Design of protein nanoparticles for cell targeting and blood brain barrier crossing

Zhikun Xu

PhD thesis 2015

Ph.D. program in Biotechnology

Design of protein nanoparticles for cell targeting and blood brain barrier crossing

Ph.D. thesis 2015

Departament de Genetica i Microbiologia

Facultat de Biociencies

Report presented by Zhikun Xu in order to complete the requirements to be granted the degree of Doctor of Philosophy in Biotechnology by Autonomous University of Barcelona

Zhikun Xu

Approval of the thesis director

Antonio Villaverde **Neus Ferrer-Miralles** **Esther Vazquez**

Contents

Contents

Contents

Contents

Introduction

Ever since humans appeared on Earth, people started to interact with nature. At early times, humans collected daily needs directly from nature, without any process. As time passed by, our ancestors gathered much more experience from collection and observation. Maybe unwittingly, they found some way to process the product and this kind of methods made better quality or easier life, and this experience led to the development of techniques, like seed selection, improving the yield of crop, cooking food etc. These techniques were soon widely used in many aspects of everyday life, and progressed towards the current concept of biotechnology.

In 1796, Edward Jenner produced the first vaccine against smallpox, and in 1927, Alexander Fleming discovered penicillin[1]. These findings improved the health condition significantly and represented two important signs that biotechnology started to participate in the medicine arena. Later in 19th century, large-scale production systems based on microbial cells were first introduced, and chemicals such as acetone or butanol were produced through this system [2]. Then, the modern fermentation industry was built up.

After that, there were some major breakthroughs that pushed the rapid development of biotechnology: in 1953, the discovery of the double helix structure of DNA by Watson and Crick [3], Marshall Nirenberg and Heinrich J. Matthaei cracked the genetic code in 1961 [4], new restriction enzymes were discovered by Paul Berg in early 1970[5], and Herbert Boyer and Stanley Cohen's first engineering of a living organism in 1973[6]. These discoveries developed the recombinant DNA technology.

In the 20th century, with the emerging of new technologies, especially nanotechnology and biotechnology had a huge development and participated more and more in the area of medicine, leading to the development of new scientific subjects such as nanobiotechnology and nanomedicine. nanobiotechnology is providing tools to achieve nanomedicine's new objectives in personalized health care, for diagnosis and therapy[7].

The goals of nanomedicine are to deliver drugs for diagnosis and for therapeutic purposes directly to a specific site, improving the efficiency while reducing the undesired side effects. Moreover, this novel approach aims to break the chemical and anatomic barriers for drug delivery, for example by improving drug solubility and stability, increasing circulation time, and transporting drugs through vascular endothelium and blood-brain barrier[8].

1. Nanobiotechnology and Nanomedicine

In 1959, Richard Feynman first brought a concept at the annual meeting of American Physical Society, which is manipulating and controlling objects on a small, nanometric scale. Since then, nanotechnology emerged and developed, and impacted all branches of the industry, from electronic, chemical to environmental and medicine [9].

There are different ways to define nanotechnology, but in general nanotechnology refers to objects within the limits between 0.1-100 nm. In 2000, the US national Nanotechnology Initiative gave us a more specific definition: “Nanotechnology is concerned with materials and systems whose structures and components exhibit novel and significantly improved physical, chemical and biological properties, phenomena and processes due to their nanoscale size” [10].

In biotechnology, most processes are performed at nanoscale. For instance, the lipid bilayer is a few nanometers thick, a protein is only 1-20 nm, virus size ranges from 20 nm-100 nm [11]. In this case, it was inevitable that these two fields cross-fertilize and develop jointly, and this led to the rising of the term nanobiotechnology.

When we speak about nanobiotechnology, people will relate that with nanomedicine; however, there are some differences between each other. nanobiotechnology is mainly about nanotechnology applied on biological systems in all basic research. It can be on plants, microorganisms and so on. When nanotechnlogy is applied in healthcare or medicine, it is in the field of nanomedicine. (Fig 1. Technologies involved in the field of nanomedicine).

Therefore, nanomedicine mainly focuses on the application of nanotechnology to medical needs, for example, by using nanoparticles and nanodevices to deliver drugs, for diagnosis or therapeutics.

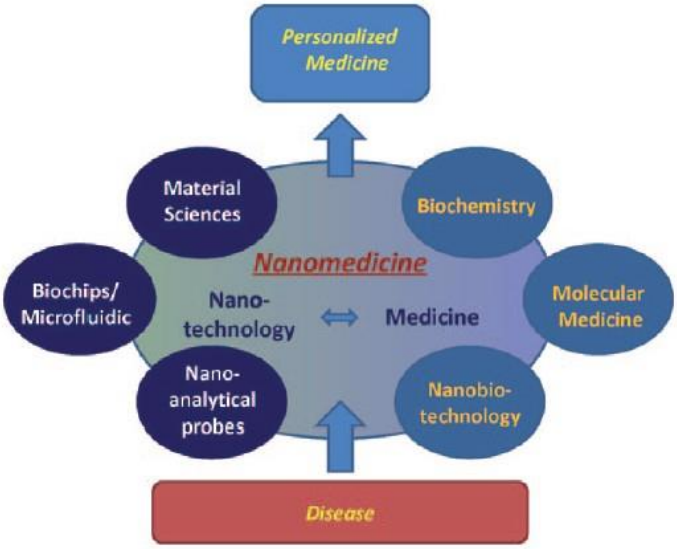

Figure 1: Technologies involved in the field of nanomedicine. Modified from *Riehemann Kristina*, et al.[10]

Compared with the traditional medicine, nanomedicine has many advantages: At nanoscale, physical and chemical characteristics can be controlled: the diffusion and sensor response could be very fast, pharmacokinetics of therapeutic compounds could have longer half live, targeting and delivery of therapeutic molecules could be more precise and effective [12, 13]. Due to these facts, when using high dose of therapeutic drugs, the system toxicity will be highly reduced. Moreover, with the help of nanomedicine, the production of small integrated devices such as biosensors and accurate drug-release systems will meet the demand of the patients. This can benefit the development of personalized medicines [14].

1.1 Applications of nanomedicine

In traditional medicine, the main goal is to improve the major areas: diagnosis and therapeutic methods, to make them more efficient, specific and cost-effective. Now with the emergence of nanomedicine, this can become real.

In the therapeutic field, because of the specificity of nanomedicine, drugs can accumulate at pathological sites, meanwhile, reducing its localization in healthy organs, and also undesirable side effects [15, 16]. This property is desirable for the strategies to treat cancer. For this reason, many efforts in nanomedicine are focused on cancer. As solid tumors present leaky vascularization, it is possible for nanoparticles with the size up to 400 nm to accumulate at cancer site; this mechanism is known as enhanced permeability and retention effect (EPR) [17, 18]. Based on the EPR effect, passive targeting improves drug delivery efficiency at tumor site. This strategy even improves the performance of targeting antibodies and peptides and can be controlled by the use of hyperthermia or ultrasound [19]. This concept is summarized in figure 2.

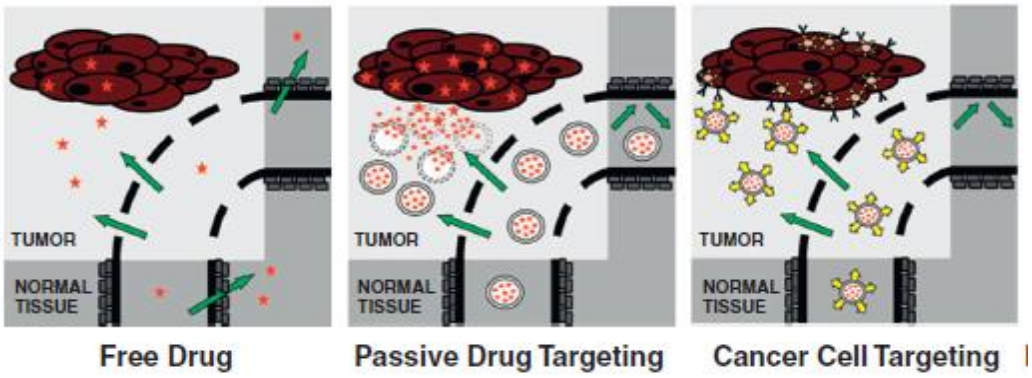

Figure 2: Drug targeting to tumors: principles, pitfalls and (pre-) clinical progress. Adopt from *Rizzo, L. Y. et al*. [8]

Moreover, in recent years, increasing number of therapeutic nanomedicines are not only used in cancer, but also used for drug delivery to other non-cancerous diseases, such as arthritis rheumatoid and atherosclerosis [20, 21] .

Recently, new nanomedicines have been designed for diagnostic purposes. Compared with traditional methods, nanomaterials labeled with contrast agents are more effective. For example, it can provide information of the circulatory system, the accumulation of therapeutic nanomedicine on target site and other organs [22], and the drug release at the target site [23]. Moreover, nanodiagnostic agents can help us to visualize and have a better understanding of some physiological disease principles, and tracking labeled cells. For example, Gadomer-17 and Resovist (new magnetic resonance, superparamagnetic iron oxide) have been used for magnetic resonance (MR) monitoring of tumor blood vessels and coronary arteries in patients [24, 25], labeling of stem cells [26] and visualization of primary liver lesions [27]. Although nanodiagnostics are very promising, many of these tools have only been tested in animal models, this is due to the stringent pharmacokinetic and elimination criteria for i.v. administered diagnostic agents. This include the use of Endorem and Sinerem, which are Resoveist-like iron oxide nanoparticles, for monitoring tumoral stem cells[28], lymph node metastases [29], cancer vaccines [30], and macrophage activity in atherosclerosis [31].

2. Nanoparticles

As described above, in nanomedicine most of the applications are based on the manufacture of different kinds of nanoparticles, and their delivery to target tissue

or cells for diagnostic or therapeutic purposes. In other words, it's mainly about nanoparticles design, production, controlling delivery and targeting. Nanoparticles for medical use have many advantages. Since nanoparticles have a nanorange size, they provide a probe that allows detection at the molecular scale. With this help, we can understand the machinery of cellular interaction and to detect abnormalities such as precancerous cells, disease marker and desigin disease marker without introducing too much interference [32], Nanoparticle-based imaging can also improve the sensitivity and specificity compared with traditional diagnostic. For therapeutic purposes, nanoparticles can improve the solubility of insoluble drugs, prolong the half-time of their systemic circulation, and display a modulatable immunogenicity. In addition, as drug delivery vehicles, nanoparticles offer promise for drug accumulation and retention at targeting site, thus lowering the frequency of administration and minimizing systemic side effects [33, 34]. Moreover, nanoparticles enable the transportation of drugs across biological barriers such as blood-brain barrier, the branching pathways of the pulmonary system and the epithelial junction of the skin [35-37], this part widely described in the next section.

In 1960s, Bangham, A. and R. Horne produced the first nanoparticle-based platform for medical application based on liposomes. [38] In the following decades nanoparticles gathered more scientific and general interest, and developed rapidly; numerous organic and inorganic nanoparticles were created for disease diagnosis and therapy. From Figure 3 we can find the rapid increasing in the number of publications per year which contain "Nanoparticles, Liposome and Monoclonal Antibody" hits from 1960-2011 [39].

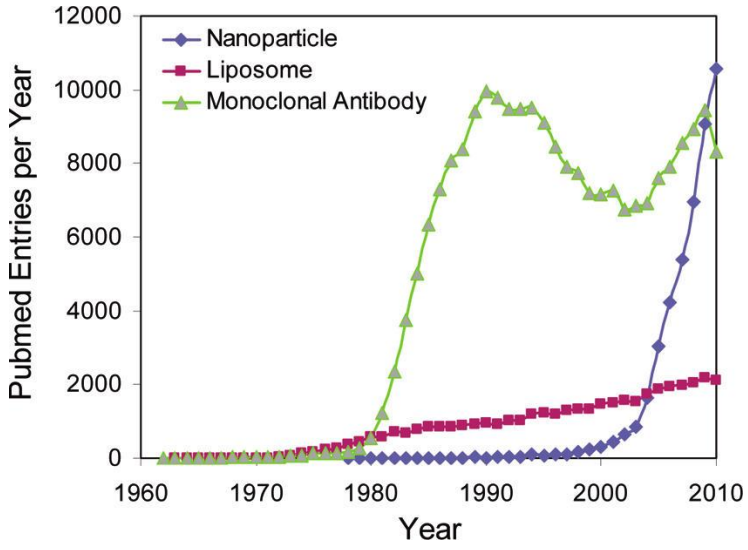

Figure 3: PubMed entries per year based on the search terms: "monoclonal antibody", "liposome", and "nanoparticle". Adapted from Shi. J., et al. [39]

Meanwhile, with the development of nanotechnology and the emergence of new nanomaterials, several types of nanoparticle platforms have been approved for clinical use, including liposomes, albumin, polymers, dendrimers and iron oxide nanoparticles for disease imaging. Here, I will introduce some of these nanoparticles.

Liposome-based nanoparticles

Liposomes are small sphere-shaped particles, formed by one or more phospholipid bilayers that can be made from cholesterol and natural phospholipids. Depending on the design, they can range from 10 nanometers up to micrometers [40]. The formation of liposomes is spontaneous, because the amphiphilic phospholipids may self-associate into bilayers. During this process, soluble drugs can be loaded inside in aqueous solution, or using solvent mechanisms and pH gradient methods [41]. Normally, liposomes will reach the

required site through a passive strategy, by extravasating into the interstitial fluid space from the bloodstream [42]. However, they can also reach the target through an active pathway. Due to existence of the lipid bilayer on the surface, it is easy to add targeting molecules to the outer surface [43]. Then, liposomes might internalize inside cells through endocytosis [44], or fusion with the cell membrane [45]. Larger liposomes might be internalized by phagocytosis [46]. However, liposomes are not stable and have a short half-time [47]. To improve this, a widely used method is to conjugate polyethylene glycol(PEG) with liposomes to change the size and properties of particles with the purpose to escape the clearance of the mononuclear phagocytic system and prolong the circulation half-time in vivo [48].

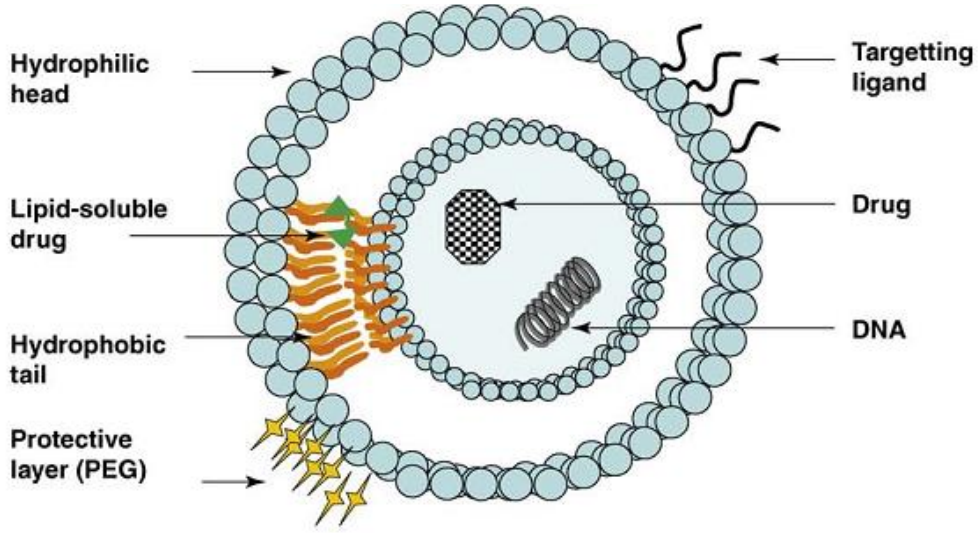

Figure 4: Diagram of a bilaminar liposome. The hydrophobic region traps drugs in the central core when the liposomes are prepared. Adapted from Malam, Y., et al.[47]

The first liposome-based nanoparticle platform was applied in medicine in 1965, and showed significant improvement on drug pharmacokinetics and

biodistribution, after then, liposomes have been widely developed as pharmaceutical carriers. [49]. Today, there are more than 11 formulations approved for clinical uses, and many more at preclinical stages. The first liposome-based drug formulation was used to treat cancer in AIDS-related Kaposi's sarcoma and multiple myeloma in this formulation.

PEGylated liposomes were encapsulated with doxorubicin (a widely used anticancer drug). This doxorubicin-liposome gave longer circulation half-time and higher concentration in tumor, meanwhile reducing the concentration of drugs in normal tissue, such as heart. It could also reduce the distribution volume from nearly 1,000 L/m^2 of normal doxorubicin to 2.8 L/m^2 in plasma [50]. There are other liposomal drugs used for clinical such as AmBisome (amphotericin B liposomes), DaunoXome (daunorubicin liposomes), DepoCyt (cytarabine liposomes), and Visudyne (verteporfin liposomes).

Polymeric nanoparticles

Polymeric nanoparticles might be the most widely used nanoparticle carriers, and have been extensively investigated in this regard. They could be formed by biodegradable, biocompatible and hydrophilic polymers such as poly (D,L-, lactide), poly (lactic acid) PLA, poly (D,L-glycolide) PLG, poly (lactide-co-glycolide) PLGA, poly-(cyanoacrylate) PCA [51-54], chitosan, gelatin, and sodium alginate. Normally, nanoparticles are prepared through two methods: dispersion of the preformed polymers and polymerization of monomers, and they form a nanoparticle with hydrophobic core and a hydrophilic surface [55]. With this property, they can bind drugs with the hydrophobic core by encapsulation, while

the hydrophilic surface will provide an external protection and may bind molecules on the surface [56]. This is suitable for delivery therapeutics such as proteins, drugs, peptides or nucleic acids. These nanopolymers are stable in blood, have low toxicity, are low immunogenic and biodegradable [57].

In recent decades, intense research has been done to develop new, effective and safe nanopolymers to transport nanomedicines. Among these new polymers, the most extensively studied and promising nanopolymer is the PLGA(poly-D,L-lactide-co-glycolide)-based nanoparticles[58]. This is because when PLGA is hydrolyzed inside the body it only produces lactic and glycolic acid which are biodegradable metabolite monomers[59]; with this property, PLGA nanoparticles have minimal systemic toxicity and constitute an efficient system for controlling and releasing therapeutics. Thus, many PLGA-based nanoparticles such as nano-antigen, nano-vaccines, and nanoparticle-based gene delivery systems have been developed [60-62]. The first FDA approved PLGA nanomedicine: Trastuzumab has been used to cure breast cancer [63, 64].

Another widely accepted polymer family is the dendrimer-based nanoparticles, and the PAMAN is the most common used dendrimer to bind and deliver molecules. That is because PAMAN is easy to prepare, its size can be controlled and that enable PAMAN to bind several molecules for diagnosis and therapy. For example, binding to metal nanoparticles improves their solubility. Other studies showed that PAMAN incorporated to a special ligand could improve the permeability to cross the blood-brain barrier [65-67].

Metal nanoparticles

Metal-based nanoparticles represent another widely used platform for nanomedicine, including gold (Au), iron oxide (Fe_2O_3), silicon dioxide or silica (SiO_2), silver. Like other nanoparticles, metal based-nanoparticles have the same properties, such as binding a variety of ligands for imaging, delivery of vehicles, and biosensors through a modifiable surface. Among these, Au is one of the most commonly used metals in nanomedicine, because it is easy to produce as nanoparticle with a favorable nano size (5-10nm), the surface could bind many therapeutics, and has a suitable absorbance and scattering of light. With those properties, Au nanoparticles have been widely used in biological diagnostics and imaging, improving the specificity and sensitivity. For example, conjugated with specific antibodies to detect cancer cells [68], and using the spectroscopic advantages of gold to detect disease cells when combined to special aptamers [69]. Iron oxide nanoparticles always have been considered to be a convenient biomarker, as they provide better and more intense color of solution with an optical signal excited from the surface [70]; and with magnetic properties, it can provide a specific localization by manipulating the magnets [71, 72]. Silicon dioxide nanoparticles conjugated with antibodies and transistors are used to detect single copies of multiple viruses [73]. Also, silicon-based nanosensors are under development [74]. Different investigations proved that metal nanoparticles are biocompatible; however, a significant amount of particles are retained in the body after administration, and the accumulation of metal particles may lead to toxicity [75].

3. Protein-based nanoparticles

With the development of nanotechnology and nanomedicine, more and more materials have been involved in these fields, beside liposomes, polymers and metal nanoparticles, protein based nanoparticles have become another biomaterial that is developing fast and attracts growing attention. Proteins are natural biological molecules indispensable for living organisms. They have unique functionalities and potential applications both in biological and material fields. Protein size is ranged from few nanometers to hundreds nanometers depending on their molecular mass; they are non-toxic, low-antigenic, biodegradable, metabolizable, and with genetic engineering, it is easy to modify their structure, surface charge, to allow heterologous ligand display, to improve stability and more importantly, proteins can be designed to form multimeric structures with the ability to self-assemble in a similar way as viral capsid proteins do. These properties open up a novel concept for imaging and therapy in nanomedicine by using the repetitive nature of protein nanoparticles to conjugate multiple drug molecules or dies on their surface. These properties enable protein particles to be widely used in targeting and delivery of therapeutic drugs, vaccine designing, diagnosis, and gene therapy; moreover, some protein particles themselves are therapeutic molecules.

Proteins can be produced in many different living hosts, such as bacteria, mammalian cells, insect cells, yeast and plants. These diverse expression systems provide different functional proteins which will meet the requirement of researches. Among these systems, *Escherichia coli* is the most common used host, because it has high productivity, it is easy to be cultured, inexpensive and well

characterized [76]. However, sometimes, recombinant proteins form inclusion bodies, which is an obstacle when the desirable product is the soluble recombinant protein version. Moreover, because bacterial hosts lack post-transcriptional modifications, this will lead to protein misfolding problems. Yeasts are another commonly used protein expression system. Like *E. coli*, yeasts also render high yields of protein production by easy processes, and as an eukaryotic organism, yeasts have a complex post-translation modification pathway that promise right folded protein production. *Pichia pastoris* and *Saccharomyces cerevisiae* are the most widely used and well genetically characterized microbial species, still applied in the pharmaceutical production [77]. However, there is a limitation in yeasts, because they are not able to produce proteins with the mammalian glycosylated pattern as they have a different glycosylation pattern modification. Another expression system is insect cell expression systems, it could provide also complex post-translation modifications although different form mammalian cells , meanwhile, more productive, easier to handle compared with mammalian cells, thus, frequently applied for high-throughput protein production [78]. To solve glycosylated protein expression problem, mammalian cell expression systems could be the choice, as they show highest similarity to human cells, have same post-translation modification and codon usage, are favorable for production of glycosylated proteins, but the cost for production is higher and yields are lower [79].

There are different ways to form protein nanoparticles. One popular method is using physical and chemical ways to change protein surface charge or protein solubility after purification; this stresses the single protein unit to form protein

aggregates and at the same time, obtaining protein nanoparticles. Another way is using genetic engineering to modify common protein for special purpose, design multi-functional protein, and produce virus and non-virus self-assembling protein nanoparticles.

The former method includes emulsification and desolvation methods. The emulsification method was developed by Ursula Schefel et al. in 1972 [80], when they tried to design the albumin particle to study the reticuloendothelial system. In this method, albumin-based aqueous solution was mixed with plant oil to form an emulsion through a hand-operated homogenizer; then they removed the oil phase by a heating-cooling method and followed with anhydrous diethyl ether (As shown in figure 5). This method could form 400-600 nm albumin nanoparticles, and these nanoparticles could be labelled with ^{99m}Tc for further study. However, this method has some disadvantages, such as high temperature that will affect protein activity, and the introduction of organic solvents that could be toxic to the body.

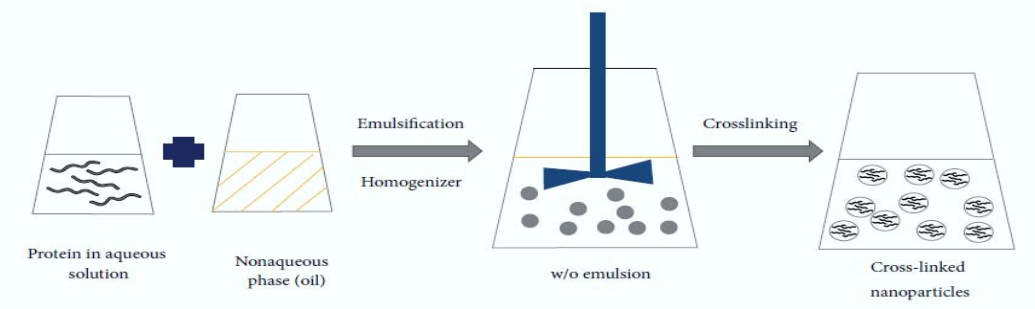

Figure 5: Preparation of protein nanoparticles by emulsification method. Adapt from Lohcharoenkal, W, et al.[81]

The desolvation method was developed by Marty et al in 1978, on the purpose to form a colloidal system for drug delivery [82]. In their experiment, albumin dissolved in water was desolvated by dropwise addition of ethanol. During this process, nanoparticles were formed, and later, cross-linkers such as glutaraldehyde were added to maintain the stability of particles. This method was developed by Lina et al [83], they incorporated an enzyme β- galactosidase with GFP to form nanoparticles (Figure 7). They form particles with a size of 270 nm, had high retention of enzyme activity, and were able to internalize inside cells to fulfill the aim of delivering therapeutic enzymes inside cells. However, when using desolvation method, big aggregates are easy to be formed, and this will cause the loss of protein activity. In fact, using a chemical process to form protein nanoparticles is always related to the change of protein properties such as hydrated layer, covalent binding and surface charge, leading to the formation of protein aggregates, while weak aggregation produces nanoparticles. The changing of protein properties somehow will affect protein structure and activities, leading to the low efficiency of protein nanoparticle for therapeutic and diagnosis use.

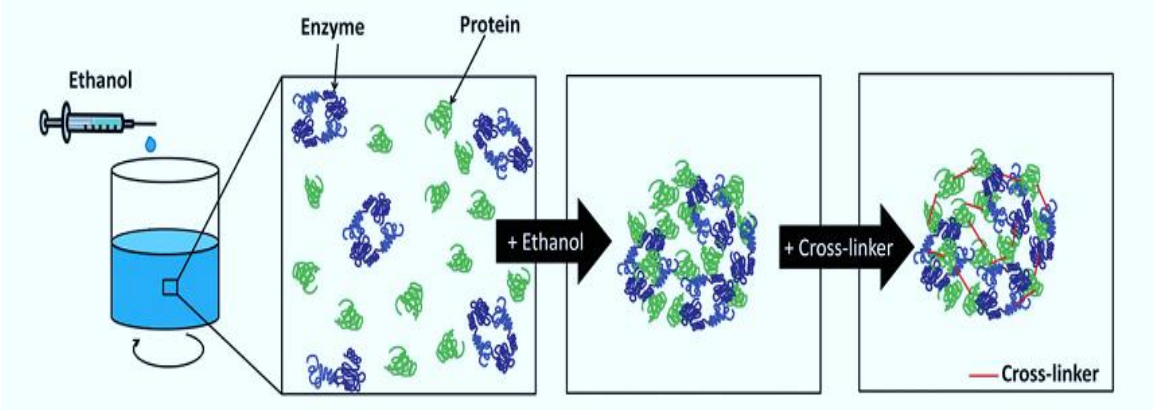

Figure 6: Schematic diagram of the desolvation process. Adopt from Estrarda L., et al.[83]

With the development of genetic engineering, new recombinant proteins can be designed from the scratch, or improved adding modifications to the existing proteins to incorporate new properties to meet patient's needs, providing strategies to design and produce multifunctional proteins to build protein-only nanoparticles. Comparing with chemical methods, genetic engineering has controllable effect on protein structure and properties after production, proteins form nanoparticles spontaneously due to the careful design.

3.1 Albumin

Another widely used protein in nanomedicine is albumin formulated in nanoparticles. Albumin is the most abundant plasma protein which is synthesized in the liver as other plasma proteins, with a molecular weight of 66.5 kDa and an average half-time of 19 days. The three-dimensional structure of human serum albumin (HSA) has been well defined by X-ray structure analysis[84], it contains three flexible sphere domains(I, II, III,) [85]as showed in Fig 6.

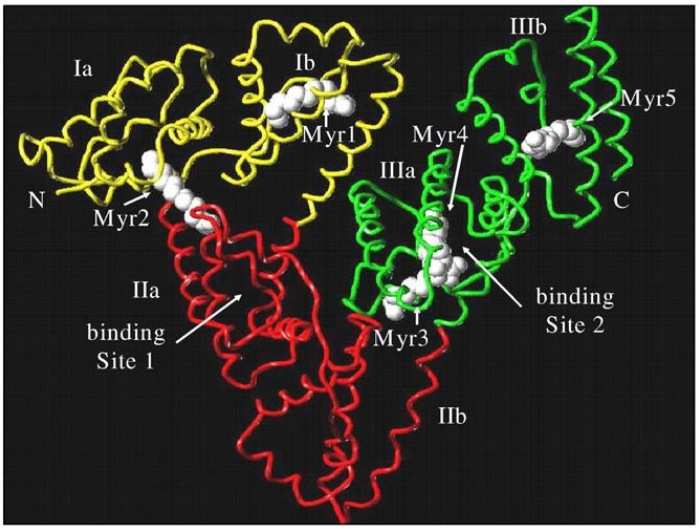

Fig 7: The 3-D structure of Human serum albumin. Adapted from D.C. Carter, et al.[86]

Albumin is an ideal protein with a nanoscale size, for delivery of therapeutics, because it is considered non-immunogenic, nontoxic, biocompatible and biodegradable. Furthermore, albumin can bind glycoprotein (gp60) receptor that mediates transcytosis [87, 88]. In addition, it can also bind many therapeutic molecules such as penicillins, sulfonamides, indole compounds and benzodiazepines; it can also transport metal ions like copper(II), nickel(II), calcium(II) and zinc(II) in blood [89].

In the middle of 20th century, a report described that different plasma proteins were accumulating in mouse tumors [90]. As albumin is the most abundant plasma protein, scientists started to think of the possibility of using albumin as a drug carrier, to deliver therapeutics to tumors. The mechanism is this: because of the leaky defective blood vessels (with a pore size of 100 nm to 1200 nm) in tumor tissue [91], it allowed macromolecules to extravasate into tumor tissue meanwhile in healthy vessels, the marcromolecules will be rejected by the endothelial barriers [92, 93]. Moreover, defective lymphatic drainage in tumors constrains proteins larger than 40 kDa to accumulate in tumors even after 100 h post application [94, 95]. Based on this, in the following years, scientists started using albumin radiolabeled or conjugated with dyes to study tumor uptake. The results showed that 3% to 25% of albumin was detected in the tumor tissue [96]. For example, after administering labeled albumin with [^{111}In]-DTPA, it was shown that more than 20% of protein accumulated in tumor after a single dose of injection [97]. Afterwards, instead of labeling radiopharmaceuticals, scientists started to conjugate therapeutic drugs to albumin for clinical uses. The most famous one was albumin-based nanoparticles conjugated with paclitaxel-

Abraxane (nab-paclitaxel), with the purpose to treat breast cancer and was approved by FDA in 2005 [98]. Compared with normal paclitaxel, nab-paclitaxel had higher tumor response rates, of 33% instead of 19%, and it was retained longer in tumor: 23 weeks compared with 16.9 weeks. This accumulation is due to the transcytosis initiated by albumin binding to its receptor gp60 (glycoprotein).

There are other albumin-based therapeutics such as methotrexate-albumin conjugate, which is an albumin-binding prodrug of doxorubicin [99], and the 6-maleimide, which is a caproyl hydrazone derivative of doxorubicin (DOXO-EMCH) [100] . Both have also been used in clinics.

3.2 Virus-like particles (VLPs).

Virus-like particles are composed by outer shell of viruses or parts of them. Without genome, they are unable to self-replicate, having a similar or highly related structure to their corresponding viruses [101, 102]. After the first VLP was generated in 1980, VLPs become an extensively accepted technology, and widely used in different fields. During the last three decades, over 110 VLPs were created from 35 different viral families [101]. VLPs were frequently used in designing vaccines. Since they have virus surface-displayed structure and densely repeated amino acids (AA)[103, 104], VLPs activate a high-immune response, and stimulates B cells to secrete high-titer antibodies. Nano sized VLPs can be taken by antigen-presenting cell, that lead to T cell activation, and generate strong cellular immune responses without using adjuvants [105, 106]. For example, scientists have designed hepatitis B (HBV) surface antigen and the human papilloma virus (HPV) capsid protein L1 as a new vaccine to fight against HBV and

HPV induced cervical cancer. This vaccine has been already commercialized [107, 108]. In addition, VLPs could be designed as vehicles to deliver nucleic acids and drugs for gene therapy. Icosahedral and lipid-enveloped virus like vectors are considered to be the most promising gene vehicles [109, 110].

Based on their structure, VLPs can be divided into two major categories: non-enveloped and enveloped VLPs. Non-enveloped VLPs are composed of one or more fragments from main capsid proteins and are able to self-assemble, not including any host components [111, 112]. Enveloped VLPs are formed by the host cell membrane with integrated antigens displayed on the surface [113, 114]. Most VLPs have been designed as recombinant proteins that can be produced in bacterial cells, mammalian cells, insect cells, yeasts and plants [115-117]. However, there are some disadvantages in the use of VLPs, such as packaging capacity, difficulty in their production, and the undesirable immunological response. All these issues should be taken into consideration.

3.3 Multi-functional proteins

The use of protein based nanoparticles for therapeutics and diagnosis always meet a lot of challenges, such as protein particle stability in blood, half-time in body, biodistribution, how to cross the biological barriers, targeting, cell internalization, endosomal escape etc. To solve those problems, recombinant proteins recruiting different functions are needed. With the help of genetic engineering, this could become true. For this purpose, many functional domains or peptides can be selected and carefully designed to combine together, then expressed in a proper host system to produce new multifunctional proteins. The

new protein has many biological activities which come from the original domains or peptides, and those activities could exhibit protein functions such as receptor interaction and binding, cell internalization, endosomal escape, therapeutics binding and releasing, intracellular trafficking, nuclear transport and crossing biological barriers such as blood-brain barrier, making the protein particles more versatile and efficient.

There are mainly two ways to design multi-functional proteins. One is known as modular protein engineering [118], which means properly design those functional domains or peptides into one polypeptide, then express them in a host system as a fusion protein with multi-functions derived from those domains [119] (Figure 8). As an example, an RGD based polypeptide contained four biological active domains was designed and produced in our lab. This RGD based recombinant protein could form 80 nm nanoparticles, and exhibited the function of promoting the proliferation and partial differentiation of neuron-like cells [120, 121]. In this method, the number and order of modules should be carefully selected and designed, and the structure is unpredictable since those domains and peptides come from different origins and have a variety of properties, and sometimes purification problems are encountered.

The other strategy is called as de novo rational protein design. In this method, a stable, no biohazard, easy to be tracked protein is selected as a backbone scaffold, then using genetic engineering technique functional domains or peptides are inserted to some specific sites of this protein, giving the scaffold protein different functions[118] (Figure 8). With this strategy, proteins with multi biological activities, high stability, clear background, easy to track, could be produced. The

insertion of amino acids should have low influence on the structure of scaffold proteins; otherwise, it will lead to unpredicted effects, so the insertion site should be carefully chosen. When selecting scaffold proteins, several factors should be taken into account, such as their background, stability, yield, whether they are easy to purify and trackable, etc. Among all the proteins, albumin is a good candidate for a scaffold protein, because it has good properties that have been described before. For example, interferon α-2b has antiviral activity, with a short half-life of 2-3 h in human body and requiring frequent injection; to improve this, interferon α-2b was genetically fused with albumin to obtain a new protein and after subcutaneous injection, this protein had a half-life of more than 140 h, and the antiviral property was highly retained, this strategy is now being used in phase III studies against hepatitis C [122, 123].

Another widely used scaffold protein is the GFP. There are countless works about GFP based fusion proteins, as it has high stability and high solubility, it is non-toxic and non-immunogenic, with the green fluorescence, their distribution, localization and internalization is easy to be tracked. In our lab, we use GFP as a backbone scaffold and functionalized it with several different ligands; also a His-tag was added for purification and endosome escape purposes [39, 124]. For example, an arginine rich peptide was added to the N terminal of GFP protein, and the functionalized GFP protein acquired internalization capacities in different cell lines, converting the recombinant protein in a carrier useful for drug delivery and gene therapy [125, 126].

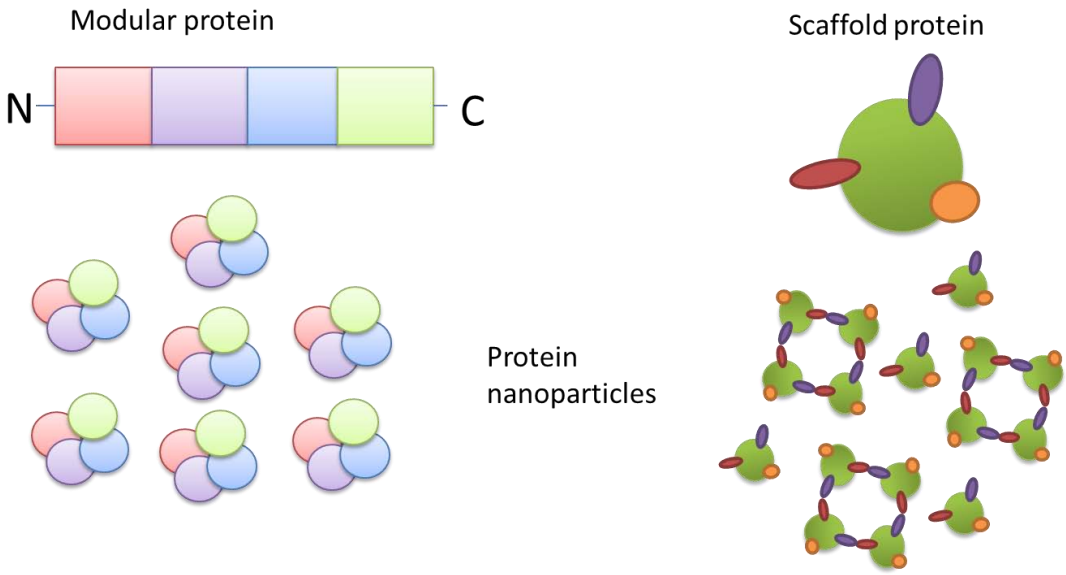

Figure 8: Schematic represent of modular protein and de novo scaffold protein approaches for multifunctional proteins.

3.3 Peptide-driven self-assembling protein nanoparticles

During the production of multifunctional proteins, many functional peptides or domains have been identified by high throughput screening or directed molecular evolution, and those peptides were used to target cell surface receptors, membrane interaction and nuclear localization [127]. However, only few peptides or domains were reported to be able to regulate the formation of nanoparticles, and most of these peptides are amyloidogenic protein segments that form fibers, membranes or hydrogels, instead of forming protein nanoparticles, they only induced protein aggregation [128, 129]. In our lab, by using the “de novo rational design” method, we designed and generated a series of peptide-driven self-assembling nanoparticles. GFP was chosen as a backbone scaffold and a His-tag

was added in the C-terminal. In the N-terminal, a cationic peptide containing polyarginines was fused. Because of the structure of GFP, as a monomer, both peptides could be exposed to the solvent, as showed in Figure 9A. Normally, with the existence of this tag pair, nanoparticles will self-assemble driven by electrostatic interactions, hydrogen bonds and van der Waals forces between monomers, and this interaction can be disrupted by increasing the concentration of salt [130]. When using highly cationic peptides such as R9 and T22 (a peptide derived from polyphemusin II which is a basic protein from horseshoe crab's blood) [125, 131], the molecular interaction is very stable forming nanoparticles of 13-20 nm (Figure 9B) even in the bloodstream, with relatively high salt concentration [132]. Apart from architectonic new abilities, these two building blocks, have other functions: H6 tag can promote endosome escape [124], while R9 peptide has the ability of bind DNA, membrane-crossing and thus enhancing cell internalization and also nuclear translocation; T22 could specifically binding CXCR4 receptor (a cell surface receptor related to several human pathologies including metastatic colorectal cancer), thus can be used to target colorectal tumors for diagnostic and therapeutic purposes. These properties enable this protein nanoparticle as a suitable vehicle for gene therapy.

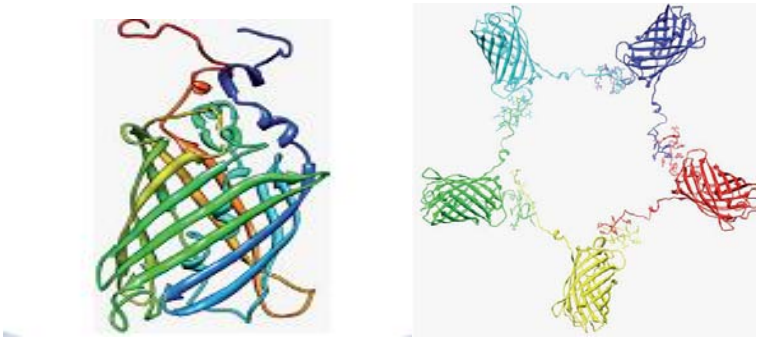

Fig 9: Molecular modeling of R9-GFP-H6 protein nanoparticles. R9 and H6 domains are the red and blue domains coming out the upper part of GFP beta barrel. Adapted from Vazquez, E., et al [125]

4. Nanoparticle Targeting and biodistribution

After nanoparticles are generated, the next step is to deliver them to required sites. This refers to the targeting delivery of nanoparticles to specific organs, tissues and cells. There are two ways to achieve this: passive targeting and active targeting.

4.1 Nanoparticle targeting

One classic example of passive targeting is the enhance permeability retention effect (EPR) presented in tumors. This is caused by the underdeveloped, leaking vasculature and poor lymphatic drainage, which allows large size molecules to accumulate in tumor tissue [133, 134]. However, there are limitations to passive targeting such as: the EPR effect is different for different tumor types, and the lack of control may lead to drug expulsion and induce drug resistance in cancer cells. [135]

This could be improved by active targeting, which means to incorporate targeting ligands on the surface of nanoparticles that could enable the nanoparticle to localize and internalize into target cells and tissues through a ligand-receptor interaction. This delivery strategy achieves a high targeting specificity and delivery efficiency, while avoiding the side effects coming from the nonspecific binding. Active targeting strategies always rely on the use of specific peptides, proteins

(mainly antibodies and their fragments) or other small molecules such as sugar moieties.

Antibodies present high binding affinity and selectivity towards the target, thus are widely used in targeting delivery of nanoparticles for therapeutic (antibody drug conjugates –ADC) and diagnosis purposes. Several nanomedicines which are conjugated to antibodies have been approved by FDA [136-138]. However, there are some limitations such as manufacturing cost, size is usually too large for an optimal tumor penetration and they may potentially induce an immunogenic response. Peptide-based targeting is another popular strategy due to their small size, easy to produce at low cost and low immunogenicity [139]. These peptides mainly originate from the binding region of a protein, thus giving the ability to the peptide to bind target cells with a specific surface marker. However, since they are just a fragment of the binding region, they may have low target affinity, and also susceptibility to proteolytic cleavage. There are also other small molecules such as folic acid [140], carbohydrates [141]and glycosylation used for targeting, as they are inexpensive to produce and have great potential as a class of targeting moieties.

The ultimate target for a nanoparticle is a subcellular compartment, where it could release their cargo and the intracellular action occurs. This makes the organelle-specific targeting an important evaluation of the effectiveness of any engineered nanoparticle. To target different organelles, nanoparticles should be designed appropriately to meet the targeting requirements. For example, transport of oligonucleotides to the nucleus requires an endosomal escape motif to avoid oligonucleotides degradation, and then a nuclear localization signal

should be present to activate the nuclear transport, driving uptake into the nucleus [142, 143]. If for example we want to deliver cargo to mitochondria, the electrostatic interactions between the engineered nanoparticle and the mitochondrial membrane should be considered at first [144]. There are also other tools and strategies to target organelles such as mitochondria, peroxisomes and endosomes/lysosomes [145-147].

Despite the promising use of ligand-receptor mediated targeting, when compared with the passive targeting *in vivo*, active targeting does not increase the drug accumulation at target site. For example, using HER2-antibody targeted liposomes or transferring-targeted gold nanoparticles do not show increased nanoparticle concentration in tumor when compared with passively targeting [148, 149]. Even though, some researchers believe that ligand-receptor mediated targeting could make sense when there is poor internalization for agents, such as DNA and siRNA which are negatively charged macromolecules [150], or in some special targeting sites where the passive targeting could not be achieved [151]. Moreover, in gene therapy, the main goal is to target on lesion's site, and deliver therapeutic gene inside diseased cells. Then, using ligand-receptor mediated targeting not only increases the specificity of targeting, but also activates the cell internalization process, leading to the high efficiency of therapeutic gene uptake [152].

4.2 Size is affecting nanoparticle targeting and distribution

Since different materials can be used to produce nanoparticles, this varies physical characteristics from one particle to another. Among all the features, size, shape and surface charge are the most critical properties. That is because these

parameters directly determine nanoparticles' function, such as the interaction with other particles, ligand and receptors, the circulation time in the body, and more importantly, directly decide the distribution on different tissues and organs, the localization on a specific target, the efficiency of internalization into target cells and intracellular trafficking; among these parameters, size is one of the most critical ones[153]. Therefore, the selection of material and nanoparticle design is very important, and for different target cells, tissues and organs, appropriate design of nanoparticles should be considered.

Our body has different systems to clear non-natural molecules, including reticuloendothelial system (RES), Kupffer cells in liver, renal clearance at kidney and mechanical filtration in spleen nanoparticles with a size around or under 5 nm will rapidly be cleared by renal filtration and urinary excretion, and when the nanoparticle is larger than 200 nm, then it will be cleaned by the spleen[154]. When the size is bigger than 500 nm, it is easily removed by RES system[155]. The size of a nanoparticle is very important for maintaining the circulating time in the body, because usually long circulation time is needed to increase the drug accumulation in target tissue. On the other hand, nanoparticles containing heavy metals should have short half-time in body, because this type of nanoparticles will lead to long-term toxicity.

At the organ level, nanoparticles of different size will be preferentially targeted to different target tissues (Table 1). Here are some examples: particles of size ranging 5-100 nm showed ability to cross BBB, but the uptake efficiency will decrease with the size, and <15nm particles targeted to the BBB showed high crossing efficiency [156, 157]. To target lymph nodes, the chosen nanoparticle

size mostly depend on the administration route. Through intrapulmonary administration, nanoparticles with a size range of 6-34nm could rapidly reach to lymph nodes, and through subcutaneously injection, the size could increase to 80 nm[158]. Nanoparticles can easily reach the liver through intravenously administration, but only particles smaller than 100 nm can reach hepatocytes, since bigger nanoparticles will accumulate in activated Kupffer cells [159]. The lungs can be accessed directly through inhalation or indirectly following intravenous administration [160]. By using intravenous administration, nanoparticles over 300 nm in diameter can reach the lung and be trapped in the intricate capillary beds of the alveoli, and smaller particles tend to diffuse to other organs after 1-2 hours after first administration[161]. In cancer tissues, the tumor vasculature may have fenestrae, and nanoparticles with a size up to 400 nm are able to accumulate in such pathological sites, through the mechanism known as EPR[162].

Target organ	Particle size	Surface property	Comments
Brain	5–100 nm: uptake efficiency decreases exponentially with size	Lipophilic moieties and neutral charge enhance brain uptake	Leukocytes can take up nanoparticles in circulation and then carry them to disease sites in the brain
Lung	>200 nm: particles are trapped in lung capillaries	Positive surface charge	Inhaled particles with low density (<0.4 g per cm^3) and of large size (>5 mm) are also retained in the lung
Liver	<100 nm, to cross liver fenestrae and target hepatocytes. >100 nm particles will be taken up by Kupffer cells	No specificity needed	Lipid and lipid-like materials tend to accumulate in the liver
Lymph nodes	6–34 nm: intra-tracheal administration. 80 nm: subcutaneous administration	Non-cationic, non-pegylated and sugar-based particles	200 nm particles in circulation can be taken up by leukocytes and trafficked to lymph nodes
Bone	Unknown	Compounds such as alendronate and aspartic acid adhere to bone and have been used for bone targeting	Despite great importance, bone targeting is under-researched

Table 1: General considerations for nanoparticle delivery to specific organs. Adapted from Avi Schroeder, et al [163]

After nanoparticles are administered into the body, the next step is to bind to target cells. Some nanoparticle internalization is mediated by ligand-receptor interaction. Once ligand is bound to the receptor, the binding will produce a localized decrease of Gibbs free energy, and induce the membrane wrap around nanoparticles to form vesicles. These vesicles are shedding from the membrane and then fused with other vesicles to form endosomes[164]. The size of the nanoparticle is quite important in this process, since with a larger size, there will be more ligand displayed on the surface, and could interact with more receptors; for example, 100 nm nanoparticles have more ligand-receptor interactions, can act as a cross-linking agent to cluster receptor and induce uptake. By contrast, a 5 nm nanoparticle only can bind to one or two receptors and this is not enough to trigger the internalization process (Figure 10). However, there is a size limitation: 20-50 nm is considered to be the optimal size [164] for receptor mediated endocytosis. In this size range, there will be enough ligands for recruiting and binding enough receptors to produce membrane wrapping, and if the size is larger than 50 nm, nanoparticles will bind to a large number of receptors, this will affect the redistribution of receptors on the membrane and may limit the binding of following nanoparticles; moreover, if nanoparticles are too big, this will also affect the formation of vesicles, thus, inhibiting the formation of endosomes[153]. Mathematical modeling showed that the optimal endocytosis only occurs when there is no shortage of ligand on the nanoparticle surface and no receptor shortage on the cell surface[165].

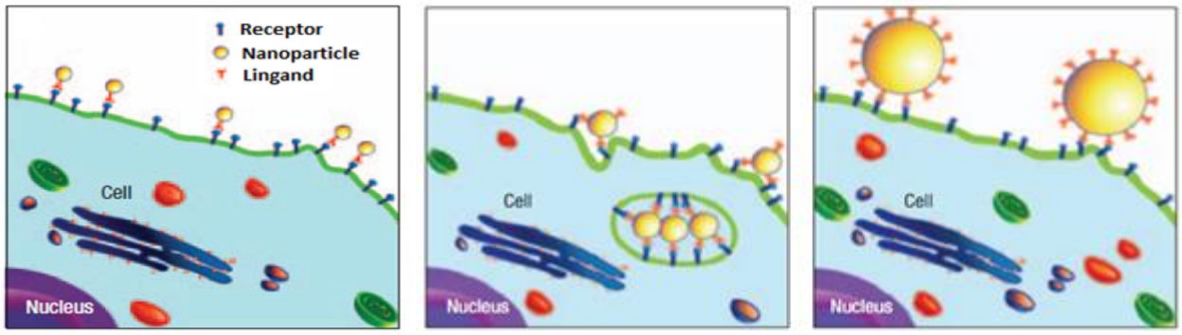

Figure 10: Effect of NP size on endocytosis. Adapted from WEN JIANG et al.[166]

After targeting to cell membrane, there are different pathways for nanoparticles' internalization, including clathrin dependent endocytosis, caveolae medidated endocytosis, micropinocytosis, macropinocytosis and phagocytosis (Figure 11). Among those, clathrin mediated endocytosis is the most common used pathway [167, 168]. It has been reported that size is the key parameter in determining which pathway will be used for nanoparticle internalization. Nanoparticle size around 120 nm could internalize through clathrin-mediated endocytosis [169], caveolin-mediated endocytosis prefer to internalize 60 nm nanoparticles, and larger nanoparticles with a size up to 1 μm tend to be uptaken by cell through micropinocytosis or phagocytosis[170].

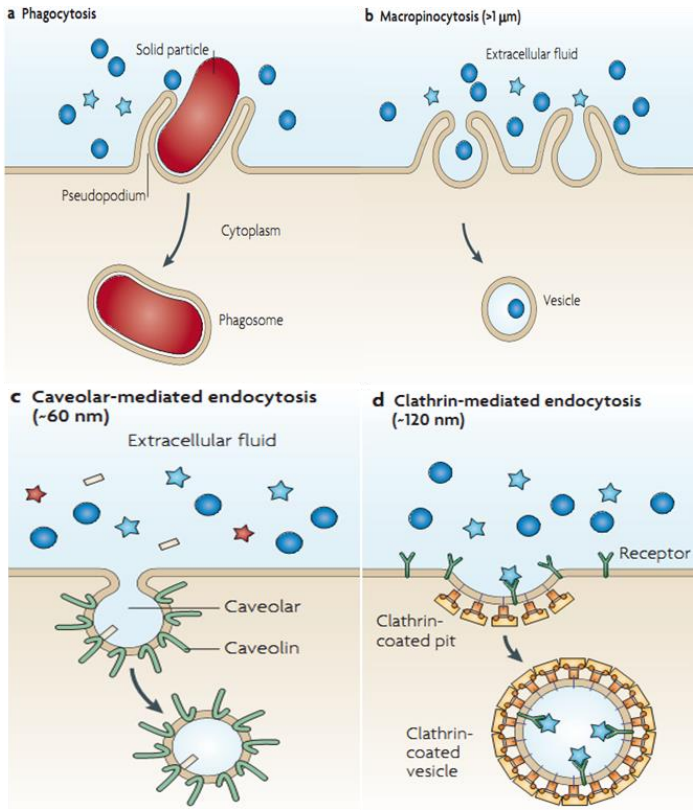

Figure 11: Modes of cellular internalization of nanoparticles and respective size limitations. Adapted from Petros et al. [155]

The behavior of nanoparticles in endolysosomal vesicles needs further study. Some researchers suggest that protease Cathepsin L could cleave nanoparticle ligand inside endosome [171], and if the nanoparticle is designed to escape the endolysosomal system, the nanoparticle could enter the cytosol, interact directly with different organelles and modulate cell behavior.[172]

The shape and charge could also affect internalization as well. Different studies suggest that rod-shaped nanoparticles show the highest uptake, followed by spheres, cylinders, and cubes [173]. Compared with spherical particles, rod-shaped nanoparticles coated with ligands could present two different orientations when interacting with cells, long axis and short axis, and the long axis could

display more ligands to interact with cell surface receptor[174], as shown in figure 11.

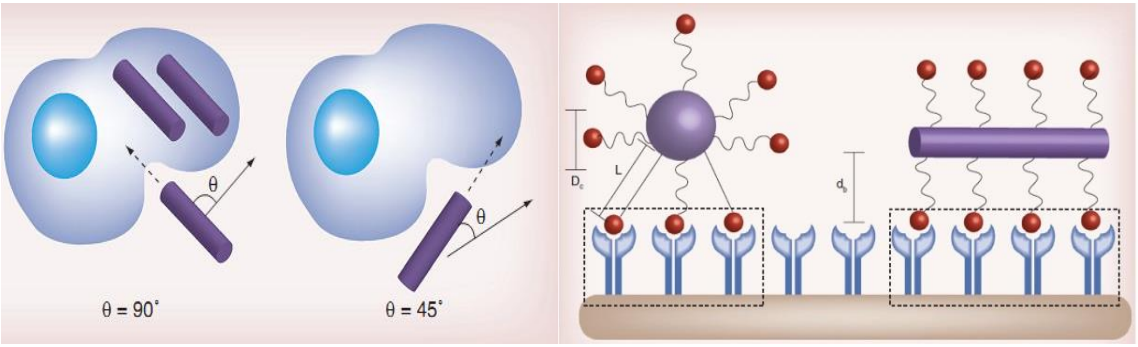

Figure 11: Effect of shape on nanoparticle binding avidity. Adapted from Randoll T., et al. [174]

Surface charge is also an important parameter in nanoparticle distribution. Nanoparticles with positive charge are easily cleared from the blood and cause several complications such as hemolysis and platelet aggregation. In addition, charged nanoparticles interact with serum proteins like immunoglobulin and lipoproteins. Cationic charged nanoparticles also tend to have a faster cell internalization compared with neutral or negative charged nanoparticles, because cell membranes have a slight negative charge due to the glycosaminoglycans of the surface and cell binding is favored by electrostatic attractions[175, 176].

4.3 Control of nanoparticle size

Since size is such an important parameter to nanoparticle, the control of size is become a critical issue in nanoparticles production. So far, the control of nanoparticle size is mainly depending on different synthesis strategies and processes. Normally, once nanoparticles were generated, the size cannot be

changed, however, there are some exceptions such as protein nanoparticle size could be altered when changing the pH or salt concentration.

Metal nanoparticles such as gold, silver and iron based nanoparticles are normally generated by simple chemical reaction processes, and their size could be controlled by changing the chemical components ratios in the reaction. For example: different size of gold nanoparticles from 10-40 nm could be generated by mixing chloroauric acid with citric acid at different ratios, and different silver nanoparticles could be obtained by mixing silver nitrate and sodium borohydride at different ratios [177]. There are different methods to produce iron oxide nanoparticles, such as aqueous co-precipitation, microemulsion and thermal decompilation. With those methods, nanoparticles of different size could be generated. There is another method named as “seeding growth” is adopted to produce larger metal nanoparticles. Small metal particles are prepared first and later used as seeds (nucleation centers) for the preparation of larger size particles. Recently, seeding growth methods were developed for size control of Au, Ag, Ir, Pd, and Pt particle [178].

Silicon nanoparticle’s size can be also controlled by changing the chemical reaction conditions. Recently, a study showed a simple approach of producing monodisperse silica nanospheres between 50-100 nm just by increasing the reaction temperature from 40 °C to 80 °C [179].

Polymeric nanoparticles can be produced by many different methods, among that, solvent evaporation is the most widely employed technique to prepare polymer nanoparticles [180]. In this method, parameters such as preparation temperature, internal aqueous phase volume, surfactant concentration, and the influence of

the molecular mass will affect nanoparticle size [181]. For example: changing of dichloromethane and acetone ratio will lead to the change of nanoparticle size from 60-120 nm [182], and when using methylene chloride as solvent in the preparation of nanoparticles, the size is larger than those prepared with ethyl acetate [183].

Proteins can be produced in many different biological systems, and the size of monomer protein particles is determined by the number of amino acids and related to the molecular weight, the more amino acids, the larger the size. For those multimeric protein nanoparticles, their size depends on the number of protein monomers which participates in its formation. However, when using desolvation method to produce protein nanoparticles, the size is also affected by the concentration of ethanol and crosslinker. Meanwhile, in our lab, when we were using combined cationic peptide and polyhistidine to produce nanoparticles, we found that after nanoparticles were generated, the size of nanoparticles can be manipulated by changing the ionic strength and the composition in the cationic residues of the N-terminal tag [130, 132], obtaining protein nanoparticles ranging in size from 10 to 50 nm.

5. Nanoparticles able to cross barriers

To reach the target tissue, organ or cell, there are some barriers that the nanoparticles have to overcome. These barriers can be classified as external barriers and internal barriers (Figure 12). The external barriers include skin and the mucous membranes, the internal barriers can be divided into en-route (blood

and extracellular matrix) and cellular barriers (the limitation of cell uptake such as endosomal/lysosomal degradation, inefficient targeting, etc).

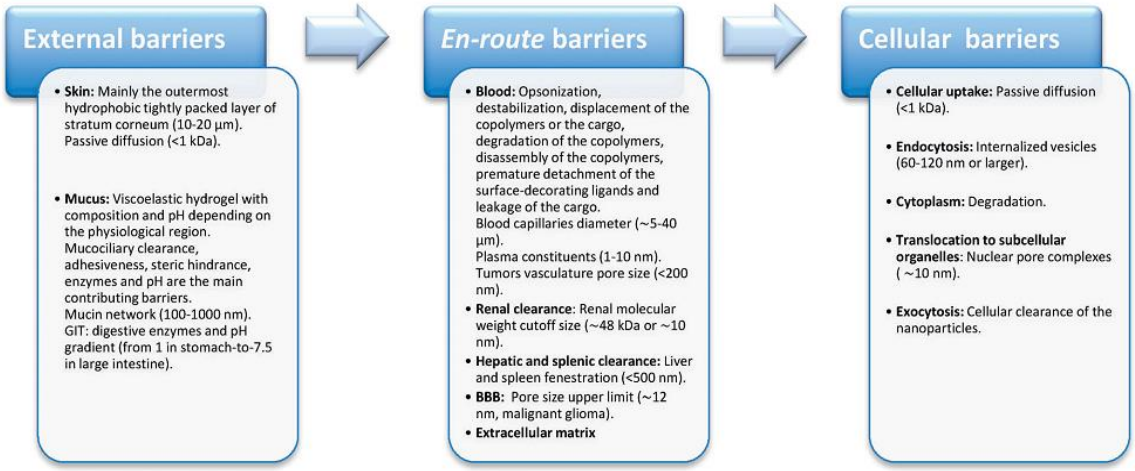

Figure 12: Barriers towards the delivery of nanoparticles can be classified into external barriers, en-route barriers and the extracellular and cellular and subcellular barriers. Adapted from Elsabahy, et al.[37]

The body is covered by either skin or mucous membranes, and they constitute the first protective barrier of our body. Based on the properties and structure of skin and mucous membranes, they could prevent nanoparticles to reach their local or systemic target through the blood, and each of them has different mechanisms to achieve that. In addition, nanoparticles that could cross the skin and mucous membranes, they could suffer surface properties modifications that alter nanoparticle's stability even before nanoparticle reaches its targeting site [37].

To circumvent skin and mucous barriers, researchers may use intravascular injection to deliver nanoparticles into blood, and for many tissues, this is the only way to reach the target tissue or organ [184-186]. However, after nanoparticles are administered into bloodstream they have to face a series of hurdles such as

renal and hepatic filtration, mononuclear phagocytic system (MPS) clearance, aggregation with serum proteins, and degradation caused by enzymes [52, 187].

The interaction between nanoparticles and plasma proteins or other blood components is the main reason causing nanoparticle's aggregation or degradation. Among this, opsonization is considered as one of the major modifications [187]. The most common opsonins include immunoglobulins, complement proteins, albumin, lipoproteins and fibrinogen [186].

The mononuclear phagocytic system (MPS) is an important immune component which consists of different types of phagocytic cells, such as macrophages from lymph nodes, macrophages, spleen and other tissues [52, 188]. MPS can protect the body by removing foreign microorganisms like viruses, bacteria and fungi. However, therapeutic nanoparticles and macromolecules can be recognized as foreign material by MPS, and MPS are highly efficient at removing nanocomplexes by initiating several immunological reactions [189].

Nanoparticles can be distributed to various tissues and organs during circulation, thus, leading to clearance at different organs. When they reach the kidney, some nanoparticles and other components from blood will be filtered and secreted into the urine [190], while in liver, they will be secreted into bile and then cleared through the feces [191]. These excretions are related to some physical characteristics of the nanoparticle (size, charge, shape etc.).

There is another physiological barrier that prevents nanoparticle diffusion from blood stream to the target site, which is the vascular endothelial barrier [192]. Because of the properties of endothelial cells and the tight junction between cells,

nanoparticles larger than 5 nm could not readily cross the capillary endothelium, remain in circulation, and then are cleared by other systems. Some tissues like the blood-brain barrier exhibits even more stringent permeability [193], which will be discussed later. Meanwhile, some tissues allow larger molecules up to 200 nm to internalize, such as liver, spleen, and tumors [194].

After nanoparticles leave the bloodstream, then have to cross the extracellular matrix, which consist of polysaccharides and fibrous proteins [195]. This dense network could resist the transport of macromolecules and nanoparticles or even trap them and provide the opportunity for the uptake by macrophages[196]. When nanoparticles reach the cell surface, there are five recognized pathway for internalization: phagocytosis, macropinocytosis, clathrin-mediated, caveolin-mediated, and clathrin/caveolin-independent endocytosis [127, 164, 197]. Then, nanoparticles will be trapped in some vesicles like endosomes or lysosomes, and often results in degradation because of the pH and the enzymes found in the late endosomes (lysosomes)[198].

6. The Blood-brain barrier

From the description above, we know that to reach the target site nanoparticles have to cross several barriers, moreover, there are some physiological barriers which are the most challenging problems for nanoparticle delivery and targeting, and one of those is the BBB. Preliminary studies described BBB as a passive impermeable barrier that separates blood and brain interstitial fluid [199]; later on, further studies proved that BBB is also a dynamic layer which could transport nutrients, proteins, peptides and even immune cells between the blood and the

brain, and the exchange of small molecules is strictly controlled[200]. The widely accepted BBB function is to protect the brain against the entry of noxious agents, and this neurovascular unit is indispensable for the protection of the underlying brain cells and the preservation of the central nervous system (CNS) homeostasis stability [200, 201].

The structure of BBB consists of endothelial cells, astrocytes, pericytes, neurons and the extracellular matrix [202] (Figure 13). The brain endothelial cells are different from peripheral vascular endothelial cells because they have unique and distinguishing properties such as the absence of fenestrations, more extensive tight junctions (TJ) and less vesicular transportation.

The inter-endothelial spaces between cells of the brain vasculature are connected with tight and adherents junctions (AJ). The TJ consist of three transmembrane proteins, claudin, occludin and junction adhesion molecules; these proteins compose the paracellular barrier of TJ, mediate the adhesion between cells, and could regulate the migration of leucocytes and the permeability of BBB [202].

The AJ is comprised by the membrane calcium-dependent protein cadherin, which could form adhesive contacts between cells through binding actin cytoskeleton together via intermediary proteins. TJ and AJ together restrict permeability to cross the BBB endothelium [202].

Astrocyte is a type of neuroglia cell with a star-shaped, which is non-neuronal and acts like support material in brain. The endfeet of astrocytes are closely opposed to the microvascular structures, thereby separating the capillaries and the neurons; astrocytes also play an important role in the maintenance of BBB

phenotype, and directly influence the dynamic circulation of the brain [203]. The space between the endothelium and the astrocytes is called basal lamina [204]; it is embedded with pericytes and filled with collagen, proteoglycans, laminin, fibronectin, and other extracellular matrix molecules. It acts like a barrier to the macromolecules and provides the possibility of cell attachment via integrins [205].

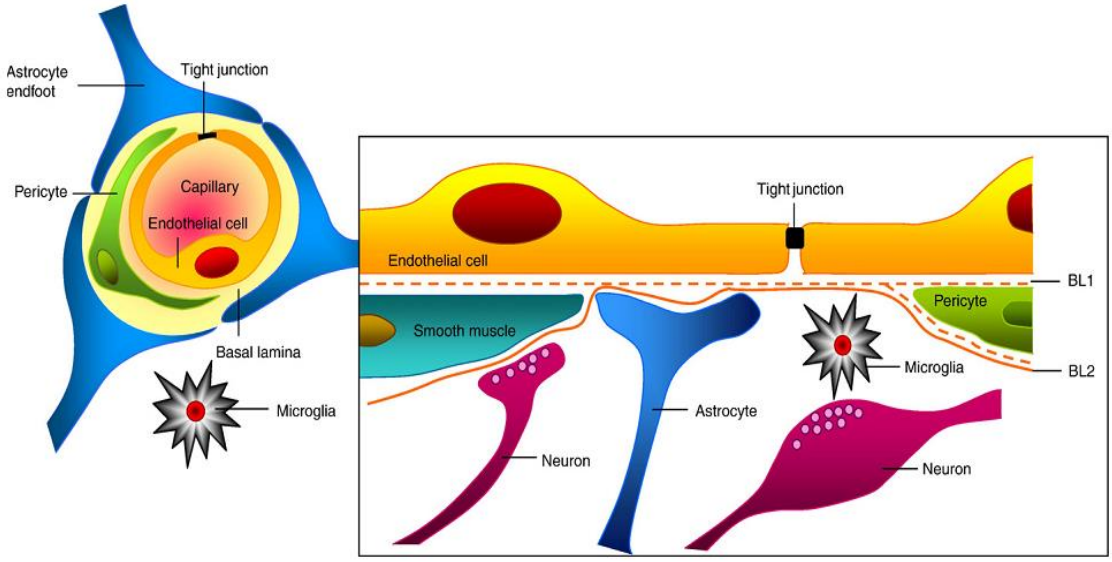

Figure 13: The BBB structure . Adapted from Abbott et al.[206]

6.1 Transportation across BBB

Because of the structure and the characteristics described above, the BBB is 50-100 times tighter than peripheral microcapillaries, it provides a good protection of the brain tissue, and allows lipid-soluble molecules to be transported across the membrane meanwhile hydrophilic solutes only have minimal permeation [36, 207]. However, on the other hand, it also creates severe restrictions for most drugs to be transported from plasma to extracellular space, thus, hinders the delivery of therapeutics inside the brain.

The transportation of substances across the BBB is mainly through three ways: (A) Passive diffusion, the general rule is that the lipid-soluble substances have higher diffusion across the BBB, for example, alcohol, nicotine, and caffeine could dissolve in lipid bilayer of the cell membrane, and then could cross the barrier easily; however, hydrophilic solutes such as penicillin can barely cross the BBB[208]; on the other hand if the hydrogen bond is reduced, the membrane permeability will increase[209]. Smaller substances (oxygen, carbon dioxide, nitric oxide, and water) could diffuse freely across BBB following their concentration gradient. (B) Active transport: substances like glucose, amines, amino acids, nucleoside, monocarboxylates, and small peptides are essential for the brain metabolism, however these substances are hydrophilic and have poor brain endothelium permeability. In brain, such solute substances could bind to specific membrane protein carriers and be transported across BBB along concentration gradients; this transportation is called carrier-mediated transport or active transport and it is independent [35, 210]. (C) Receptor-mediated transport: Endocytosis is an important mechanism to transport large molecules across membrane, however, only few none-specific endocytosis occurs in brain vasculature compared to peripheral capillaries [211](Figure 14). To maintain the brain metabolism of macromolecules such as hormones, growth factors, enzymes, transferrin, insulin and several plasma proteins can cross the BBB by receptor-mediated endocytosis [212-214]; this highly specific endocytosis is energy-dependent, and it explains why there are more mitochondrias in brain endothelial cells than that in peripheral endothelial cells [211].

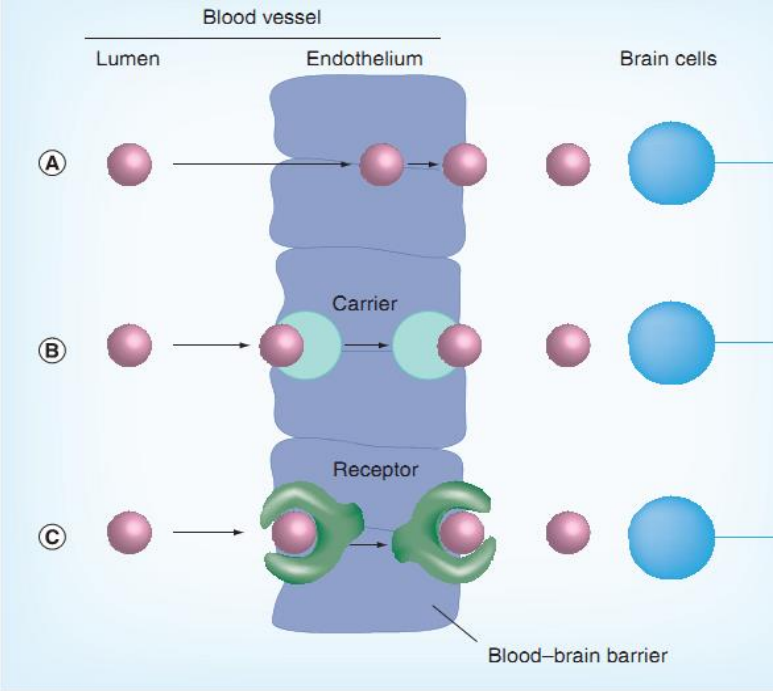

Figure 14: Mechanisms for crossing the BBB (A) Passive diffusion: fat-soluble substances dissolve in the cell membrane and cross the barrier. Water-soluble substances such as penicillin have difficulty in getting through. (B) Active transport: substances that the brain needs such as glucose and amino acids are carried across by special transport proteins. (C) Receptor-mediated transport: molecules link up to receptors on the surface of the brain and are escorted through. Adapted from Jain et al.[215]

6.2 Peptide tags for crossing the BBB

Based on the transport mechanisms of the BBB, many drugs and therapeutics were designed to cross BBB through carrier-mediated or adsorptive-mediated transcytosis, or coated with proteins or peptides to cross the BBB via receptor-mediated transcytosis pathway[216]. The former method is of low efficiency since the CNS endothelial cells (ECs) show a lower rate of transcytosis activity than

peripheral ECs, and this makes this type of nanoparticles to be more easily uptaken by other tissues [216, 217]. Thus, receptor-mediated transcytosis becomes the best option, using receptor-mediated transcytosis pathway to deliver drugs and therapeutics bound to proteins or peptides to cross BBB, and it has been widely adopted in many researches. There are mainly several types of peptides which are widely used: Low density lipoprotein peptides [218-221], transferrin [222-225] and insulin peptides [226-228], because their receptors are highly expressed on the endothelial cells from BBB, and this will make the transportation more specific and efficient.

The low-density lipoprotein (LDL) is a normal blood constituent; its biological function is to deliver cholesterol to the tissues. The corresponding receptor is the LDL-receptor (LDLR), an endocytic receptor which belongs to a varied family and can induce the uptake of cholesterol-rich lipoproteins, and it has been identified as a high affinity binding site for brain capillaries [229, 230]. The most prominent apolipoproteins for binding LDLR are the apolipoproteins B and E (ApoB and ApoE), that can bind to LDLR on the surface of target cell, and induce endocytosis [231-233]. Based on this, some nanoparticles incorporated an ApoB or ApoE derived peptide to deliver drugs and therapeutics into the brain [234, 235]. Another promising peptide named “Angiopep” showed promising ability to cross BBB through LDLR-mediated trancytosis [236]. This peptide derived from the consensus binding sequence (Kunitz domain), can be conjugated to drugs, and it has been already used in ongoing clinical trials for the treatment of brain tumors [237, 238].

Transferrin (TF) and insulin (IF) are large molecules necessary to maintain the CNS normal function; they are also transported to the brain via receptor-mediated transcytosis as these receptors are highly expressed on the brain endothelial cells[224]. Based on this, different research groups developed antibodies to target on TF and IF receptor, with the purpose to increase the transport through the BBB [239-242]. In these experiments, recombinant proteins have two functional moieties; the therapeutic peptide fused to the carboxy terminus of the IgG heavy chain and the complementary determining regions of the monoclonal antibodies that are located at the N-terminus [243].

6.3 Nanoparticles in BBB transportation

In recent years, nanoparticles have widely participated in the delivery of drugs and therapeutics across the BBB for the treatment of different CNS diseases like Alzheimer's disease, stroke, brain tumors, etc. [244, 245]. There are many advantages in the use of nanoparticles to cross the BBB. First, since the BBB only uptakes substances in a narrow size range, nanoparticles could be produced in a suitable size to meet the demand; second, nanoparticles have tunable surface properties, such as morphology and charge, but they can also be coated with BBB-crossing proteins or peptides through receptor-mediated transcytosis pathway, also increasing the specificity and efficiency of drugs, meanwhile, reducing the systemic toxicity. Moreover, nanoparticles would not disturb the barrier, thus, reducing the unnecessary damage. Based on this, many nanoparticles coated with BBB-crossing peptides were generated, and most of the BBB-crossing peptides that have been used target LDLR, transferrin and insulin receptors. For example, liposomes and polymers coated with ApoE-derived peptides could deliver drugs

crossing an in vitro BBB model [246, 247], polymeric nanoparticles such as polybutylcyanoacrylate (PBCA) coated with ApoB and E showed promising permeability crossing the BBB [248], and dendrimers like poly(amidoamine) (PAMAM) were synthesized with transferrin on the surface to enhance BBB transport and improve the drug accumulation in glioma cells[249]. Metal nanoparticles, such as gold and iron nanoparticles are also coated with varied BBB-crossing peptides like transferrin derived peptide, angiopep and insulin derived peptide [250-252].

Protein nanoparticles have increased their popularity as nanocarriers since they are low toxic, biodegradable and none-immunogenic; however, only few protein-based nanoparticles are designed and generated for crossing BBB, like the Human serum albumin (HSA) designed to be coated with transferrin, transferrin antibodies or LDL to transport drugs across the BBB [253]. However, because HSA and transferrin both are large molecules, after the conjugation, the size of nanoparticles is even larger; on the other hand, the BBB crossing process is size depended, molecules with smaller size and molecular weight (600 daltons) are favorable to BBB, large molecules always being blocked by BBB, and that is the reason why only few examples succeed to transport large size protein through the BBB. Among these examples, Schwarze et al could send protein with 120 KDa across BBB, however, the peptide they were using to targeting on BBB is derived from HIV (human immunodeficiency virus), this will bring biosafety problems [254]. Therefore, it is necessary to design efficient, biosafe, biodegradable protein based nanoparticles for drug and therapeutic delivery across the BBB.

7. Overview

Traditional drug delivery systems have many drawbacks, such as low specificity, low efficiency and undesired side-effects. However, with the development of nanomedicine, through the use of chemical or biological entities in the nanosize range, this scenario could be completely changed. In the recent years, a large number of nanoparticles have been developed as delivery systems for treatment and imaging purposes. Many different materials have been involved in nanoparticle design, aiming to improve the therapeutic efficacy and safety. Among those, natural biomolecules such as proteins are an attractive material because they are easy to produce, safer, biocompatible and biodegradable. Moreover, protein nanoparticles provide various possibilities for surface modification such as attachment of drugs and targeting ligands, thus allowing the specific delivery of drugs and therapeutics. The nanoparticle-mediated targeting delivery could be affected by different parameters, being nanoparticle's size one of the most important factors as it also affects the bio-distribution and the internalization of nanoparticles. How targeted proteins self-assemble and therefore how nanoparticle formation will affect specific cell internalization are critical issues that will be addressed in this thesis.

Nanoparticle-mediated targeting delivery is also widely used when overcoming barriers in human body, especially in the BBB. The BBB could maintain the CNS metabolic status by strictly regulating the exchange of substances between the brain and the plasma and it is considered to be the strictest barrier in human body, creating a great obstacle for delivery of drugs and imaging agents to CNS. Nanoparticles could help drugs to cross the BBB because they have suitable size and could exhibit targeting ligands on the surface. These ligands could interact

with receptors at the BBB and then transport nanoparticles across BBB by receptor mediated transcytosis. Based on this principle, in this context, we designed and produced protein based nanoparticles containing low density lipoprotein receptor (LDLR) ligands with the aim to target LDLR, and transport nanoparticles across the BBB.

Objectives

The first part of this study is aimed to deliver protein-based nanoparticles to the brain parenchyma, crossing the BBB. Regarding this, we first focused on the design, production and physico-chemical characterization of protein nanoparticles which contain low density lipoprotein receptor (LDLR) ligands; then, the uptake of protein nanoparticles both in vitro and in vivo models was extensively analyzed. To achieve these, we set the following objectives:

1. To select proper peptides with binding activity to LDLR and to design fusion recombinant proteins taking GFP as scaffold protein, to characterize those proteins as biomaterials.
2. To study cell internalization of protein nanoparticles in $LDLR^+$ and $LDLR^-$ cell lines.
3. To study the BBB permeability to nanoparticles in an in vitro model.
4. To analyze nanoparticle bio-distribution in animal models.

The second part of this thesis is aimed to study the self-assembling and dis-assembling ability of peptide-driven protein nanoparticles, and to analyze how size affects nanoparticle the performance of internalization on cells. With this purpose, protein nanoparticles were treated with high concentration of NaCl to destroy the interactions between proteins releasing the protein monomers, then comparing the internalization of the two forms of the same protein. To reach these goals, we planned the following objectives:

1. To produce CXCR4-targeted proteins with the aim to form nanoparticles
2. To set different conditions to generate either protein nanoparticles or protein monomers.

3. To characterize protein nanoparticles and protein monomers as biomaterials.
4. To compare and analyze the receptor-mediated cell internalization profile of protein nanoparticles and monomers.

Results

Paper 1

Targeting low-density lipoprotein receptors with protein-only nanoparticles

Zhikun Xu, María Virtudes Céspedes, Ugutz Unzueta, Patricia Álamo, Mireia Pesarrodona, Ramón Mangues, Esther Vázquez, Antonio Villaverde, Neus Ferrer-Miralles

Journal of Nanoparticle Research, 2015, 17(3): 1-14.

The aim of this work was to construct self-assembled protein nanoparticles targeting on LDLR (which is a high affinity binding site in brain capillaries), with the purpose of using nanostructured materials as vehicles for the systemic treatment of CNS diseases.

Four different LDLR specific ligands were fused to GFP protein and His tag; among those, only ApoB ligand, was able to promote the formation of protein nanoparticles by intermolecular interactions involving the ApoB ligand and the His tag of a neighboring monomer. This ApoB empowered protein nanoparticle showed higher internalization ability on $LDLR^+$ cells, and higher permeability in BBB in vitro model. However, when tested those proteins displaying LDLR ligands in an *in vivo* model, two proteins which were not able to form nanoparticle accumulated in at short post-administration time points, indicating that the nanoparticulate form is not favoring the accumulation apart from preventing the transient accumulation. This work brings up new concepts of BBB crossing properties by using functional protein nanoparticles.

J Nanopart Res (2015) 17:150
DOI 10.1007/s11051-015-2959-8

RESEARCH PAPER

Targeting low-density lipoprotein receptors with protein-only nanoparticles

Zhikun Xu · María Virtudes Céspedes · Ugutz Unzueta · Patricia Álamo · Mireia Pesarrodona · Ramón Mangues · Esther Vázquez · Antonio Villaverde · Neus Ferrer-Miralles

Received: 15 October 2014 / Accepted: 11 March 2015 / Published online: 20 March 2015

Abstract Low-density lipoprotein receptors (LDLR) are appealing cell surface targets in drug delivery, as they are expressed in the blood–brain barrier (BBB) endothelium and are able to mediate transcytosis of functionalized drugs for molecular therapies of the central nervous system (CNS). On the other hand, brain-targeted drug delivery is currently limited, among others, by the poor availability of biocompatible vehicles, as most of the nanoparticles under development as drug carriers pose severe toxicity issues. In this context, protein nanoparticles offer functional versatility, easy and cost-effective bioproduction, and full biocompatibility. In this study, we have designed and characterized several chimerical proteins containing different LDLR ligands, regarding their ability to bind and internalize target cells and to self-organize as viral mimetic nanoparticles of about 18 nm in diameter. While the self-assembling of LDLR-binding proteins as nanoparticles positively influences cell penetration in vitro, the nanoparticulate architecture might be not favoring BBB crossing in vivo. These findings are discussed in the context of the use of nanostructured materials as vehicles for the systemic treatment of CNS diseases.

Keywords Recombinant protein · Self-assembling · Nanoparticles, LDLR · Cell targeting · BBB · Biomedicine

Introduction

Cell-targeted drug delivery and personalized medicines strongly push toward the development of biocompatible materials adapted to deliver cargo drugs to

Z. Xu · U. Unzueta · M. Pesarrodona · E. Vázquez · A. Villaverde (✉) · N. Ferrer-Miralles (✉)
Institut de Biotecnologia i de Biomedicina, Universitat Autònoma de Barcelona, Bellaterra, 08193 Barcelona, Spain
e-mail: antoni.villaverde@uab.cat

N. Ferrer-Miralles
e-mail: neus.ferrer@uab.cat

Z. Xu · U. Unzueta · M. Pesarrodona · E. Vázquez · A. Villaverde · N. Ferrer-Miralles
Departament de Genètica i de Microbiologia, Universitat Autònoma de Barcelona, Bellaterra, 08193 Barcelona, Spain

Z. Xu · M. V. Céspedes · U. Unzueta · P. Álamo · M. Pesarrodona · R. Mangues · E. Vázquez · A. Villaverde · N. Ferrer-Miralles
CIBER de Bioingeniería, Biomateriales y Nanomedicina (CIBER-BBN), Bellaterra, 08193 Barcelona, Spain

M. V. Céspedes · P. Álamo · R. Mangues
Oncogenesis and Antitumor Drug Group, Biomedical Research Institute Sant Pau (IIB-SantPau), Hospital de la Santa Creu i Sant Pau, C/Sant Antoni Maria Claret, 167, 08025 Barcelona, Spain

specific cell types. A critical point in such design process is the selection of intrinsically non-toxic materials, which while keeping high structural and functional tunability would not induce side effects upon administration. Because of their biodegradability, biocompatibility, and functional and structural plasticity, proteins are highly convenient materials to construct carriers for the delivery of both conventional and emerging drugs (Lohcharoenkal et al. 2014). On the other hand, drug vehicles, apart from exhibiting powerful targeting properties, should overcome the sequential biological barriers encountered previous to reaching the right cell compartment in the target organ. This is compulsory when targeting the central nervous system (CNS) that is protected by the blood–brain barrier (BBB) and by the blood spinal cord barrier (Peluffo et al. 2015). Since in a therapeutic context, local administration into brain is not desirable because of its invasiveness (Lockman et al. 2002), systemic administration is mandatory and empowering drugs to cross the BBB has become a major issue in current pharmacology and nanomedicine (Pardridge 2010). BBB tightly controls the access of molecules and drugs to brain, either by paracellular or transcellular pathways, by using both functional and structural elements addressed to maintain brain homeostasis (Barbu et al. 2009). Hydrophilic and cationic small molecules show some spontaneous penetrability. However, usual chemical drugs and therapeutic proteins cannot cross the BBB or are targets for the efflux pumps acting in the BBB. A nanoparticulate organization of vehicles used for systemic drug delivery increases drug stability and circulation time (Céspedes et al. 2014), what, by preventing renal filtration, offers potential for sustained release of the cargo. Although these and other properties of nanostructured materials are highly desirable, paracellular penetration of nanoparticles targeted to the CNS is assumed to be especially problematical. Functionalization with ligands of hormone receptors or transporters for transcytosis is then mandatory despite the unexpected BBB-crossing activities exhibited by a few polymers used for nanoparticle fabrication and coating [e.g., polysorbate 80 and poly-(ethylene glycol-co-hexadecyl)-cyanoacrylate (Kim et al. 2007; Kreuter et al. 2002)].

A catalog of potential BBB-crossing peptides and proteins for functionalization is available (Van et al. 2012) (http://brainpeps.ugent.be). Among them, ligands binding transferrin, insulin, and low-density lipoprotein receptors (LDLR) have been especially appealing because of their transcytotic properties. LDLR, in particular, are of additional interest as they are overexpressed in several human conditions including lung, stomach, and cervical cancers. Several LDRL protein ligands, namely ApoB (Spencer and Verma 2007); ApoE (Re et al. 2011; Wagner et al. 2012); and Apo A-I (Fioravanti et al. 2012; Kratzer et al. 2007), have been already used to functionalize diverse types of drugs and nanoparticles to allow or enhance BBB crossing. Others, such as Kunitz-derived peptides (Angiopeps), presented in plain protein–drug complexes, have entered clinical trials addressed to brain tumors (Kurzrock et al. 2012). (http://clinicaltrials.gov/ct2/show/NCT01480583?term=ANG1005&rank=6). Although several of these LDLR ligands have proved to be promising, the ideal architecture for the drug–ligand complex to effectively cross the BBB and reach the brain remains to be elucidated. In particular, whether the ligand would be more effective when functionalizing a nanostructured vehicle than when applied in plain ligand–drug complexes remains unsolved, being a critical issue that needs further investigation (Juillerat-Jeanneret 2008).

In the present study, we have selected several peptidic LDLR ligands and explored them as BBB crossers as well as architectonic tags, in protein-only materials with alternative presentations, namely unassembled protein species or protein-only regular nanoparticles. The in vitro and in vivo analyses of cell penetrability, biodistribution, and brain targeting provide new concepts about the BBB-crossing properties of functional protein nanoparticles, and suggest divergent diffusion properties of BBB-targeted nanoparticles when acting in cell culture and upon systemic administration.

Materials and methods

Protein production and purification

Vectors derived from pET-22b and harboring *angiopep-2-GFP-H6*, *seq-1-GFP-H6*, and *apoB-GFP-H6* gene sequences had been designed in-house and constructed by Genscript. These plasmids were transformed into *Escherichia coli* BL21 (DE3) and positive clones selected in the presence of 100 μg/ml

ampicillin. Transformed bacteria were cultured in 750 ml LB (Luria–Bertani, Conda Cat. 1551.00) medium in the presence of 100 μg/ml ampicillin at 37 °C until $OD_{550} = 0.5$, and incubated further overnight at 28 °C with 1 mM isopropyl β-D-1-thiogalactopyranoside (IPTG) to trigger protein production. Bacteria were harvested through centrifugation and resuspended in Tris buffer (20 mM Tris–HCl pH 8.0, 500 mM NaCl, 10 mM Imidazol) in the presence of EDTA-free protease inhibitor (Complete EDTA-Free; Roche).Then, cells were disrupted by a French press (Thermo FA-078A) at 1100 ψ, and the soluble fraction separated from the mixture by centrifugation at 15,000×*g* for 30 min. The insoluble fraction from ApoB-GFP-H6 was stored at −80 °C for further use.

All proteins were purified by His affinity chromatography in an ÄKTA purifier FPLC (GE healthcare). After filtering the soluble fraction, samples were loaded onto HiTrap Chelating HP 1 ml columns (GE healthcare), washed with Tris wash buffer (20 mM Tris–HCl pH 8.0, 500 mM NaCl, and 10 mM Imidazol) and eluted in a lineal gradient with Tris elution buffer (20 mM Tris–HCl pH 8.0, 500 mM NaCl, and 500 mM Imidazol). After purification, corresponding fractions were collected and then dialyzed against carbonate buffer (166 mM $NaHCO_3$, pH 7.4) overnight at 4 °C. Proteins were characterized by mass spectrometry and quantified by Bradford assay. Some of these activities were technically supported by the Protein Production Platform CIBER-BBN/UAB (http://www.ciber-bbn.es/en/programas/89-plataforma-de-produccion-de-proteinas-ppp).

Protein purification from inclusion bodies

The pellet of ApoB-GFP-H6 IBs was washed with water twice, and resuspended with solubilizing buffer (40 mM Tris with 0.2 % *N*-lauroyl sarcosine, pH 8.0) in a ratio 1:40 and incubated for 24 h at room temperature. After that, the sample was centrifuged at 15,000×*g* for 30 min. Resuspended soluble protein from IBs was purified as described above with prior *N*-lauroyl sarcosine removal using a Hitrap QFF ion exchange column (GE healthcare).

Cell culture and flow cytometry

HeLa (ATCC-CCL-2) cells were cultured in DMEM (GIBCO, Rockville, MD) supplemented with 10 % Fetal Calf Serum (GIBCO) at 37 °C and 5 % CO_2. Human umbilical vein endothelial cells (HUVEC) were maintained in M199 (Invitrogen) with 5 % Fetal Calf Serum (FBS) and 1.2 mM L-glutamine, at 37 °C. Cells were incubated with recombinant proteins (1 and 9 μM) for 24 h and further treated with 1 mg/ml trypsin for 15 min to remove non-internalized protein. Then, cells were collected and analyzed on a FACSCanto system (Becton–Dickinson), using a 15 W air-cooled argon-ion laser at 488 nm excitation. GFP fluorescence emission was measured with detector D (530/30 nm band pass filter). In endosomal escape of proteins experiment, chloroquine was added 1 h before adding protein to the cell, and reach a final concentration of 100 μM, after that, cells were incubated with chloroquine and recombinant protein for 24 h, and then treated with the same procedure. For the inhibition assay, HeLa cells cultured in serum-free medium for 24 h (80 % confluence) were exposed to ApoB-GFP-H6IBs (9 μM) protein and simultaneously to increasing concentrations of suramin. After incubation for further 24 h, intracellular fluorescence was determined as described above.

Transmission electron microscopy (TEM)

Purified proteins were diluted to 0.2 mg/ml in dialysis buffer (166 mM $NaHCO_3$, pH 7.4), deposited onto carbon-coated grids for 2 min, stained with uranyl acetate, and observed in a Hitachi H-7000 transmission electron microscope.

Confocal microscopy

HeLa cells were seeded on Mat-Teck culture dishes (Mat Teck Corp., Ashland, MA, USA), and after 24 h, 2 μM of protein was added to cell culture, then it was incubated for another 24 h. The nucleus was stained with Hoechst 33342 (0.2 μg/ml, Molecular Probes) and plasma membrane was stained with CellMask™ Deep Red (2.5 μg/ml, Molecular Probes) for 5 min in darkness. Later, cells were washed with PBS (Sigma-Aldrich Chemie GmbH, Steinheim, Germany). Stained cells were examined using TCS-SP5 confocal laser scanning microscope (Leica Microsystems, Heidelberg, Germany) with a Plan Apo 63×/1.4 (oil HC × PL APO l blue) objective. Hoechst 33342 was excited by a blue diode (405 nm) and detected at the 415–460 nm range. GFP proteins were excited by an

Ar laser (488 nm) and detected at the 525–545 nm range. CellMask was excited by a HeNe laser (633 nm) and detected at the 650–775 nm range. *Z* series were collected at 0.5 μm intervals.

Fluorescence determination and dynamic light scattering (DLS)

All proteins were diluted to 400 μg/ml; then GFP fluorescence was determined by Cary Eclipse Fluorescence Spectrophotometer (Variant) at detection wavelength of 510 nm, by using an excitation wavelength of 450 nm. Volume size distribution of nanoparticles and monomeric GFP fusions were determined by dynamic light scattering at 633 nm (Zetasizer Nano ZS, Malvern Instruments Limited, Malvern, UK).

Cell permeability analysis

Permeability studies were performed at the USEF Drug Screening Platform (http://www.usc.es/en/investigacion/riaidt/usef). Briefly, CaCo2 cells were cultured in DMEM high in glucose supplemented with 10 % FBS, 1 % non-essential amino acids (100×), 1 % L-glutamine, 100 U/ml penicillin, 100 μg/ml streptomycin, 95 % air, and 5 % CO_2 and at 37 °C. The cells (CaCo2, passage 65) were seeded in the apical compartment of a sterile 6-well transwell at a density of 250,000 cells/well in 1.5 ml of medium, and 2.5 ml of fresh medium was then added to the basal compartment. Cells were maintained in this medium for 21 days until complete differentiation (renewing the medium every 2 days). After this time, the medium was changed to HBSS (0.9 mM $CaCl_2$, 0.5 mM $MgCl_2$, and 20 mM HEPES, pH 7.4).

Transepithelial resistance (TEER) measurement was conducted using a Millipore epithelial voltmeter (Millicell-ERS) in a 6-well transwell (Costar). After adding HBSS in both compartments, samples were added in the apical part at different time intervals (0, 30, 60 s, and 20 min) for TEER measurements. To determine protein transport through Caco2, the amount of transported protein was determined by the measurements of fluorescence in basal compartment over time. Experiments were performed in triplicate. Data were expressed as % of initial TEER. The % is calculated based on the formula: % Initial TEER = (TO/TI) × 100, where TO is the TEER observed in the wells with the samples under study and TI is the TEER observed before the addition of samples. The transport was assessed by the apparent permeability (cm/sec), the amount is represented as protein against time, and the slope of the linear fit (Δ amount/Δ time) was used to calculate the apparent permeability (Papp) by the formula: Papp = (Δ amount/Δ time)/($A \times C_0$), where A is the area of the growth surface (4.71 cm^2) and C_0 is the initial concentration (μM) present in the apical compartment.

In vivo model and biodistribution analyses

Five-week-old female Swiss nu/nu mice weighing between 18 and 20 g (Charles River, L-Arbresle, France) and maintained in SPF conditions were used for in vivo studies. All the in vivo procedures were approved by the Hospital de Sant Pau Animal Ethics Committee and performed according to EC directives. Proteins were injected intravenously at a dose of 500 μg/mouse ($n = 3$ mice), control mice was injected with $NaHCO_3$ buffer. At 30 min and 2 h after injection, mice were sacrificed, and brain, kidney, lung, and liver were collected and examined separately for GFP fluorescence in an IVIS Spectrum equipment (Xenogen, France). The ex vivo fluorescent recording of the brain was performed sequentially, first measuring the emission from whole brain and then of sagittal sections to achieve a complete fluorescent signal characterization.

Statistical analyses

Data were analyzed using one-way ANOVA and post hoc Tukey tests.

Results

Three chimerical genes were constructed to produce LDLR-binding recombinant proteins (Table 1), based on the following modular organization; from N- to C-termini, ligand, linker, EGFP, and H6 tail (Fig. 1a). Such organization had been previously proved useful in promoting the spontaneous formation of highly stable fluorescent protein nanoparticles, provided a sufficient positive electrostatic charge is present at the N-terminus of the whole fusion (Céspedes et al. 2014; Unzueta et al. 2012a, b). The ligands selected here were also tested for their ability to promote the

Table 1 Amino acid sequences of protein ligands and known or putative targets

Ligand	Aa sequence	Target	References
Angiopep-2	TFFYGGSRGKRNNFKTEEY	VLDLR	Demeule et al. (2008)
Seq-1	KYLAYPDSVHIW	N/A	Maggie (2011)
ApoB	SSVIDALQYKLEGTTRLTRKRGLKLATALSLSNK**F**VEGS	LDLR	Spencer and Verma (2007)

Bold amino acid letter: first amino acid detected in the short ApoB form in the soluble cell fraction

VLDLR very-low-density lipoprotein receptor, *N/A* not available but a LDLR family member, *LDLR* low-density lipoprotein receptor

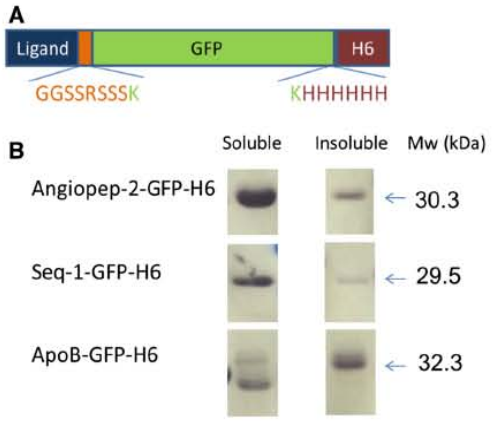

Fig. 1 Structure of the fusion proteins. **a** EGFP was used as the core of the fusions (*green*), flanked by a cell ligand at the N-terminus (*blue*) and a hexahistidine at the C-terminus (*brown*). A linker segment (*orange*) was placed between the ligand and GFP. Residues in *green* indicate the end terminal amino acids of GFP in the joining regions. The sequences of the fused N-terminal ligands are depicted in Table 1. Cationic ligands are expected to promote self-assembling in form of protein-only nanoparticles (Unzueta et al. 2012a, b; Céspedes et al. 2014). **b** Western blot analyses of disrupted bacteria producing the different fusion proteins, upon fractioning. (Color figure online)

assembling of the modular protein into nanoparticles. Angiopep-2 and Seq-1 fusions were produced in *E. coli* as fully soluble versions, while ApoB-GFP-H6 obtained from the soluble cell fraction was partially proteolized. In fact, protein sequencing by Edman degradation procedure of the soluble protein forms revealed loss of the amino-terminal 34-mer peptide of ApoB (Table 1) in approximately 50 % of the protein population (not shown). Then, since the LDLR ligand was lost in this protein fraction, the concentration of this construct was adjusted in further experiments to manage a comparative amount of full-length protein. However, in the insoluble cell fraction, the full length ApoB-GFP-H6 was detected as a unique protein band (Fig. 1b). Mass spectrometry analysis demonstrated that the insoluble protein version showed the predicted molecular mass corresponding to the intact construct. In vitro refolding of ApoB-GFP-H6 IBs rendered homogeneous soluble protein preparations.

In a preliminary screening (Unzueta et al. 2012a, b), Angiopep-2 and Seq-1 were observed as unable to promote the assembling of the fusion proteins in higher order nanoparticles, probably due to their low cationic amino acid content, although doubts remained about the potential influence of the composition of the different buffers used to store the proteins. All the proteins produced here were tested again for nanoparticle formation under homogeneous buffer conditions as described above, in 166 mM $NaHCO_3$, pH 7.4. The exclusive occurrence of unassembled forms of Seq-1-GFP-H6 and Angiopep-2-GFP-H6 was indeed confirmed (Fig. 2a), with a particle size, determined by DLS, compatible with that of GFP monomers or dimers (as GFP naturally tends to dimerization). Contrarily, ApoB-GFP-H6 formed nanoparticles in both its natural soluble form directly obtained from recombinant bacteria (ApoB-GFP-H6s), or when refolded in vitro from IBs (ApoB-GFP-H6IBs) (Fig. 2a). However, ApoB-GFP-H6s nanoparticles appeared to be unstable, as they peaked at 28 nm but also over 100 nm, indicative of aggregation. ApoB-GFP-H6IBs nanoparticles, instead, showed a unique monodisperse peak at 18 nm (Fig. 2a), compatible with the formation of robust supramolecular structures. The aggregation of ApoB-GFP-H6s suspected in DLS measures was clearly confirmed by TEM, since amorphous protein clusters abounded in the fields (Fig. 2b). This was in contrast with the highly regular architecture observed in 18 nm-ApoB-GFP-H6IBs

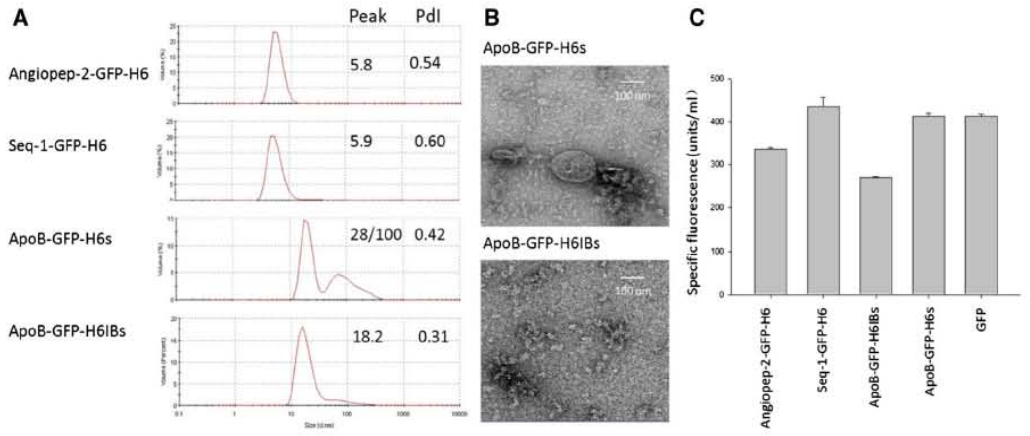

Fig. 2 Characterization of proteins and protein nanoparticles. **a** Size distribution of purified proteins, determined by DLS. Pdi is polydispersion index. **b** TEM analyses of two versions of ApoB-GFP-H6, namely straightforward soluble protein or protein species refolded from IBs. **c** Specific fluorescence emission of all protein versions, compared to that of control GFP

particles (Fig. 2b). Interestingly, all recombinant proteins retained GFP fluorescence (Fig. 2c), with only moderate reduction in the case of Angiopep-2-GFP-H6 and ApoB-GFP-H6IBs. Importantly, the preservation of fluorescence emission allowed further characterization of the constructs' biological properties by fluorescence analysis and imaging.

In this regard, we first wanted to explore cell penetrability of all constructs in cells displaying and not displaying LDLRs. Uptake of protein constructs in $LDLR^-$ HUVEC was indeed negligible when comparing with that of closely related nanoparticles empowered by the unspecific but highly efficient cell penetrating peptide R9 [nine sequential arginines, (Vazquez et al. 2010)] (Fig. 3a). In contrast, penetrability was clearly higher in $LDLR^+$ HeLa cells (Fig. 3b), especially in the case of ApoB-GFP-H6IBs. Although these data already suggested specificity in cell binding and penetration, the LDLR-dependence in the uptake of these particles was further explored using the antibiotic suramin (a symmetrical polysulfonated naphthylamine derivative of urea), a potent inhibitor of LDL–LDLR interactions (Schneider et al. 1982; Nikanjam et al. 2007; Martins et al. 2000), in the internalization assays. As expected, this drug dramatically inhibits the entrance ApoB-GFP-H6IBs into HeLa cells (Fig. 4), thus fully confirming the specific route by which the protein interacts and penetrates cells. In the presence of chloroquine, internalization of ApoB-GFP-H6IBs protein in HeLa cell population dramatically increased (Fig. 5), indicative of an endosomal route as expected for any receptor-mediated uptake (Vazquez et al. 2008). Interestingly, the penetrability of ApoB-GFP-H6s was always lower than that of ApoB-GFP-H6IBs. This fact suggests that an unstable nanoparticle might be less suitable for proper receptor binding and cell internalization. Alternatively, the folding status of the protein (probably different as derived from the soluble cell fraction or from refolding) might influence ligand exposure and/or particle performance in a biologically significant way. The efficient cell penetration of ApoB-GFP-H6IBs was fully confirmed by confocal microscopy (Fig. 6). In general, the unassembled constructs were internalized by cells in a less efficient way, and the uptake was not influenced by background protein precipitation in the extracellular medium that has been generally observed in GFP-based self-assembling proteins (Vazquez et al. 2010).

Considering these cell internalization results, the transepithelial crossing efficiency of the LDLR-ligand functionalized modular proteins was determined in a validated in vitro BBB model based on CaCo2 cells (Hellinger et al. 2012), and the results are presented in Table 2. In the two protein concentrations tested, ApoB-GFP-H6IBs presented the highest penetrability in accordance with the internalization assays presented above (Fig. 3). Angiopep-2-GFP-H6 and Seq-1-

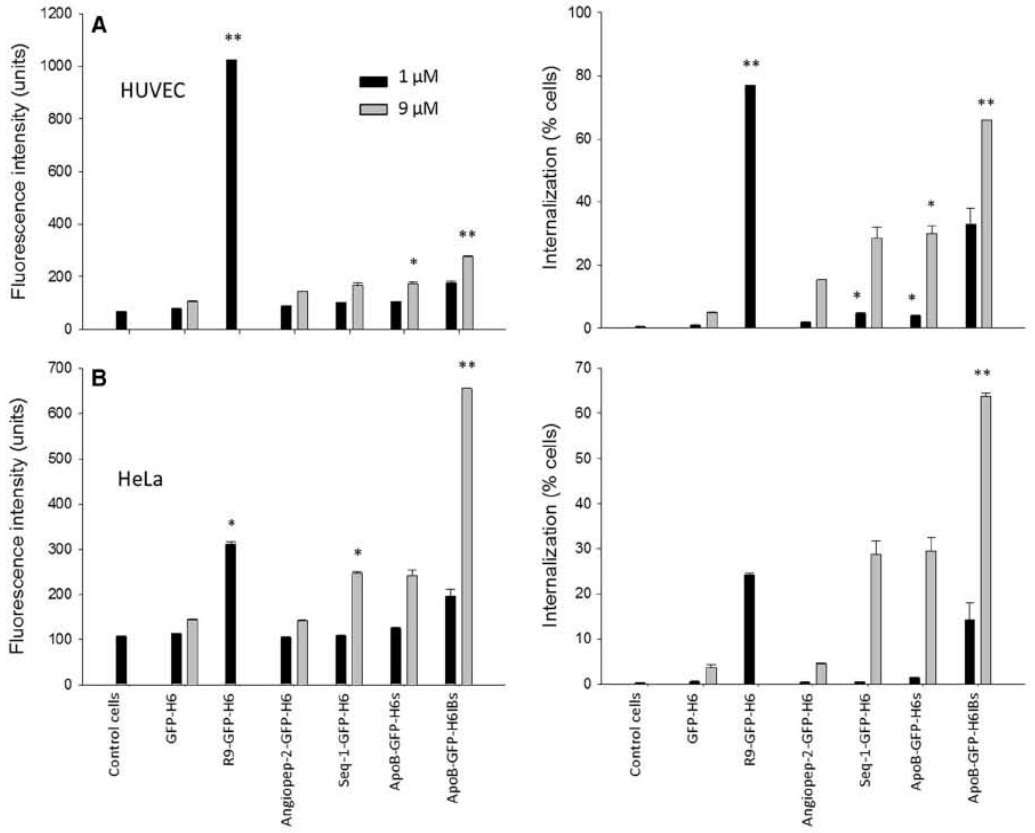

Fig. 3 Internalization of proteins and protein nanoparticles. Cell penetrability was determined by both total fluorescence emission (*left*) and by the fraction of fluorescent cells (*right*). Targets were $LDLR^-$ HUVEC (**a**) and $LDLR^+$ HeLa (**b**) cells. Proteins were added to the cultures at two alterative concentrations, namely 1 and 9 μM. Those proteins showing significant differences with GFP-H6 are labeled with *asterisks* (**$p < 0.01$; *$p < 0.05$)

GFP-H6 also displayed minor but still important penetrability in this BBB model at high protein concentration, thus suggesting a potential to effectively cross the BBB. However, when ApoB-GFP-H6s was challenged to the CaCo2 cell barrier, the apparent permeability was even lower than the negative control GFP, again indicating a failure of these protein nanoparticles to reach a fully functional status. Indeed, the integrity of the CaCo2 monolayer is maintained throughout the experiment since the Papp data of ApoB-GFP-H6s remains low at the two tested protein concentrations.

In a step further, and particularly encouraged by the good performance of ApoB-GFP-H6IBs nanoparticles, we wanted to examine the biodistribution of the protein set and the potential influence of the supramolecular protein organization, upon systemic administration through the tail vein in healthy mice in which side events that affect brain permeability such as enhanced permeability and retention (EPR) effect do not take place. We were specifically interested in this issue as at one side, LDLR are important targets in BBB crossing for drug delivery into the CNS (Demeule et al. 2008; Kim et al. 2007; Spencer and Verma 2007), and also, cationic protein nanoparticles are biocompatible materials that fulfill most of the requests posed for vehicle-mediated drug delivery into brain (Juillerat-Jeanneret 2008). Therefore, we analyzed ex vivo the signal from the whole brain to avoid the noise coming from the background

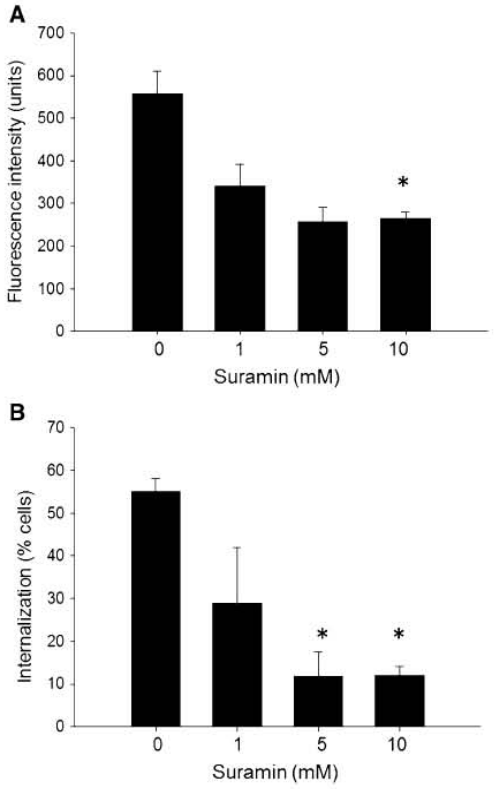

Fig. 4 Specificity in the internalization of protein nanoparticles. Suramin-mediated inhibition of ApoB-GFP-H6IBs (protein concentration at 9 μM, and Suramin concentration at 1, 5, and 10 mM, respectively) penetration in HeLa cells was determined by both total fluorescence emission (**a**) and by the fraction of fluorescent cells (**b**). Significant differences in the uptake in the presence of the inhibitor relative to the protein alone are labeled with *asterisks* (*$p < 0.05$)

of the whole body imaging followed by ex vivo recording of brain sagittal sections to complete evaluation of the extent of the emitted fluorescence. The analyses of these samples clearly indicated BBB-crossing properties of Angiopep-2-GFP-H6 and Seq-1-GFP-H6 (Fig. 7a). Angiopep-2-GFP-H6, in particular, was observed as accumulating in the brain parenchyma 30 min after administration, a fact that was fully assessed by quantitative analysis of fluorescence under conditions that not allowed GFP-H6 background signal (Fig. 7b, c). Surprisingly, not only ApoB-GFP-H6s but also ApoB-GFP-H6IBs failed to accumulate into brain (Fig. 7), indicating that the ApoB ligand, in form of nanoparticles, was unable to promote BBB crossing.

To understand better the stability in circulation and the potential renal clearance of BBB crossing and failing construct variants, GFP fluorescence was also determined in kidney. All the constructs that did not form nanoparticles (namely Angiopep-2-GFP-H6, Seq-1-GFP-H6, and the parental GFP-H6) and also the unstable ApoB-GFP-H6s nanoparticles accumulated in kidney (Fig. 8a, b). This observation strongly suggests renal clearance as it was in agreement with the hydrodynamic size of these materials being under 8 nm, the cut-off for renal filtration (Céspedes et al. 2014). This corresponds to the inability of Angiopep-2-GFP-H6 and Seq-1-GFP-H6 to self-assemble, and it also suggests that the ApoB-GFP-H6s nanoparticles, observed in vitro as unstable, probably disassemble once in the bloodstream (maybe due to the high salt content of the biological fluid). No fluorescence was recorded in lung and liver, in any case (not shown). The renal clearance is expected to dramatically reduce circulation time, what would prevent ligand-containing proteins from reaching their target (or at least, it would largely reduce the opportunities for interaction). This is exemplified by the incapability of a monomeric, T22-empowered IRFP protein to reach CXCR4 + tumoral cells in a colorectal cancer model at detectable levels, being this protein found, instead, in kidney (Céspedes et al. 2014). Contrarily, the assembled version of the same protein accumulated intracellularly in tumor but not in kidney (Céspedes et al. 2014).

These data indicate that a nanoparticulate architecture of ligand-containing proteins, promoting efficient cell penetrability and transcytosis, is neither sufficient nor necessary to reach the brain under systemic administration, and that unassembled soluble proteins, even when undergoing an effective renal clearance, are able to cross the BBB in a significant fraction.

Discussion

Proteins are excellent functional carriers for therapeutic nucleic acids and conventional drugs (Aris and Villaverde 2004; Nehate et al. 2014). When fused to the amino terminus of a His-tagged GFP, the cationic peptide ApoB promotes the formation of nanoparticles that are only composed by the modular protein acting

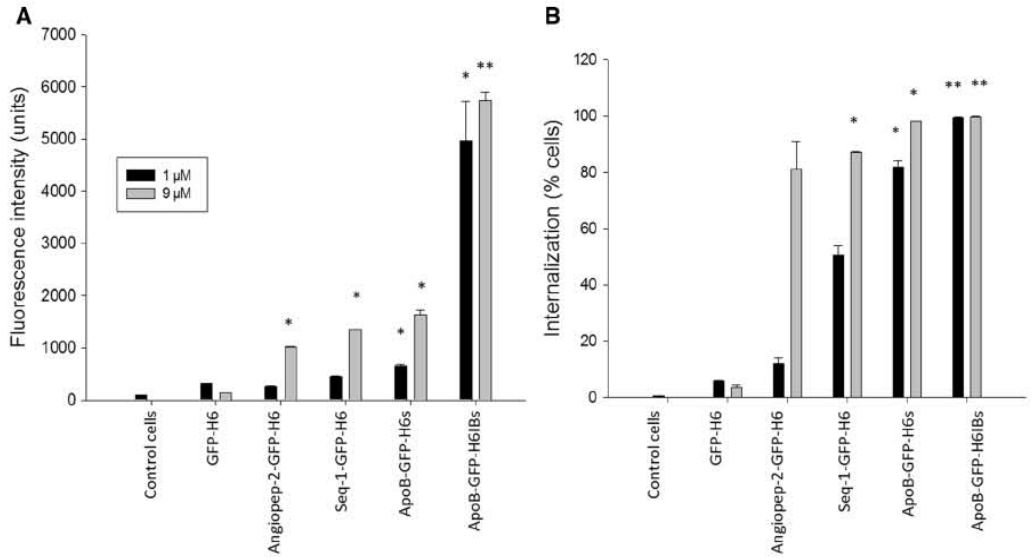

Fig. 5 Endosomal escape of proteins and protein nanoparticles. Cell penetrability was determined by both total fluorescence emission (**a**) and by the fraction of fluorescent cells (**b**). Data have been obtained in LDLR$^+$ HeLa cells in the presence of chloroquine. Those proteins showing significant differences with GFP-H6 are labeled with *asterisks* (**$p < 0.01$; *$p < 0.05$). Note the differences in the Y scale when comparing to Fig. 3

as self-interacting building block. This is based on a recently proposed protein engineering approach that allows designing protein nanoparticles by the fusion of cationic peptides to polyhistidine-tagged polypeptides. The directed formation of protein-only nanoparticles acts irrespective of the nature and sequence of the core protein, since the assembling of several unrelated proteins has been achieved by taking this architectonic principle (Céspedes et al. 2014; Unzueta et al. 2012a, b). Nanoparticle formation is promoted by the electrostatic contacts between the resulting dipolar monomers, but the whole supramolecular structure is largely stabilized by additional forces such as Van der Waals, hydrogen bond interactions (Céspedes et al. 2014; Unzueta et al. 2014), and protein–DNA interactions if used as non-viral gene therapy vehicle (Unzueta et al. 2014). Interestingly, the amino-terminal cationic peptide (ApoB in case of the current study) acts as an architectonic tag but also as a LDLR ligand with known BBB-crossing properties (see Table 1). Under the same conditions, the less cationic Seq-1 and Angiopep-2 peptides, also LDLR ligands, fail in promoting nanoparticle formation (Fig. 2).

On the other hand, ApoB-GFP-H6 nanoparticles have been obtained from two alternative protein sources, namely the soluble *E. coli* cell fraction (ApoB-GFP-H6s) or by in vitro refolding of purified ApoB-GFP-H6 IBs (ApoB-GFP-H6IBs). Although both protein versions act as self-organizing building blocks (Fig. 2), ApoB-GFP-H6s nanoparticles are poorly stable as determined by DLS and by TEM (Fig. 2). Then, the protein was found in kidney soon upon administration (Fig. 8). Renal clearance was also observed in the parental GFP-H6 and in the unassembled Seq-1-GFP-H6 and Angiopep-2-GFP-H6 (Fig. 8). In contrast, the robust ApoB-GFP-H6IBs particles with a regular size of 18 nm were not cleared by kidney, which might enable the construct for a more prolonged and stable circulation in the bloodstream. The time-extended occurrence of ApoB-GFP-H6s in kidney 2 h after administration, not observed in any strictly monomeric protein (namely GFP-H6, Seg-1-GFP-H6, and Angiopep-2-GFP-H6, Fig. 8), could be indicative of a progressive disassembling of the nanoparticles once in the bloodstream, and of a dynamic balance between assembled and disassembled forms. This would favor the hypothesis of ApoB-

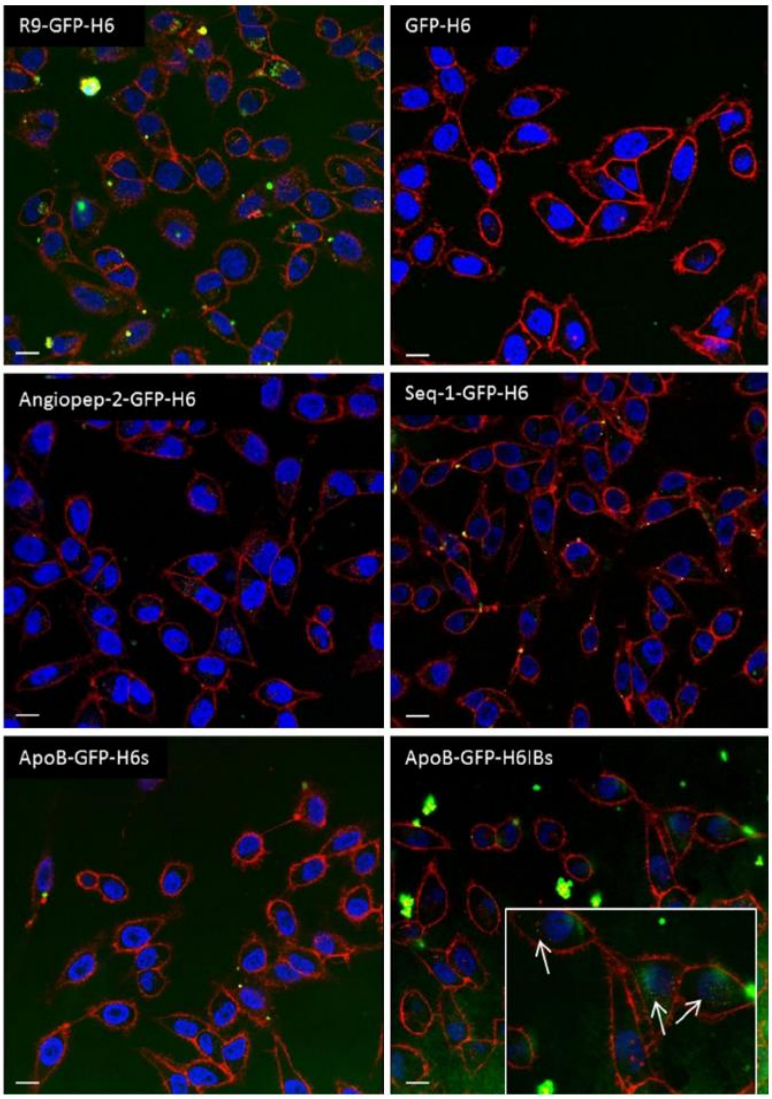

Fig. 6 Internalization of proteins and protein nanoparticles monitored by confocal microscopy in HeLa cells. The *white bars* indicate 15 μm. A magnified inset of ApoB-GFP-H6IBs has been included to stress the nanoparticulate nature of the internalized material (*arrows*), despite some extracellular protein precipitation. Nuclei are labeled in *blue* and cell membranes in *red*. (Color figure online)

GFP-H6s particles being less stable than other related constructs, which like T22-GFP-H6, maintain the multimeric structure in vivo, and completely escape from renal filtration (Céspedes et al. 2014). The differences in the stability of ApoB-GFP-H6IBs and ApoB-GFP-H6s, and also the differential cell penetrability of these constructs (Figs. 3b, 5), can be only attributed to different conformations of the protein as resulting from either the soluble cell fraction or from refolding from protein aggregates. For instance, the ApoB tail in ApoB-GFP-H6s might be more involved in cross-molecular contacts between

Table 2 In vitro transepithelial crossing activity of BBB-targeted GFP proteins

Protein	Concentration (μM)	Papp (cm/s) × 10^{-6}
Angiopep-2-GFP-H6	2	0.41 ± 0.006
	10	16.6 ± 1.5
Seq-1-GFP-H6	2	2.58 ± 0.18
	10	9.75 ± 0.004
ApoB-GFP-H6s	2	0.21 ± 0.09
	10	0.79 ± 0.09
ApoB-GFP-H6lBs	2	12.46 ± 1.03
	10	18.02 ± 4.79
GFP	2	0.69 ± 0.08
	10	2.41 ± 0.44

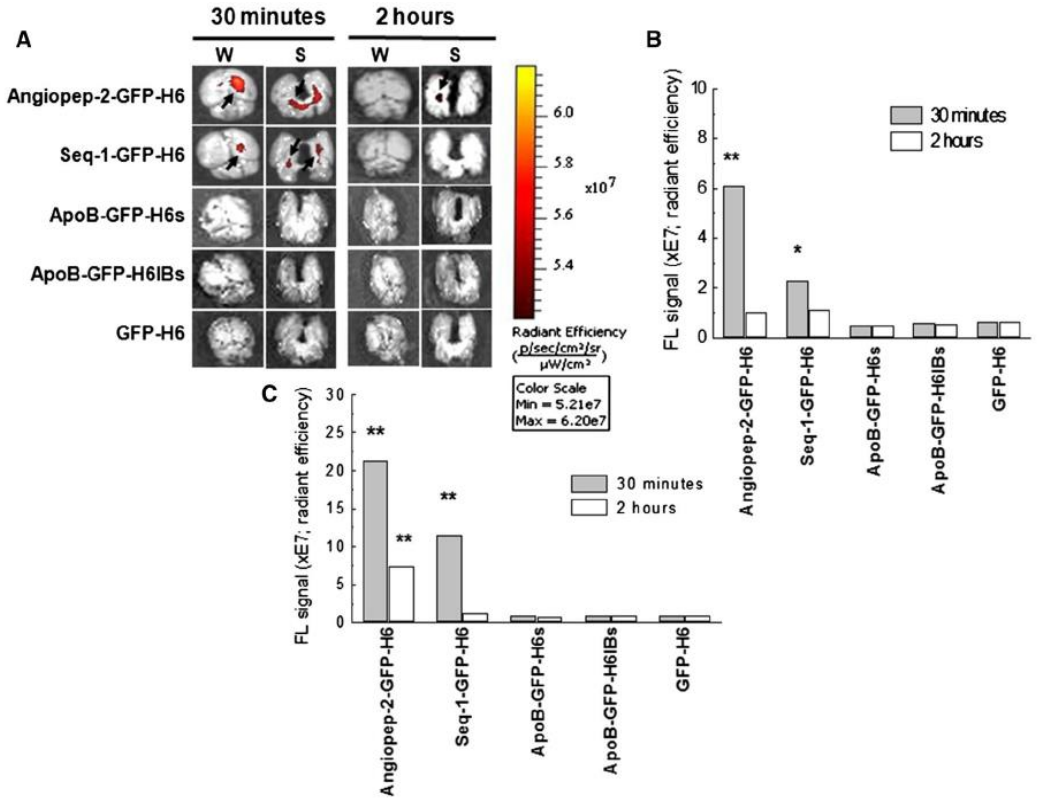

Fig. 7 Biodistribution of proteins and protein nanoparticles in ex vivo imaging. GFP fluorescence registered ex vivo in mouse whole brain (*W*) and sagittal sections (*S*) at 30 min and 2 h after I. V. administration of 500 μg of each protein. *Black arrows* show fluorescence signal accumulation in the brain parenchyma (**a**). Quantitative determination of GFP fluorescence analyzed in whole brain (**b**) and sagittal sections (**c**) expressed as the total radiant efficiency (photon/s/cm2/sr/μW/cm2). Those proteins showing significant differences with the rest of proteins are labeled with *asterisks* (**$p < 0.01$; *$p < 0.05$). Data from 30 min and 2 h samples have been compared separately

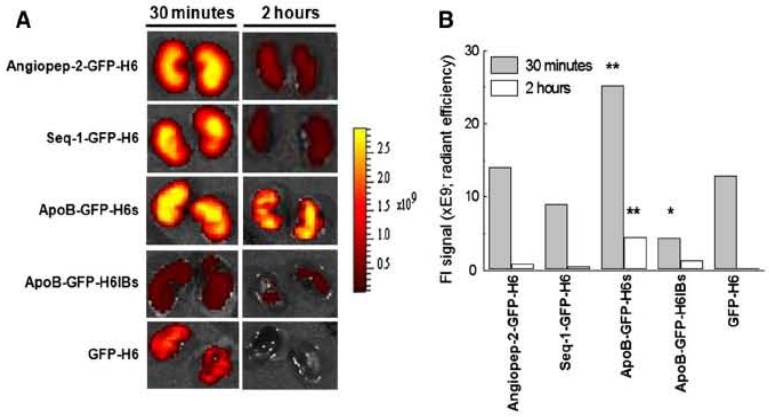

Fig. 8 Renal clearance of protein nanoparticles in ex vivo imaging. GFP fluorescence registered ex vivo in mouse kidneys 30 min and 2 h after I. V. administration of 500 μg of each construct (**a**). Quantitative determination of GFP fluorescence expressed as the total radiant efficiency (photon/s/cm2/sr/μW/cm2) (**b**). Those proteins showing significant differences with the rest of proteins are labeled with *asterisks* (**$p < 0.01$; *$p < 0.05$). Data from 30 min and 2 h samples have been compared separately

building blocks and less available for cellular interactions. Of course, the heterogeneity in protein bands detected in the Western blot analysis of the soluble *E. coli* cell fraction, probably resulting from selective proteolysis (Fig. 1b), could also contribute to this fact. Therefore, the conformational and structural status of protein building blocks of de novo designed nanoparticles, and the influence of the cell factory in the quality and properties of the final supramolecular assemblies are a currently neglected field that deserves deeper exploration (Ferrer-Miralles et al. 2013). This is especially relevant in the context of emerging biomaterials resulting from in vivo fabrication (Vazquez and Villaverde 2013), the rising number of conventional and non-conventional cell factories for protein and polymer production (Corchero et al. 2013; Ferrer-Miralles and Villaverde 2013), and the new bio-engineering strategies to improve microbial biosynthesis regarding industrial and biopharma applications (Chen 2012; Mahalik et al. 2014; Rodriguez-Carmona and Villaverde 2010).

On the other hand, ApoB-GFP-H6IBs nanoparticles internalized cultured cells more efficiently than ApoB-GFP-H6s nanoparticle versions, and also than Seq-1-GFP-H6 and Angiopep-2-GFP-H6 proteins (Figs. 3b, 6). The penetration of ApoB-GFP-H6IBs took place, as expected, in $LDLR^+$ cells but not in $LDLR^-$ cells (Fig. 3a), and it is LDLR-dependent as it was blocked by the inhibitor dug suramin (Fig. 4). The control R9-GFP-H6 nanoparticles, which are empowered by a potent Tat-inspired unspecific cell penetrating peptide (R9), do not show any LDLR-linked preference in internalization (Fig. 3). The LDLR-dependent internalization process (Fig. 4) is dramatically enhanced by chloroquine (Fig. 5), indicative of an endosomal pathway. Under these conditions, ApoB-GFP-H6IBs but no other constructs was essentially found in all cells among the population exposed to the nanoparticle, even when applied at moderate doses (1 μM).

Although based on the good performance in in vitro experiments, ApoB-GFP-H6IBs particles were highly promising regarding BBB crossing, none of the ApoB-derived protein version was found in the brain parenchyma up to 2 h after I. V. administration (Fig. 7). Surprisingly, Seq-1-GFP-H6 and Angiopep-2-GFP-H6 proteins were detected in brain in ex vivo imaging, with an occurrence that peaked at around 30 min. BBB crossing of these two proteins occurred even with important renal uptake (Fig. 8), while skipping renal clearance did not promoted, by itself, brain localization of ApoB-derivatives. The reason for the lack of correlation between kidney uptake and BBB crossing in vivo is not apparent. However, the unexpected complexity of these findings suggests two possible non-exclusive explanations: (1) the existence of differences in the capacity for transcytosis between

epithelial kidney cells and brain endothelial cells, as previously described for a different receptor (Su and Stanley 1998), and (2) the existence of differences in BBB transcytosis specificity among the different LDL family receptors (e.g., LDLR vs. VLDLR), as recently reported (Deane et al. 2008).

Finally, being ApoB a well-known BBB-crossing peptide for soluble drugs (Kreuter et al. 2002) and also when linked to nanoparticles (Kim et al. 2007), failure in a proper activity when empowering protein nanoparticles for endothelial transcytosis in the brain might be due to inappropriate presentation of the ligand in these kind of constructs. In fact, due to its cationic nature, ApoB acts as both architectonic and targeting agent with limited solvent exposure when compared to ligands in monomeric proteins. Although such a dual activity is not by itself an obstacle for proper biodistribution of protein nanoparticles (as exemplified by the peptide T22 in similar GFP-based constructs) (Céspedes et al. 2014; Unzueta et al. 2012a, b) and also for ligand-mediated cell penetrability (Figs. 3, 4, 5), the most complex biological barriers imposed by brain vessels might represent a tighter bottleneck to proper biodistribution.

Conclusions

The results presented here about the exploration of three recombinant protein-only LDLR ligands, presented in a total of four versions, reveal that high cellular penetrability in cultured cells does not guarantee efficient BBB crossing and brain targeting mediated by transcytosis-associated receptors. Interestingly, the protein versions that form nanoparticles do penetrate cultured cells more efficiently than unassembled constructs, while the contrary is true regarding in vivo BBB crossing. Such a divergent performance prompts to carefully evaluate the convenience of using nanoparticulate materials for BBB-crossing therapies, which even being highly efficient in cell culture might find in vivo bottlenecks essentially distinguishable from those encountered when targeting organs other than brain. In addition, our findings suggest possible differences in the transcytosis capacity between epithelial and endothelial cells and among the different LDL receptor family members.

Acknowledgments We are grateful to the Protein Production Platform (CIBER-BBN—UAB) for helpful technical assistance and for protein production and purification services (http://www.ciber-bbn.es/en/programas/89-plataforma-de-produccion-de-proteinas-ppp). We are indebted to FIS PI12/01861, Marató 416/C/2013-2030 and NanoMets to RM, MINECO BIO2013-41019-P to AV, AGAUR (2014SGR-132), and CIBER de Bioingeniería, Biomateriales y Nanomedicina (project NANOPROTHER) for funding our research on protein-based therapeutics. We thank the CIBER-BBN Nanotoxicology Unit for fluorescent in vivo follow-up using the IVIS equipment. We are also indebted to the Cell Culture and Citometry Units of the Servei de Cultius Cel·lulars, Producció d'Anticossos i Citometria (SCAC), and to the Servei de Microscòpia, both at the UAB, and to the Soft Materials Service (ICMAB-CSIC/CIBER-BBN). CIBER-BBN is an initiative funded by the VI National R&D&i Plan 2008–2011, Iniciativa Ingenio 2010, Consolider Program, CIBER Actions and financed by the Instituto de Salud Carlos III with assistance from the European Regional Development Fund. Z. X. and M. P. acknowledge financial support from China Scholarship Council and Universitat Autònoma de Barcelona through pre-doctoral fellowships, respectively. AV received an ICREA ACADEMIA award.

References

Aris A, Villaverde A (2004) Modular protein engineering for non-viral gene therapy. Trends Biotechnol 22:371–377

Barbu E, Molnar E, Tsibouklis J, Gorecki DC (2009) The potential for nanoparticle-based drug delivery to the brain: overcoming the blood–brain barrier. Expert Opin Drug Deliv 6:553–565

Cespedes MV, Unzueta U, Tatkiewicz W, Sanchez-Chardi A, Conchillo-Sole O, Alamo P et al (2014) In vivo architectonic stability of fully de novo designed protein-only nanoparticles. ACS Nano 8(5):4166–4176

Chen GQ (2012) New challenges and opportunities for industrial biotechnology. Microb Cell Fact 11:111

Corchero JL, Gasser B, Resina D, Smith W, Parrilli E, Vazquez F et al (2013) Unconventional microbial systems for the cost-efficient production of high-quality protein therapeutics. Biotechnol Adv 31:140–153

Deane R, Sagare A, Hamm K, Parisi M, Lane S, Beth M et al (2008) apoE isoform-specific disruption of amyloid beta peptide clearance from mouse brain. J Clin Invest 118:4002–4013

Demeule M, Regina A, Che C, Poirier J, Nguyen T, Gabathuler R et al (2008) Identification and design of peptides as a new drug delivery system for the brain. J Pharmacol Exp Ther 324:1064–1072

Ferrer-Miralles N, Villaverde A (2013) Bacterial cell factories for recombinant protein production; expanding the catalogue. Microb Cell Fact 12:113

Ferrer-Miralles N, Rodriguez-Carmona E, Corchero JL, Garcia-Fruitos E, Vazquez E, Villaverde A (2013) Engineering protein self-assembling in protein-based nanomedicines for drug delivery and gene therapy. Crit Rev Biotechnol. doi:10.3109/07388551.2013.833163

Fioravanti J, Medina-Echeverz J, Ardaiz N, Gomar C, Parra-Guillen ZP, Prieto J et al (2012) The fusion protein of IFN-alpha and apolipoprotein A-I crosses the blood–brain barrier by a saturable transport mechanism. J Immunol 188:3988–3992

Hellinger E, Veszelka S, Tóth AE, Walter F, Kittel A, Bakk ML, Tihanyi K, Háda V, Nakagawa S, Duy TD, Niwa M, Deli MA, Vastag M (2012) Comparison of brain capillary endothelial cell-based and epithelial (MDCK-MDR1, Caco-2, and VB-Caco-2) cell-based surrogate blood–brain barrier penetration models. Eur J Pharm Biopharm 82:340–351

Juillerat-Jeanneret L (2008) The targeted delivery of cancer drugs across the blood–brain barrier: chemical modifications of drugs or drug-nanoparticles? Drug Discov Today 13:1099–1106

Kim HR, Andrieux K, Gil S, Taverna M, Chacun H, Desmaele D et al (2007) Translocation of poly(ethylene glycol-co-hexadecyl)cyanoacrylate nanoparticles into rat brain endothelial cells: role of apolipoproteins in receptor-mediated endocytosis. Biomacromolecules 8:793–799

Kratzer I, Wernig K, Panzenboeck U, Bernhart E, Reicher H, Wronski R et al (2007) Apolipoprotein A-I coating of protamine–oligonucleotide nanoparticles increases particle uptake and transcytosis in an in vitro model of the blood–brain barrier. J Control Release 117:301–311

Kreuter J, Shamenkov D, Petrov V, Ramge P, Cychutek K, Koch-Brandt C et al (2002) Apolipoprotein-mediated transport of nanoparticle-bound drugs across the blood–brain barrier. J Drug Target 10:317–325

Kurzrock R, Gabrail N, Chandhasin C, Moulder S, Smith C, Brenner A et al (2012) Safety, pharmacokinetics, and activity of GRN1005, a novel conjugate of angiopep-2, a peptide facilitating brain penetration, and paclitaxel, in patients with advanced solid tumors. Mol Cancer Ther 11:308–316

Lockman PR, Mumper RJ, Khan MA, Allen DD (2002) Nanoparticle technology for drug delivery across the blood–brain barrier. Drug Dev Ind Pharm 28:1–13

Lohcharoenkal W, Wang L, Chen YC, Rojanasakul Y (2014) Protein nanoparticles as drug delivery carriers for cancer therapy. Biomed Res Int 2014. doi:10.1155/2014/180549

Maggie JM (2011) Peptide for transmigration across blood brain barrier and delivery systems comprising the same. United States Patent Application Publication US 2011/0165079 A1

Mahalik S, Sharma AK, Mukherjee KJ (2014) Genome engineering for improved recombinant protein expression in *Escherichia coli*. Microb Cell Fact 13:177

Martins IJ, Hone E, Chi C, Seydel U, Martins RN, Redgrave TG (2000) Relative roles of LDLr and LRP in the metabolism of chylomicron remnants in genetically manipulated mice. J Lipid Res 41:205–213

Nehate C, Jain S, Saneja A, Khare V, Alam N, Dubey R et al (2014) Paclitaxel formulations: challenges and novel delivery options. Curr Drug Deliv 1(6):666–686

Nikanjam M, Gibbs AR, Hunt CA, Budinger TF, Forte TM (2007) Synthetic nano-LDL with paclitaxel oleate as a targeted drug delivery vehicle for glioblastoma multiforme. J Control Release 124:163–171

Pardridge WM (2010) Biopharmaceutical drug targeting to the brain. J Drug Target 18(3):157–167

Peluffo H, Unzueta U, Negro-Demontel ML, Xu Z, Váquez E, Ferrer-Miralles N, Villaverde A (2015) BBB-targeting, protein-based nanomedicines for drug and nucleic acid delivery to the CNS. Biotechnol Adv 33:277–287

Re F, Cambianica I, Sesana S, Salvati E, Cagnotto A, Salmona M et al (2011) Functionalization with ApoE-derived peptides enhances the interaction with brain capillary endothelial cells of nanoliposomes binding amyloid-beta peptide. J Biotechnol 156:341–346

Rodriguez-Carmona E, Villaverde A (2010) Nanostructured bacterial materials for innovative medicines. Trends Microbiol 18:423–430

Schneider WJ, Beisiegel U, Goldstein JL, Brown MS (1982) Purification of the low density lipoprotein receptor, an acidic glycoprotein of 164,000 molecular weight. J Biol Chem 257:2664–2673

Spencer BJ, Verma IM (2007) Targeted delivery of proteins across the blood–brain barrier. Proc Natl Acad Sci USA 104:7594–7599

Su T, Stanley KK (1998) Opposite sorting and transcytosis of the polymeric immunoglobulin receptor in transfected endothelial and epithelial cells. J Cell Sci 111(Pt 9):1197–1206

Unzueta U, Ferrer-Miralles N, Cedano J, Zikung X, Pesarrodona M, Saccardo P et al (2012a) Non-amyloidogenic peptide tags for the regulatable self-assembling of protein-only nanoparticles. Biomaterials 33:8714–8722

Unzueta U, Cespedes MV, Ferrer-Miralles N, Casanova I, Cedano JA, Corchero JL et al (2012b) Intracellular CXCR4 + cell targeting with T22-empowered protein-only nanoparticles. Int J Nanomed 7:4533–4544

Unzueta U, Saccardo P, Domingo-Espin J, Cedano J, Conchillo-Sole O, Garcia-Fruitos E et al (2014) Sheltering DNA in self-organizing, protein-only nano-shells as artificial viruses for gene delivery. Nanomedicine 10:535–541

Van DS, Bronselaer A, Nielandt J, Stalmans S, Wynendaele E, Audenaert K et al (2012) Brainpeps: the blood–brain barrier peptide database. Brain Struct Funct 217:687–718

Vazquez E, Villaverde A (2013) Microbial biofabrication for nanomedicine: biomaterials, nanoparticles and beyond. Nanomedicine (Lond) 8:1895–1898

Vazquez E, Ferrer-Miralles N, Villaverde A (2008) Peptide-assisted traffic engineering for nonviral gene therapy. Drug Discov Today 13:1067–1074

Vazquez E, Roldan M, Diez-Gil C, Unzueta U, Domingo-Espin J, Cedano J et al (2010) Protein nanodisk assembling and intracellular trafficking powered by an arginine-rich (R9) peptide. Nanomedicine (Lond) 5:259–268

Wagner S, Zensi A, Wien SL, Tschickardt SE, Maier W, Vogel T et al (2012) Uptake mechanism of ApoE-modified nanoparticles on brain capillary endothelial cells as a blood–brain barrier model. PLoS One 7(3):e32568

Paper 2

Formulating tumor-homing peptides as regular nanoparticles enhances receptor-mediated cell penetrability

Zhikun Xu, Ugutz Unzueta, Mónica Roldán, Ramón Mangues, Alejandro Sánchez-Chardi, Neus Ferrer-Miralles, Antonio Villaverde, Esther Vázquez

Materials Letters, 2015.

This work is aimed to produce size-controllable protein nanoparticles towards CXCR4 receptor (CXCR4, a cell surface receptor marker associated with metastasis-forming colorectal cancer cells and other human pathologies) expressing cells. In a previous work, a recombinant GFP fused at the N-terminus with the CXCR4 ligand T22 and the Hisx6 tag at the C-terminus was able to self-assemble in protein nanoparticles under defined experimental conditions. In this article, by using a new scaffold protein iRFP to replace GFP, we determined that it could also self-assemble into nanoparticles, showing high penetration into $CXCR4^{+}$ cells. This indicates that the o scaffold protein has neither affect on the formation of nanoparticles, nor on the ligand targeting ability. The force which drives nanoparticle formation mainly is based on electrostatic interactions between protein monomers, and this can be interrupted by the presence of high salt concentration. Moreover, when this T22 empowered nanoparticle is transferred to a high salt concentration buffer, protein naaparticles disassemble into monomers reducing its cell penetrability efficiency, proving again that size and perhaps the multivalency of the protein nanoparticle versus the monovalency of

protein monomers is a key factor in receptor mediated cell targeting and penetration.

Materials Letters 154 (2015) 140–143

Contents lists available at ScienceDirect

Materials Letters

journal homepage: www.elsevier.com/locate/matlet

Formulating tumor-homing peptides as regular nanoparticles enhances receptor-mediated cell penetrability

Zhikun Xu [a,b,c,1], Ugutz Unzueta [c,d,1], Mónica Roldán [e], Ramón Mangues [c,d], Alejandro Sánchez-Chardi [e], Neus Ferrer-Miralles [a,b,c], Antonio Villaverde [a,b,c,*], Esther Vázquez [a,b,c]

[a] Institut de Biotecnologia i de Biomedicina, Universitat Autònoma de Barcelona, Bellaterra, 08193 Barcelona, Spain
[b] Departament de Genètica i de Microbiologia, Universitat Autònoma de Barcelona, Bellaterra, 08193 Barcelona, Spain
[c] CIBER de Bioingeniería, Biomateriales y Nanomedicina (CIBER-BBN), Bellaterra, 08193 Barcelona, Spain
[d] Oncogenesis and Antitumor Drug Group and Nanotoxicology Unit, Biomedical Research Institute Sant Pau (IIB-SantPau), Hospital de la Santa Creu i Sant Pau, C/ Sant Antoni Maria Claret, 167, 08025 Barcelona, Spain
[e] Servei de Microscòpia, Universitat Autònoma de Barcelona, Bellaterra, Barcelona, Spain

ARTICLE INFO

Article history:
Received 8 March 2015
Accepted 10 April 2015
Available online 20 April 2015

Keywords:
Biomaterials
Biomimetic
Nanoparticles
Protein materials

ABSTRACT

Homing peptides are exploited in nanomedicine to functionalize either free drugs or nanostructured materials used as drug carriers. However, the influence of multivalent versus monovalent peptide presentation on the interaction with the receptor and on the consequent intracellular delivery of the associated cargo remains poorly explored. By using a tumor-homing peptide (T22) with regulatable self-assembling properties we have investigated here if its display in a either a monomeric form or as multimeric, self-assembled protein nanoparticles might determine the efficacy of receptor-mediated penetrability into target cells. This has been monitored by using a fluorescent cargo protein (iRFP), which when fused to the homing peptide acts as convenient reporter. The results indicate that the nanoparticulate protein versions are significantly more efficient in mediating receptor-dependent uptake than their unassembled counterparts. These finding stresses an additional benefit of nanostructured materials based on repetitive building blocks, regarding the multivalent presentation of cell ligands that facilitate cell penetration in drug delivery applications.

1. Introduction

Cell targeted drug delivery is expected to result in high concentration levels of drugs in desired cells and tissues, aiming to minimize side effects of chemotherapies and to thereby improve the patient's quality of life. Tumor-homing peptides specifically internalize cancer cells via specific binding to over-expressed cell-surface receptors. Therefore, they have been explored for use as targeting tools in drug delivery, either fused to therapeutic proteins [5], coupled to drugs or therapeutic nucleic acids [2,17], or as functionalizing agents of different types of nanoparticles intended as drug carriers [1,8]. Under the combined development of materials sciences and nanomedicine it is however unclear whether tumor-homing peptides are more effective in promoting passenger drug penetration when formulated as plain molecular preparations or as multimeric presentations on nanoparticulate entities.

Recently, we have developed a new protein engineering principle to construct protein-only nanoparticles for targeted drug and DNA delivery in cancer [12,14,15]. This has been possible through the construction of self-assembling building blocks containing tumor homing peptides, which organized as highly stable nanoscale entities. The size of these constructs (> 8 nm) allow them to escape renal filtration [4], thus exhibiting a convenient biodistribution upon administration and exclusively accumulating in primary tumor and metastatic foci [13]. Among the set of different building blocks generated under this principle, the protein T22-IRFP-H6 exhibits unique assembling properties. In a standard physiological buffer, it organizes as toroidal nanoparticles but in presence of high salt content, the building blocks remain fully disassembled. The possibility to regulate the assembling of T22-IRFP-H6 offers an exceptional opportunity to comparatively explore, in the same molecular species, whether the cell targeting

* Corresponding author at: Institut de Biotecnologia i de Biomedicina, Universitat Autònoma de Barcelona, Bellaterra, 08193 Barcelona, Spain.
E-mail address: Antoni.Villaverde@uab.cat (A. Villaverde).
[1] Equally contributed.

http://dx.doi.org/10.1016/j.matlet.2015.04.055
0167-577X/

and internalization properties of T22, a potent ligand of CXCR4 [13], are influenced by its presentation as either free protein molecules or as regular assembled, protein-only nanoparticles.

2. Materials and methods

Protein production and characterization: T22-IRFP-H6 was produced by standard procedures [4]. After purification, the protein was collected and dialyzed against two alternative buffers: $NaHCO_3$ 166 mM, pH=7.4 and $NaHCO_3$ 166 mM, NaCl 333 mM, pH = 7.8, overnight at 4 °C. Fluorescence emission spectrum was measured at 710 nm, by using a JASCO FP-8000 spectrofluorometer (JASCO, US), with an excitation wavelength of 635 nm. Volume size distribution of nanoparticles and monomeric proteins were determined by dynamic light scattering (DLS, Zetasizer Nano ZS, Malvern Instruments Limited, Malvern, UK), at 633 nm. Size exclusion chromatography (SEC) was done in a calibrated Superdex200 10/300GL (Tricorn) column (GE Healthcare).

Cell culture, flow cytometry and competition assay: HeLa cells (ATCC-CCL-2) were grown on 24 wells plate for 24 h in OptiPRO™ SFM medium (Life technologies) supplemented with 3 mM L-Glutamine. Recombinant proteins were added to each well at a final concentration of 2 μM and further incubated for 24 h. After that, the medium was removed and cells washed with PBS and incubated with 1 mg/ml trypsin for 15 min to remove protein bound to cell surface. Cells were centrifuged at 400g for 5 min to remove trypsin, and collected and resuspended in PBS. Cells were analyzed on a FACSCanto system (Becton Dickinson), using a 15 W air-cooled argon-ion laser at 635 nm excitation. IRFP fluorescence was measured with detector A (780/60 nm band pass filter). For the competition assay, AMD3100 was added 1 h before proteins. Protein internalization was determined 24 h later by flow cytometry.

Confocal microscopy: HeLa cells were cultured on Mat-Teck culture dishes (Mat Teck Corp., Ashland, MA, USA) with serum-free medium for 24 h. Proteins were added with a final concentration of 2 μM. After 24 h, cells were washed with PBS and nuclei and membranes stained with Hoechst 33342 and concanavalin A respectively for 10 min. After washing with PBS complete medium was added and stained cells were examined using a TCS-SP5 confocal laser scanning microscope (Leica Microsystems, Heidelberg, Germany) with a Plan Apo 63 × /1.4 (oil HC × PL APO l blue) objective.

Cryo transmission electron microscopy (CryoTEM): Microdrops of purified proteins (3 μL) were deposited on Quantifoil R1.2/1.3 grids, put in liquid ethane in a Leica EM CPC and immediately placed in a Gatan cryo-transfer specimen holder. Samples were observed in a Jeol JEM 2011 transmission electron microscope, operating at 200 kV and equipped with a CCD Gatan 895 USC 4000 camera.

Field emission scanning electron microscopy (FESEM): Microdrops (5 μl) of protein sample were added to a silicon wafer and air-dried at room temperature. Native structure of samples was observed in a FESEM Zeiss Merlin operating at 2 kV equipped with a high-resolution in-lens secondary electron detector.

3. Results and discussion

Features of protein materials: Upon production in bacteria, T22-IRFP-H6 occurred as an individual molecular species of 38.6 kDa that partially adopted a dimeric form (77.2 kDa) (Fig. 1A), the natural organization of iRFP [6]. Further dialysis in front a physiological buffer or a buffer containing 500 mM salt, did not alter the integrity of the protein (Fig. 1B). However, in low salt buffer, T22-IRFP-H6 organized as supramolecular entities formed by around 10 monomers (Fig. 1C), that were seen as regular nanoparticles of 15 nm by DLS (Fig. 1D). Particle formation was fully confirmed by FESEM (Fig. 1E) and by cryo-TEM (Fig. 1F). No

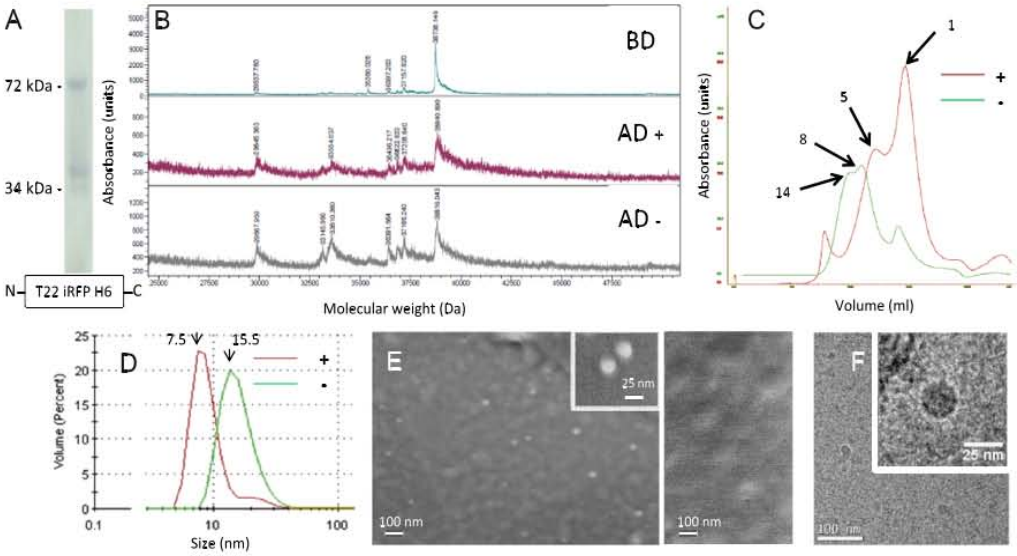

Fig. 1. Characterization of T22-iRFP-H6-based materials. (A) Western blot of purified T22-iRFP-H6 revealed with an anti-His antibody, indicating the molecular weight of markers. At the bottom, scheme of the modular composition of T22-iRFP-H6. (B) Mass spectrometry of purified T22-iRFP-H6 before dialysis (BD), and after dialysis (AD) against low salt (−) and high salt buffers (+). (C) SEC of T22-iRFP-H6 in low salt (green line) and in high salt (red) buffers. Figures indicate the approximate number of monomers forming the plotted structures. (D) DLS plots of the same samples. (E) FESEM images of T22-iRFP-H6 nanoparticles (left) at two magnification levels. No nanoparticles were observed in high salt buffer (right). (F) Cryo-TEM images of T22-iRFP-H6 nanoparticles at two magnification levels. (For interpretation of the references to color in this figure legend, the reader is referred to the web version of this article.)

nanoparticles were observed when T22-IRFP-H6 was dialyzed against high salt buffer (Fig. 1C–E).

Comparative analysis of cellular internalization: Upon approving the robustness of the analytical system we approached the comparative testing of the CXCR4-mediated cell penetrability of free T22-IRFP-H6 protein and T22-IRFP-H6 nanoparticles. We aimed to determine if the nanostructured display of the CXCR4 ligand T22 might significantly influence receptor binding and subsequent cell uptake or contrarily, if such a formulation is irrelevant regarding the performance of the tumor-homing peptide. iRFP constructs, being fully fluorescent [4], are convenient reporters in internalization assays, as free and nanostructured versions of T22-IRFP-H6 showed indistinguishable specific emission values of 13.4 ± 0.14 and 12.8 ± 0.23 U/mg respectively. At the same molar ratio, both forms of T22-IRFP-H6 were internalized into CXCR4$^+$ HeLa cells, while the control, IRFP-H6 remained extracellular (Fig. 2A). However, T22-IRFP-H6 nanoparticles were internalized much more efficiently than T22-IRFP-H6 free protein, and under the same conditions, the amount of protein uptake as nanoparticles doubled that of penetrating target cells as disassembled entities.

Interestingly, the CXCR4 antagonist AMD3100, a very specific and highly potent inhibitor of CXCR4 binding [3,7], blocks the entry of T22-IRFP-H6 nanoparticles more efficiently than that of soluble protein (Fig. 2A). The milder blocking of disassembled protein uptake might be indicative that, not only the cell penetrability of T22 is enhanced by a nanoparticulate formulation but also the specificity of binding to the cell surface receptor. However, very low background binding of free T22-IRFP-H6 to CXCR4$^-$ SW1417 cells was also observed (Fig. 2B), thereby discarding the possibility of a significant interaction of this species to an alternative receptor.

The confocal analysis of CXCR4$^+$ HeLa cells exposed to both protein versions confirmed the enhanced cell penetrability of the nanoparticulate T22-IRFP-H6 isoform (Fig. 2C). This protein version was visualized as discrete intracellular entities found in endosomal vesicles, free in the cytoplasm and perinuclear area (Fig. 2D), and in agreement with the endosome-mediated penetration previously described for T22-empowered polypeptides [4]. Altogether, these results confirm that despite both assembled and disassembled versions of T22-IRFP-H6 internalize target cells via the tumor marker CXCR4, the penetrability of the nanostructured version is clearly higher than that of the free version. This fact is probably related to the multiple presentation of T22 on regular nanoparticles, and to the consequent multivalent receptor binding that enhances endosome formation and penetration [11], as it occurs in natural viruses [9].

4. Conclusions

In summary, we described here an enhanced performance of the tumor-homing peptide T22 as multimeric versus monomeric

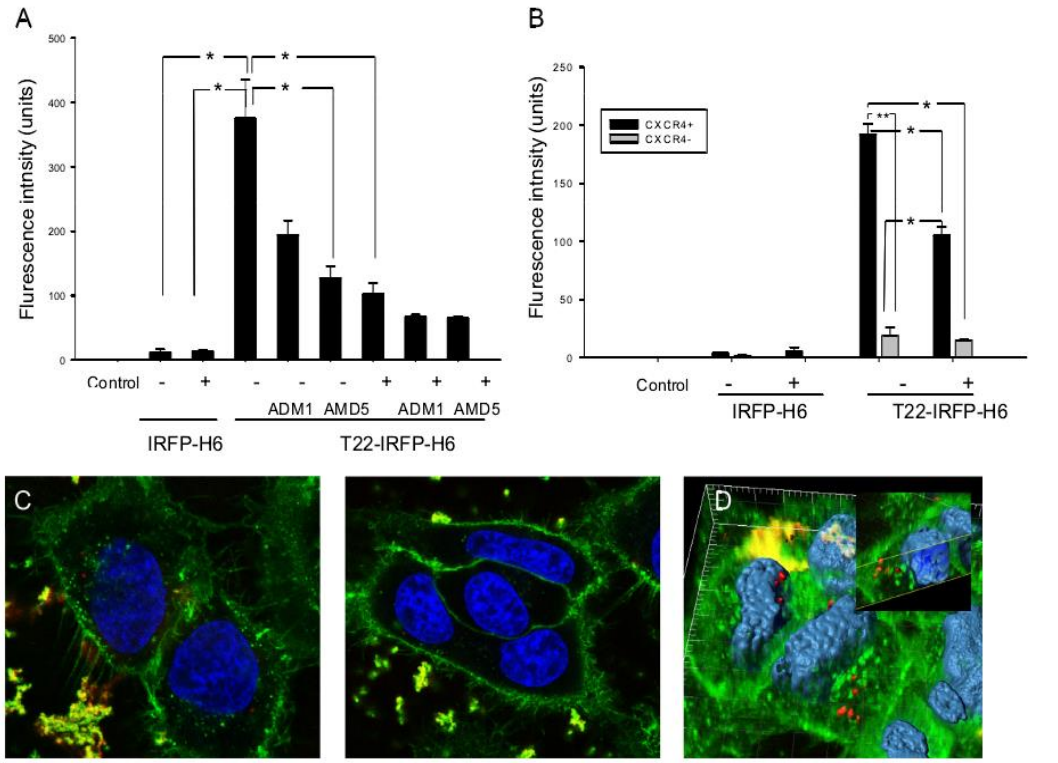

Fig. 2. Determination of CXCR4-mediated cell penetrability of T22-IRFP-H6 under alternative formulations. (A) Internalized fluorescence in CXCR4$^+$ HeLa cells. (B) Penetrability into SW1417 cells overexpressing (black bars) or devoid of (gray bars) CXCR4, proteins being formulated in either low salt buffer (−) or high salt buffer (+). Protein/AMD3100 molar ratios (either 1 or 5) are indicated (AMD1, AMD5). (*), $p < 0.01$; (**), $p < 0.001$, upon One-way ANOVA and a Tukey significance test. (C) Confocal images of CXCR4$^+$ HeLa cells incubated with protein nanoparticles (left) or monomers (right). (D) 3D confocal imaging reconstruction of CXCR4$^+$ cells internalizing nanoparticles. Cell membranes are visualized in green, nucleic acids in blue and iRFP-derived proteins in red. (For interpretation of the references to color in this figure legend, the reader is referred to the web version of this article.)

forms, regarding receptor-mediated cell internalization. This finding stresses the convenience to formulate targeting peptides, used for Trojan horse approaches of molecular medicine, in multivalent material arrangements. Therefore, drug delivery through carrier nanoparticles would profit not only from a higher penetrability, longer circulation time and improved stability compared to free drug versions [16], but they will also offer a convenient platform for the multiple and regular display of homing peptides. Therefore, the "artificial virus" concept in nanomedicine [10] to describe mimetic virus-like vehicles should be extended to cover not only the nanoscale nature of relevant materials, but also their potential to support a multivalent and regular display of cell binding sites in a virus-like pattern.

Acknowledgments

The authors acknowledge the financial support granted to E.V. (PI12/00327) and R.M. (PI12/01861) from FIS, to E.V. (TV32013-133930) and to R.M. and A.V. (TV32013-132031) from La Marató de TV3 (416/C/2013), to A.V. from MINECO (Grant BIO2013-41019-P) and from the Centro de Investigación Biomédica en Red (CIBER) de Bioingeniería, Biomateriales y Nanomedicina (NANOPROTHER and NANOCOMETS projects). We are grateful to the Protein Production Platform (CIBER-BBN-UAB) for protein production and purification services (http://www.ciber-bbn.es/en/programas/89-plataforma-de-produccion-de-proteinas-ppp), to the Servei de Cultius Cel·lulars, Producció d'Anticossos i Citometria (SCAC), to the Servei de Microscòpia, both at the UAB and to the Soft Materials Service (ICMAB-CSIC/CIBER-BBN). Z.X. received a fellowship grant from China Scholarship Council (Grant no. 2011630065) and U.U. from ISCIII. AV received an ICREA ACADEMIA award.

References

[1] Alkilany AM, Boulos SP, Lohse SE, Thompson LB, Murphy CJ. Homing peptide-conjugated gold nanorods: the effect of amino acid sequence display on nanorod uptake and cellular proliferation. Bioconjug Chem 2014;25:1162–71.
[2] Arap W, Pasqualini R, Ruoslahti E. Cancer treatment by targeted drug delivery to tumor vasculature in a mouse model. Science 1998;279:377–80.
[3] Burger JA, Stewart DJ. CXCR4 chemokine receptor antagonists: perspectives in SCLC. Expert Opin Investig Drugs 2009;18:481–90.
[4] Cespedes MV, Unzueta U, Tatkiewicz W, Sanchez-Chardi A, Conchillo-Sole O, Alamo P, et al. In vivo architectonic stability of fully de novo designed protein-only nanoparticles. ACS Nano 2014;8:4166–76.
[5] Cieslewicz M, Tang J, Yu JL, Cao H, Zavaljevski M, Motoyama K, et al. Targeted delivery of proapoptotic peptides to tumor-associated macrophages improves survival. Proc Natl Acad Sci U S A 2013;110:15919–24.
[6] Filonov GS, Piatkevich KD, Ting LM, Zhang J, Kim K, Verkhusha VV. Bright and stable near-infrared fluorescent protein for in vivo imaging. Nat Biotechnol 2011;29:757–61.
[7] Hatse S, Princen K, Bridger G, De CE, Schols D. Chemokine receptor inhibition by AMD3100 is strictly confined to CXCR4. FEBS Lett 2002;527:255–62.
[8] Makela AR, Matilainen H, White DJ, Ruoslahti E, Oker-Blom C. Enhanced baculovirus-mediated transduction of human cancer cells by tumor-homing peptides. J Virol 2006;80:6603–11.
[9] Mammen M, Choi SK, Whitesides GM. Polyvalent interactions in biological systems: implications for design and use of multivalent ligands and inhibitors. Angew Chem Int Ed 1998;37:2754–94.
[10] Mastrobattista E, van der Aa MA, Hennink WE, Crommelin DJ. Artificial viruses: a nanotechnological approach to gene delivery. Nat Rev Drug Discov 2006;5:115–21.
[11] Muro S, Koval M, Muzykantov V. Endothelial endocytic pathways: gates for vascular drug delivery. Curr Vasc Pharmacol 2004;2:281–99.
[12] Pesarrodona M, Ferrer-Miralles N, Unzueta U, Gener P, Tatkiewicz W, Abasolo I, et al. Intracellular targeting of CD44 cells with self-assembling, protein only nanoparticles. Int J Pharm. 2014;473:286–95.
[13] Unzueta U, Cespedes MV, Ferrer-Miralles N, Casanova I, Cedano JA, Corchero JL, et al. Intracellular CXCR4$^+$ cell targeting with T22-empowered protein-only nanoparticles. Int J Nanomed 2012;7:4533–44.
[14] Unzueta U, Ferrer-Miralles N, Cedano J, Zikung X, Pesarrodona M, Saccardo P, et al. Non-amyloidogenic peptide tags for the regulatable self-assembling of protein-only nanoparticles. Biomaterials 2012;33:8714–22.
[15] Unzueta U, Saccardo P, Domingo-Espin J, Cedano J, Conchillo-Sole O, Garcia-Fruitos E, et al. Sheltering DNA in self-organizing, protein-only nano-shells as artificial viruses for gene delivery. Nanomedicine 2014;10:535–41.
[16] Villaverde A. Nanoparticles in translational science and medicine. London: Academic Press (Elsevier); 2011.
[17] Yang W, Luo D, Wang S, Wang R, Chen R, Liu Y, et al. TMTP1, a novel tumor-homing peptide specifically targeting metastasis. Clin Cancer Res 2008;14:5494–502.

Discussion

The major purpose in the design and generation of nanoparticles is to create a new and efficient drug carrier platform for the delivery of therapeutics and imaging agents to specific sites. With this goal, materials of different nature such as lipids, cationic polymers, metals, carbon and proteins have been selected for the production of nanoparticles of different shapes and geometries [255]. Among them, protein-based nanoparticles are attracting increasing attention because they are biodegradable, and biocompatible. Furthermore, this type of nanoparticles have an amenable surface which allows modification and attachment of drugs and targeting ligands [81]. Moreover, proteins could be produced in many different cost-effective platforms. In addition, by genetic engineering, different functions can be incorporated into the same protein.

To produce protein nanoparticles, the common method is to modify already known natural proteins such as albumin, gelatin and elastin by linking them with chemicals like polymers [81], or to generate recombinant proteins finding inspiration in viruses or bacteria [256-259]; selecting those proteins or protein modules that have a tendency to oligomerize into nanoparticles [260, 261]. With these methods, many protein nanoparticles have been generated and are widely used in different biomedical applications such as delivery of drugs and antigen presentation [262, 263]. However, since those nanoparticles are from matured natural protein or viruses, they always lack structural versatility. There is another type of amyloidogenic proteins that can self-assemble into nanoparticles through cross-molecular beta sheet-based interactions, but when those ligands are fused as a tag to other proteins, it always induces protein aggregation [264-266], which is not appropriate for intravenous administration.

To overcome those drawbacks, a new strategy called “rational design protein method” was explored [118, 125]. The rational design protein method is based on the modification or insertion of selected amino acids or domains in a backbone protein to incorporate new and modifiy protein properties. This method offers a good way to construct multi-functional proteins with domains for cell targeting, self-assembling, etc. However, so far, only few successful examples of protein nanoparticle construction and structure modulation have been reported [81, 83, 267, 268]; it is important to develop a new modular platform to generate protein inexpensive and technically reachable multi-functional nanoparticles [131, 269].

Nanoparticles have many medical applications, the most common being the delivery of therapeutics and imaging agents [40, 75, 182] to specific target cells or tissues. The delivery process always includes barrier overcoming, including blood brain-barrier (BBB), one of the strictest barrier in human body, when the intended delivery is to the CNS. The BBB only allows non lipophilic molecules up to 400 Da to freely cross it; this is a huge obstacle for delivery therapeutics and drugs into CNS [202]. However, larger molecular weight proteins such as lipoproteins, insulin, transferrin and leptins are able to cross BBB through a receptor mediated pathway; this provides a viable method for transportation of drugs and therapeutics across BBB [36, 270, 271]. Based on this, proteins or ligands which are able to cross the BBB through receptor mediated transport are decorated on the surface of nanoparticles with the purpose of increasing the efficiency of nanoparticle transportation. The proteins or ligands used to be incorporated in nanoparticles are antibodies against BBB receptors, or special binding domains originated from BBB crossing proteins like lipoproteins, insulin or transferrin [213,

272-274]. However, using antibodies to transport nanoparticles across BBB has some drawbacks, as it usually produces nanoparticles of large size and molecular weight, and those nanoparticles could not be taken by BBB although they showed high affinity to receptors, that because the receptor-mediated transcytosis is size dependent [153]. Meanwhile, the strategy of using ligands to be incorporated in nanoparticles for crossing BBB is showing great potential. Ligands originated from low density lipoproteins like ApoB, ApoE, and Angiopep have shown outstanding performance transporting drugs, therapeutics and nanoparticles across BBB [232, 275-280].

Size plays a very important role not only in nanoparticle biodistribution, but also in the uptake of target cell and toxicity[155]. It has been reported that nanoparticles with a size under 5 nm are easily cleared from our body before they reach the target site, and if the size is too large, over 200 nm, they could not cross the capillaries and then are eventually filtered by kidney [154, 176]. When using materials such as liposomes, polymers, metals or silicon to produce nanoparticles, nanoparticle size is easy to control, and size control methods have been extensively explored [52]. However, the size of protein nanoparticles is not easy to manipulate. This is because natural protein size is determined. With the strategy of rational design, repetitive protein monomeric building blocks could assemble into regular size particles, and this provides the possibility of size control regarding protein nanoparticles.

Our lab has used the rational design method to generate a series of protein nanoparticles. In those studies, GFP was chosen as the backbone or scaffold because it is safer, stable and traceable, then a versatile ligand (R9, T22) at the N-

terminus and a His-tag at the C-terminus were fused to the scaffold protein as architectonic tags; the interactions between the cationic ligand and the His-tag induce the formation of nanoparticles, and provides multi-functions such as self-assembling, cell endocytosis, barrier crossing, and tumor targeting [121, 130-132, 269]. This is a convenient strategy, since with rational design, recombinant proteins could form nanoparticles and exhibit a variety of functions; moreover, it has been demonstrated that the size of those nanoparticles can be controlled by engineering electrostatic protein charge [130].

Based on this background, we aimed to use the rational design method to construct a new protein nanoparticle with a suitable size, presenting BBB receptor binding ligands that could be transported across the BBB through receptor mediated transportation.

First of all, suitable ligands which could bind to the receptor in BBB were carefully selected based on reliable scientific references. We have selected three candidate ligands: Angiopep-2, Seq-1 and ApoB. Angiopep-2 is a ligand derived from the consensus binding sequence (Kunitz domain), exhibiting high transcytosis capacity both in vitro and in vivo, and able to bind pharmaceuticals for the treatment of brain tumors[278, 280-283]. ApoB derived ligand is adapted from amino acids 3371-3409 of human ApoB protein. This peptide has been designed as a gene vector, and when expressed in mouse is able to accumulate in brain [233, 234, 275]. Seq-1 is a peptide whose sequence was obtained by phage-display and has been selected from an US patent; it is a synthetic peptide capable of targeting and transmigration across BBB both in vivo and in vitro [268].

Then, like in previous work, GFP was chosen as the scaffold protein, candidate peptides were fused to the N-terminus of GFP and a His-tag was added to the C-terminus, as shown in figure 15. This design was based on the recently proposed protein engineering principle by our group that predicts the generation of protein nanoparticles by the fusion of cationic peptides to polyhistidine tagged polypeptides [130, 132]. Then, all recombinant proteins were expressed in *E. coli* and purified from the soluble cell fraction. ApoB protein was also obtained from the inclusion bodies of *E. coli* since it was unstable in the soluble cellular fraction. **(Paper1, figure 1)**

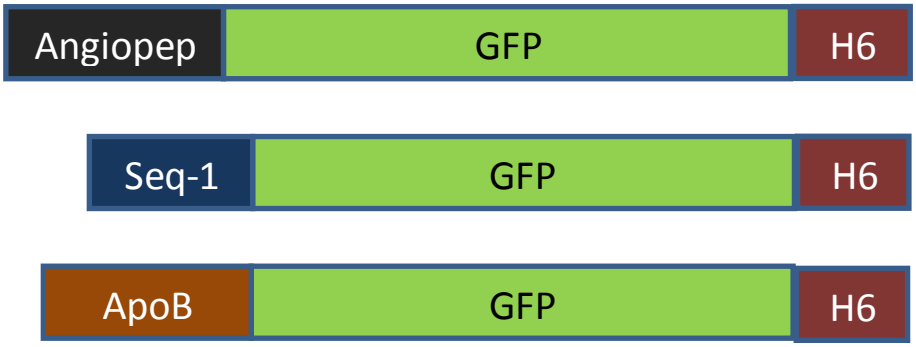

Figure 15: The design of recombinant proteins. From the top: Angiopep-2-GFP-H6, Seq-1-GFP-H6 and ApoB-GFP-H6.

From the Dynamic light scanning (DLS) and Transmission electron microscopy (TEM) results **(paper 1, figure 2)** we found that although all the proteins were GFP-based proteins, different particle sizes were present. Angiopep-2-GFP-H6 and Seq-1-GFP-H6 had a size around 6 nm, similar to GFP monomer, meanwhile, ApoB-GFP-H6s and ApoB-GFP-H6IBs proteins had a larger size around 20 nm.

However, the ApoB-GFP-H6 particles had poor stability as observed by TEM and DLS when compared with soluble protein samples obtained from inclusion bodies and the size is range from 20 nm to 120 nm. These results indicate that ApoB-GFP-H6 could self-organize into nanoparticles. The mechanism behind that is the cationic peptide ApoB which could interact with the polyhistidine tag between dipolar monomers, which induced the nanoparticle formation; moreover, the supramolecular stability was also probably driven by additional forces such as Van der Waals and hydrogen bond interactions [132, 269]. Meanwhile, Seq-1 and Angiopep-2 peptides failed in promoting nanoparticle formation under the same conditions because they are less cationic peptides **(paper1, figure 2)**. These conclusions are consistent with previous findings of architectonic tagging for protein nanoscale construction by using peptide pairs with high content of arginines and lysines [125, 130, 131].

As discussed in the introduction section, nanoparticle size enormously affects the cell targeting and endocytosis. In our experiment, although all the chosen peptides were LDLR ligands and showed promising transcytosis capacity in BBB crossing in previous studies, when fused to GFP and His-tag, the protein exhibited different crossing abilities. At the cellular level, Angiopep-2-GFP-H6, Seq-1-GFP-H6 and ApoB-GFP-H6 proteins showed low internalization ability both in $LDLR^+$ cells and in $LDLR^-$ cells. On the contrary, ApoB-GFP-H6 solubilized from IBs showed higher efficiency of internalization in $LDLR^+$ cells than other proteins **(paper1, figure 3B),** and as expected, the penetration took place in $LDLR^+$ cells but not in $LDLR^-$ cells **(paper1, figure 3A)**. The size of nanoparticles was playing a key role in this internalization assay [166, 174, 284, 285], Angiopep-2-GFP-H6 and Seq-1-GFP-

H6 are monomeric proteins with smaller size around 8 nm; in this format, only one ligand is presented on the surface of each particle, and only can bind one or two receptors; this is not enough to trigger an efficient internalization process. On the other hand, ApoB-GFP-H6 could form larger nanoparticles, displaying more ligands on the surface, and therefore binding more receptors and then leading to the LDL-receptor mediated internalization of nanoparticles **(paper 1, figure 4**). However, when the cells were treated with chloroquine, the internalization was dramatically enhanced, and this is indicative of the use of an endosomal pathway **(paper1, figure 5)**. Furthermore, the permeability of those LDLR-ligand functionalized modular proteins was determined in a validated BBB model in vitro based on CaCo2 cells, and showed consistent results with the cellular experiment, again proving the idea that nanoparticle size is important for cell uptake [272, 273].

In a further step, we tested the biodistribution of those proteins, and whether they could cross BBB through LDLR-mediated transportation, since those proteins were all fused with a LDLR derived ligand. After i.v. injected to mice, Angiopep-2-GFP-H6, Seq-1-GFP-H6 and ApoB-GFP-H6s proteins with a size around 8nm were rapidly cleared by kidney, while ApoB-GFP-H6IBs nanoparticles were not detected in kidney **(paper 1, figure 8)**. This is because small size nanoparticles are easily cleared by the renal system [153, 155, 157]. Although ApoB-GFP-H6s could form nanoparticles, it showed to be quite unstable, and it may disassemble in the blood stream and then be cleared by kidneys. To our surprise, the highly promising BBB-crossing nanoparticle formed by ApoB-GFP-H6 solubilized from IBs failed to accumulate in brain[286], and none ApoB-derived protein version was

found in the brain parenchyma up to two hours after i.v. administration **(paper 1, figure 7)** . Instead of that, Angiopep-2-GFP-H6 and Seq-1-GFP-H6 proteins were detected in brain at 30 min, and then disappeared at 2 h after administration **(paper1, figure 8)**. The failure of ApoB derived nanoparticles might be because the ApoB ligand was present unsuitably on the nanoparticle surface; because ApoB is a cationic peptide and it acts as an architectonic agent in forming nanoparticles, this can possibly limit its solvent exposure when compared to the ligands in monomeric proteins, somehow reducing the ability of targeting. The ability of ApoB to form nanoparticles should not be an obstacle for proper biodistribution (as exemplified by the peptide T22 in similar GFP-based constructs) [131, 132], and for ligand-mediated penetration; the most complex biological barrier imposed by brain vessels might represent a tighter bottleneck for proper biodistribution.

The differences in stability and cell penetrability between ApoB-GFP-H6s and ApoB-GFP-H6 solubilized from IBs nanoparticles are mainly because their different origins, one from the soluble cell fraction, the other from inclusion bodies. For example, the ApoB tail in ApoB-GFP-H6s is favorable in cross-molecular contacts between building blocks and less available for cellular interactions. And the Western blot result showed that selective proteolysis was occurred in the soluble *E. coli* cell fraction (**paper1, figure 1B**), and proteins from inclusion bodies were not affected. Thus, the status of protein conformation and structure in *de novo* designed nanoparticles, and how cell factory affects the quality and the properties of final supramolecular assemblies still remains under study and deserves deeper exploration [267, 287]. This is closely related to the

improvement of conventional cell factories for protein and peptide production and the rising number of new strategies for microbial biosynthesis regarding industrial and biopharmaceutical applications [288].

Protein nanoparticle size control and cell penetration

As described above, nanoparticle size is quite critical not only in cell penetration, but also in biodistribution [165, 176, 289]. When materials such as liposomes, polymers, silicon or metals were used to produce nanoparticles, the size of those nanoparticles have been predefined, and the fine fabrication procedures are mainly chemical or mechanical [161, 174]. The size of proteins is also predictable when using protein material such as albumin, gelatin or GFP protein since the size of those proteins have already been determined [81, 191]; however, when referred to self-assembled protein nanoparticles, size is still not fully controlled. That is mainly because the mechanisms which direct the formation of nanoparticles are still unclear. In previous studies, our laboratory has built a system to construct protein nanoparticles by the use of peptide pairs consisting of a cationic peptide and a His-tag; this provides a suited platform to study the mechanism of protein nanoparticle formation, thus achieving the protein nanoparticle size control [131, 132, 269].

T22 is a cationic peptide derived from polyphemusin II from the horseshoe crab that has shown specific binding to CXCR4 receptor [290, 291], and it has been adopted to form protein nanoparticles using *de novo* rational design method [131]. This T22-empowered nanoparticle showed excellent CXCR4-dependent cell internalization in metastasis-forming CXCR4+ cancer stem cells. The protein

nanoparticle design was based on the concept of rational assembling of repetitive monomeric building blocks driven by the interaction between a cationic peptide and a His-tag, and when changed for another cationic peptide R9 [125], it did not disturb the formation of protein nanoparticles, thus, proving that this is a reliable method. To further prove this concept, instead of changing the N-terminal peptide, we changed the scaffold protein, to check if this platform is or not dependent on the scaffold protein but on the N- and C- terminus pair.

As discussed above, we used iRFP which is a dimeric fluorescent protein to replace GFP protein [292], and fused T22 peptide to the N-terminal and His-tag to the C-terminal **(paper2, figure 1A)**. As expected, nanoparticles with a size around 15 nm were formed in a low salt buffer, because of the interaction between the T22 cationic peptide and the His-tag, leading to the self-assembling of repetitive proteins **(paper2, figure 1D)**. There are many forces that may induce the formation of protein nanoparticles, including Van der Waals, hydrogen bond, and electrostatic interactions [130, 132]. In order to study which forces were driving the formation of protein nanoparticles, T22-iRFP-H6 protein was dialyzed in a buffer containing high concentration of NaCl. The results showed that the T22-iRFP-H6 nanoparticles where not stable at high concentration of salt, and they disassembled into protein dimers with a size around 8 nm **(paper2, figure 1D)**, indicating that dimer self-assembling was mainly governed by electrostatic interactions.

The T22-iRFP-H6 protein nanoparticles also showed promising cell internalization ability toward $CXCR4^+$ cell line **(paper 2, figure 2A, 2B)**, which means T22 ligand triggered this receptor mediated cell internalization. By contrast, T22-iRFP-H6

monomer had a lower cell penetration ability, which again, proved that size is a key parameter in receptor-mediated cell uptake of nanoparticles. However, when compared with previous T22-GFP-H6 nanoparticles, the internalization ability of T22-iRFP-H6 nanoparticle declined. That could be because iRFP protein is a dimeric fluorescent protein, and the formation of iRFP based nanoparticles is different from the GFP based nanoparticles, affecting then the exposure of the T22 ligand, thus lowering its internalization ability.

Conclusions

1. Multifunctional GFP proteins fused to LDLR ligands (name the ligands here) s and polyhistidine tag were produced by using rational design method.
2. Physico-chemical characterization of those GFP variants corroborate the previously described principle that predicts that cationic architectonic tag pairs (cationic peptide and polyhistidine) can induce the formation of protein nanoparticles.
3. The formation of protein nanoparticles is mainly driven by electrostatic interactions between protein monomers.
4. ApoB-GFP-H6 protein purification from inclusion bodies helps to increase the stability only of this protein nanoparticles.
5. Protein nanoparticles containing the ApoB ligand are efficient in targeting and in internalization into $LDLR^{+}$ cells, and this has been proven to be an independent event.
6. ApoB empowered protein nanoparticles showed higher permeability in BBB vitro model than monomeric Seq-1 and Angiopeps containing proteins.
7. Nanoparticle size is a critical parameter in LDLR mediated cell targeting and internalization.
8. T22 is an efficient tag for $CXCR4^{+}$ receptor mediated targeting and penetration irrespective of the scaffold protein.
9. Replacing scaffold protein GFP to iRFP protein does not affect the interaction between cationic protein T22 and polyhistidine, thus has no effect on the formation of protein nanoparticles.
10. High concentration of NaCl can disrupt the interaction between protein monomers, leading to the disassembling of protein nanoparticles.

11. T22 monomer protein has lower receptor targeting ability and penetrability than its nanoparticulate counterpart.

Annex

Annex 1

BBB-targeting, protein-based nanomedicines for drug and nucleic acid delivery to the CNS

Hugo Peluffo, Ugutz Unzueta, María Luciana Negro-Demontel, Zhikun Xu, Esther Váquez, Neus Ferrer-Miralles, Antonio Villaverde

Biotechnology advances, 2015, 33(2): 277-287.

Biotechnology Advances 33 (2015) 277–287

Contents lists available at ScienceDirect

Biotechnology Advances

journal homepage: www.elsevier.com/locate/biotechadv

Research review paper

BBB-targeting, protein-based nanomedicines for drug and nucleic acid delivery to the CNS

Hugo Peluffo [a,b], Ugutz Unzueta [c,d,e], María Luciana Negro-Demontel [a,b], Zhikun Xu [c,d,e], Esther Vázquez [c,d,e], Neus Ferrer-Miralles [c,d,e,*], Antonio Villaverde [c,d,e,**]

[a] Neuroinflammation Gene Therapy Laboratory, Institut Pasteur de Montevideo, Montevideo, Uruguay
[b] Departamento de Histología y Embriología, Facultad de Medicina, Universidad de la República (UDELAR), Montevideo, Uruguay
[c] Institut de Biotecnologia i de Biomedicina, Universitat Autònoma de Barcelona, Bellaterra, 08193 Barcelona, Spain
[d] Department de Genètica i de Microbiologia, Universitat Autònoma de Barcelona, Bellaterra, 08193 Barcelona, Spain
[e] CIBER en Bioingeniería, Biomateriales y Nanomedicina (CIBER-BBN), Bellaterra, 08193 Barcelona, Spain

ARTICLE INFO

Article history:
Received 23 February 2014
Received in revised form 14 January 2015
Accepted 9 February 2015
Available online 16 February 2015

Keywords:
Nanoparticles
BBB
Protein engineering
Recombinant proteins
Artificial viruses
Drug delivery
Gene therapy

ABSTRACT

The increasing incidence of diseases affecting the central nervous system (CNS) demands the urgent development of efficient drugs. While many of these medicines are already available, the Blood Brain Barrier and to a lesser extent, the Blood Spinal Cord Barrier pose physical and biological limitations to their diffusion to reach target tissues. Therefore, efforts are needed not only to address drug development but specially to design suitable vehicles for delivery into the CNS through systemic administration. In the context of the functional and structural versatility of proteins, recent advances in their biological fabrication and a better comprehension of the physiology of the CNS offer a plethora of opportunities for the construction and tailoring of plain nanoconjugates and of more complex nanosized vehicles able to cross these barriers. We revise here how the engineering of functional proteins offers drug delivery tools for specific CNS diseases and more transversally, how proteins can be engineered into smart nanoparticles or 'artificial viruses' to afford therapeutic requirements through alternative administration routes.

Contents

1. Introduction

The maintenance of the central nervous system (CNS) homeostasis is essential for its normal function. The limits of the CNS tissue are

* Correspondence to: N. Ferrer-Miralles, Department de Genètica i de Microbiologia, Universitat Autònoma de Barcelona, Bellaterra, 08193 Barcelona, Spain. ** Correspondence to: A. Villaverde, Institut de Biotecnologia i de Biomedicina, Universitat Autònoma de Barcelona, Bellaterra, 08193 Barcelona, Spain.

http://dx.doi.org/10.1016/j.biotechadv.2015.02.004
0734-9750/

established by the astrocytic glia limitans facing the meninges and the blood vessels, and by the ependymocytes of the choroid plexus where the cerebrospinal fluid is produced (Fig. 1A). Astrocyte end-feet wrap the meningeal fibroblasts and the endothelial cells (ECs) of the capillaries, leaving between them the basement membrane. Brain capillaries display a large surface area (~20 m^2 per 1.3 kg brain), and thus possess a predominant role in regulating the brain microenvironment. The blood–brain-barrier (BBB) limits the entry of blood-derived molecules and circulating leukocytes, protecting the CNS from fluctuations in plasma compositions or circulating agents such as neurotransmitters and xenobiotics. It is composed of specialized ECs held together by multiprotein complexes known as tight junctions, astrocytes, pericytes and basement membrane (Abbott et al., 2006; Reese and Karnovsky, 1967) (Fig. 1B). CNS ECs display more efficient cell-to-cell tight junctions than other ECs (Wolburg and Lippoldt, 2002), rest on a continuous basement membrane and express a series of transporters responsible for the regulated exchange of nutrients and toxic products. These characteristics make the CNS ECs a continuous and selective physical barrier for hydrophilic substances, and a key player in the regulated trafficking of molecules into the CNS (Abbott et al., 2006) (Fig. 2). Interestingly, the Blood Spinal Cord Barrier (BSCB) displays similarities to the BBB, but it also has some unique properties, among them being slightly more permeable (Bartanusz et al., 2011). Transit restrictions imposed by the BBB (and at lesser extent by BSCB) represent the most important barrier to overcome in the drug delivery to the CNS. In the context of emerging neurological diseases, targeting drugs to the CNS is under strong pushing demands, but vehicles for BBB crossing are still in their infancy, with a long run until full tailoring.

2. Cross-transportation through BBB

The BBB gradually develops in humans during the first postnatal year (Adinolfi, 1979) and it's nearly complete in rats after the second postnatal week (Stewart and Hayakawa, 1987). This highly differentiated EC phenotype is induced and maintained in the long term by interactions with the surrounding cells, mainly astrocytes and pericytes but also perivascular macrophages and even neurons (Abbott et al., 2006; Alvarez et al., 2011; Arthur et al., 1987; Janzer and Raff, 1987). For instance, in vivo, astrocytes secrete Sonic Hedgehog (Shh), that will act on endothelial cells and promote BBB integrity (Alvarez et al., 2011). In addition to the role in long-term barrier induction and maintenance, astrocytes and other cells can release chemical factors that modulate local endothelial permeability over a time-scale of seconds to minutes. Thus, both natural stimuli for BBB leakage and pharmacological compounds acting on endogenous BBB induction pathways like Shh inhibitors (Alvarez et al., 2011) can be used to transiently increase the entrance of molecules into the CNS parenchyma. Moreover, the phenotypical characteristics of the BBB ECs include both uptake mechanisms (e.g. GLUT-1 glucose carrier, L1 amino acid transporter, transferrin receptor) and efflux transporters (e.g. P-glycoprotein), and thus transporter/receptor-mediated transit across the BBB has also been used to deliver molecules of pharmacological interest into the CNS parenchyma (Fig. 2). In this case, specific transcellular receptor-mediated transcytosis transports molecules from the luminal membrane, lining the internal surface of the vessels, to the abluminal membrane on the external CNS-lining surface. In addition, less specific adsorptive-mediated transcytosis can also be used for the delivery of molecules, but CNS ECs show a lower rate of transcytosis activity than peripheral ECs (Rubin and Staddon, 1999), making this a less efficient process for the incorporation of circulating molecules.

A final consideration regarding potential limiting steps for the delivery of hydrophilic substances into the CNS across the BBB is that both intracellular and extracellular enzymes provide an additional barrier. Extracellular enzymes such as peptidases and nucleotidases are capable of metabolizing peptides and ATP respectively. Intracellular enzymes, that are involved in hepatic drug metabolism, have been found in the

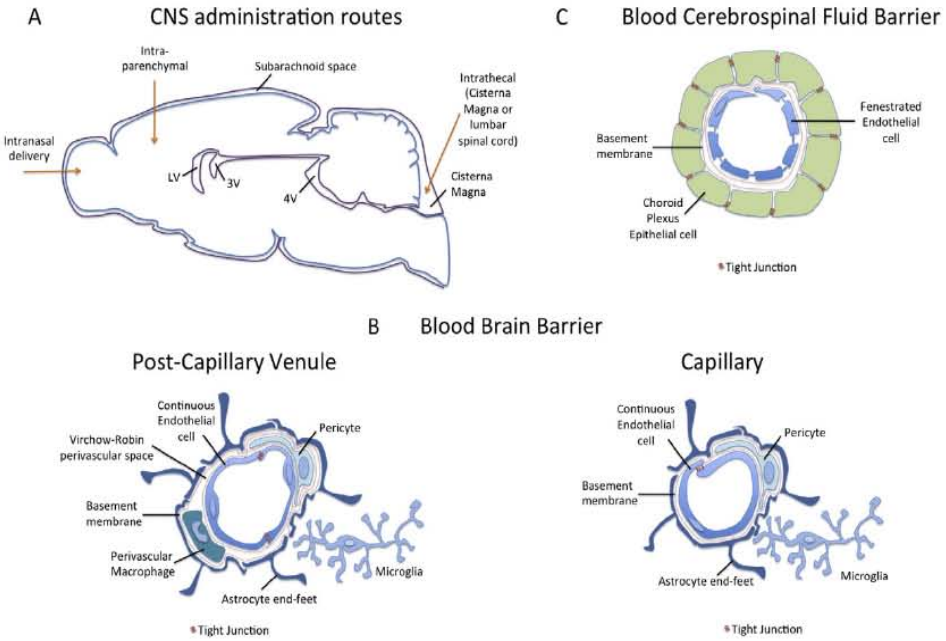

Fig. 1. Anatomical basis of the BBB. Boundaries of the CNS tissue contacting the blood vessels, meninges and the cerebrospinal fluid are depicted (A), and also alternative routes for administration of substances to the CNS to bypass the BBB. The intimate relationship between ECs, continuous basement membrane, astrocytes, pericytes and perivascular macrophages contributing to various degrees to the BBB formation and maintenance can be observed (B). Moreover, ependymocytes of the choroid plexus produce the cerebrospinal fluid and conform, in addition, the Blood Cerebrospinal Fluid Barrier (BCFB) (C).

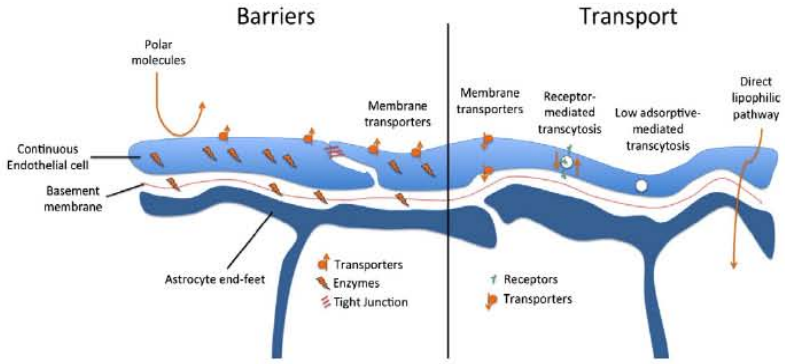

Fig. 2. Main barriers and transport mechanisms of the BBB. Physical barriers as endothelial cell membranes or intercellular tight junctions are the principal obstacles to overcome for polar macromolecules to enter the CNS (left). Moreover, intracellular and extracellular enzymes, basal membrane and astrocyte endfeet can also constitute additional barriers. Endogenous protein mediated selective transport mechanisms for small polar substances and macromolecules are responsible for the communication of the CNS with the blood flow (right). These can be exploited for targeted delivery of different types of nanocomplexes.

small microvessels from the brain, the choroid plexuses, and the leptomeninges (pia plus arachnoid mater), such as monoamine oxidase and cytochrome P450, and they can inactivate many lipophilic neuroactive and toxic compounds (el-Bacha and Minn, 1999).

The delivery of substances across the Blood Cerebrospinal Fluid Barrier (BCFB) may also be considered as an interesting option. This barrier shows a morphological correlate with the BBB at the level of tight junctions between the cells. These, however, are not located at the EC capillaries that are in fact fenestrated (Fig. 1C), but on the apical surface of the epithelial cells of the choroid plexus and the arachnoid fibroblasts along the blood vessels, inhibiting paracellular diffusion of hydrophilic molecules across this barrier. When a substance reaches the cerebrospinal fluid it can diffuse through the Virchow–Robin's perivascular spaces (Bechmann et al., 2001), which are located between the basement membrane around pericytes and ECs and the basement membrane at the surface of the glia limitans of the brain vessels (Fig. 1B). These perivascular spaces are in direct contact with the subarachnoid space and thus with the cerebrospinal fluid. When small tracers are injected into the cerebrospinal fluid they follow the fluids flow through the perivascular spaces and the ventricles, and they may enter the brain parenchyma (Iliff et al., 2012). In fact, after an intracisternal injection, small hydrophilic molecules can be observed around the ventricle walls and the superficial layers of the CNS in contact with the meninges or in the whole brain parenchyma depending on the size of the molecule (Iliff et al., 2012). Larger molecules will not enter the brain parenchyma after intraventricular or intracisternal injection due to the ependymocytes and the glia limitans and its basal lamina (Bechmann et al., 2001; Iliff et al., 2012; Kim et al., 2006), being only observed in the perivascular compartment. Thus, after intravenous administration, a hydrophilic drug will not reach the cerebrospinal fluid, but if administered intracisternally it may enter the brain parenchyma in a size-depending fashion. The engineering of appropriate vehicles for cargo drug delivery using these administration routes may be useful to envisage potential therapeutic strategies.

3. Disturbed BBB permeability

BBB disruption is a central and early characteristic of many acute and chronic CNS injuries such as stroke, trauma, inflammatory and infectious processes, Multiple Sclerosis, Alzheimer, Parkinson, epilepsy, pain, and brain tumors (Abbott et al., 2006; Rosenberg, 2012). In these cases, the increase in BBB permeability is linked to the dysfunction of the CNS (Rosenberg, 2012). For instance, inflammation is a common feature of both chronic and acute CNS injuries and it is one of the main causes of the expansion of the neuropathology to adjacent CNS tissue areas. Many inflammatory mediators, like tumor necrosis factor-α (TNFα), induce BBB permeability acting directly on ECs (Deli et al., 1995) or indirectly by activating astrocytes to secrete other proinflammatory mediators like IL-1β (Didier et al., 2003), and in this way contribute to the disease severity. In the Multiple Sclerosis model termed Experimental Allergic Encephalomyelitis (EAE), the major BBB disruption occurs in the white matter post-capillary venules in response to inflammatory stimuli (Tonra, 2002), showing that these locations can also constitute important places for the entry of circulating molecules and cells into the brain. After a traumatic brain injury there is a rapid extravasation of blood in the central damaged areas, and intravascular coagulation and significant reduction in blood flow in the pericontusional brain areas. This is followed by two peaks of BBB opening at 4–6 h and 2–3 days after the insult (Chodobski et al., 2011). Thus, though the extent and particular moments of BBB permeability vary in the different pathologies, it can be used as a therapeutic time-window to deliver molecules into the CNS (Rosenberg, 2012).

Transient pharmacological stimulation of BBB opening for drug delivery is tempting, and it can be achieved by the injection of hypertonic solutions with mannitol. However, the potential toxic effects, especially under pathological conditions, are notable. Though the permeability of the BBB may be spontaneously enhanced at certain time-windows post-injury, as for example after traumatic brain or spinal cord injury (Bartanusz et al., 2011), that will allow the desired drugs entering the CNS, the pharmacological disruption of the BBB under pathological conditions may in contrast worsen the disease progression. For instance, the pharmacological disruption of the BBB enhanced the clinical severity in an EAE model (Alvarez et al., 2011), indicating that the integrity of the BBB is involved in the pathology and it also modulates the recovery. In this context, the dysfunction of the BBB and BSCB has been well documented in the etiology or progression of several CNS pathologies (Bartanusz et al., 2011), making the enhancement of BBB barrier permeability not indicated for the delivery of drugs into the damaged CNS. Again, specific BBB crossing vehicles would be required to provide the drugs with CNS transit properties.

4. Viral and viral-based vectors for BBB crossing

Recent reports have demonstrated that some non-pathogenic, single-stranded DNA human parvoviruses, in particular the adeno-associated virus (AAV) serotypes 6 and 9, enter the CNS following intravenous (i.v.) administration without the use of any BBB-permeabilizing agents (Duque et al., 2009; Foust et al., 2009, 2010; Towne et al., 2008). This observation generated important expectations regarding the identification of surface protein motifs capable of inducing transport of vectors across the BBB.

Recombinant vectors for AAV-derived gene therapy (rAAVs) can infect a broad range of both dividing and post-mitotic cells, and their DNA persists in an episomal state thus enabling efficient and stable transduction (Grieger and Samulski, 2005; Mandel et al., 2006). These vehicles are highly efficient in the nervous system and infect mainly neurons by intrathecal (Federici et al., 2012) or intracerebral injections (Burger et al., 2005; Mandel et al., 2006; McCown, 2005). Towne et al. (2008) observed that motor neurons could be transduced along the entire spinal cord through a single noninvasive i.v. delivery of rAAV6 in 42 days old wt and SOD1 G93A transgenic mice model of Amyotrophic Lateral Sclerosis. The transduction of astrocytes and other non-motor neuron cells, along with the finding that the motor neurons were not transduced following intramuscular injection, suggested that the mechanism of transduction was independent of retrograde transport, and that the vector was in fact able to cross the BBB (Towne et al., 2008). Moreover, rAAV9 was found to be very efficient for transducing spinal cord cells including motor neurons after i.v. delivery in both neonate and adult mice (Duque et al., 2009). Kaspar and colleagues (Foust et al., 2009) have demonstrated that delivery of rAAV9 through the systemic circulation leads to widespread transduction of the neonatal and adult mice brain, with marked differences in cell tropism in relation to the stage of development and complexity of the BBB (Foust et al., 2009; Lowenstein, 2009). In accordance, Gray et al. (2011) reported the ability of rAAV9 to transduce neurons and glia in the brain and spinal cord of adult mice and nonhuman primates. They suggest that AAV9 enters the nervous system by an active transport mechanism across the BBB rather than by passive slipping through the tight junctions between endothelial cells, as the co-administration of mannitol prior to rAAV injection resulted in only a 50% increase in brain delivery. They observed extensive transduction of neurons and glia throughout the mice brain and spinal cord (with neurons outnumbering astrocytes ~2:1 in the hippocampus and striatum and 1:1 in the cortex). However, the overall transduction efficiency was considerably lower in non-human primates, being glial cells the main cell type transduced. These rodent/non-human primate differences are important for clinical applications, and may reflect a variety of species-specific factors including differential BBB transport, capsid-interacting blood factors to promote or inhibit rAAV9 transduction, neural cell tropism within the brain, and/or intracellular trafficking and vector persistence. A summary of the AAV9 viral-based administration strategies to cross the BBB for therapeutic purposes is summarized in Fig. 3. Nevertheless, the identification of the functional motifs of the surface proteins of AVV6 and AVV9 will surely contribute to the engineering of more effective vectors for the treatment of central nervous system injuries. In fact, AAV capsid DNA shuffling and subsequent directed evolution generated AVV novel clones able to cross selectively the seizure-compromised BBB after i.v. administration (Gray et al., 2010).

Obviously, in the context of biological risks associated to administration of viruses (Edelstein et al., 2007) and the inflammatory conditions linked to AVV administration and immune responses (Daya and Berns, 2008), molecular carriers or non-infectious virus-inspired constructs (artificial viruses) would be preferred for drug BBB-cross delivery. Artificial viruses are nanostructured, manmade molecular oligomers that mimic viral behavior regarding cell penetrability, targeted delivery of associated drugs and nucleic acids and other key functions relevant to encapsulation, cell surface receptor targeting, intracellular trafficking and eventual nuclear delivery, among others (Mastrobattista et al., 2006). In this regard, peptides and proteins are enough versatile to functionalize these vehicles, or the drug itself in simpler nanoconjugates. When the building blocks of drug carries are proteins, these functions can be recruited by the incorporation, in a single polypeptide chain, of functional peptides from diverse origins that supply desired biological activities to the whole construct (Ferrer-Miralles et al., 2008; Ferrer-Miralles et al. Epub ahead of print; Vazquez et al., 2008, 2009). Also, principles for the rational control of self-assembling of natural and fully de novo designed polypeptides as nanostructured materials are being established (Domingo-Espin et al., 2011; Unzueta et al., 2012a, 2012b, 2014; Vazquez and Villaverde, 2010; Vazquez et al., 2010), thus opening a plethora of possibilities for the design and biological production of nanostructured, protein-based artificial viruses (Ferrer-Miralles et al., Epub ahead of print; Rodriguez-Carmona and Villaverde, 2010; Vazquez and Villaverde, 2013) with good clinical grade formulation profile. The BBB-crossing abilities of AAVs prove, in any case, the potential penetrability of nanosized protein entities in the context of emerging nanomedicines of CNS.

5. BBB-crossing protein tags in artificial drug carriers

From a different angle, chemical modification of a drug can enhance its penetrability into the CNS, for example by adding domains for glycosylation (Poduslo and Curran, 1992), methylation (Hansen et al., 1992) and pegylation (Witt et al., 2001), lipophilic domains (Egleton and Davis, 2005), or coating it with polysorbates (Bhaskar et al., 2010). Also, precursors can cross the BBB when the drug cannot, as is the

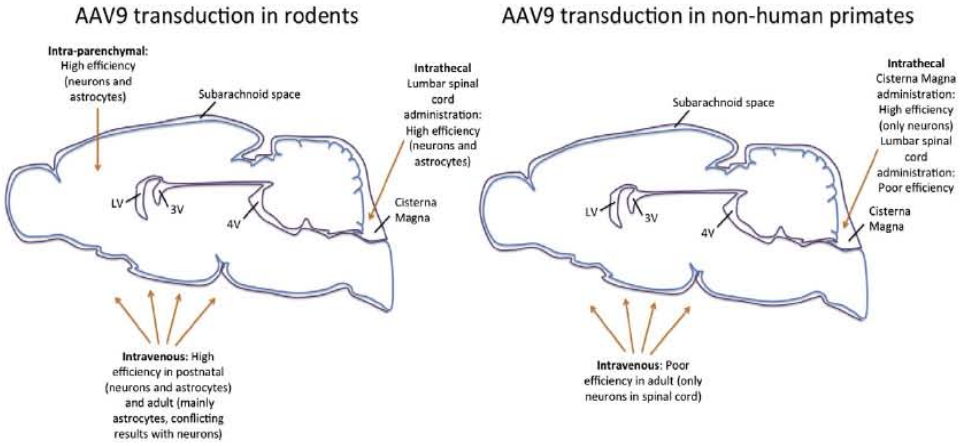

Fig. 3. AAV9 administration routes and transduction efficiencies. Different results have been obtained when AAV9 was administered by i.v. or intra-thecal delivery, but also in postnatal or adult animals, and importantly in mice or in non-human primates. While i.v. delivery efficiently transduces neurons and astrocytes in postnatal and adult mice, very low efficiency and mainly astrocyte transduction was observed in non-human primates. Moreover, intrathecal delivery into the Cisterna Magna resulted in the widest transduction in non-human primates.

case of L-Dopa in the treatment of Parkinson's disease (Wade and Katzman, 1975). In a very different context, adequate engineering of natural proteins can offer, at different extents, tools to functionalize free drugs or nanosized carriers to reach the CNS parenchyma (Table 1). For that, receptor-mediated transcytosis can be reached by the incorporation of proteins or short peptides that act as ligands of insulin, transferrin or low density lipoprotein receptors (Table 1). For instance, monoclonal antibodies covalently bound to therapeutic proteins have been targeted to insulin and transferrin receptors (TfRs) in both in vitro and in vivo models (Fu et al., 2010b, 2011; Lu et al., 2011). In these experiments, recombinant proteins have two functional moieties; the therapeutic peptide fused to the carboxy terminus of the IgG heavy chain and the complementarily determining regions of the monoclonal antibodies that are located at the N-terminus (Pardridge and Boado, 2012). This delivery platform, dubbed Molecular Trojan Horse and extensively exploited by Pardridge (2006), can be adapted to any therapeutic protein as long as its production in recombinant organisms maintains its biological function. In this context, recent insights in industrial-oriented metabolic engineering (Lee et al., 2012) and the wide diversity of microbial species that are now under exploration as cell factories for therapeutic proteins (Corchero et al., 2013) offer alternatives to conventional hosts for the production of highly functional protein species. In addition, monoclonal antibodies conjugated to polymeric micelles (Yue et al., 2012), liposomes (Mamot et al., 2005; Schnyder and Huwyler, 2005b; Zhang et al., 2002) and polymeric nanoparticles (Reukov et al., 2011a) can improve the performance of the chemical entities in the transport of therapeutic molecules across the BBB. Recent results suggest that low affinity binding and monovalent binding to the cellular receptors are highly effective for successful transcytosis (Niewoehner et al., 2014; Yu et al., 2011).

In the development of photothermal therapy, gold nanoparticles conjugated to peptides carrying the motif THR target transferrin receptor (TfR) and they are delivered to the CNS (Prades et al., 2012b). Also, pegylated Fe_3O_4 nanoparticles conjugated with lactoferrin (Qiao et al., 2012b) have been proposed as MRI molecular probes for imaging diagnostic purposes. In some instances, intravenously administered nanoparticles of different chemical origins get adsorbed to apolipoproteins and the entrance to the CNS is mediated by low density lipoprotein receptors (Gessner et al., 2001; Kim et al., 2007). This is the case of human serum albumin (HSA) nanoparticles loaded with loperamide (Ulbrich et al., 2011). Therefore, some nanoparticulate carriers have been modified to include low-density lipoproteins (LDLs) or LDL receptor binding peptides (ApoB (Spencer and Verma, 2007); APoE (Re et al., 2011; Wagner et al., 2012) and Apo A-I (Fioravanti et al., 2012; Kratzer et al., 2007a)) in their formulation, which results in significantly improved entrance to the brain parenchyma when compared with naked nanoparticles. In that sense, HSA nanoparticles with covalently bound ApoA-I or ApoE are able to transport drugs to the brain with similar efficiency as HSA nanoparticles conjugated to antibodies against insulin or transferrin receptors, or HSA nanoparticles conjugated to insulin or transferrin (Zensi et al., 2009, 2010). Among successful examples, peptides derived from the consensus binding sequence (Kunitz domain) of proteins transported through LDL receptors, such as aprotinin and Kunitz precursor inhibitor 1 (Demeule et al., 2008b; Gabathuler, 2010b), must be stressed as very promising (Table 1). Kunitz-derived peptides (angiopeps), covalently bound to drugs, have been already used or are in ongoing clinical trials for the treatment of brain tumors. The main objective of the targeting peptides in clinics is the treatment of brain metastases from solid tumors (breast and lung cancers) as an alternative to the surgical removal of the primary brain tumor. Particularly, it has been demonstrated that angiopep conjugated to paclitaxel (ANG1005, also named GRN1005, http://clinicaltrials.gov/ct2/show/NCT01480583?term=ANG1005&rank=6) is well tolerated and shows activity in patients with advanced solid tumors previously treated with antitumor drugs (Kurzrock et al., 2012). In addition, there are three ongoing clinical trials in the same direction (http://clinicaltrials.gov). Apart from the endogenous ligands, other peptides with high affinity for brain receptors (or strong cell-penetrating peptides) have also been explored as functional materials, including pegylated-gelatin siloxane nanoparticles conjugated with HIV-1-derived Tat peptide (Tian et al., 2012), rabies virus glycoprotein conjugated to liposomes (Tao et al., 2012), and variable heavy-chain domain of camel homodimeric antibodies (VHH) (Li et al., 2012) for receptor-homing peptides obtained from phage display screening (Maggie et al., 2010; Malcor et al., 2012). To gather all published information related to peptides with activity to cross the BBB, Van Dorpe and collaborators designed a

Table 1
Main transversal approaches to address BBB-crossing in nanomedicine, illustrated by representative examples.

Method	Target	Ligand and references	Application and reference	NP size
Therapeutic proteins conjugated to mAbs raised against insulin and transferrin receptors	Transferrin receptor	Carboxy terminus of the IgG heavy chain (mAb) against the mouse transferrin receptor	Erythropoietin fused to the mAb to treat stroke (Fu et al., 2011)	ND
	Insulin receptor	Monoclonal antibodies conjugated to polymeric micelles, liposomes (Mamot et al., 2005; Schnyder and Huwyler, 2005a; Ulbrich et al., 2011) and polymeric nanoparticles (Reukov et al., 2011b) against insulin receptor	Insulin or an anti-insulin receptor mAbs were covalently coupled to the human serum albumin NP (Zensi et al., 2010)	157 ± 11 nm
Adsorption of apolipoproteins on chemical NPs to interact with LDLR	LDLR	Apolipoproteins	Adsorption of apolipoprotein B-100 (ApoB-100) onto PEG-PHDCA NPs (Kim et al., 2007)	135 ± 41 nm
Conjugation or covalent binding of endogenous ligands (proteins or peptides) to nanocarriers	Transferrin receptor	THR derived peptide	Gold nanoparticles conjugated to THR peptide target transferrin receptor and can deliver gold NPs to the CNS (Prades et al., 2012a)	519 ± 10 nm
	Transferrin receptor	Lactoferrin	Pegylated Fe_3O_4 NPS conjugated with lactoferrin used for imaging diagnostic purposes (Qiao et al., 2012a)	48.9 nm
	LDLR	Peptides derived from $ApoE^{20,29}$, $ApoB^{23}$ and ApoA-I (Kratzer et al., 2007b; Lu et al., 2011)	LDLR binding-domain of ApoB was cloned into lentivirus vector (Spencer and Verma, 2007)	ND
	LDLR	Peptides originated from Kunitz protein (angiopeps)	Covalently bound to drugs used for the treatment of brain tumors (Demeule et al., 2008a)	ND

mAbs: monoclonal antibodies.
LDLR: low density lipoprotein receptor.
Apo: apolipoprotein.
NP: nanoparticle.
ND: not determined.
THR: tri-peptide motif (thre-his-arg).

peptide database to organize scattered information (Van et al., 2012) (http://brainpeps.ugent.be). The main approaches to protein-guided BBB delivery of therapeutic nanoparticles are summarized in Fig. 4.

6. BBB-crossing for the treatment of CNS diseases

Among CNS diseases, only three are currently treated with drugs that naturally cross the BBB, namely epilepsy, chronic pain and psychiatric disorders (Ghose et al., 1999). For degenerative diseases, vascular diseases, trauma aftermaths, viral infections and congenital diseases occurring in the CNS, there is a pushing need to develop BBB-crossing strategies for drug delivery, preferentially based on non-viral carriers (Table 2). The most representative examples of how BBB-crossing is addressed in these conditions are discussed in the next sections.

6.1. Neurodegenerative disorders

Therapeutic approaches to neurodegenerative diseases are concentrating most of the efforts on the design of therapeutic compounds able to cross the BBB. For Parkinson's disease, the first drug used clinically was the dopamine precursor L-Dopa, that contrarily to dopamine itself, crosses the BBB by using a large amino acid transporter (Wade and Katzman, 1975). On the other hand, in a Trojan Horse approach, Pardridge's group normalized striatal tyrosine hydroxylase levels and reversed functional signs in a Parkinson model. A tyrosine hydroxylase gene empowered by a nervous system-specific promoter was injected, carried by pegylated liposomes decorated with OX26 antibody against TfR (Zhang et al., 2003, 2004a). The team was also successful entering erythropoietin (Zhou et al., 2011b) and glial derived neurotrophic factor (GDNF) (Fu et al., 2010a) by joining these therapeutic proteins to mice anti-TfR antibodies, and subsequently reaching clear neuroprotective effects.

Regarding Alzheimer, again, by means of this anti-TfR antibody as BBB transporter and by fusion to an anti-Abeta amyloid antibody, the levels of beta amyloid peptide were dramatically reduced (Zhou et al., 2011a). In this context, Genentech is developing a lower affinity variant of anti-TfR antibody (that favors release from the BBB towards the CNS) fused to an antibody against the enzyme BACE1, involved in amyloidal plaque formation. When the bifunctional molecule is applied systemically, a decrease of 47% in plaques was observed in mouse models (Yu et al., 2011). Interestingly, the fusion of a monovalent sFab of an anti-TfR antibody to an anti-Abeta antibody mediated effective uptake transcytosis and TfR recycling, while the presence of two Fab fragments on the anti-Abeta antibody resulted in uptake followed by trafficking to lysosomes and an associated reduction in TfR levels (Niewoehner et al., 2014). This approach exhibited enhanced in vivo targeting of Abeta plaques after i.v. administration. Nerve growth factor (NGF) fused to an anti-TfR antibody has also been used successfully to prevent neuronal degeneration when applied intravenously in a Huntington disease model (Kordower et al., 1994). In a similar context, a poly(mannitol-co-PEI) gene transporter modified with a rabies virus glycoprotein is able to ameliorate Alzheimer symptoms by transporting a therapeutic RNAi (Park et al., 2015). Alternatively, the intranasal route to the CNS (Hanson and Frey, 2008), through the olfactory and trigeminal nerve has been largely explored to introduce important factors in neurogenesis and memory such as NGF (De et al., 2005), insulin-like growth factor 1 (IGF-I) (Liu et al., 2004), fibroblast growth factor 2 (FGF-2) (Jin et al., 2003), insulin (Benedict et al., 2004), interferon beta (IFN beta (Ross et al., 2004)) and the octapeptide NAP (Matsuoka et al., 2008) which is currently in Phase II clinical trials in patients with incipient Alzheimer's disease (Gozes et al., 2009).

6.2. Brain tumors

Diverse BBB-crossing anti-tumor vectors are under development in both pre-clinical and clinical phases, empowered by a spectrum of BBB-crossing tags. Angiochem Inc. entered into Phase I clinical trials a product (ANG1005) that uses the peptide Angiopep-2, capable of driving the cargo paclitaxel by transcytosis through the BBB by using the LDL receptor LRP-1. This conjugate showed previously intracranial tumor regression in murine models when administered i.v. (Bichat et al., 2008). Melanotransferrin associated with doxorubicin increased the survival in mice with intracranial tumors (Gabathuler, 2005; Karkan et al., 2008). Albumin is being used at the University of California, San Francisco (UCSF), in a Phase I clinical trial as a carrier of paclitaxel (nab-paclitaxel) to treat brain and CNS tumors (Chien et al., 2009) (it is already in the market for breast cancer). Targeting the transmembrane protein TMEM30A, the ligand FC5 (discovered by phage display, a single domain antibody — sdAb —), drives liposomes through the BBB to release doxorubicin into the CNS (Gabathuler, 2010a). On the other hand, by taking a

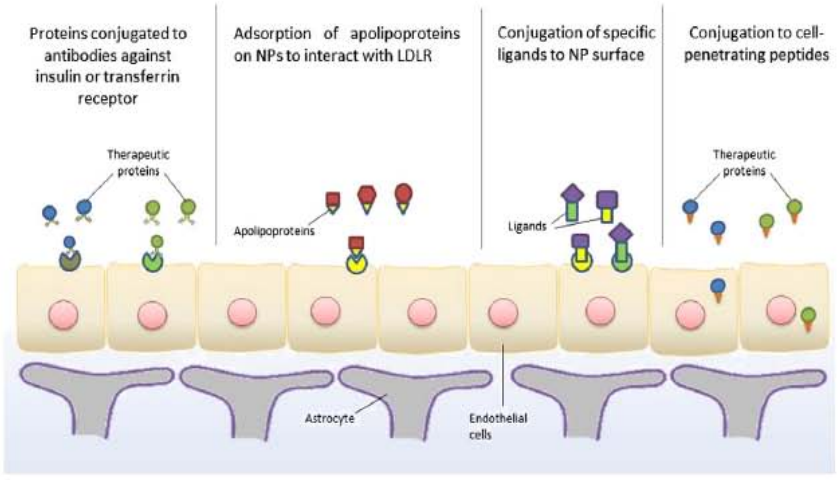

Fig. 4. Receptor-mediated approaches used in nanomedicine to cross the BBB. Different types of proteins (including antibodies) showing specific binding to BBB transporters and cell surface receptors that are relevant to transcytosis are used to functionalize nanoparticles (NPs). Cell-penetrating peptides carrying therapeutic proteins are also depicted. More details and specific examples are given in Table 1.

Table 2
Disease-focused main approaches to BBB drug transdelivery.

Disease	Drug	Target	Ligand and strategy	References
Neurodegenerative disorders				
Parkinson	L-Dopa	Large amino acid transporter	L-Dopa	Wade and Katzman (1975)
	Tyrosine hydroxylase gene	TfR	Pegylated liposome decorated with OX26 ab against TfR.	Zhang et al. (2003, 2004a)
	Erythropoietin	TfR	Fusion protein joined to TfR ab.	Zhou et al. (2011b)
	GDNF	TfR	Fusion protein joined to TfR ab.	Fu et al. (2010b)
Alzheimer	Ab against beta-amyloid	TfR	Fusion protein joined to TfR ab.	Zhou et al. (2011a)
	Ab against BACE1 enzyme	TfR	Fusion protein joined to low affinity TfR ab.	Yu et al. (2011)
Huntington disease	NGF	TfR	Fusion protein joined to TfR ab.	Kordower et al. (1994)
Brain tumors				
Intracranial tumor	Antiangiogenic oligonucleotides	ND	Polycefin polymer	Ljubimova et al. (2008)
	DO-FUdR	ND	Drug incorporated in solid lipid nanoparticles	Wang et al. (2002)
	Paclitaxel	LRP-1 (LDL receptor)	Drug conjugated to Angiopep-2 peptide.	Bichat et al. (2008)
	Paclitaxel	Melanotransferrin receptor	Drug associated with melanotransferrin	Karkan et al. (2008)
	Paclitaxel	ND	Drug conjugated to albumin	Chien et al. (2009)
	Doxorubicin	TMEM30A transmembrane protein	Liposomes decorated with FC5 ligand	Gabathuler (2010a)
	shRNAs against EGFR	Insulin receptor/transferrin receptor	Pegylated immunopolysomes associated to TfR ab and insulin receptor ab.	Boado (2007), Pardridge (2004)
	Doxorubicin	LDL receptor via ApoB/E enrichment	Drug bound to polysorbate-coated polymer	Steiniger et al. (2004)
	Oligonucleotides against protein kinase C alpha	ND	Nude oligonucleotide administration	Yazaki et al. (1996)
Anti-nociception				
	Loperamide	TfR	Human serum albumin coupled to TfR ab.	Ulbrich et al. (2009)
	Loperamide	Possible adsorption-mediated endocytosis	PLGA nanoparticle derivatized with a glycosylated heptapeptide	Tosi et al. (2007)
	Dalargine	ND	Drug joined to cell penetrating peptides	Rousselle et al. (2003)
	Dalargine	TMEM30A transmembrane protein	Drug joined to a FC5–Fc fusion antibody	Farrington et al. (2014)
Cerebral ischemia				
	BDNF	TfR	Protein linked to TfR ab.	Wu and Pardridge (1999)
	FGF-2	TfR	Protein linked to TfR ab.	Song et al. (2002)
	VIP	TfR	Protein linked to TfR ab.	Bickel et al. (1993)
	Erythropoietin	TfR	Protein linked to TfR ab.	Fu et al. (2011)
	NGF gene	TfR	Lipoplexes decorated with transferrin	da Cruz et al. (2005)
	NR2B	ND	Protein fused to cell penetrating peptide	Aarts et al. (2002)
	Bcl-XI	ND	Protein fused to cell penetrating peptide	Kilic et al. (2002)
	GDNF	ND	Protein fused to cell penetrating peptide	Kilic et al. (2003)
	JNKI	ND	Protein fused to cell penetrating peptide	Borsello et al. (2003)
Infectious diseases				
	siRNA	ND	9R-RVG fusion protein	Kumar et al. (2007)
	Anti-VIH drugs	ND	Drug associated to liposomes	Dusserre et al. (1995)
	Anti-VIH drugs	ND	Drug associated to micelles	Spitzenberger et al. (2007)
	Anti-VIH drugs	ND	Drug associated to cell penetrating peptide	Rao et al. (2009)
	Diminazenediaceturate	LDL receptor via ApoE enrichment	Lipid-drug conjugate	Gessner et al. (2001)
Mucopolysaccharidosis				
	Beta-glucuronidase gene	TfR	Liposomes associated to TfR ab.	Zhang et al. (2008)
	Alpha-L-iduronidase enzyme	TfR	Protein linked to TfR ab.	Boado et al. (2008)
	Beta-glucuronidase	ND	Protein fused to cell penetrating peptide	Xia et al. (2001)

ND: not determined.
PLGA: poly(lactic-co-glycolic) acid.
TfR: transferrin receptor.

Trojan Horse strategy based on pegylated immunoliposomes targeted to TfR (Boado et al., 2007), the delivery of shRNAs expression vectors against the epidermal growth factor receptor (EGFR) increased the survival in mice with intracranial tumors (Boado, 2007; Pardridge, 2004; Zhang et al., 2004b). Doxorubicin ferried by polysorbate-coated polymer nanoparticles promoted long-term glioblastoma remission in rats, probably by an unspecific BBB crossing (Steiniger et al., 2004), and a polycefin polymer variant that specifically targets human brain, which is associated to antiangiogenic oligonucleotides inhibits tumor angiogenesis and improves animal survival (Ljubimova et al., 2008).

On the other hand, despite no direct CNS targeting, it has been possible to increase the intracranial levels of anticancer 3′5′-dioctanoyl-5-fluoro-2′deoxyuridine (DO-FUdR), by incorporating it into a solid lipid nanoparticle (Wang et al., 2002). Furthermore, when administered systemically, nude phosphorothioate oligonucleotides against protein kinase C alpha, also reduced intracranial glioblastoma tumor size and doubled mice survival time (Yazaki et al., 1996). On the basis of these results, a Phase II clinical trial has been completed (http://www.clinicaltrials.gov/ct2/results?term=pkc-alpha). In a more recent example, an intravenously injected cell penetrating peptide (LNP) decorating

a polylysine-PEG gene vector extended the median survival time of glioma-bearing mice (Yao et al., 2014).

6.3. Pain

Anti-nociception is usually achieved by methylation (Hansen et al., 1992) or glycosylation (Polt et al., 1994) of active molecules to stimulate their penetrability into the CNS. On the other hand, coupling human serum albumin to an anti-TfR permits the transport of loperamide into the CNS for anti-nociception effects (Ulbrich et al., 2009). The same drug is delivered into the CNS by injecting i.v. a poly(lactic-co-glycolic) acid (PLGA) nanoparticle, derivatized with the peptide H_2N-Gly-L-Phe-D-Thr-Gly-L-Phe-L-Leu-L-Ser(O-β-D-Glucose)-$CONH_2$ (g7) (Tosi et al., 2007). The analgesic dalargine joined to a cationic cell-penetrating peptide (Syn-B) increases brain uptake in two orders of magnitude. This peptide crosses the BBB using a nonspecific route, that is, without association with a receptor (Rousselle et al., 2003). Other polyarginine-based peptides as CNS transporters are in preclinical phases (Gabathuler, 2010a).

6.4. Ischemia

Sequelae of cerebral ischemia can be lessened by CNS delivery of brain-derived neurotrophic factor (BDNF) (Wu and Pardridge, 1999; Zhang and Pardridge, 2001), fibroblast growth factor (FGF-2) (Song et al., 2002), inhibitor of caspase-3 (Yemisci et al., 2014), vasoactive intestinal peptide (VIP) (Bickel et al., 1993; Wu and Pardridge, 1996) and erythropoietin (EPO) (Fu et al., 2011) linked to an anti-TfR antibody. The nerve growth factor (NGF) gene has been introduced into the CNS while inside lipoplexes decorated with the TfR natural ligand, transferrin (da Cruz et al., 2005). The cell penetrating Tat peptide has also proven to carry efficiently N-methyl D-aspartate receptor subtype 2B (NR2B) domain (Aarts et al., 2002), B-cell lymphoma-extra large protein ($Bcl\text{-}X_L$) (Kilic et al., 2002), glial cell-derived neurotrophic factor (GDNF) (Kilic et al., 2003) and c-Jun domain (Borsello et al., 2003), to protect neurons in brain infarct models. On the other side, sniffing insulin-like growth factor (IGF-1) (Liu et al., 2004) and EPO (Yu et al., 2005) protects the brain against stroke in animal models (Hanson and Frey, 2008). Modular protein/DNA nanoparticles have been shown to induce biologically relevant transgenic protein levels and therapeutic effects after acute excitotoxic injuries when injected intracerebrally (Negro-Demontel et al., 2014; Peluffo et al., 2003, 2006, 2012). The addition of CNS targeting domains to these particles may enable intravenous delivery retaining its neuroprotective potential.

6.5. Infectious diseases

CNS infectious diseases have also been treated in vivo using different approaches. By administering i.v. siRNA into Japanese encephalitis virus-infected mice, Manjunath and colleagues afforded specific viral gene silencing and protection. The siRNA carrier was a two-domain peptide formed by nine arginines (R9) and a peptide derived from rabies virus glycoprotein (RVG) (Kumar et al., 2007). On the other hand, the brain levels of different anti-HIV drugs have been increased several folds through association with liposomes (foscarnet, (Dusserre et al., 1995)), micelles (zidovudine, lamivudine, nelfinavir, (Spitzenberger et al., 2007)) and the Tat protein (ritonavir, (Rao et al., 2009)). Furthermore, second stage African trypanosomiasis was treated intravenously in a mouse model by conjugating the active water-soluble drug to liposomes using polysorbate 80 as surfactant (Olbrich et al., 2002).

6.6. Other conditions

Other diseases in which the BBB crossing has been successfully achieved are Hurler's Syndrome (mucopolysaccharidosis), using the mouse anti-TfR antibody associated to a liposome with beta-glucuronidase gene (Zhang et al., 2008) or fusioned to the alpha-L-iduronidase enzyme (Boado et al., 2008). A cell-penetrating Tat peptide improves the beta-glucuronidase biodistribution when organized as a single chain fusion protein (Xia et al., 2001). Narcolepsy has also been treated with good results with nasal hypocretin I (Hanson and Lobner, 2004).

7. Administration routes

The intravenous administration of functionalized nanoparticles is the most used therapeutic route. However, in some cases, patient compliance is not easy to achieve, and alternative administration routes need to be explored. In fact, there are standardized methods for drug delivery by osmotic disruption (Kroll and Neuwelt, 1998; Yang et al., 2011), by local delivery placing polymer wafers after tumor excision (Balossier et al., 2010), by convection-enhanced delivery (White et al., 2012a, 2012b) or by intranasal administration (Grassin-Delyle et al., 2012; Tsai, 2012; Wolf et al., 2012; Zhu et al., 2012) (Fig. 1A). Some of these treatments are still highly invasive and are only addressed to high grade glioma patients. In the milder intranasal delivery, the drug is being accumulated in the olfactive bulb and then diffusing inside the brain. This approach has been proven to be quite effective in the treatment of various disease models, acting through the olfactory pathway and trigeminal nerve (Born et al., 2002; Hanson and Frey, 2008). Regarding gene therapy, only 1.9% of current clinical trials are performed on the CNS, and almost all of them are applied by intracranial injection or performed ex vivo (Ginn et al., 2013), pointing to the importance of the delivery of BBB-crossing gene therapy vectors.

8. Conclusions and future prospects

Numerous examples of basic research and ongoing clinical trials illustrate how proteins can be engineered to overcome the complexity of both BBB and BSCB in drug delivery contexts. In this regard, a few CNS diseases are already treated with protein-based targeted drugs, and much more are expected to be released for use in the next future. Hopefully, and based on current insights on the engineering of protein self-assembling, functional proteins would be desirably adapted as building blocks of nanosized entities, acting at the same time as BBB crossers, targeting agents and drug carriers. Although the fully de novo design of such protein-based artificial viruses is in its infancy, the accumulation of data about the physiology of the CNS and of relevant cell receptors, the widening spectrum of drugs potentially useful in CNS therapies and the exploration of alternative routes for administration on the bases of result from the use of natural viruses envisage the generation of these sophisticated vehicles as a forthcoming routine strategy.

Acknowledgments

The authors acknowledge the financial support granted to H.P. and L.N. from Fundació Marató TV3, Catalunya, Spain (TV32011-110533), Comisión Sectorial de Investigación Científica de la Universidad de la República (CSIC-UDELAR), Uruguay, Agencia Nacional de Investigación e Innovación (ANII), Uruguay, and FOCEM (MERCOSUR Structural Convergence Fund), COF 03/11, to E.V. from FIS (PI12/00327) and Fundació Marató TV3 (TV32013-133930) and to A.V. from Fundació Marató TV3 (TV32013-132031), MINECO (BIO2013-41019-P) and from the Centro de Investigación Biomédica en Red (CIBER) de Bioingeniería, Biomateriales y Nanomedicina, with assistance from the European Regional Development Fund, for their nanomedical research. Z.X. and U.U. acknowledge financial support from China Scholarship Council (2011630065) and from ISCIII (FI09/00150) respectively, both through pre-doctoral fellowships. A.V. has been distinguished with an ICREA ACADEMIA award.

References

Aarts M, Liu Y, Liu L, Besshoh S, Arundine M, Gurd JW, et al. Treatment of ischemic brain damage by perturbing NMDA receptor–PSD-95 protein interactions. Science 2002; 298:846–50.

Abbott NJ, Ronnback L, Hansson E. Astrocyte–endothelial interactions at the blood–brain barrier. Nat Rev Neurosci 2006;7:41–53.

Adinolfi M. The permeability of the blood-CSF barrier during foetal life in man and rat and the effect of brain antibodies on the development of the CNS. In: Hemmings WA, editor. Protein transmission through living membranes. Amsterdam: Elsevier/North-Holland Biomedical Press; 1979. p. 349–64.

Alvarez JI, Dodelet-Devillers A, Kebir H, Ifergan I, Fabre PJ, Terouz S, et al. The Hedgehog pathway promotes blood–brain barrier integrity and CNS immune quiescence. Science 2011;334:1727–31.

Arthur FE, Shivers RR, Bowman PD. Astrocyte-mediated induction of tight junctions in brain capillary endothelium: an efficient in vitro model. Brain Res 1987;433:155–9.

Balossier A, Dorner L, Emery E, Heese O, Mehdorn HM, Menei P, et al. Incorporating BCNU wafers into malignant glioma treatment European case studies. 2010;30:195–204.

Bartanusz V, Jezova D, Alajajian B, Digicaylioglu M. The blood–spinal cord barrier: morphology and clinical implications. Ann Neurol 2011;70:194–206.

Bechmann I, Priller J, Kovac A, Bontert M, Wehner T, Klett FF, et al. Immune surveillance of mouse brain perivascular spaces by blood-borne macrophages. Eur J Neurosci 2001; 14:1651–8.

Benedict C, Hallschmid M, Hatke A, Schultes B, Fehm HL, Born J, et al. Intranasal insulin improves memory in humans. Psychoneuroendocrinology 2004;29:1326–34.

Bhaskar S, Tian F, Stoeger T, Kreyling W, de la Fuente JM, Grazu V, et al. Multifunctional nanocarriers for diagnostics, drug delivery and targeted treatment across blood–brain barrier: perspectives on tracking and neuroimaging. Part Fibre Toxicol 2010; 7:3.

Bichat F, Demeule M, Lawrence B, Raguin O, Sourzat B, Gabathuler R, et al. Enhanced drug delivery to brain tumours with a new paclitaxel–peptide conjugate. Eur J Cancer 2008(Suppl. 6):139.

Bickel U, Yoshikawa T, Landaw EM, Faull KF, Pardridge WM. Pharmacologic effects in vivo in brain by vector-mediated peptide drug delivery. Proc Natl Acad Sci U S A 1993;90: 2618–22.

Boado RJ. Blood–brain barrier transport of non-viral gene and RNAi therapeutics. Pharm Res 2007;24:1772–87.

Boado RJ, Zhang Y, Zhang Y, Pardridge WM. Humanization of anti-human insulin receptor antibody for drug targeting across the human blood–brain barrier. Biotechnol Bioeng 2007;96:381–91.

Boado RJ, Zhang Y, Zhang Y, Xia CF, Wang Y, Pardridge WM. Genetic engineering of a lysosomal enzyme fusion protein for targeted delivery across the human blood–brain barrier. Biotechnol Bioeng 2008;99:475–84.

Born J, Lange T, Kern W, McGregor GP, Bickel U, Fehm HL. Sniffing neuropeptides: a transnasal approach to the human brain. Nat Neurosci 2002;5:514–6.

Borsello T, Clarke PG, Hirt L, Vercelli A, Repici M, Schorderet DF, et al. A peptide inhibitor of c-Jun N-terminal kinase protects against excitotoxicity and cerebral ischemia. Nat Med 2003;9:1180–6.

Burger C, Nash K, Mandel RJ. Recombinant adeno-associated viral vectors in the nervous system. Hum Gene Ther 2005;16:781–91.

Chien AJ, Illi JA, Ko AH, Korn WM, Fong L, Chen LM, et al. A phase I study of a 2-day lapatinib chemosensitization pulse preceding nanoparticle albumin-bound paclitaxel for advanced solid malignancies. Clin Cancer Res 2009;15:5569–75.

Chodobski A, Zink BJ, Szmydynger-Chodobska J. Blood–brain barrier pathophysiology in traumatic brain injury. Transl Stroke Res 2011;2:492–516.

Corchero JL, Gasser B, Resina D, Smith W, Parrilli E, Vazquez F, et al. Unconventional microbial systems for the cost-efficient production of high-quality protein therapeutics. Biotechnol Adv 2013;31:140–53.

da Cruz MT, Cardoso AL, de Almeida LP, Simoes S, de Lima MC. Tf-lipoplex-mediated NGF gene transfer to the CNS: neuronal protection and recovery in an excitotoxic model of brain injury. Gene Ther 2005;12:1242–52.

Daya S, Berns KI. Gene therapy using adeno-associated virus vectors. Clin Microbiol Rev 2008;21:583–93.

De RR, Garcia AA, Braschi C, Capsoni S, Maffei L, Berardi N, et al. Intranasal administration of nerve growth factor (NGF) rescues recognition memory deficits in AD11 anti-NGF transgenic mice. Proc Natl Acad Sci U S A 2005;102:3811–6.

Deli MA, Descamps L, Dehouck MP, Cecchelli R, Joo F, Abraham CS, et al. Exposure of tumor necrosis factor-alpha to luminal membrane of bovine brain capillary endothelial cells cocultured with astrocytes induces a delayed increase of permeability and cytoplasmic stress fiber formation of actin. J Neurosci Res 1995;41:717–26.

Demeule M, Regina A, Che C, Poirier J, Nguyen T, Gabathuler R, et al. Identification and design of peptides as a new drug delivery system for the brain. J Pharmacol Exp Ther 2008a;324:1064–72.

Demeule M, Regina A, Che C, Poirier J, Nguyen T, Gabathuler R, et al. Identification and design of peptides as a new drug delivery system for the brain. 2008b; 324:1064–72.

Didier N, Romero IA, Creminon C, Wijkhuisen A, Grassi J, Mabondzo A. Secretion of interleukin-1beta by astrocytes mediates endothelin-1 and tumour necrosis factor-alpha effects on human brain microvascular endothelial cell permeability. J Neurochem 2003;86:246–54.

Domingo-Espin J, Vazquez E, Ganz J, Conchillo O, Garcia-Fruitos E, Cedano J, et al. Nanoparticulate architecture of protein-based artificial viruses is supported by protein–DNA interactions. Nanomedicine (Lond) 2011;6:1047–61.

Duque S, Joussemet B, Riviere C, Marais T, Dubreil L, Douar AM, et al. Intravenous administration of self-complementary AAV9 enables transgene delivery to adult motor neurons. Mol Ther 2009;17:1187–96.

Dusserre N, Lessard C, Paquette N, Perron S, Poulin L, Tremblay M, et al. Encapsulation of foscarnet in liposomes modifies drug intracellular accumulation, in vitro anti-HIV-1 activity, tissue distribution and pharmacokinetics. AIDS 1995;9:833–41.

Edelstein ML, Abedi MR, Wixon J. Gene therapy clinical trials worldwide to 2007—an update. J Gene Med 2007;9:833–42.

Egleton RD, Davis TP. Development of neuropeptide drugs that cross the blood–brain barrier. NeuroRx 2005;2:44–53.

el-Bacha RS, Minn A. Drug metabolizing enzymes in cerebrovascular endothelial cells afford a metabolic protection to the brain. Cell Mol Biol 1999;45:15–23.

Farrington GK, Caram-Salas N, Haqqani AS, Brunette E, Eldredge J, Pepinsky B, et al. A novel platform for engineering blood–brain barrier-crossing bispecific biologics. FASEB J 2014;28:4764–78.

Federici T, Taub JS, Baum GR, Gray SJ, Grieger JC, Matthews KA, et al. Robust spinal motor neuron transduction following intrathecal delivery of AAV9 in pigs. Gene Ther 2012; 19:852–9.

Ferrer-Miralles N, Vazquez E, Villaverde A. Membrane-active peptides for non-viral gene therapy: making the safest easier. Trends Biotechnol 2008;26:267–75.

Ferrer-Miralles N, Rodríguez-Carmona E, Corchero JL, García-Fruitós E, Vázquez E, Villaverde A. Engineering protein self-assembling in protein-based nanomedicines for drug delivery and gene therapy. Crit Rev Biotechnol 2013 Oct 9. [PMID: 24102113, Epub ahead of print].

Fioravanti J, Medina-Echeverz J, Ardaiz N, Gomar C, Parra-Guillen ZP, Prieto J, et al. The fusion protein of IFN-alpha and Apolipoprotein A-I crosses the blood–brain barrier by a saturable transport mechanism. 2012;188:3988–92.

Foust KD, Nurre E, Montgomery CL, Hernandez A, Chan CM, Kaspar BK. Intravascular AAV9 preferentially targets neonatal neurons and adult astrocytes. Nat Biotechnol 2009;27:59–65.

Foust KD, Wang X, McGovern VL, Braun L, Bevan AK, Haidet AM, et al. Rescue of the spinal muscular atrophy phenotype in a mouse model by early postnatal delivery of SMN. Nat Biotechnol 2010;28:271–4.

Fu A, Zhou QH, Hui EK, Lu JZ, Boado RJ, Pardridge WM. Intravenous treatment of experimental Parkinson's disease in the mouse with an IgG–GDNF fusion protein that penetrates the blood–brain barrier. Brain Res 2010a;1352:208–13.

Fu AL, Zhou QH, Hui EKW, Lu JZ, Boado RJ, Pardridge WM. Intravenous treatment of experimental Parkinson's disease in the mouse with an IgG–GDNF fusion protein that penetrates the blood–brain barrier. 2010b;1352:208–13.

Fu AL, Hui EKW, Lu JZ, Boado RJ, Pardridge WM. Neuroprotection in stroke in the mouse with intravenous erythropoietin–Trojan horse fusion protein. 2011;1369:203–7.

Gabathuler RAGKMLCQTSYJsWVTZJWA. Development of a potential protein vector(NeuroTrans) to deliver drugs across the blood–brain barrier. Int Congr Ser 2005;1277:171–84.

Gabathuler R. Approaches to transport therapeutic drugs across the blood–brain barrier to treat brain diseases. Neurobiol Dis 2010a;37:48–57.

Gabathuler R. An engineered peptide compound platform technology incorporating angiopep for crossing the BBB. 999 Riverview Dr, Ste 208, Totowa, NJ 07512-1165 USA: Humana Press Inc.; 2010b.

Gessner A, Olbrich C, Schroder W, Kayser O, Muller RH. The role of plasma proteins in brain targeting: species dependent protein adsorption patterns on brain-specific lipid drug conjugate (LDC) nanoparticles. 2001;214:87–91.

Ghose AK, Viswanadhan VN, Wendoloski JJ. A knowledge-based approach in designing combinatorial or medicinal chemistry libraries for drug discovery. 1. A qualitative and quantitative characterization of known drug databases. J Comb Chem 1999;1: 55–68.

Ginn SL, Alexander IE, Edelstein ML, Abedi MR, Wixon J. Gene therapy clinical trials worldwide to 2. J Gene Med 2013;15:65–77.

Gozes I, Stewart A, Morimoto B, Fox A, Sutherland K, Schmeche D. Addressing Alzheimer's disease tangles: from NAP to AL-108. Curr Alzheimer Res 2009;6:455–60.

Grassin-Delyle S, Buenestado A, Naline E, Faisy C, Blouquit-Laye S, Couderc LJ, et al. Intranasal drug delivery: an efficient and non-invasive route for systemic administration focus on opioids. 2012;134:366–79.

Gray SJ, Blake BL, Criswell HE, Nicolson SC, Samulski RJ, McCown TJ, et al. Directed evolution of a novel adeno-associated virus (AAV) vector that crosses the seizure-compromised blood–brain barrier (BBB). Mol Ther 2010;18:570–8.

Gray SJ, Matagne V, Bachaboina L, Yadav S, Ojeda SR, Samulski RJ. Preclinical differences of intravascular AAV9 delivery to neurons and glia: a comparative study of adult mice and nonhuman primates. Mol Ther 2011;19:1058–69.

Grieger JC, Samulski RJ. Adeno-associated virus as a gene therapy vector: vector development, production and clinical applications. Adv Biochem Eng Biotechnol 2005;99:119–45.

Hansen Jr DW, Stapelfeld A, Savage MA, Reichman M, Hammond DL, Haaseth RC, et al. Systemic analgesic activity and delta-opioid selectivity in [2,6-dimethyl-Tyr1, D-Pen2, D-Pen5]enkephalin. J Med Chem 1992;35:684–7.

Hanson LR, Frey WH. Intranasal delivery bypasses the blood–brain barrier to target therapeutic agents to the central nervous system and treat neurodegenerative disease. BMC Neurosci 2008;9(Suppl. 3):S5.

Hanson M, Lobner D. In vitro neuronal cytotoxicity of latex and nonlatex orthodontic elastics. Am J Orthod Dentofacial Orthop 2004;126:65–70.

Iliff JJ, Wang M, Liao Y, Plogg BA, Peng W, Gundersen GA, et al. A paravascular pathway facilitates CSF flow through the brain parenchyma and the clearance of interstitial solutes, including amyloid beta. Sci Transl Med 2012;4:147ra111.

Janzer RC, Raff MC. Astrocytes induce blood–brain barrier properties in endothelial cells. Nature 1987;325:253–7.

Jin K, Xie L, Childs J, Sun Y, Mao XO, Logvinova A, et al. Cerebral neurogenesis is induced by intranasal administration of growth factors. Ann Neurol 2003;53:405–9.

Karkan D, Pfeifer C, Vitalis TZ, Arthur G, Ujiie M, Chen Q, et al. A unique carrier for delivery of therapeutic compounds beyond the blood–brain barrier. PLoS One 2008;3:e2469.

Kilic E, Dietz GP, Hermann DM, Bahr M. Intravenous TAT-Bcl-XL is protective after middle cerebral artery occlusion in mice. Ann Neurol 2002;52:617–22.
Kilic U, Kilic E, Dietz GP, Bahr M. Intravenous TAT-GDNF is protective after focal cerebral ischemia in mice. Stroke 2003;34:1304–10.
Kim WK, Alvarez X, Fisher J, Bronfin B, Westmoreland S, McLaurin J, et al. CD163 identifies perivascular macrophages in normal and viral encephalitic brains and potential precursors to perivascular macrophages in blood. Am J Pathol 2006;168:822–34.
Kim HR, Andrieux K, Gil S, Taverna M, Chacun H, Desmaele D, et al. Translocation of poly(-ethylene glycol-co-hexadecyl)cyanoacrylate nanoparticles into rat brain endothelial cells: role of apolipoproteins in receptor-mediated endocytosis. Biomacromolecules 2007;8:793–9.
Kordower JH, Charles V, Bayer R, Bartus RT, Putney S, Walus LR, et al. Intravenous administration of a transferrin receptor antibody–nerve growth factor conjugate prevents the degeneration of cholinergic striatal neurons in a model of Huntington disease. Proc Natl Acad Sci U S A 1994;91:9077–80.
Kratzer I, Wernig K, Panzenboeck U, Bernhart E, Reicher H, Wronski R, et al. Apolipoprotein A-I coating of protamine-oligonucleotide nanoparticles increases particle uptake and transcytosis in an in vitro model of the blood–brain barrier. J Control Release 2007a;117:301–11.
Kratzer I, Wernig K, Panzenboeck U, Bernhart E, Reicher H, Wronski R, et al. Apolipoprotein A-I coating of protamine-oligonucleotide nanoparticles increases particle uptake and transcytosis in an in vitro model of the blood–brain barrier. 2007b;117:301–11.
Kroll RA, Neuwelt EA. Outwitting the blood–brain barrier for therapeutic purposes: osmotic opening and other means. 1998;42:1083–99.
Kumar P, Wu H, McBride JL, Jung KE, Kim MH, Davidson BL, et al. Transvascular delivery of small interfering RNA to the central nervous system. Nature 2007;448:39–43.
Kurzrock R, Gabrail N, Chandhasin C, Moulder S, Smith C, Brenner A, et al. Safety, pharmacokinetics, and activity of GRN1005, a novel conjugate of Angiopep-2, a peptide facilitating brain penetration, and paclitaxel, in patients with advanced solid tumors. 2012;11:308–16.
Lee SY, Mattanovich D, Villaverde A. Systems metabolic engineering, industrial biotechnology and microbial cell factories. Microb Cell Fact 2012;11:156.
Li T, Bourgeois JP, Celli S, Glacial F, Le Sourd AM, Mecheri S, et al. Cell-penetrating anti-GFAP VHH and corresponding fluorescent fusion protein VHH-GFP spontaneously cross the blood–brain barrier and specifically recognize astrocytes: application to brain imaging. FASEB J 2012;26:3969–79.
Liu XF, Fawcett JR, Hanson LR, Frey WH. The window of opportunity for treatment of focal cerebral ischemic damage with noninvasive intranasal insulin-like growth factor-I in rats. J Stroke Cerebrovasc Dis 2004;13:16–23.
Ljubimova JY, Fujita M, Ljubimov AV, Torchilin VP, Black KL, Holler E. Poly(malic acid) nanoconjugates containing various antibodies and oligonucleotides for multitargeting drug delivery. Nanomedicine (Lond) 2008;3:247–65.
Lowenstein PR. Crossing the rubicon. Nat Biotechnol 2009;27:42–4.
Lu JZ, Boado RJ, Hui EK, Zhou QH, Pardridge WM. Expression in CHO cells and pharmacokinetics and brain uptake in the Rhesus monkey of an IgG-iduronate-2-sulfatase fusion protein. Biotechnol Bioeng 2011;108:1954–64.
Maggie J, Hsiang-Fa L, Sing-Ming C, Yi-Ju K, Li-Wen C. Peptide for transmigration across brain blood barrier and delivery systems comprising the same; 2010 [12/979, 804 [US2011/0165079 A1]. US].
Malcor JD, Payrot N, David M, Faucon A, Abouzid K, Jacquot G, et al. Chemical optimization of new ligands of the low-density lipoprotein receptor as potential vectors for central nervous system targeting. 2012;55:2227–41.
Mamot C, Drummond DC, Noble CO, Kallab V, Guo Z, Hong K, et al. Epidermal growth factor receptor-targeted immunoliposomes significantly enhance the efficacy of multiple anticancer drugs in vivo. Cancer Res 2005;65:11631–8.
Mandel RJ, Manfredsson FP, Foust KD, Rising A, Reimsnider S, Nash K, et al. Recombinant adeno-associated viral vectors as therapeutic agents to treat neurological disorders. Mol Ther 2006;13:463–83.
Mastrobattista E, van der Aa MA, Hennink WE, Crommelin DJ. Artificial viruses: a nanotechnological approach to gene delivery. Nat Rev Drug Discov 2006;5:115–21.
Matsuoka Y, Jouroukhin Y, Gray AJ, Ma L, Hirata-Fukae C, Li HF, et al. A neuronal microtubule-interacting agent, NAPVSIPQ, reduces tau pathology and enhances cognitive function in a mouse model of Alzheimer's disease. J Pharmacol Exp Ther 2008;325:146–53.
McCown TJ. Adeno-associated virus (AAV) vectors in the CNS. Curr Gene Ther 2005;5:333–8.
Negro-Demontel ML, Saccardo P, Giacomini C, Yáñez-Muñoz RJ, Ferrer-Miralles N, Vazquez E, et al. Comparative analysis of lentiviral vectors and modular protein nanovectors for traumatic brain injury gene therapy. Mol Ther Methods Clin Dev 2014;1:14047.
Niewoehner J, Bohrmann B, Collin L, Urich E, Sade H, Maier P, et al. Increased brain penetration and potency of a therapeutic antibody using a monovalent molecular shuttle. Neuron 2014;81:49–60.
Olbrich C, Gessner A, Kayser O, Muller RH. Lipid-drug-conjugate (LDC) nanoparticles as novel carrier system for the hydrophilic antitrypanosomal drug diminazenediaceturate. J Drug Target 2002;10:387–96.
Pardridge WM. Intravenous, non-viral RNAi gene therapy of brain cancer. Expert Opin Biol Ther 2004;4:1103–13.
Pardridge WM. Molecular Trojan horses for blood–brain barrier drug delivery. Curr Opin Pharmacol 2006;6:494–500.
Pardridge WM, Boado RJ. Reengineering biopharmaceuticals for targeted delivery across the blood–brain barrier. San Diego: Elsevier Academic Press Inc.; 2012.
Park TE, Singh B, Li H, Lee JY, Kang SK, Choi YJ, et al. Enhanced BBB permeability of osmotically active poly(mannitol-co-PEI) modified with rabies virus glycoprotein via selective stimulation of caveolar endocytosis for RNAi therapeutics in Alzheimer's disease. Biomaterials 2015;38:61–71.
Peluffo H, Aris A, Acarin L, Gonzalez B, Villaverde A, Castellano B. Nonviral gene delivery to the central nervous system based on a novel integrin-targeting multifunctional protein. Hum Gene Ther 2003;14:1215–23.
Peluffo H, Acarin L, Aris A, Gonzalez P, Villaverde A, Castellano B, et al. Neuroprotection from NMDA excitotoxic lesion by Cu/Zn superoxide dismutase gene delivery to the postnatal rat brain by a modular protein vector. BMC Neurosci 2006;7:35.
Peluffo H, Ii-Ruiz D, Ejarque-Ortiz A, Heras-Alvarez V, Comas-Casellas E, Martinez-Barriocanal A, et al. Overexpression of the immunoreceptor CD300f has a neuroprotective role in a model of acute brain injury. Brain Pathol 2012;22(3):318–28.
Poduslo JF, Curran GL. Increased permeability across the blood–nerve barrier of albumin glycated in vitro and in vivo from patients with diabetic polyneuropathy. Proc Natl Acad Sci U S A 1992;89:2218–22.
Polt R, Porreca F, Szabo LZ, Bilsky EJ, Davis P, Abbruscato TJ, et al. Glycopeptide enkephalin analogues produce analgesia in mice: evidence for penetration of the blood–brain barrier. Proc Natl Acad Sci U S A 1994;91:7114–8.
Prades R, Guerrero S, Araya E, Molina C, Salas E, Zurita E, et al. Delivery of gold nanoparticles to the brain by conjugation with a peptide that recognizes the transferrin receptor. Biomaterials 2012a;33:7194–205.
Prades R, Guerrero S, Araya E, Molina C, Salas E, Zurita E, et al. Delivery of gold nanoparticles to the brain by conjugation with a peptide that recognizes the transferrin receptor. 2012b;33:7194–205.
Qiao R, Jia Q, Huwel S, Xia R, Liu T, Gao F, et al. Receptor-mediated delivery of magnetic nanoparticles across the blood–brain barrier. ACS Nano 2012a;6:3304–10.
Qiao RR, Jia QJ, Huwel S, Xia R, Liu T, Gao FB, et al. Receptor-mediated delivery of magnetic nanoparticles across the blood–brain barrier. 2012b;6:3304–10.
Rao KS, Ghorpade A, Labhasetwar V. Targeting anti-HIV drugs to the CNS. Expert Opin Drug Deliv 2009;6:771–84.
Re F, Cambianica I, Sesana S, Salvati E, Cagnotto A, Salmona M, et al. Functionalization with ApoE-derived peptides enhances the interaction with brain capillary endothelial cells of nanoliposomes binding amyloid-beta peptide. 2011;156:341–6.
Reese TS, Karnovsky MJ. Fine structural localization of a blood–brain barrier to exogenous peroxidase. J Cell Biol 1967;34:207–17.
Reukov V, Maximov V, Vertegel A. Proteins conjugated to poly(butyl cyanoacrylate) nanoparticles as potential neuroprotective agents. Biotechnol Bioeng 2011a;108:243–52.
Reukov V, Maximov V, Vertegel A. Proteins conjugated to poly(butyl cyanoacrylate) nanoparticles as potential neuroprotective agents. 2011b;108:243–52.
Rodriguez-Carmona E, Villaverde A. Nanostructured bacterial materials for innovative medicines. Trends Microbiol 2010;18:423–30.
Rosenberg GA. Neurological diseases in relation to the blood–brain barrier. J Cereb Blood Flow Metab 2012;32:1139–51.
Ross TM, Martinez PM, Renner JC, Thorne RG, Hanson LR, Frey WH. Intranasal administration of interferon beta bypasses the blood–brain barrier to target the central nervous system and cervical lymph nodes: a non-invasive treatment strategy for multiple sclerosis. J Neuroimmunol 2004;151:66–77.
Rousselle C, Clair P, Smirnova M, Kolesnikov Y, Pasternak GW, Gac-Breton S, et al. Improved brain uptake and pharmacological activity of dalargin using a peptide-vector-mediated strategy. J Pharmacol Exp Ther 2003;306:371–6.
Rubin LL, Staddon JM. The cell biology of the blood–brain barrier. Annu Rev Neurosci 1999;22:11–28.
Schnyder A, Huwyler J. Drug transport to brain with targeted liposomes. NeuroRx 2005a;2:99–107.
Schnyder A, Huwyler J. Drug transport to brain with targeted liposomes. 2005b;2:99–107.
Song BW, Vinters HV, Wu D, Pardridge WM. Enhanced neuroprotective effects of basic fibroblast growth factor in regional brain ischemia after conjugation to a blood–brain barrier delivery vector. J Pharmacol Exp Ther 2002;301:605–10.
Spencer BJ, Verma IM. Targeted delivery of proteins across the blood–brain barrier. Proc Natl Acad Sci U S A 2007;104:7594–9.
Spitzenberger TJ, Heilman D, Diekmann C, Batrakova EV, Kabanov AV, Gendelman HE, et al. Novel delivery system enhances efficacy of antiretroviral therapy in a animal model for HIV-1 encephalitis. J Cereb Blood Flow Metab 2007;27:1033–42.
Steiniger SC, Kreuter J, Khalansky AS, Skidan IN, Bobruskin AI, Smirnova ZS, et al. Chemotherapy of glioblastoma in rats using doxorubicin-loaded nanoparticles. Int J Cancer 2004;109:759–67.
Stewart PA, Hayakawa EM. Interendothelial junctional changes underlie the developmental 'tightening' of the blood–brain barrier. Brain Res 1987;429:271–81.
Tao YH, Han JF, Dou HY. Brain-targeting gene delivery using a rabies virus glycoprotein peptide modulated hollow liposome: bio-behavioral study. 2012;22:11808–15.
Tian XH, Wei F, Wang TX, Wang D, Wang J, Lin XN, et al. Blood–brain barrier transport of Tat peptide and polyethylene glycol decorated gelatin–siloxane nanoparticle. 2012;68:94–6.
Tonra JR. Cerebellar susceptibility to experimental autoimmune encephalomyelitis in SJL/J mice: potential interaction of immunology with vascular anatomy. Cerebellum 2002;1:57–68.
Tosi G, Costantino L, Rivasi F, Ruozi B, Leo E, Vergoni AV, et al. Targeting the central nervous system: in vivo experiments with peptide-derivatized nanoparticles loaded with Loperamide and Rhodamine-123. J Control Release 2007;122:1–9.
Towne C, Raoul C, Schneider BL, Aebischer P. Systemic AAV6 delivery mediating RNA interference against SOD1: neuromuscular transduction does not alter disease progression in fALS mice. Mol Ther 2008;16:1018–25.
Tsai SJ. Peripheral administration of brain-derived neurotrophic factor to Rett syndrome animal model: a possible approach for the treatment of Rett syndrome. 2012;18:HY33–6.

Ulbrich K, Hekmatara T, Herbert E, Kreuter J. Transferrin- and transferrin-receptor-antibody-modified nanoparticles enable drug delivery across the blood–brain barrier (BBB). Eur J Pharm Biopharm 2009;71:251–6.
Ulbrich K, Knobloch T, Kreuter J. Targeting the insulin receptor: nanoparticles for drug delivery across the blood–brain barrier (BBB). J Drug Target 2011;19:125–32.
Unzueta U, Cespedes MV, Ferrer-Miralles N, Casanova I, Cedano JA, Corchero JL, et al. Intracellular CXCR4^{+} cell targeting with T22-empowered protein-only nanoparticles. Int J Nanomedicine 2012a;7:4533–44.
Unzueta U, Ferrer-Miralles N, Cedano J, Zikung X, Pesarrodona M, Saccardo P, et al. Non-amyloidogenic peptide tags for the regulatable self-assembling of protein-only nanoparticles. Biomaterials 2012b;33:8714–22.
Unzueta U, Saccardo P, Domingo-Espin J, Cedano J, Conchillo-Sole O, Garcia-Fruitos E, et al. Sheltering DNA in self-organizing, protein-only nano-shells as artificial viruses for gene delivery. Nanomedicine 2014;10:535–41.
Van DS, Bronselaer A, Nielandt J, Stalmans S, Wynendaele E, Audenaert K, et al. Brainpeps: the blood–brain barrier peptide database. Brain Struct Funct 2012;217:687–718.
Vazquez E, Villaverde A. Engineering building blocks for self-assembling protein nanoparticles. Microb Cell Fact 2010;9:101.
Vazquez E, Villaverde A. Microbial biofabrication for nanomedicine: biomaterials, nanoparticles and beyond. Nanomedicine (Lond) 2013;8:1895–8.
Vazquez E, Ferrer-Miralles N, Villaverde A. Peptide-assisted traffic engineering for nonviral gene therapy. Drug Discov Today 2008;13:1067–74.
Vazquez E, Ferrer-Miralles N, Mangues R, Corchero JL, Schwartz Jr S, Villaverde A. Modular protein engineering in emerging cancer therapies. Curr Pharm Des 2009;15:893–916.
Vazquez E, Roldan M, Diez-Gil C, Unzueta U, Domingo-Espin J, Cedano J, et al. Protein nanodisk assembling and intracellular trafficking powered by an arginine-rich (R9) peptide. Nanomedicine (Lond) 2010;5:259–68.
Wade LA, Katzman R. Synthetic amino acids and the nature of L-DOPA transport at the blood–brain barrier. J Neurochem 1975;25:837–42.
Wagner S, Zensi A, Wien SL, Tschickardt SE, Maier W, Vogel T, et al. Uptake mechanism of ApoE-modified nanoparticles on brain capillary endothelial cells as a blood–brain barrier model. 2012;7.
Wang JX, Sun X, Zhang ZR. Enhanced brain targeting by synthesis of 3′,5′-dioctanoyl-5-fluoro-2′-deoxyuridine and incorporation into solid lipid nanoparticles. Eur J Pharm Biopharm 2002;54:285–90.
White E, Bienemann A, Pugh J, Castrique E, Wyatt M, Taylor H, et al. An evaluation of the safety and feasibility of convection-enhanced delivery of carboplatin into the white matter as a potential treatment for high-grade glioma. 2012a;108:77–88.
White E, Bienemann A, Taylor H, Hopkins K, Cameron A, Gill S. A phase I trial of carboplatin administered by convection-enhanced delivery to patients with recurrent/progressive glioblastoma multiforme. 2012b;33:320–31.
Witt KA, Huber JD, Egleton RD, Roberts MJ, Bentley MD, Guo L, et al. Pharmacodynamic and pharmacokinetic characterization of poly(ethylene glycol) conjugation to met-enkephalin analog [D-Pen2, D-Pen5]-enkephalin (DPDPE). J Pharmacol Exp Ther 2001;298:848–56.
Wolburg H, Lippoldt A. Tight junctions of the blood–brain barrier: development, composition and regulation. Vascul Pharmacol 2002;38:323–37.
Wolf DA, Hanson LR, Aronovich EL, Nan Z, Low WC, Frey WH, et al. Lysosomal enzyme can bypass the blood–brain barrier and reach the CNS following intranasal administration. 2012;106:131–4.
Wu D, Pardridge WM. Central nervous system pharmacologic effect in conscious rats after intravenous injection of a biotinylated vasoactive intestinal peptide analog coupled to a blood–brain barrier drug delivery system. J Pharmacol Exp Ther 1996;279:77–83.
Wu D, Pardridge WM. Neuroprotection with noninvasive neurotrophin delivery to the brain. Proc Natl Acad Sci U S A 1999;96:254–9.
Xia H, Mao Q, Davidson BL. The HIV Tat protein transduction domain improves the biodistribution of beta-glucuronidase expressed from recombinant viral vectors. Nat Biotechnol 2001;19:640–4.
Yang WL, Huo TY, Barth RF, Gupta N, Weldon M, Grecula JC, et al. Convection enhanced delivery of carboplatin in combination with radiotherapy for the treatment of brain tumors. 2011;101:379–90.
Yao H, Wang K, Wang Y, Wang S, Li J, Lou J, et al. Enhanced blood–brain barrier penetration and glioma therapy mediated by a new peptide modified gene delivery system. Biomaterials 2014;37C:345–52.
Yazaki T, Ahmad S, Chahlavi A, Zylber-Katz E, Dean NM, Rabkin SD, et al. Treatment of glioblastoma U-87 by systemic administration of an antisense protein kinase C-alpha phosphorothioate oligodeoxynucleotide. Mol Pharmacol 1996;50:236–42.
Yemisci M, Caban S, Gursoy-Ozdemir Y, Lule S, Novoa-Carballal R, Riguera R, et al. Systemically administered brain-targeted nanoparticles transport peptides across the blood–brain barrier and provide neuroprotection. J Cereb Blood Flow Metab 2014. http://dx.doi.org/10.1038/jcbfm.2014.220. [Epub ahead of print].
Yu YP, Xu QQ, Zhang Q, Zhang WP, Zhang LH, Wei EQ. Intranasal recombinant human erythropoietin protects rats against focal cerebral ischemia. Neurosci Lett 2005;387:5–10.
Yu YJ, Zhang Y, Kenrick M, Hoyte K, Luk W, Lu Y, et al. Boosting brain uptake of a therapeutic antibody by reducing its affinity for a transcytosis target. Sci Transl Med 2011;3:84ra44.
Yue J, Liu S, Wang R, Hu X, Xie Z, Huang Y, et al. Fluorescence-labeled immunomicelles: preparation, in vivo biodistribution, and ability to cross the blood–brain barrier. 2012;12:1209–19.
Zensi A, Begley D, Pontikis C, Legros C, Mihoreanu L, Wagner S, et al. Albumin nanoparticles targeted with Apo E enter the CNS by transcytosis and are delivered to neurones. 2009;137:78–86.
Zensi A, Begley D, Pontikis C, Legros C, Mihoreanu L, Buchel C, et al. Human serum albumin nanoparticles modified with apolipoprotein A-I cross the blood–brain barrier and enter the rodent brain. J Drug Target 2010;18:842–8.
Zhang Y, Pardridge WM. Neuroprotection in transient focal brain ischemia after delayed intravenous administration of brain-derived neurotrophic factor conjugated to a blood–brain barrier drug targeting system. Stroke 2001;32:1378–84.
Zhang Y, Lee HJ, Boado RJ, Pardridge WM. Receptor-mediated delivery of an antisense gene to human brain, cancer cells. 2002;4:183–94.
Zhang Y, Calon F, Zhu C, Boado RJ, Pardridge WM. Intravenous nonviral gene therapy causes normalization of striatal tyrosine hydroxylase and reversal of motor impairment in experimental parkinsonism. Hum Gene Ther 2003;14:1–12.
Zhang Y, Schlachetzki F, Zhang YF, Boado RJ, Pardridge WM. Normalization of striatal tyrosine hydroxylase and reversal of motor impairment in experimental parkinsonism with intravenous nonviral gene therapy and a brain-specific promoter. Hum Gene Ther 2004a;15:339–50.
Zhang Y, Zhang YF, Bryant J, Charles A, Boado RJ, Pardridge WM. Intravenous RNA interference gene therapy targeting the human epidermal growth factor receptor prolongs survival in intracranial brain cancer. Clin Cancer Res 2004b;10:3667–77.
Zhang Y, Wang Y, Boado RJ, Pardridge WM. Lysosomal enzyme replacement of the brain with intravenous non-viral gene transfer. Pharm Res 2008;25:400–6.
Zhou QH, Fu A, Boado RJ, Hui EK, Lu JZ, Pardridge WM. Receptor-mediated abeta amyloid antibody targeting to Alzheimer's disease mouse brain. Mol Pharm 2011a;8:280–5.
Zhou QH, Hui EK, Lu JZ, Boado RJ, Pardridge WM. Brain penetrating IgG–erythropoietin fusion protein is neuroprotective following intravenous treatment in Parkinson's disease in the mouse. Brain Res 2011b;1382:315–20.
Zhu JH, Jiang YJ, Xu GL, Liu XF. Intranasal administration: a potential solution for cross-BBB delivering neurotrophic factors. 2012;27:537–48.

Annex 2

In Vivo Architectonic Stability of Fully de Novo Designed Protein-Only Nanoparticles

María Virtudes Céspedes,Ugutz Unzueta,Witold Tatkiewicz,Alejandro Sánchez-Chardi,Oscar Conchillo-Solé,Patricia Álamo,Zhikun Xu,Isolda Casanova,José Luis Corchero,Mireia Pesarrodona,Juan Cedano,Xavier Daura,Imma Ratera,Jaume Veciana,Neus Ferrer-Miralles,Esther Vazquez,Antonio Villaverde, andRamón Mangues

ACS nano, 2014, 8(5): 4166-4176.

ARTICLE

In Vivo Architectonic Stability of Fully *de Novo* Designed Protein-Only Nanoparticles

María Virtudes Céspedes,[†,‡] Ugutz Unzueta,[‡,§,∥] Witold Tatkiewicz,[‡,⊥] Alejandro Sánchez-Chardi,[#] Oscar Conchillo-Solé,[§] Patricia Álamo,[†,‡] Zhikun Xu,[‡,§,∥] Isolda Casanova,[†,‡] José Luis Corchero,[‡,§,∥] Mireia Pesarrodona,[‡,§,∥] Juan Cedano,[▽] Xavier Daura,[§,⊗] Imma Ratera,[‡,⊥] Jaume Veciana,[‡,⊥] Neus Ferrer-Miralles,[‡,§,∥] Esther Vazquez,[‡,§,∥] Antonio Villaverde,[‡,§,∥,*] and Ramón Mangues[†,‡]

[†]Oncogenesis and Antitumor Drug Group, Biomedical Research Institute Sant Pau (IIB-SantPau), Hospital de la Santa Creu i Sant Pau, C/Sant Antoni Maria Claret, 167, 08025 Barcelona, Catalonia, Spain, [‡]CIBER de Bioingeniería, Biomateriales y Nanomedicina (CIBER-BBN), Bellaterra, 08193 Barcelona, Catalonia, Spain, [§]Institut de Biotecnologia i de Biomedicina, Universitat Autònoma de Barcelona, Bellaterra, 08193 Barcelona, Catalonia, Spain, [∥]Departament de Genètica i de Microbiologia, Universitat Autònoma de Barcelona, Bellaterra, 08193 Barcelona, Catalonia, Spain, [⊥]Department of Molecular Nanoscience and Organic Materials, Institut de Ciencia de Materials de Barcelona (CSIC), Bellaterra, 08193 Barcelona, Catalonia, Spain, [#]Servei de Microscòpia, Universitat Autònoma de Barcelona, Bellaterra, 08193 Barcelona, Catalonia, Spain, [▽]Laboratory of Immunology, Universidad de la República, General Rivera 1350, Regional Norte, Salto, 50.000, Uruguay, and [⊗]Institució Catalana de Recerca i Estudis Avançats (ICREA), 08010 Barcelona, Catalonia, Spain

ABSTRACT The fully *de novo* design of protein building blocks for self-assembling as functional nanoparticles is a challenging task in emerging nanomedicines, which urgently demand novel, versatile, and biologically safe vehicles for imaging, drug delivery, and gene therapy. While the use of viruses and virus-like particles is limited by severe constraints, the generation of protein-only nanocarriers is progressively reachable by the engineering of protein−protein interactions, resulting in self-assembling functional building blocks. In particular, end-terminal cationic peptides drive the organization of structurally diverse protein species as regular nanosized oligomers, offering promise in the rational engineering of protein self-assembling. However, the *in vivo* stability of these constructs, being a critical issue for their medical applicability, needs to be assessed. We have explored here if the cross-molecular contacts between protein monomers, generated by end-terminal cationic peptides and oligohistidine tags, are stable enough for the resulting nanoparticles to overcome biological barriers in assembled form. The analyses of renal clearance and biodistribution of several tagged modular proteins reveal long-term architectonic stability, allowing systemic circulation and tissue targeting in form of nanoparticulate material. This observation fully supports the value of the engineered of protein building blocks addressed to the biofabrication of smart, robust, and multifunctional nanoparticles with medical applicability that mimic structure and functional capabilities of viral capsids.

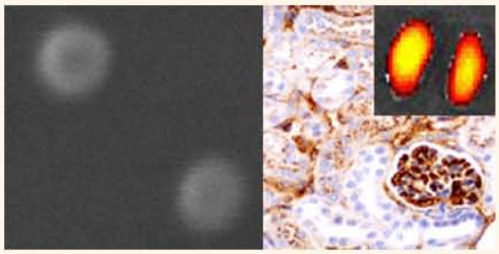

KEYWORDS: protein nanoparticles · building blocks · genetic engineering · biodistribution · targeting · drug delivery · nanoparticles · self-assembling · architectonic stability · protein folding · artificial viruses

Different types of materials are under examination for the construction of nanoparticles as molecular carriers in diagnosis and therapy, including lipids, diverse types of polymers, dendrimers, carbon nanotubes, and metals.[1] While the usage of many of these candidates is technically appealing and their manufacture economically feasible, biocompatibility issues severely compromise *in vivo* applicability.[2] Instead, proteins are ideal biomaterials for therapeutic applications, because of their natural structural roles, easy and cost-effective biological production, functional tunability by genetic engineering and full biocompatibility. Regarding drug delivery, several categories of entities found in nature support the concept of proteins as ideal nano- or microcages for molecular carriage. Infectious viruses,[3,4] virus-like particles (VLPs),[5] and more recently bacterial microcompartments (BMC)[6] and eukaryotic vaults[7] are being explored to transport and deliver nucleic acids, peptides or proteins,

* Address correspondence to antoni.villaverde@uab.cat.

Received for review May 5, 2013 and accepted April 7, 2014.

Published online April 07, 2014
10.1021/nn4055732

chemicals, metals, and quantum dots, among others. However, biosafety concerns in the case of viruses and narrow flexibility in readapting tropism and geometry in VLPs, vaults and BMCs, stress the need of novel protein nanocages that, being highly tunable and functionally versatile, would not be limited by the above constraints.

The highly organized protein shells of viruses and other natural protein nanocages are formed by self-assembling building blocks that interact through a complex combination of electrostatic, hydrophobic, van der Waals, and hydrogen bond forces.[8] So far, the *de novo* design of self-assembling protein monomers for tailored construction has poorly advanced and it is reluctant to generic rational design.[9] Self-assembling amyloidogenic peptides, although showing a wide spectrum of applications in nanomedicine,[9] are unable to generate regular sized shells for controlled drug encapsulation, and their biological fabrication poses important challenges. Concerning full proteins, a limited number of engineering approaches have rendered self-organizing cages or filaments, by adapting oligomerization domains from natural oligomeric proteins,[10−13] through the *in silico* assisted fine engineering of protein−protein interfaces[14] or by designing disulfide bonds between cysteine-carrying modified stretches.[15]

Recently,[16] we have described a new protein engineering principle for the construction of self-assembling, protein-only nanoparticles, based on the combined use of one cationic peptide plus a polyhistidine. These peptides, fused at either end termini of recombinant proteins, confer tagged monomers (structurally different protein species such as GFP and p53) with a strong dipolar charge distribution that supports spontaneous self-organization as monodisperse nanoparticulate materials. The size of these particles can be regulated by the ionic strength and, specially, by the composition in the cationic residues of the N-terminal tag (larger particle size when tails contain more cationic residues, under a lineal dependence).[16] The N-terminal peptide acts, in addition, as a cell-receptor specific ligand that confers targeting properties to the particle.[16] The relevance of this engineering principle relies on its generic applicability, since contrarily to other proposed approaches it is not limited to any particular protein species and it does not require precise amino acid stretches or composition in the building block to ensure proper assembly, as, potentially, any protein can be tagged to promote self-organization. These peptide-driven nanoparticles have been proven useful for the targeted intracellular delivery of proteins[17] and expressible DNA,[18] so far in absence of detectable cellular or organic toxicity.[19]

In particular, the modular protein T22-GFP-H6 was constructed under such tag-based principle, and it forms regular, 13 nm-nanoparticles that internalize, in a particulate form, in CXCR4-expressing cells (T22 being a peptidic ligand of CXCR4[20]).[19] When administered in metastatic colorectal cancer animal models in which CXCR4 overexpression is clinically relevant, T22-GFP-H6 shows an excellent biodistribution and it is internalized by $CXCR4^+$ cells in the primary tumor and also in the metastatic foci.[16] While this fact is highly promising regarding medical applicability of this platform, it is not clear whether the intermolecular interactions promoted by these nanoarchitectonic peptides are strong enough to ensure the stability of nanoparticles *in vivo*. In fact, the occurrence of T22-GFP-H6 in target cells and tissues determined by immunohistochemistry does not ensure that the nanoparticulate structure has been maintained during *in vivo* administration. The *in vivo* stability of the nanoparticle formed *in vitro* needs to be confirmed in order to implement this platform as a generic tool for drug design. In fact, if the protein−protein interactions promoted by the peptidic tags are weaker and less complex than those supporting assembling of infectious viruses, VLPs, vaults, and BMC shells, it could be not ruled out that the nanoparticles formed *in vitro* by artificial monomers would be immediately disassembled once administered, as the bloodstream and intracellular media are rich in charged molecules. In this context, limited stability and a premature release of cargo drugs or imaging agents would fully invalidate the system for further development.

In this regard, determining if a multifunctional protein reaches its target tissue in a nanoparticulate form or as disassembled monomers is not easily approachable experimentally. The *a priori* choice transmission electron microscopy (TEM) does not offer enough resolution to discriminate between monomeric and nanoparticulate forms (~6 *versus* ~13 nm) of protein materials inside target cells (a complex and heterogeneous protein-rich media with similar electrodensity than recombinant proteins), and also between internalized and endogenous protein structures within this size range. Antibodies and gold nanoparticles used in immunolabeling techniques for TEM are also within the same size range. Therefore, we have determined here the *in vivo* architectonic stability of *de novo* designed protein nanoparticles (and therefore, the validity of the whole architectonic principle) by an approach alternative to direct TEM observation that permits a rapid and feasible *in vivo* translation and a refined analysis at the whole body level. This is based on the monitoring of renal clearance and biodistribution of several reporter building blocks (constructs R9-GFP-H6, T22-GPP-H6, T22-IRFP-H6) administered as either monomers (<7 nm) or assembled entities (>7 nm). Parental monomeric species, as well as closely related protein variants that do not form nanoparticles, have been also used as controls. As renal filtration occurs for compounds with a size lower or around

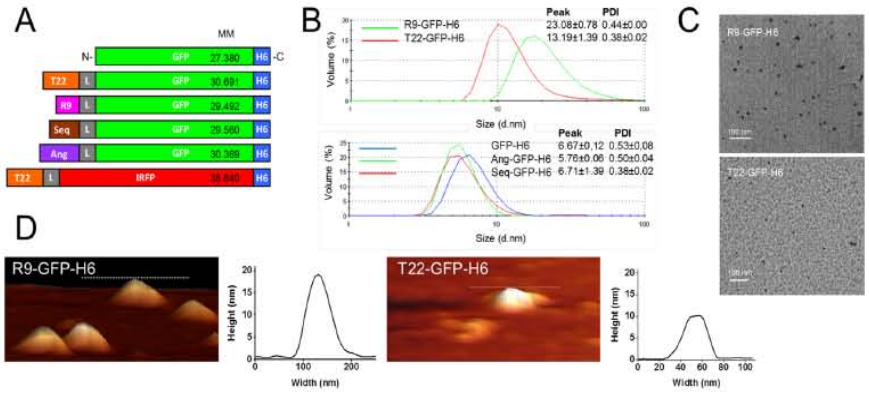

Figure 1. *In vitro* **assembling of protein-only nanoparticles. (A) Schematic representation of all protein constructs used in the study. Precise amino acid sequences of R9, T22, Ang (Angiopep-2), and Seq (Seq-1) have been given elsewhere.[18,19] L is a linker peptide commonly used in phage display (GGSSRSS).[42] The molecular masses (MM) of proteins were determined by mass spectroscopy, and they were coincident with predicted values. (B) Size of protein complexes formed by distinct GFP variants, measured by DLS in representative experiments. Peak and polydispersion index (PDI) are shown for each plot. (C) TEM images of protein nanoparticles upon purification from producing bacteria. (D) AFM images of randomly selected nanoparticles and topography cross sections of isolated entities. Measurements have been done in liquid with a tip radius of 10 nm. Then, the width (but not the high) of the particles is inherently overestimated.**

7 nm,[21] accumulation of the administered material in kidney but not in target tissues would be indicative of disassembling, while occurrence in target tissues but not in kidney would prove the *in vivo* stability of nanoparticles. Interestingly, the obtained results indicate that nanoparticles formed *in vitro* are highly stable during systemic circulation, thus proving the structural robustness and strong potential of end-terminal cationic tags as nanoarchitectonic tools for medical applications.

RESULTS AND DISCUSSION

The fusion of N-terminal cationic peptides to H6-tagged GFP promotes the self-organization of the construct into protein-only nanoparticles of sizes ranging from 10 to 50 nm.[16] These particles are immediately observed upon protein purification from recombinant bacteria and they probably assemble in the storage buffer against which the protein is dialyzed after elution. Being highly cationic, peptides R9 and T22 (used in nanomedicine for brain targeting and $CXCR4^+$ cell targeting respectively, Figure 1A) support the self-assembling of GFP-H6 as fully fluorescent particles of ~20 and ~13 nm (Figure 1B). The sizes of these particles, primarily determined by DLS, were confirmed by TEM (Figure 1C) and atomic force microscopy (AFM) (Figure 1D, and Supporting Information S Figures 1 and 2). In contrast, the noncationic peptides Ang-and Seq fail in promoting any supramolecular organization of the fusion proteins, and the size of the monomers was coincident in both cases with that of GFP-H6 (around 6 nm, Figure 1 B).

In mice, upon single intravenous (iv) administration at equal doses, Ang-GFP-H6, Seq-GFP-H6, and the parental GFP-H6 accumulated in kidney (Figure 2A–C), indicative of renal clearance and in agreement with the occurrence of these proteins in a monomeric form also *in vivo*. Contrarily, R9-GFP-H6 and T22-GFP-H6 were not observed in kidney (Figure 2A–C), suggesting that the nanoparticulate architecture reached by these proteins *in vitro* (Figure 1C,D) was maintained *in vivo* during circulation in blood. No protein was detected in lung, heart, spleen or liver in any case (Figure 2A). Consistently with their lack of renal clearance, the fluorescence emitted by R9-GFP-H6 and T22-GFP-H6 was detectable in plasma showing a first fast half-life of rapid distribution in the blood compartment, followed by a second and slow half-life of long-lasting permanence in blood (Figure 2D, and Supporting Information Table 1). Leucocytes and platelets showed lack of fluorescence accumulation for R9-GFP-H6, whereas fluorescence after T22-GFP-H6 administration was slightly increased in these blood cells as compared to background fluorescence in nonaccumulating tissues, but it was until 100 times lower than fluorescence reached by T22-GFP-H6 in tumor tissue. No accumulation was observed in red blood cells (Supporting Information S Figure 3). Although *a priori* it could be not discarded that the absence of protein in kidney would be due to a proteolytic instability and fast degradation, T22-GFP-H6 was observed to be highly stable in plasma and when administered to colorectal cancer mice models it accumulated in primary tumors and metastatic foci.[19] The combination of all these data was indicative that the protein reached its target in a full-length form. In this particular construct, the N-terminal peptide T22 was at the same time an architectonic tag and a cell-specific ligand, as it binds the cell surface receptor CXCR4 and internalizes $CXCR4^+$ cells.[19,20] Interestingly,

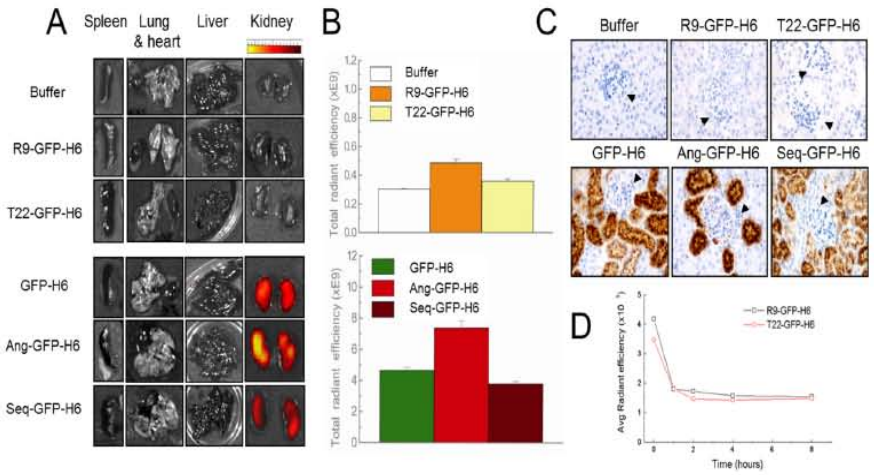

Figure 2. Stability and biodistribution of protein constructs. (A) GFP signal registered *ex vivo* in mouse spleen, lung, heart, liver sections, and kidneys 2 h after iv administration of 500 μg of each protein or buffer alone. (B) Quantitative determination of fluorescence in analyzed kidneys expressed as the total radiant efficiency (photon/s/cm^2/sr/μW/cm^2) of right and left kidneys for each mouse. The slight variations found when comparing proteins could be due to differences in the specific fluorescence, as protein sizes are rather similar (Figure 1). (C) Immunohistochemical anti-GFP detection of the administered proteins in the renal tissue, which is only observed if the small size (<7 nm) of the administered material determines its filtration and accumulation in the renal glomeruli while being excreted (400× magnification). Arrowheads show high density of hematoxylin stained nuclei (blue) corresponding to cells in the renal tissue, including glomerular cells. Note the absence of GFP staining in animals administered with R9- and T22-containing proteins, and the presence of signal when Ang- and Seq-derived proteins were administered (brown staining). (D) Pharmacokinetics of R9-GFP-H6 and T22-GFP-H6 after a 200 μg intravenous bolus administration. GFP fluorescence was recorded in plasma obtained after blood centrifugation at time 0, 1, 2, 4, 8 h. The elimination rate constant (Kel), and half-life of elimination (t1/2), were calculated using a one-compartment model and a semi-log plot of plasma concentration *versus* time curve (see Supporting Information Table 1). R9-GFP-H6 and T22-GFP-H6 showed a fast distribution in the blood compartment followed by a slow half-life of recirculation in blood.

no enhancement of apoptosis was observed in any of the checked organs, namely, nontumoral lung, heart, spleen, and liver (Supporting Information S Figure 4), and no loss of weight or other pathological signs of toxicity were observed in any of the administered animals as compared to buffer-treated animals (not shown). The absence of cellular toxicity of T22-GFP-H6 *in vitro* had been already reported,[19] altogether indicating a potential of these protein particles for *in vivo* applications.

To complement these data, we first confirmed the proteolytic stability of R9-GFP-H6 and related monomeric proteins in plasma and serum (Figure 3A) that was as high as that observed in T22-GFP-H6.[19] Then, the biodistribution analysis of R9-GFP-H6 upon administration determined that this protein nanoparticles localized in brain (a background occurrence of GFP-H6 was also determined; Figure 3B,C). This was not completely unexpected as previous findings suggested a BBB-crossing potential of R9 and related arginine rich peptides.[22,23] Since neither R9- nor T22-empowered proteins were detected in lung or heart (Figure 2A), the possibility of unspecific protein aggregation can be strongly excluded, whereas the lack of accumulation in spleen or liver indicate that they are not taken by the mononuclear phagocyte system that affects other categories of nanoparticles.[24,25] Again, the absence of these proteins in kidney must be exclusively attributed to their nanoparticulate organization that prevents size-dependent clearance. Renal filtration of parental GFP-H6 and related nonassembling proteins also indicated that these constructs, with a size very close to the threshold for filtration, do not tend to aggregate or assemble *in vivo* and that they keep their monomeric form during circulation in blood.

While offering an enormous potential in the design of artificial viruses and protein nanoparticles for medical purposes,[26] the high *in vivo* architectonic stability of R9-GFP-H6 and T22-GFP-H6 observed here was not anticipated. As R9 and T22 are highly cationic and the whole chimerical constructs show a dipolar charge distribution,[16] we expected electrostatic charges to be the main drivers of protein assembly. Then, nanoparticle stability in media with a high load of charged components, such as bloodstream (negatively charged proteins and a wide catalogue of ions), was at least initially surprising, as we could presume molecular competitions between charged agents and building blocks and consequent particle dissociation. Experimental data indicated, instead, that nanoparticles formed *in vitro* keep such organization also *in vivo*. To test this "structural memory", we evaluated renal clearance of a novel modular protein generated in this

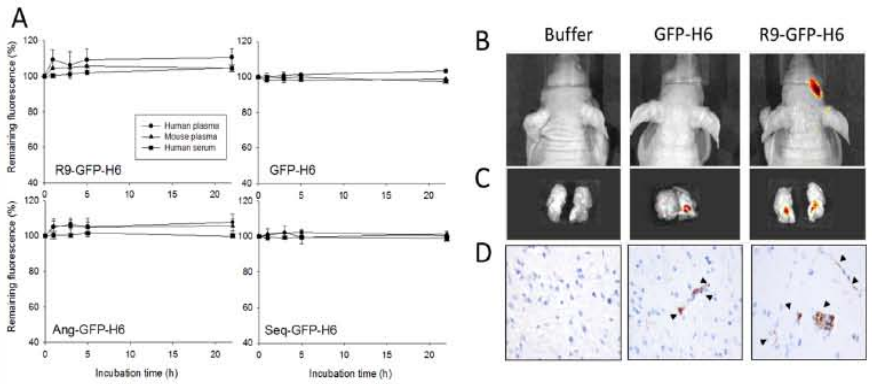

Figure 3. Stability and biodistribution of R9-GFP-H6. (A) *In vitro* stability of protein R9-GFP-H6 and control proteins GFP-H6, Ang-GFP-H6, and Seq-GFP-H6 in human plasma (circles), mouse plasma (triangles), and human serum (squares), monitored by fluorescent emission. (B) *In vivo* whole-body recording of a representative mouse 2 h after iv administration with buffer alone, with 500 μg of GFP-H6 or R9-GFP-H6, showing occurrence of fluorescence in the brain. (C) GFP fluorescence signal recording in *ex vivo* brain sagittal sections of a representative mouse. (D) Inmunohistochemical detection of the protein using and anti-GFP antibody, in mouse brain sections 2 h after iv administration of 500 μg of GFP-H6 and R9-GFP-H6 of buffer alone (400×). Arrows show protein accumulation in the brain parenchyma.

study (T22-IRFP-H6). In this construct, the core of the building block is iRFP, a dimeric fluorescent protein with primary sequence and structure unrelated to those of GFP. Once purified in low salt buffer, this construct self-organizes as nanoparticles of ~14 nm (Figure 4A,B), while it remains disassembled (probably as natural dimers) in high salt buffer (Figure 4A). Furthermore, adding salt to the protein when already assembled in low salt buffer (to reach the same salt concentration than in high salt buffer) does not alter particle size (Figure 4C). This is indicative of a tight organization of the protein assemblies and of robust cross-molecular interactions between monomers that are not responsive to alterations of the media conditions upon assembling. In this context, NP40 had also no effect on the stability of nanoparticles (Figure 4D) while the strong denaturant detergent SDS used as a control disassembled the constructs already at 0.1% (Figure 4E). The progressive reduction of the protein size observed at 0.1 and 1% could reflect a hierarchical disassembly of nanoparticles first releasing dimeric T22-IRFP-H6 building blocks and later individual denatured monomers.

To assess more robustly the *in vivo* stability and architectonic memory of protein nanoparticles, we administered the polypeptide T22-IRFP-H6 to colorectal cancer mice models, either in disassembled (high salt buffer) or assembled (low salt buffer) forms. Upon iv injection, renal clearance was observed only in the case of the disassembled protein, while tumor targeting was only observed in the nanoparticulate form (Figure 5A,B). This fact indicated again the preservation in the bloodstream of the molecular organization adopted *in vitro*, but also it proved that tissue targeting by efficient cell surface ligands is impaired by renal clearance, as it prevents individual proteins reaching the intended target. Presentation of the failing polypeptide in a nanostructured form with a size higher than 7 nm instead avoids renal excretion and it confers a high recirculation time in blood, thus offering opportunities for its accumulation in the target tissue. Importantly, since the cell ligand is the peptide T22 in both cases, no biased biodistribution could be potentially attributed to the use of different ligands but exclusively to the presentation in disassembled or assembled forms.

To explore the fine architecture of these nanoparticles, we first estimated the number of monomers forming them, by size-exclusion chromatography. Interestingly, the 23 nm R9-GFP-H6 particles peaked out of the column range, but still, an important fraction peaked at a value compatible with a pentameric organization of the protein, in agreement with previous *in silico* modeling.[16,18,19] There, the basic structure of R9-GFP-H6 nanoparticles has been suggested to be star-shaped discoidal pentamers, in which monomers are organized as a ring around an empty center.[18] On the other hand, T22-GFP-H6 and T22-IRFP-H6 were majorly organized in clusters of 10 monomers (Figure 6A), but minor peaks corresponding to 15 T22-IRFP-H6 monomers, to the T22-IRFP-H6 dimer (the natural form of IRFP), and to T22-GFP-H6 monomers were also observed. The occurrence of oligomers formed at least by 5, 10, and 15 monomers would account for the slight polydispersion of the particle size determined by DLS (Figure 1B) and strongly suggested the stacking of basic pentameric blocks in higher order structures. In this regard, the tubular organization observed in R9-GFP-H6-DNA complexes[27] is again fitting with a model in which nanodisks are piled as cylinders. The

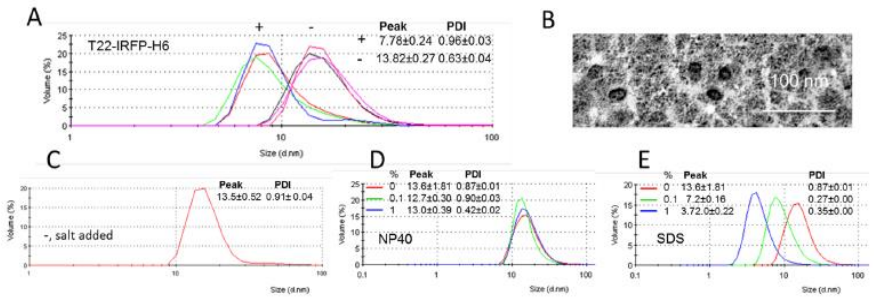

Figure 4. Structural memory of protein-only nanoparticles *in vitro*. (A) DLS size analysis of T22-IRFP-H6 purified in low salt (carbonate buffer, −) and high salt (carbonate buffer +334 mM NaCl, +). Different measures are plotted to evidence robustness of data. (B) TEM analysis of T22-IRFP-H6 purified in low salt buffer (assembled). (C) DLS size analysis of T22-IRFP-H6 purified in low salt buffer and in which additional salt was added later to reach 500 mM NaCl. Alternatively, NP40 (D) and SDS (E) were added up to 1%. Peak and PDI values are shown for each DLS plot.

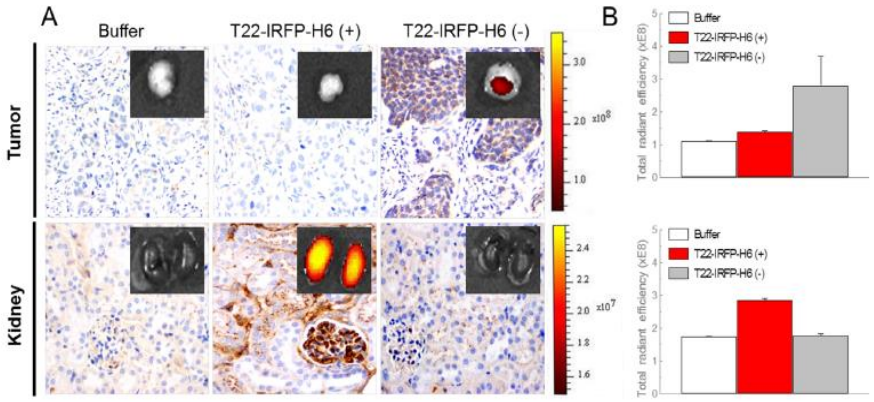

Figure 5. Structural memory of protein-only nanoparticles *in vivo*. Mouse tumor and kidney sections were registered 24 h after 50 μg iv administration of T22-IRFP-H6 in either high (+, disassembled) or low (−, assembled) salt buffers. (A) Immunohistochemical analysis of the tumor and glomeruli using an anti-His-tag antibody (400× magnification). Insets show IRFP fluorescence signal detected *ex vivo* in tissues of a representative mouse for each group, after subtracting the autofluorescence. (B) The total radiant efficiency (photon/s/cm^2/sr/μW/cm^2) as determined for each group in tumor (top) and kidney (bottom).

robustness of the emission spectra of assembled GFP variants when compared with regular GFP (Figure 6B) indicated little or no conformational changes in the GFP barrel associated with nanoparticle formation. In this context, the overhanging tails (R9 or T22 and H6) rather than the monomer core itself could be the main structure responsible for protein−protein interactions in the nanoparticle, as previously suggested.[16,18] In a last structural analysis, Cryo-TEM and especially high-resolution FESEM (Figure 6C) showed a ring shaped organization of all protein particles that, in the case of T22-GFP-H6, would be compatible with two staked pentamers. These new data confirmed again the particle sizes determined primarily by DLS, TEM, and AFM (Figure 1 and Supporting Information S Figures 1 and 2) and the circular distribution of the protein material (Figure 6C).

All these results clearly indicate that, once nanoparticles are formed, their architecture remains stable both *in vitro* and *in vivo*, and that while salt content modulates the initial configuration of protein−protein interactions, it does not disturb the structure of the formed supramolecular complexes. The cross-molecular contacts between monomers would be then more complex than mere electrostatic interactions and probably similar to those occurring in viruses and related entities. At a neutral pH, the polyhistidine tail is not charged, and the interaction between arginines and neutral histidines is known to be strong, as it may combine polar, hydrophobic, and cation-pi (between the guanidinium positive charge and the aromatic imidazole ring) interactions. These interactions may be favorable even when H6 is positively charged, as expected under slightly acidic environments.[28,29]

Because of the especially high definition of ring-shaped FESEM images and the occurrence of pentameric structures in R9-GFP-H6 nanoparticles, we

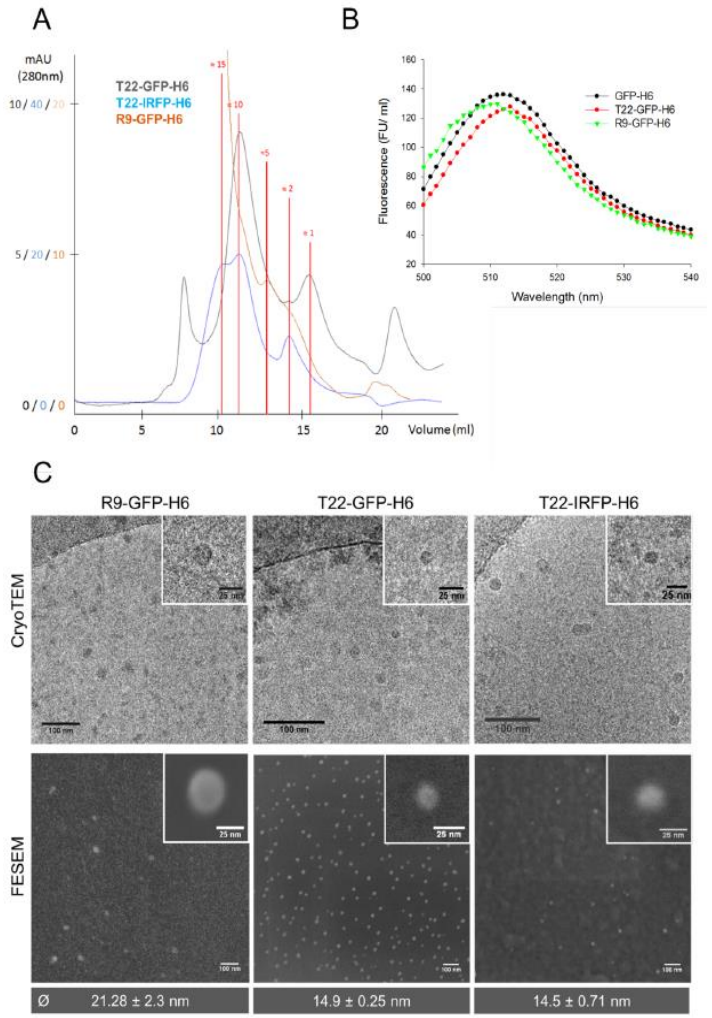

Figure 6. Fine architecture of protein-only nanoparticles. (A) Overlap of size exclusion chromatograms of different protein nanoparticles. Vertical red lines indicate the occurrence of nanoparticles by the position of peaks, indicating the estimated number of monomers that form them. (B) Overlap of fluorescence emission spectra of assembled protein nanoparticles (T22-GFP-H6, R9-GFP-H6) compared with that of the monomeric control protein (GFP-H6). (C) Wide field CryoTEM and FESEM images of protein nanoparticles formed by different proteins. The average size of each type of particle was determined by SEM and depicted. The insets show magnifications of single nanoparticles.

modeled protein−protein interactions in this particular construct.[16,18] Different probable star-shaped nanoparticles resulted from the docking process depending on the conformation adopted by the overhanging end-terminal peptides, all of them in the range of 15−30 nm and compatible with the nanoparticle size (Figure 7). When resolving the energetics organizing the monomers, complex combinations of electrostatic interactions, van der Waals forces, and hydrogen bonds were found in all cases (Table 1), as in those occurring in natural protein complexes.[30] The strong weight of van der Waals forces and hydrogen bonds revealed that electrostatic contacts, although important, were not the unique actors in the self-assembling of modular monomers. In this context, capsid proteins interact mainly through a combination of electrostatic repulsion, hydrophobic attraction and specific contacts between given pairs of amino acids. These interactions impose a certain restriction in the orientation of the interaction during complex formation, and once this is formed, the weaker van der Waals forces complete the assembly. Varying the acidity and salinity conditions (or the concentration of Ca^{2+} ions) adjusts the relative balance between these competing interactions, thereby

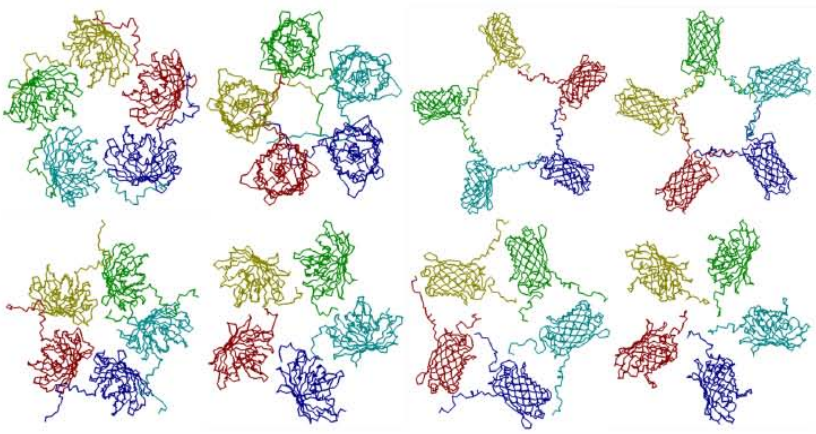

Figure 7. Different conformations of R9-GFP-H6 nanoparticles obtained in the docking process by using different configurations of overhanging R9 and H6 peptides. Models in the top row were generated with HADDOCK[40] using R9 residues as active and H6 residues as passive. Models in the bottom row were generated declaring only R9 residues as active. The energetics governing protein–protein interactions in each of these models are given in Table 1.

TABLE 1. Summary of Energetics Governing Monomer–monomer Interactions in the Molecular Models Depicted in Figure 4

model[a]	hydrogen bond[b]	van der Waals[b]	electrostatics[b]
UP 1	−47.34	−65	−21.56
UP 2	−44.97	−57.16	−6.61
UP 3	−29.13	−42.38	−7.33
UP 4	−31.6	−38.18	−10.85
DOWN 1	−26.45	−30.56	2.86
DOWN 2	−23.13	−25.79	−4.6
DOWN 3	−12.64	−20.78	1.02
DOWN 4	−7.57	−11.83	12.21

[a] Models refer to those depicted in Figure 7, in top and bottom rows, numbered from left to right. [b] Values were calculated with FoldX and are given in kcal/mol.

favoring assembly or disassembly. Electrostatic contacts might be the starting force promoting initial protein–protein contacts in artificial protein nanoparticles, which are later complemented with other type of interactions by slight conformational/spatial adjustments.

Linked to their high functional versatility, proteins (in form of ligands or antibodies) are preferred to functionalize most of the currently developed drug vehicles targeted to specific cell types.[31] In addition, because of the high protein biocompatibility and versatility offered by genetic engineering, protein-only nanoparticles are extremely promising in nanomedicine as they can recruit, apart from cell targeting, a diversity of functions that are appealing in drug delivery such as self-assembling, cage formation, nucleic acid binding, endosomal escape, and nuclear transport.[32−34] The less desired immunogenicity associated with proteins is expected to be solved by using homologous and biologically inert proteins (such as albumin) as scaffolds for nanoparticle construction.[35] However, protein self-assembling is far from full rational control. This is due to the current inability in linking molecular architecture with the forces that regulate cross-molecular interactions.[30] In fact, the actual complexity that allows correct assembling of viral shells is not reflected by the apparent simplicity of the capsid components and it cannot be predicted in advance from the analysis of the monomers. Here we prove that the assembly promoted by a short cationic peptide (such as R9 or T22) combined with a hexahistidine tail, fused to the end termini of different proteins acting as building blocks, mimic the organization of natural protein complexes such as viral shells, conferring a high stability of the nanoparticle once administered in the bloodstream. Importantly, the efficient tissue targeting combined with absence of renal filtration indicates that R9 and T22 peptides maintain their activities as ligands while promoting the cross-molecular interactions between monomers in tightly assembled nanoparticles. In the particular case of T22, its targeting to $CXCR4^+$ cells makes this tag not only appealing for drug delivery in colorectal cancer but also in the treatment of other neoplasias (e.g., breast, ovary, prostate cancer, or acute myeloid leukemia),[36] in which high membrane expression of CXCR4 correlates with poor prognosis. Protein nanoparticles displaying effective T22 tags could also be used as vehicles for targeting other diseases in which the pathological mechanisms involve CXCR4 expression, such as pulmonary fibrosis[37] or myocardial infarction.[38]

Since the tags tested here promote self-assembling of structurally diverse proteins such as GFP,[16] p53,[16] and iRFP (the present study), it opens a plethora of opportunities in selecting monomer cores that could be more convenient to avoid immune responses (namely homologous proteins) when administering

protein nanoparticles in a clinical context. Furthermore, proteins such as p53 with an intrinsic therapeutic value might gain stability and therefore activity when delivered with a particulate organization, in a step beyond the purpose of acting as mere carriers for the delivery of cargo drugs. Although ionic strength appears to be important during nanoparticle organization, this parameter does not affect the stability of already formed particles. This fact allows these entities to overcome biological barriers and reach their target in a nanoparticulate form. The engineering platform based on the addition of architectonic tags other than oligomerization domains offers a wide and unexpected plasticity in the design of multifunctional modular monomers (a diversity of protein species being suitable as cores), and it opens a spectrum of opportunities for the fully *de novo* design of robust protein-based carriers (artificial viruses) for emerging nanomedical applications.

CONCLUSIONS

We have here determined the functional robustness and architectonic stability of fully *de novo* designed protein-only nanoparticles, based on a generic engineering principle in which modular monomers are tagged with end-terminal cationic peptides. A sharp coincidence between nanoparticle formation *in vitro* and the *in vivo* escape from renal filtration has been revealed for several model proteins, proving the maintenance of protein−protein interactions in the bloodstream. Then, the architectonic principles described here offer promise to approach a rational design of self-assembling artificial viruses based on recombinant proteins for nanomedical applications *in vivo*.

METHODS

Proteins and Protein Purification. R9-GFP-H6 and T22-GFP-H6 are modular proteins in which the cationic peptides R9 (nine arginines,[23]) and T22 (derived from polyphemusin II,[20]) are fused to the amino terminus of a hexahistine C-tagged GFP (GFP-H6). These peptides, apart from providing positive charges that create a dipolar building block,[19] confer targeting properties to the resulting nanoparticle. In the case of T22, a ligand of CXCR4,[20] this has been experimentally confirmed as the administered protein accumulates in primary and metastatic foci in a colorectal cancer model.[19] Ang-GFP-H6 and Seq-GFP-H6 are closely related proteins that do not form nanoparticles, since the amino-terminal tags are not cationic.[19] T22-IRFP-H6 was designed in house, and synthetic genes were provided and subcloned into pET22b plasmid vector (using NdeI and HindIII restriction sites) by Genescript (Piscataway, NJ). T22-IRFP-H6 has a similar modular scheme as T22-GFP-H6, but in this case, the central part of the fusion was not GFP but the near-infrared fluorescent dimeric protein IRFP.[39] All proteins were encoded by pET22b in *Escherichia coli* Origami B (BL21, OmpT$^-$, Lon$^-$, TrxB, Gor$^-$ (Novagen)), produced overnight at 20 °C upon 1 mM IPTG addition, and purified by Histidine-tag affinity chromatography as described.[16] In short, we used HiTrap Chelating HP 1 mL columns (GE Healthcare) in an AKTA purifier FPLC (GE Healthcare). Cell extracts were disrupted at 1100 psi in a French Press (Thermo FA-078A), and soluble and insoluble fractions were separated by centrifugation at 20000*g* for 45 min at 4 °C. The soluble fraction was charged onto HiTrap column and subsequently washed with Tris 20 mM, NaCl 500 mM, Imidazole 10 mM, pH = 8 buffer. Proteins were eluted by linear gradient of high Imidazole concentration buffer (20 mM Tris, 500 mM NaCl, 500 mM Imidazole, pH = 8). Once in elution buffer, they were dialyzed against the most appropriate buffer regarding stability (empirically determined to minimize unspecific aggregation), which was found to be carbonate buffer (166 mM $NaHCO_3$, pH 7.4) for Ang-GFP-H6, Seq-GFP-H6, and T22-IRFP-H6, Tris NaCl (20 mM Tris, 500 mM NaCl, pH 7.4) for T22-GFP-H6, and Tris dextrose (20 mM Tris, 5% dextrose, pH 7.4) for GFP-H6 and R9-GFP-H6. The high salt buffer was always obtained by adding NaCl to reach a final concentration of 500 mM. Once dialyzed, protein samples were stored at −80 °C until use. Protein integrity was systematically assessed by Western blot analysis, MALDI-TOF, and N-terminal sequencing.

Analysis of Protein Stability. The stability of proteins GFP-H6, R9-GFP-H6, Ang-GFP-H6, and Seq-GFP-H6 was analyzed by measuring fluorescence emission after incubation in different media. R9-GFP-H6 was diluted, in triplicate, in either human serum (Sigma, ref: S2257-5ML, final concentration of 0.23 μg/μL) or in human and mouse plasma (final concentration of 0.11 μg/μL). GFP-H6, Ang-GFP-H6, and Seq-GFP-H6 were also diluted, in duplicate, in the same media, at final concentrations of 0.23, 0.13, and 0.08 μg/μL, respectively. Human blood was obtained from a healthy donor in the Hospital de Sant Pau. Murine blood (approximately 250 μL per mouse) was obtained from the submandibular facial vein of five control mice (25 g) in heparinized tubes. A plasma pool sample was obtained by centrifugation of total blood at 600*g* for 10 min at 4 °C. Immediately after dilution, samples were harvested (time 0) and their fluorescence signals were taken as the initial reference value (100%). Proteins were further incubated (at 37 °C, with agitation), and samples were taken, at different time points, up to 22 h. Protein functional stability during incubations was analyzed by fluorescence determination at 510 nm in a Cary Eclipse fluorescence spectrophotometer (Variant, Inc., Palo Alto, CA) using an excitation wavelength of 450 nm.

Dynamic Light Scattering. Volume size distribution of nanoparticles and monomeric protein versions were measured using a dynamic light scattering (DLS) analyzer at the wavelength of 633 nm, combined with noninvasive backscatter technology (NIBS) (Zetasizer Nano ZS, Malvern Instruments Limited, Malvern, U.K.). Samples were measured at 20 °C. DLS measurements of solvents were used as controls. The measurements were performed in triplicate.

Fluorescence Emission Spectra Determination. Nanoparticles fluorescence emission spectra from 500 to 540 nm was determined by a Cari Eclipse fluorescence spectrophotometer (Variant, Inc., Palo Alto, CA) using an excitation wavelength of 450 nm.

Transmission Electron Microscopy (TEM). Droplets of each protein sample (5 μL, 0.150 mg/mL) were deposited in duplicate onto carbon-coated copper grids for 2 min, and excess specimen was then withdrawn. A set of samples was submitted to negative staining with uranyl acetate, whereas the other set was rotary shadowed by evaporation of atomized platinum−carbon at an angle of 25°. Samples were observed with a Jeol 1400 transmission electron microscope, equipped with a CCD Gatan ES1000W Erlangshen camera.

Cryo Transmission Electron Microscopy (CryoTEM). Drops of protein solutions (3 μL) were deposited on Quantifoil R 1.2/1.3 grids and blotted to eliminate the excess of sample. Then, grids were plunged in liquid ethane in a Leica EM CPC, placed in a Gatan cryo-transfer specimen holder and observed in a Jeol JEM 2011 transmission electron microscope operating at 200 kV and equipped with a CCD Gatan 895 USC 4000 camera.

Field Emission Scanning Electron Microscopy (FESEM). To characterize the native morphology and distribution of protein nanoparticles, 5 μL of protein solution samples was deposited into a

silicon substrate, and excess of material was then removed. Samples were air-dried and observed without coating in a FESEM Zeiss Merlin operating at 2 kV. Images were acquired with a high-resolution in-lens secondary electron detector. ImageJ 1.46n software was used for nanoparticle size distribution analysis in FESEM images.

Atomic Force Microscopy (AFM). The analyses were performed in liquid with a commercial atomic force microscope (PicoSPM 5100 from Molecular Imaging Agilent Technologies, Inc., Santa Clara, CA) operating in acoustic mode. R9-GFP-H6 in 20 mM Tris buffer, pH 7.5, and 5% dextrose (4 μg/μL, 20 μL) was dropped onto a freshly cleaved mica surface and imaged in liquid. T22-GFP-H6 in sodium bicarbonate 1.4% buffer, pH 7.4 (4.3 μg/μL, 50 μL), was dropped onto a freshly cleaved mica surface and imaged in liquid. For the acoustic mode measurements, a silicon (Applied NanoStructures, Inc.) tip, with a radius of 10 nm, a nominal spring constant of 0.6−3.7 N/m, and a resonance frequency of 43−81 kHz was used.

Size Exclusion Chromatography. The molecular weight distribution of protein nanoparticles was determined by size exclusion chromatography after injection of 100 μL of samples in a previously calibrated Superdex200 10/300 GL (Tricorn) column (GE Healthcare).

Animals and Administration Regime. Five-week-old female Swiss nu/nu mice weighing between 18 and 20 g (Charles River, L-Abreslle, France), maintained in SPF conditions, were used for *in vivo* studies. All the *in vivo* procedures were approved by the Hospital de Sant Pau Animal Ethics Committee. We assessed stability, biodistribution, and renal clearance of protein constructs 2 h after iv administration of 500 μg/mouse (n = 3 mice). The control mice (n = 3) were administered iv in the appropriate buffer (20 mM Tris, 5% dextrose, pH 7.5, for R9-GFP-H6; 20 mM Tris, 500 mM NaCl, pH 7.4 for T22-GFP-H6; and 166 mM $NaCO_3H$, pH 7.5, for Seq- and Ang-empowered constructs). We also assessed the stability and renal clearance of T22-IRFP-H6 dissolved in high salt carbonate buffer (+) or low salt carbonate buffer (−) by iv administration of 50 μg/mouse (n = 3 mice), 24 h postadministration. Control mice were administered iv with the same buffer. The animal model for metastatic colorectal cancer has been described in detail elsewhere.[19]

Biodistribution of Nanoparticles in Mice. At 2 h post administration, mice were anesthetized with isofluorane and whole-body fluorescence was monitored using the IVIS Spectrum equipment (Xenogen, France). Subsequently, mice blood was collected, necropsy was performed, and all organs were removed and placed individually into wells to determine GFP or IRFP fluorescence in an IVIS Spectrum. Then, these organs were collected, fixed in 4% formaldehyde in phosphate buffer for 24 h, and finally embedded in paraffin for histological and immunohistochemical evaluation. Nanoparticle biodistribution in blood was determined after centrifugation using a ficoll gradient. In the resulting blood fractions, we registered GFP-derived fluorescence using an IVIS Spectrum. In all cases, the fluorescence signal was digitalized, and after subtracting the autofluorescence, it was displayed as a pseudocolor overlay and expressed in terms of Radiant efficiency for each protein group (control or experimental), dose, and time. To calculate half-life of elimination and the elimination rate constant (kel), GFP fluorescence signal was recorded in plasma at time 0, 1, 2, 4, 8 h after a single 200 μg intravenous dose of R9-GFP-H6 or of T22-GFP-H6.

Histopathology and Immunohistochemistry for GFP-His-Tag Proteins. Four-micrometer-thick sections were stained with hematoxylin−eosin (H&E) and a complete histopathological analysis was performed by two independent observers. In addition, a quantitation of the number of dead cells, as measured determining apoptotic bodies, in spleen, lung liver, kidney, and brain tissues, were counted in 10 microscopic fields (400×). The presence and location of the GFP-His tagged proteins in tissue sections were demonstrated by inmunohistochemistry. Paraffin-embedded tissue sections (4 μm) were deparaffinized, rehydrated, and washed in PBS-T. Antigen retrieval was performed by citrate buffer at 120 °C. After peroxidase activity was quenched by incubating the slides in 3% H_2O_2 for 10 min, the slides were washed in PBS-T. Slides were incubated 30 min with a primary antibody against GFP (1:100; Santa Cruz Biotechnology, Inc., Santa Cruz, CA) or histidine (1:1000; GE Healthcare, U.K.), washed in PBS-T, and incubated with the secondary horseradish peroxidase (HRP) conjugated antibody for 30 min at room temperature. The antibody interaction was then visualized using the chromogenic detection, in which the HRP cleaved the DAB substrate (DAKO, Denmark) to produce a brown precipitate at the location of the protein. Finally, sections were counterstained with hematoxylin, dehydrated with decreasing percentages of ethanol (100−95−70−50%) and mounted using DPX mounting medium. Representative pictures were taken using Cell^B software (Olympus Soft Imaging v 3.3, Japan) at 400× magnification.

Molecular Modeling. Models of R9-GFP-H6 monomers were built using Modeller 9v2 (24) and docked using HADDOCK v 2.0,[40] enforcing C5 symmetry and using N-terminal arginine residues as the active residues (Figure 4). The models were generated using the same protocols previously described.[18] The energetics of the models were analyzed with FoldX using the function AnalyseComplex.[41]

Conflict of Interest: The authors declare no competing financial interest.

Acknowledgment. We appreciate the technical support of Fran Cortés from the Cell Culture Unit of Servei de Cultius Cel.lulars Producció d'Anticossos i Citometria (SCAC, UAB), of Emma Rossinyol to Carmen Cabrera from Oncogenesis and Antitumor Drug Group, from Servei de Microscòpia (UAB), and of Amable Bernabé from Soft Materials Service (ICMAB-CSIC/CIBER-BBN). We are also indebted to the Nanotoxicology Platform and Protein Production Platform (http://www.ciber-bbn.es/en/programas/89-plataforma-de-produccion-de-proteinas-ppp). The authors also acknowledge the financial support granted to E.V. (PI12/00327) and R.M. (PI12/01861) from FIS, to A.V., J.V., and R.M. from Agència de Gestió d'Ajuts Universitaris i de Recerca (Grants 2009SGR-108 to A.V., SGR2009-516 to J.V. and 2009-SGR-1437 to R.M.), to R.M. and to A.V. from La Marató de TV3 (416/C/2013), to J.V. from DGI (Grant CTQ2010-19501) and from the Centro de Investigación Biomédica en Red (CIBER) de Bioingeniería, Biomateriales y Nanomedicina (NANOPROVIR, NANOCOMETS and PROGLIO projects), financed by the Instituto de Salud Carlos III with assistance from the European Regional Development Fund. U.U. received a fellowship grant from ISCIII. W.T. is grateful to the Consejo Superior de Investigaciones Cientificas (CSIC) for a "JAE-pre" fellowship. A.V. has been distinguished with an ICREA ACADEMIA Award.

Supporting Information Available: Wider AFM fields, biodistribution of nanoparticles and control proteins in blood cells, analysis of nanoparticle toxicity *in vivo* and stability in blood. This material is available free of charge *via* the Internet at http://pubs.acs.org.

REFERENCES AND NOTES

1. Villaverde, A. *Nanoparticles in Translational Science and Medicine*; Academic Press (Elsevier): London, 2011.
2. Sharifi, S.; Behzadi, S.; Laurent, S.; Forrest, M. L.; Stroeve, P.; Mahmoudi, M. Toxicity of Nanomaterials. *Chem. Soc. Rev.* **2012**, *41*, 2323–2343.
3. Giacca, M.; Zacchigna, S. Virus-Mediated Gene Delivery for Human Gene Therapy. *J. Controlled Release* **2012**, *161*, 377–388.
4. Edelstein, M. L.; Abedi, M. R.; Wixon, J. Gene Therapy Clinical Trials Worldwide to 2007—An Update. *J. Gene Med.* **2007**, *9*, 833–842.
5. Ma, Y.; Nolte, R. J.; Cornelissen, J. J. Virus-Based Nanocarriers for Drug Delivery. *Adv. Drug Delivery Rev.* **2012**, *64*, 811–825.
6. Corchero, J. L.; Cedano, J. Self-Assembling, Protein-Based Intracellular Bacterial Organelles: Emerging Vehicles for Encapsulating, Targeting and Delivering Therapeutical Cargoes. *Microb. Cell Fact.* **2011**, *10*, 92.
7. Rome, L. H.; Kickhoefer, V. A. Development of the Vault Particle as a Platform Technology. *ACS Nano* **2013**, *7*, 889–902.
8. Zlotnick, A. Are Weak Protein-Protein Interactions the General Rule in Capsid Assembly? *Virology* **2003**, *315*, 269–274.

9. Lakshmanan, A.; Zhang, S.; Hauser, C. A. Short Self-Assembling Peptides as Building Blocks for Modern Nanodevices. *Trends Biotechnol.* **2012**, *30*, 155–165.
10. Doll, T. A.; Raman, S.; Dey, R.; Burkhard, P. Nanoscale Assemblies and Their Biomedical Applications. *J. R. Soc., Interface* **2013**, *10*, No. 20120740.
11. Lai, Y.T.; Cascio, D.; Yeates, T. O. Structure of a 16-nm Cage Designed by Using Protein Oligomers. *Science* **2012**, *336*, 1129.
12. Bai, Y.; Luo, Q.; Zhang, W.; Miao, L.; Xu, J.; Li, H.; Liu, J. Highly Ordered Protein Nanorings Designed by Accurate Control of Glutathione S-Transferase Self-Assembly. *J. Am. Chem. Soc.* **2013**, *135*, 10966–10969.
13. Yang, Y.; Burkhard, P. Encapsulation of Gold Nanoparticles into Self-Assembling Protein Nanoparticles. *J. Nanobiotechnol.* **2012**, *10*, 42.
14. King, N. P.; Sheffler, W.; Sawaya, M. R.; Vollmar, B. S.; Sumida, J. P.; Andre, I.; Gonen, T.; Yeates, T. O.; Baker, D. Computational Design of Self-Assembling Protein Nanomaterials with Atomic Level Accuracy. *Science* **2012**, *336*, 1171–1174.
15. Usui, K.; Maki, T.; Ito, F.; Suenaga, A.; Kidoaki, S.; Itoh, M.; Taiji, M.; Matsuda, T.; Hayashizaki, Y.; Suzuki, H. Nanoscale Elongating Control of the Self-Assembled Protein Filament with the Cysteine-Introduced Building Blocks. *Protein Sci.* **2009**, *18*, 960–969.
16. Unzueta, U.; Ferrer-Miralles, N.; Cedano, J.; Zikung, X.; Pesarrodona, M.; Saccardo, P.; Garcia-Fruitos, E.; Domingo-Espin, J.; Kumar, P.; Gupta, K. C.; *et al.* Non-Amyloidogenic Peptide Tags for the Regulatable Self-Assembling of Protein-Only Nanoparticles. *Biomaterials* **2012**, *33*, 8714–8722.
17. Vazquez, E.; Cubarsi, R.; Unzueta, U.; Roldan, M.; Domingo-Espin, J.; Ferrer-Miralles, N.; Villaverde, A. Internalization and Kinetics of Nuclear Migration of Protein-Only, Arginine-Rich Nanoparticles. *Biomaterials* **2010**, *31*, 9333–9339.
18. Vazquez, E.; Roldan, M.; Diez-Gil, C.; Unzueta, U.; Domingo-Espin, J.; Cedano, J.; Conchillo, O.; Ratera, I.; Veciana, J.; Daura, X.; *et al.* Protein Nanodisk Assembling and Intracellular Trafficking Powered by an Arginine-Rich (R9) Peptide. *Nanomedicine (London, U.K.)* **2010**, *5*, 259–268.
19. Unzueta, U.; Cespedes, M. V.; Ferrer-Miralles, N.; Casanova, I.; Cedano, J. A.; Corchero, J. L.; Domingo-Espin, J.; Villaverde, A.; Mangues, R.; Vazquez, E. Intracellular CXCR4$^+$ Cell Targeting with T22-Empowered Protein-Only Nanoparticles. *Int. J. Nanomed.* **2012**, *7*, 4533–4544.
20. Murakami, T.; Zhang, T. Y.; Koyanagi, Y.; Tanaka, Y.; Kim, J.; Suzuki, Y.; Minoguchi, S.; Tamamura, H.; Waki, M.; Matsumoto, A.; *et al.* Yamamoto, N. Inhibitory Mechanism of the CXCR4 Antagonist T22 against Human Immunodeficiency Virus Type 1 Infection. *J. Virol.* **1999**, *73*, 7489–7496.
21. Feng, B.; LaPerle, J. L.; Chang, G.; Varma, M. V. Renal Clearance in Drug Discovery and Development: Molecular Descriptors, Drug Transporters and Disease State. *Expert Opin. Drug Metab. Toxicol.* **2010**, *6*, 939–952.
22. Kumar, P.; Wu, H.; McBride, J. L.; Jung, K. E.; Kim, M. H.; Davidson, B. L.; Lee, S. K.; Shankar, P.; Manjunath, N. Transvascular Delivery of Small Interfering RNA to the Central Nervous System. *Nature* **2007**, *448*, 39–43.
23. Saccardo, P.; Villaverde, A.; Gonzalez-Montalban, N. Peptide-Mediated DNA Condensation for Non-Viral Gene Therapy. *Biotechnol. Adv.* **2009**, *27*, 432–438.
24. Moghimi, S. M.; Hunter, A. C. Capture of Stealth Nanoparticles by the Body's Defences. *Crit Rev. Ther. Drug Carrier Syst.* **2001**, *18*, 527–550.
25. Moghimi, S. M.; Hunter, A. C.; Murray, J. C. Long-Circulating and Target-Specific Nanoparticles: Theory to Practice. *Pharmacol. Rev.* **2001**, *53*, 283–318.
26. Ferrer-Miralles, N.; Rodriguez-Carmona, E.; Corchero, J. L.; Garcia-Fruitos, E.; Vazquez, E.; Villaverde, A. Engineering Protein Self-Assembling in Protein-Based Nanomedicines for Drug Delivery and Gene Therapy. *Crit. Rev. Biotechnol.* [Epub ahead of print]. DOI: 10.3109/07388551.2013.833163. Published online Oct 9, **2013**.
27. Unzueta, U.; Saccardo, P.; Domingo-Espin, J.; Cedano, J.; Conchillo-Sole, O.; Garcia-Fruitos, E.; Cespedes, M. V.; Corchero, J. L.; Daura, X.; Mangues, R.; *et al.* Sheltering DNA in Self-Organizing, Protein-Only Nano-Shells as Artificial Viruses for Gene Delivery. *Nanomedicine* **2014**, *10*, 535–541.
28. Heyda, J.; Mason, P. E.; Jungwirth, P. Attractive Interactions between Side Chains of Histidine-Histidine and Histidine-Arginine-Based Cationic Dipeptides in Water. *J. Phys. Chem. B* **2010**, *114*, 8744–8749.
29. Vondrasek, J.; Mason, P. E.; Heyda, J.; Collins, K. D.; Jungwirth, P. The Molecular Origin of Like-Charge Arginine-Arginine Pairing in Water. *J. Phys. Chem. B* **2009**, *113*, 9041–9045.
30. Leckband, D. Measuring the Forces That Control Protein Interactions. *Annu. Rev. Biophys. Biomol. Struct.* **2000**, *29*, 1–26.
31. Mout, R.; Moyano, D. F.; Rana, S.; Rotello, V. M. Surface Functionalization of Nanoparticles for Nanomedicine. *Chem. Soc. Rev.* **2012**, *41*, 2539–2544.
32. Aris, A.; Feliu, J. X.; Knight, A.; Coutelle, C.; Villaverde, A. Exploiting Viral Cell-Targeting Abilities in a Single Polypeptide, Non-Infectious, Recombinant Vehicle for Integrin-Mediated DNA Delivery and Gene Expression. *Biotechnol. Bioeng.* **2000**, *68*, 689–696.
33. Vazquez, E.; Ferrer-Miralles, N.; Mangues, R.; Corchero, J. L.; Schwartz, S., Jr.; Villaverde, A. Modular Protein Engineering in Emerging Cancer Therapies. *Curr. Pharm. Des* **2009**, *15*, 893–916.
34. Vazquez, E.; Ferrer-Miralles, N.; Villaverde, A. Peptide-Assisted Traffic Engineering for Nonviral Gene Therapy. *Drug Discovery Today* **2008**, *13*, 1067–1074.
35. Elzoghby, A. O.; Samy, W. M.; Elgindy, N. A. Albumin-Based Nanoparticles as Potential Controlled Release Drug Delivery Systems. *J. Controlled Release* **2012**, *157*, 168–182.
36. Balkwill, F. The Significance of Cancer Cell Expression of the Chemokine Receptor CXCR4. *Semin. Cancer Biol.* **2004**, *14*, 171–179.
37. Xu, J.; Mora, A.; Shim, H.; Stecenko, A.; Brigham, K. L.; Rojas, M. Role of the SDF-1/CXCR4 Axis in the Pathogenesis of Lung Injury and Fibrosis. *Am. J. Respir. Cell Mol. Biol.* **2007**, *37*, 291–299.
38. Frangogiannis, N. G. The Stromal Cell-Derived Factor-1/CXCR4 Axis in Cardiac Injury and Repair. *J. Am. Coll. Cardiol.* **2011**, *58*, 2424–2426.
39. Filonov, G. S.; Piatkevich, K. D.; Ting, L.-M.; Zhang, J.; Kim, K.; Verkhusha, V. V. Bright and Stable Near-Infrared Fluorescent Protein for *in Vivo* Imaging. *Nat. Biotechnol.* **2011**, *29*, 757–761.
40. Dominguez, C.; Boelens, R.; Bonvin, A. M. HADDOCK: A Protein-Protein Docking Approach Based on Biochemical or Biophysical Information. *J. Am. Chem. Soc.* **2003**, *125*, 1731–1737.
41. Guerois, R.; Nielsen, J. E.; Serrano, L. Predicting Changes in the Stability of Proteins and Protein Complexes: A Study of More Than 1000 Mutations. *J. Mol. Biol.* **2002**, *320*, 369–387.
42. Andris-Widhopf, J.; Steinberger, P.; Fuller, R.; Rader, C.; Barbas, C. F., III. Generation of Human Fab Antibody Libraries: PCR Amplification and Assembly of Light- and Heavy-Chain Coding Sequences. *Cold Spring Harbor Protoc.* **2011**, *2011*, No. pdb.prot065565.

Annex 3

Non-amyloidogenic peptide tags for the regulatable self-assembling of protein-only nanoparticles

Ugutz Unzueta, Neus Ferrer-Miralles, Juan Cedano, Xu Zikung, Mireia Pesarrodona, Paolo Saccardo, Elena García-Fruitós, Joan Domingo-Espín, Pradeep Kumar, Kailash C. Gupta, Ramón Mangues, Antonio Villaverde, Esther Vazquez

Biomaterials, 2012, 33(33): 8714-8722.

Biomaterials 33 (2012) 8714–8722

Contents lists available at SciVerse ScienceDirect

Biomaterials

journal homepage: www.elsevier.com/locate/biomaterials

Non-amyloidogenic peptide tags for the regulatable self-assembling of protein-only nanoparticles

Ugutz Unzueta [a,b,c], Neus Ferrer-Miralles [a,b,c], Juan Cedano [d], Xu Zikung [a,b,c], Mireia Pesarrodona [a,b,c], Paolo Saccardo [a,b,c], Elena García-Fruitós [a,b,c], Joan Domingo-Espín [a,b,c], Pradeep Kumar [e], Kailash C. Gupta [f], Ramón Mangues [c,g], Antonio Villaverde [a,b,c,*], Esther Vazquez [a,b,c]

[a] Institut de Biotecnologia i de Biomedicina, Universitat Autònoma de Barcelona, Bellaterra, 08193 Barcelona, Spain
[b] Department de Genètica i de Microbiologia, Universitat Autònoma de Barcelona, Bellaterra, 08193 Barcelona, Spain
[c] CIBER de Bioingeniería, Biomateriales y Nanomedicina (CIBER-BBN), Bellaterra, 08193 Barcelona, Spain
[d] Laboratory of Immunology, Regional Norte, Universidad de la Republica, Gral. Rivera 1350, Salto 50.000, Uruguay
[e] CSIR, Institute of Genomics and Integrative Biology, University Campus, Mall Road, Delhi 110007, India
[f] CSIR, Indian Institute of Toxicology Research, Mahatma Gandhi Marg, Lucknow 226001, Uttar Pradesh, India
[g] Grup d'Oncogènesi i Antitumorals, Institut de Recerca, Hospital de la Santa Creu i Sant Pau, Barcelona, Spain

ARTICLE INFO

Article history:
Received 31 July 2012
Accepted 15 August 2012
Available online 3 September 2012

Keywords:
Nanoparticles
Artificial viruses
Peptide tags
Protein engineering
Cationic peptides
Electrostatic interactions

ABSTRACT

Controlling the self-assembling of building blocks as nanoscale entities is a requisite for the generation of bio-inspired vehicles for nanomedicines. A wide spectrum of functional peptides has been incorporated to different types of nanoparticles for the delivery of conventional drugs and nucleic acids, enabling receptor-specific cell binding and internalization, endosomal escape, cytosolic trafficking, nuclear targeting and DNA condensation. However, the development of architectonic tags to induce the self-assembling of functionalized monomers has been essentially neglected. We have examined here the nanoscale architectonic capabilities of arginine-rich cationic peptides, that when displayed on His-tagged proteins, promote their self-assembling as monodisperse, protein-only nanoparticles. The scrutiny of the cross-molecular interactivity cooperatively conferred by poly-arginines and poly-histidines has identified regulatable electrostatic interactions between building blocks that can also be engineered to encapsulate cargo DNA. The combined use of cationic peptides and poly-histidine tags offers an unusually versatile approach for the tailored design and biofabrication of protein-based nano-therapeutics, beyond the more limited spectrum of possibilities so far offered by self-assembling amyloidogenic peptides.

1. Introduction

Viral capsid proteins self-assemble as complex, highly symmetric particles that act as natural cages for the cell-targeted delivery of their genomes. The tailored construction of virus-inspired complexes is a promising route to drug delivery [1–7]. Being devoid of any infectious material, "artificial viruses" [8] do not show the undesired biological side effects associated to administration of viruses in viral gene therapy [9]. In this context, virus-like particles (VLPs), microbial organelles, [10], multifunctional proteins [11] and a spectrum of diverse vesicular materials are under development as carriers for therapeutic nucleic acids or conventional drugs. Many functional peptides have been identified from nature or selected by directed molecular evolution as ligands for cell surface receptors, membrane-active peptides and nuclear localization signals [4–6,12]. When conveniently pooled, these tag-mediated activities confer virus-like properties to the resulting multifunctional entities. In protein-only vehicles, all these domains can be covalently combined in single chain molecules that constitute the monomeric building blocks [11]. However, peptides enabling their holding proteins to organize as nanosized particles have so far been unidentified. The so-called self-assembling peptides, that might have been potentially promising for nanoparticle generation, are in general amyloidogenic protein segments that form fibers, membranes or hydrogels [13,14]. When used in fusion proteins, these peptides induce protein aggregation [15,16], being useless as tags for nanoparticle formation. Therefore, promoting the assembling of a selected protein as nanoparticles is so far excluded from rational engineering.

* Corresponding author. Institut de Biotecnologia i de Biomedicina, Universitat Autònoma de Barcelona, Bellaterra, 08193 Barcelona, Spain.
E-mail addresses: antoni.villaverde@uab.cat, prof.a.villaverde@gmail.com (A. Villaverde).

0142-9612/$ – see front matter © 2012 Elsevier Ltd. All rights reserved.
http://dx.doi.org/10.1016/j.biomaterials.2012.08.033

We have very recently described that a nine-arginine peptide (R9), when displayed on the surface of a recombinant, His-tagged EGFP, promotes the self-assembling of the whole fusion protein as regular nanoparticles of about 20 nm in diameter [17]. These constructs efficiently penetrate cultured mammalian cells by an endocytic pathway [18], cross the nuclear membrane, accumulate in the nucleus and allow the expression of a carried transgene [17]. The formation of these supramolecular complexes is completely distinguishable from unspecific protein aggregation [7,19,20]. Cationic peptides, including poly-arginines of different lengths, are well known by their membrane-crossing and DNA-condensation abilities, and widely used in gene therapy and more generally in drug delivery [5,6,12,21]. However, if showing a general applicability, such a newly described architectonic ability would be specially promising for the easy engineering of protein nanoparticles formed by specific proteins with desired biological activities.

To explore the possibility of effectively controlling the assembly of protein nanoparticles, we have examined here the role of cationic peptides and poly-histidines as an architectonic tag pair. These agents, upon incorporated into monomeric building blocks, synergistically cooperate in promoting nanoparticle formation by balancing, in a regulatable way, protein–protein and protein–DNA interactions. The potential of the 'nano-architectonic tag' concept is discussed here in the context of the design of smart, protein-based particles by conventional genetic engineering.

2. Materials and methods

2.1. Protein design and gene cloning

Several derivatives of R9–GFP–H6 containing decreasing numbers of arginine residues were constructed in house by site directed mutagenesis of the parental clone, by replacing these residues by glycines and alanines to keep the length of the peptide tag constant (Table 1). The new constructs R7–GFP–H6, R6–GFP–H6 and R3–GFP–H6 were efficiently produced in *Escherichia coli* Rosetta from the vector pET21b (Novagen 69744-3). Nine additional derivatives of GFP–H6 containing diverse amino terminal peptides of variable amino acid sequence, length and charge (Table 2), were designed in-house, provided by Geneart (Regensburg, Germany) or Genscript (Piscataway, USA), and produced from pET22b in *Escherichia coli* Origami B (BL21, OmpT$^-$, Lon$^-$, TrxB$^-$, Gor$^-$ (Novagen)) and the related strain BL21(DE3) for characterization.

2.2. Protein production and purification

Bacterial cells carrying the appropriate plasmid vectors were grown in shaker flask in Luria–Bertani (LB) medium containing 34 μg/ml chloramphenicol, 12.5 μg/ml tetracycline (strain resistance) and 100 μg/ml amplicillin (vector resistance) at 37 °C to A_{550} = 0.5–0.7. Recombinant gene expression was induced overnight at 20 °C by 0.1 mM isopropyl-β-D-thiogalactopyronaside (IPTG). Cell cultures were then centrifuged for 45 min (5,000*g* at 4 °C) and resuspended in Tris buffer (Tris 20 mM pH 8.0, NaCl 500 mM, Imidazol 10 mM) in the presence of EDTA-Free protease inhibitor (Complete EDTA-Free; Roche). The cells were then disrupted at 1100 psi using a French Press (Thermo FA-078A).

Table 1
Peak size (in nm) of Rn–GFP–H6 nanoparticles in low salt and high salt buffers. The occurrence of larger soluble particles and their size is also indicated. Relevant properties of the cationic tag are also depicted.

Tag name	Sequence	Size in low salt buffer[a] (larger particles)/PDI	Size in high salt buffer[b] (larger particles)/PDI	Number of arginines
R9	RRRRRRRRR	23.0/0.2	20.4/0.3	9
R7	RRRGRGRRR	37.9/0.2	6.5/0.5	7
R6	RARGRGRRR	15.5 (827.1)/0.7	8.5/0.4	6
R3	RARGRGGGA	14 (240.9, 526.9)/0.7	7.0/0.7	3

PDI: polydispersion index.
[a] Tris–dextrose.
[b] Tris–NaCl.

Proteins were purified by 6×His-tag affinity chromatography using HiTrap Chelating HP 1 ml columns (GE healthcare) by ÄKTA purifier FPLC (GE healthcare). Filtered cell extracts were loaded onto the HiTrap column after insoluble cell fraction separation by centrifugation (15,000*g* at 4 °C). The column was washed with Tris 20 mM, 500 mM NaCl, 10 mM Imidazole, pH 8.0. Proteins were eluted with a high imidazole content buffer (Tris 20 mM pH 8.0, 500 mM NaCl, 500 mM Imidazol) in a lineal gradient. The recombinant protein production has been performed in the Protein Production Platform (CIBER-BBN-UAB) (http://bbn.ciberbbn.es/programas/plataformas/equipamiento).

After purification, selected protein fractions were dialyzed overnight at 4 °C. Protein stability had been previously tested in several buffers from which the most appropriates regarding protein stability were selected in a per case basis. Low salt buffers were carbonate buffer (166 mM $NaHCO_3$, pH 7.4), Tris dextrose (20 mM Tris 500 mM + 5% dextrose pH 7.4) and PBS glycerol (140 mM NaCl, 7.5 mM Na_2HPO_4, 2.5 mM NaH_2PO_4 + 10% glycerol pH 7.4). The high salt buffer was always Tris–NaCl (20 mM Tris 500 mM NaCl pH 7.4). Proteins were finally aliquoted in small samples (30 μl) after 0.22 μm pore membrane filtration. Proteins were characterized by mass spectrometry and N-terminal sequencing and their amounts determined by Bradford's assay [22].

2.3. Fluorescence determination and dynamic light scattering (DLS)

Protein fluorescence was determined by Cary Eclipse Fluorescence Spectrophotometer (Variant) at detection wavelength of 510 nm by using an excitation wavelength of 450 nm. Volume size distribution of nanoparticles and monomeric GFP fusions were determined by dynamic light scattering at 633 nm (Zetasizer Nano ZS, Malvern Instruments Limited, Malvern, UK).

2.4. Transmission electron microscopy (TEM)

For transmission electron microscopy, proteins purified as described above were diluted to 0.2 mg/ml, deposited onto carbon-coated grids and contrasted by the evaporation of 1 nm platinum layer. These samples were observed in a Hitachi H-7000 transmission electron microscope.

2.5. Determination of protein physicochemical properties

Protein physicochemical properties including molecular weight, isoelectric point, aliphatic index, hydrophobicity and stability index were determined in silico by "ProtParam" software (Expasy). Protein solubility was determined by conventional western-blot analysis from whole cell extracts using Quantity One software (Bio-Rad), upon estimation of soluble and insoluble protein fractions. Bands corresponding to the recombinant protein were revealed with a commercial monoclonal antibody that recognizes the C-terminal His-tag (GE Healthcare), using dilutions of GFP–H6 as a reference. Protein charge and accessible surface were calculated from model structures. PDB2PQR was used to calculate protein protonation states to infer electrostatic charge at a particular pH [23], and solvent accessible surface areas were calculated by means of the Pops algorithms [24].

2.6. Modeling protein monomers and protein–DNA interactions

Homology models of the protein models were generated using Modeller [25], Phyre [26] and Swiss-PdbViewer [27]. The quality and stereochemical properties of the models were evaluated using Vadar [28]. The electrostatic interactions between the R9–GFP–H6 monomer and double stranded DNA were explored at acidic pH by using Haddock [29]. After obtaining the solution, a molecular dynamics was performed through NAMD [30] to minimize the energy of the system and to obtain the sequence of frames. The resulting movie was generated using VMD [31].

2.7. Cell culture and transfection and confocal microscopy

HeLa (ATCC-CCL-2) cells were cultured in MEM (GIBCO, Rockville, MD) supplemented with 10% Fetal Calf Serum (GIBCO) and incubated at 37 °C and 5% CO_2. For confocal analysis, cells were grown on Mat-Teck culture dishes and processed as described [17]. For the analysis of cell transfection, cells were exposed to R9–GFP–H6 nanoparticles combined with pCDNA 3.1 encoding the *td Tomato* gene. Red fluorescence in cells was analyzed on a FACS Calibur system (Becton Dickinson) after detachment with 0.5 mg/ml trypsin. DNA retardation assays were carried out according to previously reports [32]. Detailed protocols can be found elsewhere [17,18].

2.8. Statistic analysis

Mean data, standard deviations and errors were calculated by Microsoft Office Excel 2003 (Microsoft). Pair-wise correlations, regressions and statistical significances were calculated by Sigmaplot 10.0. All the potential parametric correlations were analyzed by a lineal regression statistic assay.

Table 2
Peak size (in nm) of peptide tagged GFP–H6 nanoparticles in low salt and high salt buffers. The occurrence of larger soluble particles and their size is also indicated. Relevant properties of the respective building blocks are also listed.

Peptide name	Sequence	Reference	Size in low salt buffer (larger particles)/PDI	Size in high salt buffer[c] (larger particles)/PDI	Number of arginines	Number of positively charged residues (arg + lys)
T22	RRWCYRKCYKGYCYRKCR	[73]	35.3/0.4[a]	10.92/0.4	5	8
CXCL12	KPVSLSYRCPCRFFESHVARANVKHL KILNTPNCALQIVARLKNNNRQVCIDP KLKWIQEYLEKALN	[74]	145.6/0.4[a]	14.6/0.2	5	12
vCCL2	LGASWHRPDKCCLGYQKRPLPQVLL SSWYPTSQLCSKPGVIFLTKRGRQV CADKSKDWVKKLMQQLPVTA	[75]	46.24 (342.1)/0.2[a]	83.3/0.2	4	12
V1	LGASWHRPDKCCLGYQKRPLP	[76]	9.4 (227.0)/0.4[a]	8.0 (20)/0.3	2	4
Angiopep-2	TFFYGGSRGKRNNFKTEEY	[77]	5.8/0.5[b]	nd	2	4
Seq-1	KYLAYPDSVHIW	[78]	5.9/0.6[b]	nd	0	1
Laminin 5alfa peptide A5G27	RLVSYNGIIFFLK	[79]	26.2/0.4[b]	nd	1	2
Fibronectin peptide I	KNNQKSEPLIGRKKT	[80]	4.0/0.6	nd	1	5
Fibronectin peptide V	WQPPRARI	[80]	4.1/0.8	nd	2	2

PDI: polydispersion index.
[a] PBS–glycerol.
[b] Carbonate.
[c] Tris–NaCl.

3. Results

3.1. Mapping the architectonic abilities of poly-arginines

While His-tagged GFP is exclusively found in a disassembled monomeric form (of around 5 nm), the addition of the cell-penetrating poly-arginine (R9) peptide at the amino terminus promoted the spontaneous organization of R9–GFP–H6 as building blocks of regularly sized nanoparticles of around 20 nm [17]. To map the architectonic properties of poly-arginines we constructed a series of arginine-based tags (Rn) with a decreasing number of arginine residues, to evaluate if they retained the ability to promote protein self-assembling. Soluble versions of R7–GFP–H6, R6–GFP–H6 and R3–GFP–H6 were all found in the form of relatively monodispersed nanoparticulate entities of sizes ranging from 14 nm (R3–GFP–H6) to 38 nm (R7–GFP–H6, Table 1). This was indicative that a lower number of arginine residues (3) were already able to promote self-assembling of the monomers as protein-only nanoparticles. However, R3–GFP–H6 and R6–GFP–H6 showed secondary peaks of larger sizes (Table 1 and Figure 1), indicative of structural instability. On the other side, when Rn–GFP–H6 fusions were dialyzed against a high salt buffer upon purification, these proteins (at exception of R9–GFP–H6) did not form nanoparticles (Table 1). These data demonstrated the electrostatic nature of the protein–protein interactions supporting their self-assembling, that were much stronger when promoted by the highly cationic peptide R9, resulting in the formation of tightly assembled, highly stable particles.

3.2. Architectonic properties of non poly-arginine cationic peptides

To discriminate between a potential specific role of arginine residues and a generic influence of the cationic nature of the tag, in promoting ordered monomer self-assembling, other protein segments with unrelated amino acid sequences and lengths were fused to the amino terminus of GFP–H6 and challenged for nanoparticle formation. Four ligands of the cell surface cytokine receptor CXCR4 (T22, V1, CXCL12 and vCCL2), three ligands of CD44 (the fibronectin segments I and V, and the laminin 5alfa peptide A5G27), and the membrane-active peptides Seq-1 and Angiopep-2 (Table 2) were incorporated as N-terminal GFP–H6 fusions. Among them, T22, in form of T22–GFP–H6, had been recently observed as tending to form regular oligomers [33]. Interestingly, most of these peptides enabled GFP–H6 to form stable nanoparticles of different sizes, ranging from around 20 to 150 nm (Table 2, Fig. 2a, and Supplementary Fig. S1). Again, a high salt content in the buffer tended to minimize particle formation and to reduce the resulting size of the complexes (Table 2). This was especially evident in the case of CXCL12-empowered constructs, for which size dropped from 145 to 15 nm (Fig. 2a, Table 2). On the other hand, the addition of V1 resulted in a mixed population of monomers and nanoparticles, the last fraction being reduced by high salt content (Fig. 2a). However, even in a high salt buffer, V1-empowered particles organized as regular entities of 8 and 20 nm, whose occurrence was fully confirmed by TEM (Fig. 2b). In fact, the larger CXCL12- and V1-empowered particles observed in absence of salt (see Fig. 2b) seemed to be due to clusters of smaller particles. Such a hierarchic supramolecular organization was not so apparent in T22–GFP–H6, in which different sized but tight nanoparticles were observed in both high and low salt buffers (Fig. 2b), indicative of architectonic robustness. Angiopep-2, Seq-1 and the fibronectin peptides I and V failed in promoting assembling of their respective functionalized monomers (Table 2, Supplementary Fig. S1).

At that point, we wanted to explore any potential parameter of the tags that might be determinative of nanoparticle formation and size. We unsuccessfully explored dependences between diverse biochemical properties of the peptides and of full fusion proteins (including length, molecular mass, hydrophobicity, aliphatic index and accessibility to the solvent) with particle size (not shown). However, the formation of nanoparticles was slightly but clearly influenced by the number of arginine residues of the amino terminal tag, in the border of the statistic significance (Fig. 3). While considering the total number of positively charged amino acids (lysines and arginines), the significance of the dependence dramatically increased (Fig. 3). In these plots, the highly unstable construct CXCL12–GFP–H6 is shown but the data was excluded from the analysis because of the instability of the assembled construct as discussed above (Fig. 2a, Table 2). As a control, no relationship between the total length of the tag and nanoparticle size was observed (Fig. 3). These data clearly supported the concept that not arginines as specific amino acids but the whole cationic nature of the tag determined its architectonic potential and influenced the size of the resulting constructs.

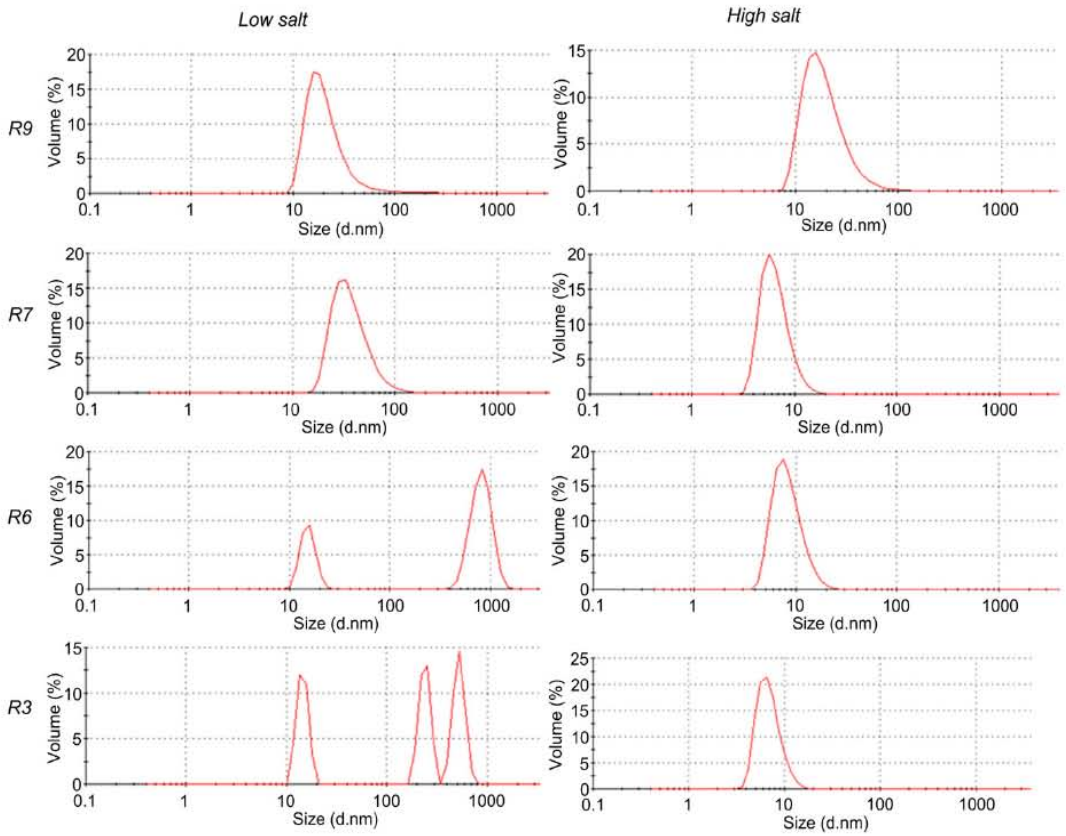

Fig. 1. Size distribution of GFP–H6 monomers tagged with amino terminal arginine-rich peptides (Table 1). Upon purification, proteins were dialyzed against PBS–glycerol (low salt buffer) or Tris–NaCl (high salt buffer). All the constructs were fluorescent.

3.3. Regulatable functional properties of poly-histidines in protein-only nanoparticles

Once confirmed the structural potential of cationic peptides, we also wanted to explore if poly-histidines would contribute to the supramolecular organization of tagged building blocks, apart from their utility as protein purification tags and as endosomolytic agents in drug delivery [34]. We suspected a role of H6 since the pKa of the imidazole group of histidines is 6.10, and its charge, at difference of poly-arginines (pKa of 12.48), is expected to be unstable at pH close to neutral. In this regard, several functional properties of R9–GFP–H6 nanoparticles were highly dependent on pH. Indeed, cell penetrability of R9–GFP–H6 was optimal at pH 5.8 and progressively decreased at higher pH (Fig. 4a), suggesting a gradual inactivation of R9 activities under alkaline media. At pH 4, the protein precipitated and remained externally attached to the plasma membrane, showing poor internalization. When analyzed by DLS (Fig. 4b), the size of R9–GFP–H6 particles remained constant at pH values between 5.8 and 10 (17–20 nm), and marginally increased up to 35 nm at pH 4 (some aggregation was observed at pH 4 and 10). When R9–GFP–H6 was combined with plasmid DNA at pH 5.8 and further exposed to cultured mammalian cells, about 50% of the population expressed the transgene (Fig. 4c). However, this value dropped to about 3% at pH 4 and to even lower values at neutral and basic pH, indicating pH-dependent functional variability and probably structural rearrangements of the polyplexes. Interestingly, the differential effectiveness of the polyplexes in transfection experiments that were all performed in MEM culture media at neutral pH indicated that the specific properties of the nanoparticles reached at different pHs are stable and did not revert when further incubated under physiological conditions.

On the other hand, the ability of R9–GFP–H6 nanoparticles to bind DNA was null at neutral and basic pH, clear at pH 5.8 and maximal at pH 4 (Fig. 4d). These data suggested that at pH over 6.1, H6 having no charge, R9 might be overtitrated by electrostatic protein–protein interactions, rendering the tag unavailable for other activities such as cell penetration and DNA binding. Below pH = 6.1, protonation of histidines would enable H6 for protein–protein and protein–DNA contacts, releasing R9 for plasma membrane translocation, DNA loading and efficient transgene delivery and expression. At pH 4, protein denaturation and aggregation is expected to eclipse the enhanced cross-molecular abilities of H6.

3.4. Architectonic potential of poly-histidines

The above data suggested cross-molecular reactivity of H6. However, no architectonic abilities of poly-histidines regarding

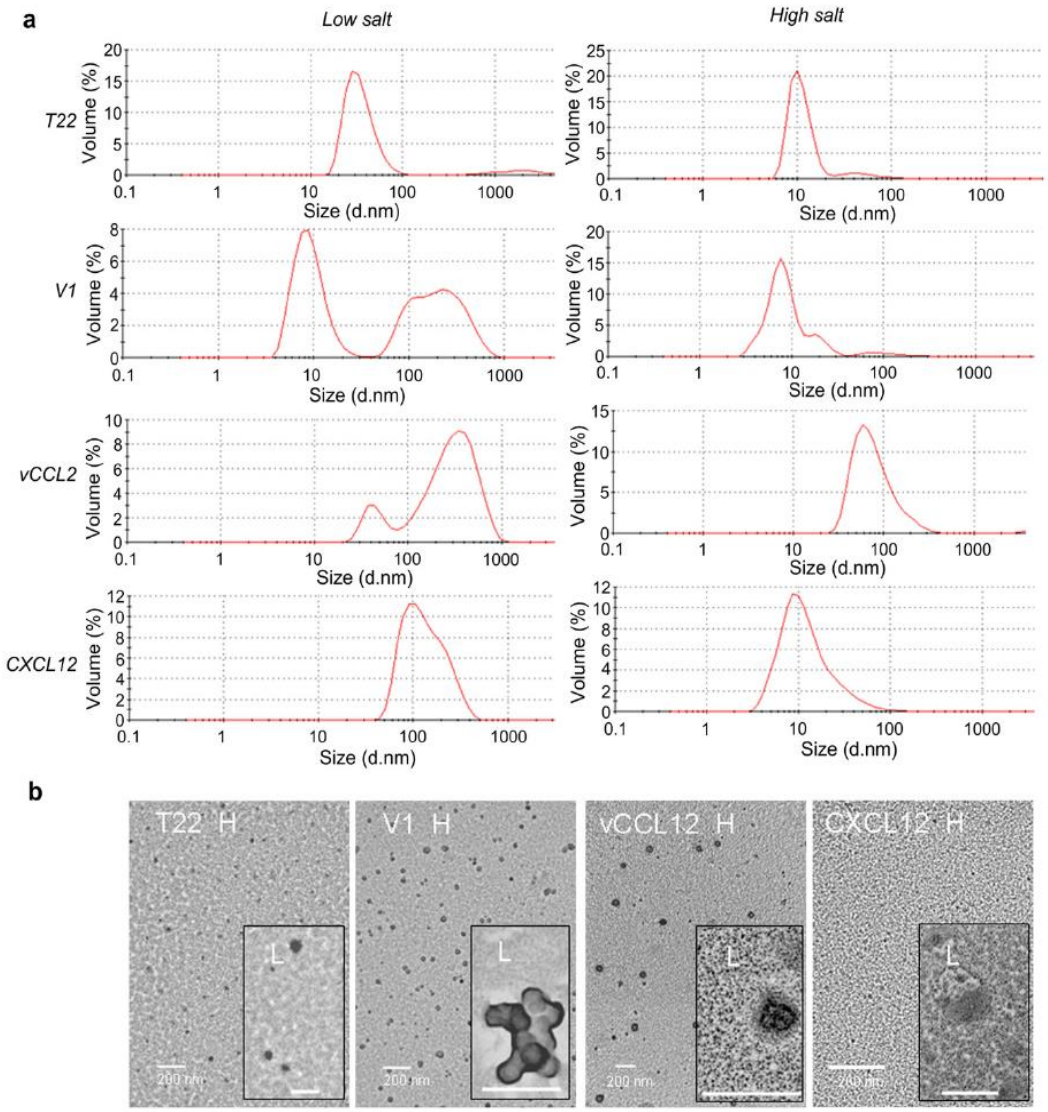

Fig. 2. Architecture of GFP-derived nanoparticles empowered with different amino terminal cationic peptides (Table 2). Upon purification, proteins were dialyzed against PBS–glycerol (low salt buffer) or Tris–NaCl (high salt buffer). (A) Size distribution of the resulting GFP–H6 constructs monitored by DLS. (B) TEM micrographs of these particles formed in either high salt (H) or low salt (L) buffers. All the constructs were fluorescent.

nanoparticle formation had been so far reported. Therefore, the potential assembling of GFP–H6 (lacking any amino terminal cationic peptide) was explored at different pHs. At pH 7 and 8, size of GFP–H6 peaked at around 5 nm (Fig. 5a), a value compatible with monomer size (at pH 10 the protein fully precipitated; not shown). However, at pH 5.8, a minor but regular size up-shift was observed, that was more even pronounced at pH 4. Also, under acidic conditions, a minor but significant fraction of GFP–H6 organized as regular particles of about 22 nm. On the other hand, with protonated H6 tails, GFP–H6 was able to bind DNA at pH 4 (although not at 5.8, Fig. 5b and Supplementary Video S1). These data confirmed that charged H6 was able to promote, as suspected, stable protein–protein and protein–DNA interactions. In R9–GFP–H6, showing a marked dipolar charge distribution (Fig. 5c), H6 intervened in nanoparticle formation by promoting electrostatic protein–protein contacts, as modeled in Fig. 5d. H6-mediated interactions would be more favored than those driven by R9, because of the more extended arm of H6 (Fig. 5d). Although at pH 4, H6 also binds DNA (modeled in Fig. 5b), at this condition the nanoparticle itself is not stable as the protein aggregates (Fig. 4a and b). Then, the efficiency of the nanoparticles in mediating transgene delivery showed an optimal when assembled at pH 5.8

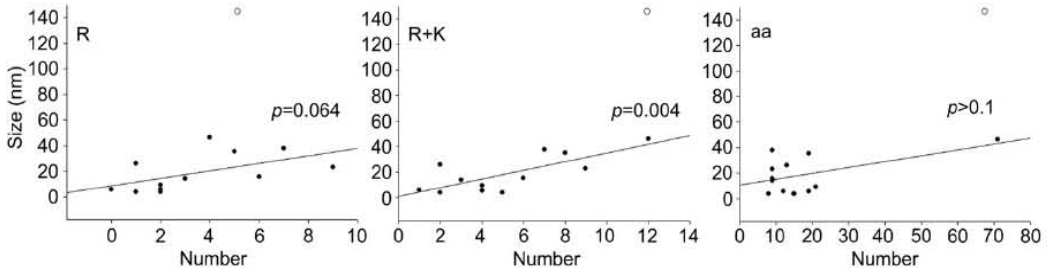

Fig. 3. Regression analyses between selected properties of all peptide tags used in this study (Tables 1 and 2) and the peak size of the chimerical constructs determined in low salt buffer. *R* stands for the number of arginine residues, $R + K$ indicates the number of all cationic residues (arginines and lysines), and aa reefers to the total number of residues of the peptide. The white symbol refers to data from CXCL12-empowered particles, and it has been excluded from the analyses.

(Fig. 4c), where R9 is free for non-architectonic functions. Again, this is irrespective of the conditions at with the particles are finally used in biological interfaces, that are expected to be around physiological pH.

Supplementary data related to this article can be found at doi: 10.1016/j.biomaterials.2012.08.033.

3.5. Generic tagging of building blocks with R9 and H6

As demonstrated above, the combination of a cationic peptide at the amino terminus of GFP with a poly-histidine enables this protein to self-assemble as regular sized nanoparticles through electrostatic interactions. In particular, R9 and T22 are excellent tags for this purpose, as they induce the formation of very stable regular sized entities poorly sensitive to high salt content. We wondered at which extent nanoparticle formation could be strictly linked to the particular structure of GFP (beta-barrel), and if a peptide pair such as R9 and H6 could functionalize proteins others than GFP to act as monomers of self-organizing protein nanoparticles. This was explored by using the structurally different, tumor suppressor protein p53 (tetrameric, 43.7 kDa per monomer), that was functionalized with R9 and H6 following the same scheme than previously used for GFP. Interestingly, the addition of the end terminal tags to this protein resulted in a significant up-shift of their size (Fig. 6). This fact confirmed that the pair R9–H6 can confer self-organizing properties to proteins other GFP, and that the architectonic tag concept could be considered as a principle with generic applicability in bionanotechnology.

4. Discussion

The construction of self-assembling protein-only nanoparticles from repetitive building blocks has been a rather neglected issue in nanomedicine, in contrast to the long run expertise accumulated in the fabrication of liposomes and polymeric particles with predefined nanoscale features [35–39]. Consequently, the current protein-based vehicles for drug delivery generated de novo include a catalog of rather amorphous entities [40] that are produced under no previous design. On the other hand, viruses [41–43], virus-like particles [44–47], parts of viral capsids [48], flagella-based devices

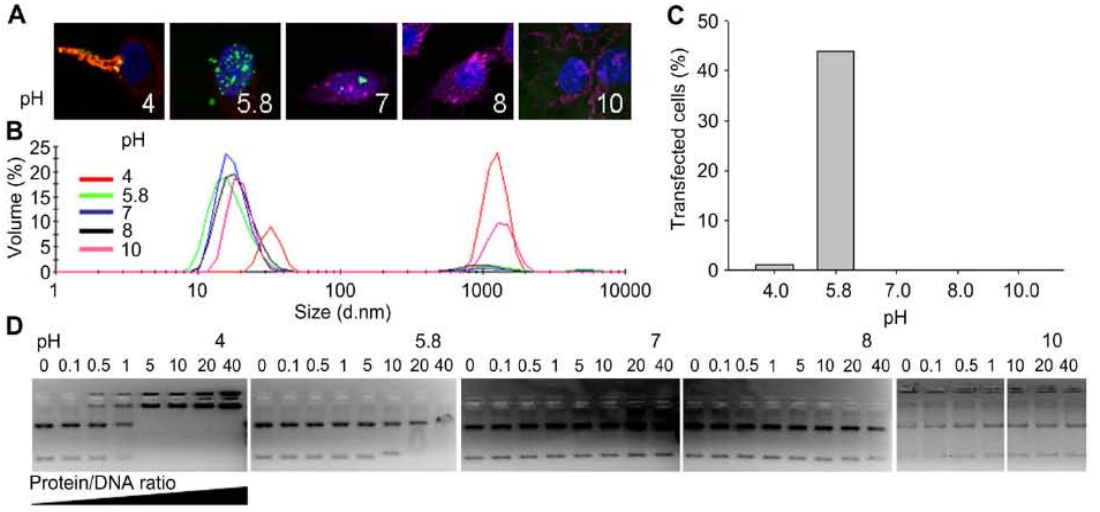

Fig. 4. Functional and structural characterization of R9–GFP–H6-based nanoparticles. (A) Confocal snap-shots of cultured HeLa cells exposed to protein-only R9–GFP–H6 nanoparticles for 24 h. Nanoparticles emitted green fluorescence, the cell membrane was stained will CellMask (rendering pink-reddish signal) and cell DNA with Hoechst 3342 (blue). (B) Size distribution of R9–GFP–H6 nanoparticles in absence of DNA. (C) Percentage of HeLa cells expressing a reported gene carrier by polyplexes formed at distinct pH values, at a protein/DNA ratio of 50. (D) DNA-binding abilities of R9–GFP–H6 nanoparticles at different pH values. (For interpretation of the references to color in this figure legend, the reader is referred to the web version of this article.)

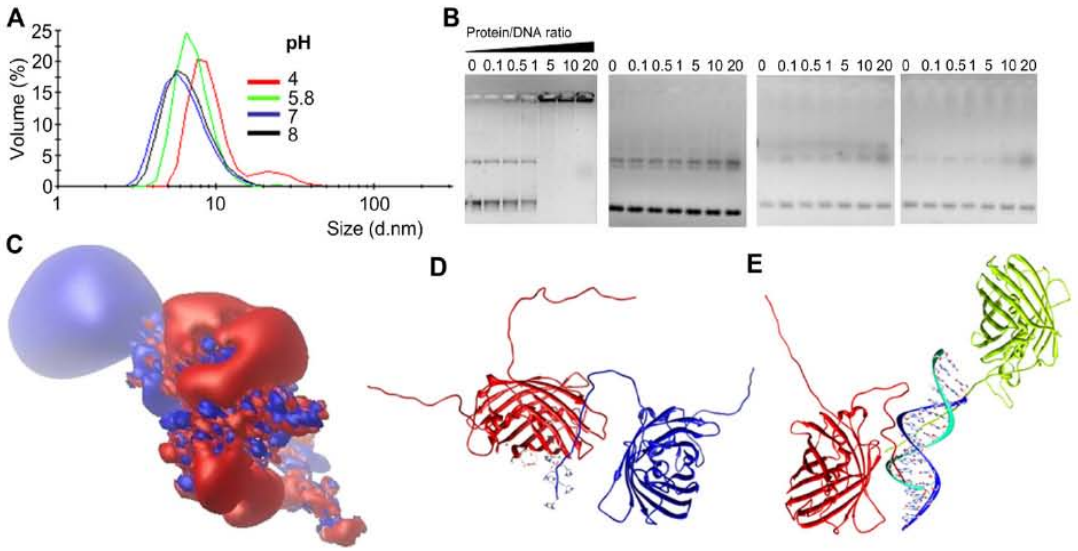

Fig. 5. Cross-interacting abilities of the protonated His-tag in R9–GFP–H6. (A) Size distribution measured by DLS of GFP–H6 constructs at different pH values. (B) DNA binding of GFP–H6 monitored by retardation assays at different pH values. (C) Polatization in the charge distribution of the R9–GFP–H6 monomer (blue cationic, red anionic) in which the electrostatic potencial has been calculated in aqueous media by means of the Adaptive Poisson–Boltzmann Solver method [81]. (D) Interaction of the positively charged H6 peptide with the anionic pole of the R9–GFP–H6 monomer, modeled at pH 5.8. (E) Conformation of the positively charged H6 peptide of R9–GFP–H6 interacting with double stranded DNA, modeled at pH 5.8. (For interpretation of the references to color in this figure legend, the reader is referred to the web version of this article.)

[49–51], organelles [10] and other constructs formed by the natural oligomerization of natural proteins [52,53] maintain their natural self-organization pattern and are exploited for nanomedical purposes such as drug delivery, antigen presentation or as scaffolds for nano-fabrication [54,55], but with limited or null structural versatility. Conventional self-assembling peptides organize in aqueous solutions by the formation of cross-molecular beta sheet-based interactions, similar to those supporting amyloidal deposition [56–60]. Such interactions result in fibril formation [56,57,61,62], that can finally derive in tailored materials such as membranes [14] of gels [13]. Unfortunately, when fused as tags to large proteins, self-assembling peptides prompt aggregation [15,16]. Therefore, the rational generation of man-made protein nanoparticles based on selected protein monomers, that is, polypeptides with appealing biological functions, has been so far poorly reached.

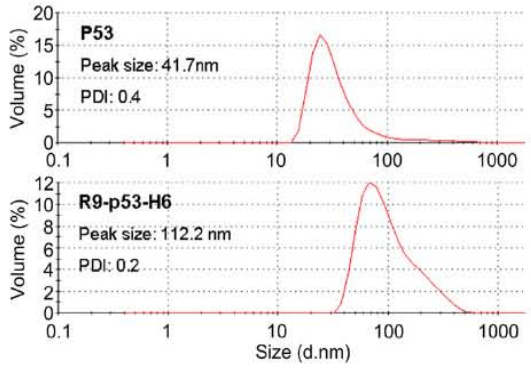

Fig. 6. Size distribution of p53 and R9–p53–H6 in elution buffer. PDI is polydispersion index.

In this context, the few successful insights on the construction and modulation of protein-only nanoparticles have derived from unanticipated observations. As an illustrative example, the mixture of a fusogenic peptide from viral origin and a poly-lysine (K_{16}) renders the unexpected formation of spherical microparticles from 120 to 800 nm, whose size is regulated by salt concentration, pH and temperature [63]. Furthermore, the design of short peptides with appropriate charge distribution permits a semi-rational control of peptide self-assembling as 2D or 3D nanofiber-based complexes [64]. For larger proteins, the construction of elastin-mimetic protein polymers with self-assembling properties is among the most advanced examples of self-organizing, net-shaped materials [65].

In a previous study [17], we have observed that a poly-arginine peptide (R9) was able to promote the self-organization of a modular chimerical protein (His-tagged GFP) into regular 20 nm-sized nanoparticles suitable for drug delivery [18]. This finding revealed a novel potential of the well-known family of cell-penetrating Rn peptides [3–6,21,66–70], in promoting self-organization of holding proteins at the nanoscale level. The possibility of using specific peptide tags as directors of protein self-organization into nanoparticles with pre-defined properties is particularly appealing, as it should potentially allow the manipulation of their properties by conventional genetic engineering. To determine if this unsuspected architectonic ability could be shared by other cationic stretches we tested here nanoparticle formation of GFP–H6 as driven by R7, R6 and R3 (Table 1), and by nine additional peptides with unrelated amino acid sequences (Table 2). Interestingly, most of these tags induced the formation of fluorescent GFP oligomers of regular architecture (pseudo-spherical nanoparticles, Fig. 2), ranging from 20 to 100 nm (Tables 1 and 2). The fact that their formation and size was influenced in most cases by salt concentration (Figs. 1 and 2) indicates that monomer self-assembling was governed by electrostatic interactions between monomers. However, two particular constructs namely R9–GFP–

H6 and at a minor extent T22–GFP–H6, empowered by highly cationic tags, were especially stable under variable salt content. The fact that diverse unrelated cationic peptides enabled monomers to self-organize into monodisperse nanoparticles confirms the self-organizing properties as a general property of cationic peptides (other than R9, Fig. 3), and also that the structure of the peptide tag itself is not critical for the assembling of the building blocks. Also, the beta-barrel core of GFP was nicely preserved in all the constructs as inferred from the fluorescence emission observed in all the particles (not shown, legends of Figs. 1–3).

On the other hand, data presented here reveal that the histidine tag (H6), commonly used for protein purification and as endosomal escaping agent promotes protein–protein and protein–DNA contacts, when the pH at which particles or polyplexes are formed decreases (Fig. 5 and Supplementary Video S1). Then, the structural dynamism offered by the partially protonated H6 tag and its competition with the cationic R9 tail for molecular interactions allows an unusual molecular flexibility that permits to adapt the protein particles as efficient carriers for DNA delivery by slightly decreasing the pH under neutral values. The H6 peptide, as an unusually versatile, pH-controlled architectonic tag complements the activities of R9 (or those of alternative cationic peptides), being the dual peptide set as a whole, a promising platform for the activation of defined protein monomers for regulatable cross-molecular interactions.

In summary, in this work we propose a novel concept of architectonic tagging for nanoscale construction by the use of a peptide pair. The fusion of a H6 tag at the carboxy terminus and a cationic peptide at the amino terminus of diverse proteins enable them to act as self-assembling monomers of protein-only nanoparticles. Both model proteins tested in this study namely GFP and p53, self-assembled when tagged with R9, T22 (and other cationic peptides) and H6 (Figs. 1, 2 and 6). At least in the case of GFP, in which biological activity of the monomer can be straightforward determined by fluorescence emission, it has been determined that assembly does not impair functionality. This fact makes the proposed peptidic platform very appealing to generate nanoparticles with potential for the delivery of either active proteins or associated nucleic acids. The administration of protein drugs as nanoparticles (by engineering them as building blocks) could largely increase stability, bioavailability and intracellular drug delivery [71], when comparing with the soluble, non-particulate counterpart. Interestingly, the size of the resulting construct, a critical parameter in nanomedicine [72], seems to be strongly influenced by the charge of the cationic tag (Fig. 3), which can be easily defined in anticipation by simple *in silico* protein design. Although further studies are obviously required to fully understand the mechanics of self-assembling and to adjust the methodological aspects of this principle, the observations reported here open intriguing possibilities for the pioneering rational design of tailored protein nanoparticles by conventional engineering of the primary amino acid sequence.

5. Conclusion

The combination of a cationic peptide and a hexa-histidine tail fused to the amino and carboxy termini, respectively, of different proteins enable them to act as building blocks of self-assembling nanoparticles whose properties are regulatable by pH during particle formation. These vehicles are also able to condense and deliver expressible DNA into mammalian cells. The architectonic properties of the tag pair at the nanoscale are supported by electrostatic contacts, primarily driven by the cationic tag and subsidiarily by H6. When protonated at slightly acidic pH, positively charged H6 replaces by competition the cationic tag and intervenes in the formation of stable contacts. The further implementation of this bi-armed peptide platform should allow the biofabrication and formulation of desired drug proteins as protein-only nanoparticles, as an exciting alternative to the limited use of conventional, amyloidgenic self-assembling peptides in nanomedicine.

Acknowledgments

We appreciate the technical support of Fran Cortés from the Cell Culture Unit of Servei de Cultius Cel·lulars, Producció d'Anticossos i Citometria (SCAC), and from Servei de Microscòpia, both at the UAB, and the Protein Production Platform (PPP) of the CIBER de Bioingeniería, Biomateriales y Nanomedicina. We also acknowledge the financial support received for the design and production of artificial viruses for gene therapy to EV and AV from FISS (PS0900165), MINECO (ACI2009-0919), AGAUR (2009SGR-108) and CIBER de Bioingeniería, Biomateriales y Nanomedicina, an initiative funded by the VI National R&D&i Plan 2008–2011, Iniciativa Ingenio 2010, Consolider Program, CIBER Actions and financed by the Instituto de Salud Carlos III with assistance from the European Regional Development Fund. XZ is a recipient of a scholarship under the Post-graduate Study Abroad Program of The China Scholarship Council, China. UU and PS have received predoctoral fellowships from ISCIII, Spain, while JDE was supported through a FPU fellowship from MINECO, Spain. AV has been distinguished with an ICREA ACADEMIA award. EGF is supported by the Programa Personal de Tecnico de Apoyo (Modalidad Infraestructuras Científico-Tecnológicas, MICINN).

Appendix A. Supplementary data

Supplementary data related to this article can be found at http://dx.doi.org/10.1016/j.biomaterials.2012.08.033

References

[1] Uchida M, Klem MT, Allen M, Suci P, Flenniken M, Gillitzer E, et al. Biological containers: protein cages as multifunctional nanoplatforms. Adv Mater 2007;19:1025–42.
[2] Kim HH, Choi HS, Yang JM, Shin S. Characterization of gene delivery in vitro and in vivo by the arginine peptide system. Int J Pharm 2007;335:70–8.
[3] Futaki S, Suzuki T, Ohashi W, Yagami T, Tanaka S, Ueda K, et al. Arginine-rich peptides. An abundant source of membrane-permeable peptides having potential as carriers for intracellular protein delivery. J Biol Chem 2001;276:5836–40.
[4] Vazquez E, Ferrer-Miralles N, Mangues R, Corchero JL, Schwartz Jr S, Villaverde A. Modular protein engineering in emerging cancer therapies. Curr Pharm Des 2009;15:893–916.
[5] Vazquez E, Ferrer-Miralles N, Villaverde A. Peptide-assisted traffic engineering for nonviral gene therapy. Drug Discov Today 2008;13:1067–74.
[6] Ferrer-Miralles N, Vazquez E, Villaverde A. Membrane-active peptides for non-viral gene therapy: making the safest easier. Trends Biotechnol 2008;26:267–75.
[7] Toledo-Rubio V, Vazquez E, Platas G, Domingo-Espín J, Unzueta U, Steinkamp E, et al. Protein aggregation and soluble aggregate formation screened by a fast microdialysis assay. J Biomol Screen 2010;15:453–7.
[8] Mastrobattista E, van der Aa MA, Hennink WE, Crommelin DJ. Artificial viruses: a nanotechnological approach to gene delivery. Nat Rev Drug Discov 2006;5:115–21.
[9] Edelstein ML, Abedi MR, Wixon J. Gene therapy clinical trials worldwide to 2007 – an update. J Gene Med 2007;9:833–42.
[10] Corchero JL, Cedano J. Self-assembling, protein-based intracellular bacterial organelles: emerging vehicles for encapsulating, targeting and delivering therapeutical cargoes. Microb Cell Fact 2011;10:92.
[11] Aris A, Villaverde A. Modular protein engineering for non-viral gene therapy. Trends Biotechnol 2004;22:371–7.
[12] Saccardo P, Villaverde A, Gonzalez-Montalban N. Peptide-mediated DNA condensation for non-viral gene therapy. Biotechnol Adv 2009;27:432–8.
[13] Koutsopoulos S, Unsworth LD, Nagai Y, Zhang S. Controlled release of functional proteins through designer self-assembling peptide nanofiber hydrogel scaffold. Proc Natl Acad Sci U S A 2009;106:4623–8.
[14] Zhang S, Holmes T, Lockshin C, Rich A. Spontaneous assembly of a self-complementary oligopeptide to form a stable macroscopic membrane. Proc Natl Acad Sci U S A 1993;90:3334–8.
[15] Wu W, Xing L, Zhou B, Lin Z. Active protein aggregates induced by terminally attached self-assembling peptide ELK16 in *Escherichia coli*. Microb Cell Fact 2011;10:9.

[16] Zhou B, Xing L, Wu W, Zhang XE, Lin Z. Small surfactant-like peptides can drive soluble proteins into active aggregates. Microb Cell Fact 2012;11:10.
[17] Vazquez E, Roldan M, Diez-Gil C, Unzueta U, Domingo-Espín J, Cedano J, et al. Protein nanodisk assembling and intracellular trafficking powered by an arginine-rich (R9) peptide. Nanomedicine (Lond) 2010;5:259–68.
[18] Vazquez E, Cubarsi R, Unzueta U, Roldán M, Domingo-Espín J, Ferrer-Miralles N, et al. Internalization and kinetics of nuclear migration of protein-only, arginine-rich nanoparticles. Biomaterials 2010;31:9333–9.
[19] Vazquez E, Corchero JL, Villaverde A. Post-production protein stability: trouble beyond the cell factory. Microb Cell Fact 2011;10:60.
[20] Martinez-Alonso M, Gonzalez-Montalban N, Garcia-Fruitos E, Villaverde A. Learning about protein solubility from bacterial inclusion bodies. Microb Cell Fact 2009;8:4.
[21] Kumar P, Wu H, McBride JL, Jung KE, Kim MH, Davidson BL, et al. Transvascular delivery of small interfering RNA to the central nervous system. Nature 2007;448:39–43.
[22] Bradford MM. A rapid and sensitive method for the quantitation of microgram quantities of protein utilizing the principle of protein-dye binding. Anal Biochem 1976;72:248–54.
[23] Dolinsky TJ, Czodrowski P, Li H, Nielsen JE, Jensen JH, Klebe G, et al. PDB2PQR: expanding and upgrading automated preparation of biomolecular structures for molecular simulations. Nucleic Acids Res 2007;35:W522–5.
[24] Cavallo L, Kleinjung J, Fraternali F. POPS: a fast algorithm for solvent accessible surface areas at atomic and residue level. Nucleic Acids Res 2003;31:3364–6.
[25] Eswar N, Eramian D, Webb B, Shen MY, Sali A. Protein structure modeling with MODELLER. Methods Mol Biol 2008;426:145–59.
[26] Kelley LA, Sternberg MJ. Protein structure prediction on the Web: a case study using the Phyre server. Nat Protoc 2009;4:363–71.
[27] Guex N, Peitsch MC. SWISS-MODEL and the Swiss-PdbViewer: an environment for comparative protein modeling. Electrophoresis 1997;18:2714–23.
[28] Willard L, Ranjan A, Zhang H, Monzavi H, Boyko RF, Brian D, et al. VADAR: a web server for quantitative evaluation of protein structure quality. Nucleic Acids Res 2003;31:3316–9.
[29] Dominguez C, Boelens R, Bonvin AM. HADDOCK: a protein–protein docking approach based on biochemical or biophysical information. J Am Chem Soc 2003;125:1731–7.
[30] Phillips JC, Braun R, Wang W, Gumbart J, Tajkhorshid E, Villa E, et al. Scalable molecular dynamics with NAMD. J Comput Chem 2005;26:1781–802.
[31] Hsin J, Arkhipov A, Yin Y, Stone JE, Schulten K. Using VMD: an introductory tutorial. Curr Protoc Bioinformatics 2008. Chapter 5: Unit 5.7.
[32] Aris A, Villaverde A. Molecular organization of protein–DNA complexes for cell-targeted DNA delivery. Biochem Biophys Res Commun 2000;278:455–61.
[33] Unzueta U, Cespedes MV, Ferrer-Miralles N, Casanova I, Cedano JA, Corchero JL, et al. Intracellular CXCR4+ cell targeting with T22-empowered protein-only nanoparticles. Int J Nanomed 2012;7:4533–44.
[34] Ferrer-Miralles N, Corchero JL, Kumar P, Cedano JA, Gupta KC, Villaverde A, et al. Biological activities of histidine-rich peptides; merging biotechnology and nanomedicine. Microb Cell Fact 2011;10:101.
[35] Zhang L, Pornpattananangku D, Hu CM, Huang CM. Development of nanoparticles for antimicrobial drug delivery. Curr Med Chem 2010;17:585–94.
[36] Sarker DK. Sculpted amphiphilic liposomal particles for modifiable medicinal applications. Curr Drug Discov Technol 2009;6:52–8.
[37] Sarker DK. Engineering of nanoemulsions for drug delivery. Curr Drug Deliv 2005;2:297–310.
[38] Huynh NT, Passirani C, Saulnier P, Benoit JP. Lipid nanocapsules: a new platform for nanomedicine. Int J Pharm 2009;379:201–9.
[39] Patel D, Sawant KK. Self micro-emulsifying drug delivery system: formulation development and biopharmaceutical evaluation of lipophilic drugs. Curr Drug Deliv 2009;6:419–24.
[40] Maham A, Tang Z, Wu H, Wang J, Lin Y. Protein-based nanomedicine platforms for drug delivery. Small 2009;5:1706–21.
[41] Mao C, Flynn CE, Hayhurst A, Sweeney R, Qi J, Georgiou G, et al. Viral assembly of oriented quantum dot nanowires. Proc Natl Acad Sci U S A 2003;100:6946–51.
[42] Mao C, Solis DJ, Reiss BD, Kottmann ST, Sweeney RY, Hayhurst A, et al. Virus-based toolkit for the directed synthesis of magnetic and semiconducting nanowires. Science 2004;303:213–7.
[43] Nam KT, Kim DW, Yoo PJ, Chiang CY, Meethong N, Hammond PT, et al. Virus-enabled synthesis and assembly of nanowires for lithium ion battery electrodes. Science 2006;312:885–8.
[44] Goldmann C, Stolte N, Nisslein T, Hunsmann G, Luke W, Petry H. Packaging of small molecules into VP1–virus–like particles of the human polyomavirus JC virus. J Virol Methods 2000;90:85–90.
[45] Georgens C, Weyermann J, Zimmer A. Recombinant virus like particles as drug delivery system. Curr Pharm Biotechnol 2005;6:49–55.
[46] Xu YF, Zhang YQ, Xu XM, Song GX. Papillomavirus virus-like particles as vehicles for the delivery of epitopes or genes. Arch Virol 2006;151:2133–48.
[47] Malboeuf CM, Simon DA, Lee YE, Lankes HA, Dewhurst S, Frelinger JG, et al. Human papillomavirus-like particles mediate functional delivery of plasmid DNA to antigen presenting cells in vivo. Vaccine 2007;25:3270–6.
[48] Lee TJ, Schwartz C, Guo P. Construction of bacteriophage phi29 DNA packaging motor and its applications in nanotechnology and therapy. Ann Biomed Eng 2009;37:2064–81.
[49] Hiratsuka Y, Miyata M, Tada T, Uyeda TQ. A microrotary motor powered by bacteria. Proc Natl Acad Sci U S A 2006;103:13618–23.
[50] Kumara MT, Muralidharan S, Tripp BC. Generation and characterization of inorganic and organic nanotubes on bioengineered flagella of mesophilic bacteria. J Nanosci Nanotechnol 2007;7:2260–72.
[51] Deplanche K, Woods RD, Mikheenko IP, Sockett RE, Macaskie LE. Manufacture of stable palladium and gold nanoparticles on native and genetically engineered flagella scaffolds. Biotechnol Bioeng 2008;101:873–80.
[52] Aris A, Feliu JX, Knight A, Coutelle C, Villaverde A. Exploiting viral cell-targeting abilities in a single polypeptide, non-infectious, recombinant vehicle for integrin-mediated DNA delivery and gene expression. Biotechnol Bioeng 2000;68:689–96.
[53] Hassane FS, Ivanova GD, Bolewska-Pedyczak E, Abes R, Arzumanov AA, Gait MJ, et al. A peptide-based dendrimer that enhances the splice-redirecting activity of PNA conjugates in cells. Bioconjug Chem 2009;20:1523–30.
[54] Rodriguez-Carmona E, Villaverde A. Nanostructured bacterial materials for innovative medicines. Trends Microbiol 2010;18:423–30.
[55] Villaverde A. Nanotechnology, bionanotechnology and microbial cell factories. Microb Cell Fact 2010;9:53.
[56] Straub JE, Thirumalai D. Principles governing oligomer formation in amyloidogenic peptides. Curr Opin Struct Biol 2010;20:187–95.
[57] Reddy G, Straub JE, Thirumalai D. Dynamics of locking of peptides onto growing amyloid fibrils. Proc Natl Acad Sci U S A 2009;106:11948–53.
[58] Espargaro A, Villar-Pique A, Sabate R, Ventura S. Yeast prions form infectious amyloid inclusion bodies in bacteria. Microb Cell Fact 2012;11:89.
[59] Villar-Pique A, Espargaro A, Sabate R, de Groot NS, Ventura S. Using bacterial inclusion bodies to screen for amyloid aggregation inhibitors. Microb Cell Fact 2012;11:55.
[60] Garcia-Fruitos E, Sabate R, de Groot NS, Villaverde A, Ventura S. Biological role of bacterial inclusion bodies: a model for amyloid aggregation. FEBS J 2011;278:2419–27.
[61] Martinez-Alonso M, Gonzalez-Montalban N, Garcia-Fruitos E, Villaverde A. The functional quality of soluble recombinant polypeptides produced in *Escherichia coli* is defined by a wide conformational spectrum. Appl Environ Microbiol 2008;101:1353–8.
[62] Schrodel A, de MA. Characterization of the aggregates formed during recombinant protein expression in bacteria. BMC Biochem 2005;6:10.
[63] Collins L, Parker AL, Gehman JD, Eckley L, Perugini MA, Separovic F, et al. Self-assembly of peptides into spherical nanoparticles for delivery of hydrophilic moieties to the cytosol. ACS Nano 2010;4:2856–64.
[64] Yang YL, Khoe U, Wang XM, Horii A, Yokoi H, Zhang SG. Designer self-assembling peptide nanomaterials. Nano Today 2009;4:193–210.
[65] Wright ER, Conticello VP. Self-assembly of block copolymers derived from elastin-mimetic polypeptide sequences. Adv Drug Deliv Rev 2002;54:1057–73.
[66] Futaki S, Nakase I, Tadokoro A, Takeuchi T, Jones AT. Arginine-rich peptides and their internalization mechanisms. Biochem Soc Trans 2007;35:784–7.
[67] Melikov K, Chernomordik LV. Arginine-rich cell penetrating peptides: from endosomal uptake to nuclear delivery. Cell Mol Life Sci 2005:622739–49.
[68] Satheshkumar PS, Lokesh GL, Murthy MR, Savithri HS. The role of arginine-rich motif and beta-annulus in the assembly and stability of Sesbania mosaic virus capsids. J Mol Biol 2005;353:447–58.
[69] Ejima D, Yumioka R, Arakawa T, Tsumoto K. Arginine as an effective additive in gel permeation chromatography. J Chromatogr A 2005;1094:49–55.
[70] Tsumoto K, Umetsu M, Kumagai I, Ejima D, Philo JS, Arakawa T. Role of arginine in protein refolding, solubilization, and purification. Biotechnol Prog 2004;20:1301–8.
[71] Ferrari M. Frontiers in cancer nanomedicine: directing mass transport through biological barriers. Trends Biotechnol 2010;28:181–8.
[72] Jiang W, Kim BY, Rutka JT, Chan WC. Nanoparticle-mediated cellular response is size-dependent. Nat Nanotechnol 2008;3:145–50.
[73] Murakami T, Zhang TY, Koyanagi Y, Tanaka Y, Kim J, Suzuki Y, et al. Inhibitory mechanism of the CXCR4 antagonist t22 against human immunodeficiency virus type 1 infection. Journal of Virology 1999;73:7489–96.
[74] Amara A, Gall SL, Schwartz O, Salamero J, Montes M, Loetscher P, et al. HIV coreceptor downregulation as antiviral principle: SDF-1alpha-dependent internalization of the chemokine receptor CXCR4 contributes to inhibition of HIV replication. J Exp Med 1997;186:139–46.
[75] Kledal TN, Rosenkilde MM, Coulin F, Simmons G, Johnsen AH, Alouani S, et al. A broad-spectrum chemokine antagonist encoded by Kaposi's sarcoma-associated herpesvirus. Science 1997;277:1656–9.
[76] Zhou NM, Luo ZW, Luo JS, Hall JW, Huang ZW. A novel peptide antagonist of CXCR4 derived from the N-terminus of viral chemokine vMIP-II. Biochemistry 2000;39:3782–7.
[77] Demeule M, Regina A, Che C, Poirier J, Nguyen T, Gabathuler R, et al. Identification and design of peptides as a new drug delivery system for the brain. Journal of Pharmacology and Experimental Therapeutics 2008;324:1064–72.
[78] Maggie J, Hsiang-Fa L, Sing-Ming C, Yi-Ju K, Li-Wen C. Peptide for trans-migration across brain blood barrier and delivery systems comprising the same. 12/979, 804 [US2011/0165079 A1] 2010. US.
[79] Hibino S, Shibuya M, Engbring JA, Mochizuki M, Nomizu M, Kleinman HK. Identification of an active site on the laminin alpha 5 chain globular domain that binds to CD44 and inhibits malignancy. Cancer Res 2004;64:4810–6.
[80] Jalkanen S, Jalkanen M. Lymphocyte CD44 binds the COOH-terminal heparin-binding domain of fibronectin. J Cell Biol 1992;116:817–25.
[81] Baker NA, Sept D, Joseph S, Holst MJ, McCammon JA. Electrostatics of nanosystems: application to microtubules and the ribosome. Proc Natl Acad Sci U S A 2001;98:10037–41.

References

References

1. Fleming, A., *On the antibacterial action of cultures of a penicillium, with special reference to their use in the isolation of B. influenzae. 1929.* Bull World Health Organ, 1929. **79**(8): p. 780-90.
2. Demain, A.L. and P. Vaishnav, *Production of recombinant proteins by microbes and higher organisms.* Biotechnology advances, 2009. **27**(3): p. 297-306.
3. Watson, J.D. and F.H. Crick, *Molecular structure of nucleic acids; a structure for deoxyribose nucleic acid.* Nature, 1953. **171**(4356): p. 737-8.
4. Matthaei, J.H., et al., *Characteristics and composition of RNA coding units.* Proc Natl Acad Sci U S A, 1962. **48**: p. 666-77.
5. Jackson, D.A., R.H. Symons, and P. Berg, *Biochemical method for inserting new genetic information into DNA of Simian Virus 40: circular SV40 DNA molecules containing lambda phage genes and the galactose operon of Escherichia coli.* Proceedings of the National Academy of Sciences, 1972. **69**(10): p. 2904-2909.
6. Cohen, S.N., et al., *Construction of biologically functional bacterial plasmids in vitro.* Proceedings of the National Academy of Sciences, 1973. **70**(11): p. 3240-3244.
7. Jain, K.K., *The handbook of nanomedicine*. 2012: Springer Science & Business Media.
8. Rizzo, L.Y., et al., *Recent progress in nanomedicine: therapeutic, diagnostic and theranostic applications.* Curr Opin Biotechnol, 2013. **24**(6): p. 1159-66.
9. Gleiter, H., *Nanocrystalline materials.* progress in Materials Science, 1989. **33**(4): p. 223-315.
10. Riehemann, K., et al., *Nanomedicine—challenge and perspectives.* Angewandte Chemie International Edition, 2009. **48**(5): p. 872-897.
11. Suh, W.H., Y.-H. Suh, and G.D. Stucky, *Multifunctional nanosystems at the interface of physical and life sciences.* Nano Today, 2009. **4**(1): p. 27-36.
12. Tang, M., et al., *Recent progress in nanotechnology for cancer therapy.* Chin J Cancer, 2010. **29**(9): p. 775-80.
13. Park, J.H., et al., *Cooperative nanoparticles for tumor detection and photothermally triggered drug delivery.* Advanced Materials, 2010. **22**(8): p. 880-885.
14. Cho, K., et al., *Therapeutic nanoparticles for drug delivery in cancer.* Clinical cancer research, 2008. **14**(5): p. 1310-1316.
15. Kim, B.Y., J.T. Rutka, and W.C. Chan, *Nanomedicine.* New England Journal of Medicine, 2010. **363**(25): p. 2434-2443.
16. Lammers, T., W.E. Hennink, and G. Storm, *Tumour-targeted nanomedicines: principles and practice.* Br J Cancer, 2008. **99**(3): p. 392-7.
17. Matsumura, Y. and H. Maeda, *A new concept for macromolecular therapeutics in cancer chemotherapy: mechanism of tumoritropic accumulation of proteins and the antitumor agent smancs.* Cancer research, 1986. **46**(12 Part 1): p. 6387-6392.
18. Maeda, H., H. Nakamura, and J. Fang, *The EPR effect for macromolecular drug delivery to solid tumors: Improvement of tumor uptake, lowering of systemic toxicity, and distinct tumor imaging in vivo.* Advanced Drug Delivery Reviews, 2013. **65**(1): p. 71-79.
19. Lammers, T., et al., *Drug targeting to tumors: principles, pitfalls and (pre-) clinical progress.* J Control Release, 2012. **161**(2): p. 175-87.
20. Liu, X.M., S.C. Miller, and D. Wang, *Beyond oncology--application of HPMA copolymers in non-cancerous diseases.* Adv Drug Deliv Rev, 2010. **62**(2): p. 258-71.
21. Lobatto, M.E., et al., *Perspectives and opportunities for nanomedicine in the management of atherosclerosis.* Nat Rev Drug Discov, 2011. **10**(11): p. 835-52.
22. Lammers, T., et al., *Nanotheranostics and image-guided drug delivery: current concepts and future directions.* Mol Pharm, 2010. **7**(6): p. 1899-912.

23. Janib, S.M., A.S. Moses, and J.A. MacKay, *Imaging and drug delivery using theranostic nanoparticles.* Advanced Drug Delivery Reviews, 2010. **62**(11): p. 1052-1063.
24. Chiribiri, A., et al., *Visualization of the cardiac venous system using cardiac magnetic resonance.* American Journal of Cardiology, 2008. **101**(3): p. 407-412.
25. Fink, C., et al., *High‐resolution three‐dimensional MR angiography of rodent tumors: Morphologic characterization of intratumoral vasculature.* Journal of Magnetic Resonance Imaging, 2003. **18**(1): p. 59-65.
26. Politi, L.S., et al., *Magnetic-resonance-based tracking and quantification of intravenously injected neural stem cell accumulation in the brains of mice with experimental multiple sclerosis.* Stem Cells, 2007. **25**(10): p. 2583-92.
27. Reimer, P. and T. Balzer, *Ferucarbotran (Resovist): a new clinically approved RES-specific contrast agent for contrast-enhanced MRI of the liver: properties, clinical development, and applications.* European radiology, 2003. **13**(6): p. 1266-1276.
28. Zhu, J., L. Zhou, and F. XingWu, *Tracking neural stem cells in patients with brain trauma.* N Engl J Med, 2006. **355**(22): p. 2376-8.
29. Harisinghani, M.G., et al., *Noninvasive detection of clinically occult lymph-node metastases in prostate cancer.* N Engl J Med, 2003. **348**(25): p. 2491-9.
30. de Vries, I.J., et al., *Magnetic resonance tracking of dendritic cells in melanoma patients for monitoring of cellular therapy.* Nat Biotechnol, 2005. **23**(11): p. 1407-13.
31. Tang, T.Y., et al., *The ATHEROMA (Atorvastatin Therapy: Effects on Reduction of Macrophage Activity) Study. Evaluation using ultrasmall superparamagnetic iron oxide-enhanced magnetic resonance imaging in carotid disease.* J Am Coll Cardiol, 2009. **53**(22): p. 2039-50.
32. Taton, T.A., *Nanostructures as tailored biological probes.* Trends in Biotechnology, 2002. **20**(7): p. 277-279.
33. Emerich, D.F. and C.G. Thanos, *Targeted nanoparticle-based drug delivery and diagnosis.* Journal of drug targeting, 2007. **15**(3): p. 163-183.
34. Groneberg, D.A., et al., *Nanoparticle-based diagnosis and therapy.* Current drug targets, 2006. **7**(6): p. 643-648.
35. Tsuji, A., *Small molecular drug transfer across the blood-brain barrier via carrier-mediated transport systems.* NeuroRx, 2005. **2**(1): p. 54-62.
36. Shityakov, S., et al., *Blood-brain barrier transport studies, aggregation, and molecular dynamics simulation of multiwalled carbon nanotube functionalized with fluorescein isothiocyanate.* Int J Nanomedicine, 2015. **10**: p. 1703-13.
37. Elsabahy, M. and K.L. Wooley, *Design of polymeric nanoparticles for biomedical delivery applications.* Chem Soc Rev, 2012. **41**(7): p. 2545-61.
38. Bangham, A. and R. Horne, *Negative staining of phospholipids and their structural modification by surface-active agents as observed in the electron microscope.* Journal of molecular biology, 1964. **8**(5): p. 660-IN10.
39. Shi, J., et al., *Self-assembled targeted nanoparticles: evolution of technologies and bench to bedside translation.* Acc Chem Res, 2011. **44**(10): p. 1123-34.
40. Torchilin, V.P., *Recent advances with liposomes as pharmaceutical carriers.* Nature Reviews Drug Discovery, 2005. **4**(2): p. 145-160.
41. Qiu, L., N. Jing, and Y. Jin, *Preparation and in vitro evaluation of liposomal chloroquine diphosphate loaded by a transmembrane pH-gradient method.* International journal of pharmaceutics, 2008. **361**(1): p. 56-63.
42. Malam, Y., M. Loizidou, and A.M. Seifalian, *Liposomes and nanoparticles: nanosized vehicles for drug delivery in cancer.* Trends in Pharmacological Sciences, 2009. **30**(11): p. 592-599.

43. Ghosh, P., et al., *Gold nanoparticles in delivery applications.* Adv Drug Deliv Rev, 2008. **60**(11): p. 1307-15.
44. Duzgunes, N., et al., *Fusion of liposomes containing a novel cationic lipid, N-[2, 3-(dioleyloxy) propyl]-N, N, N-trimethylammonium: induction by multivalent anions and asymmetric fusion with acidic phospholipid vesicles.* Biochemistry, 1989. **28**(23): p. 9179-9184.
45. van der Woude, I., et al., *Parameters influencing the introduction of plasmid DNA into cells by the use of synthetic amphiphiles as a carrier system.* Biochimica et Biophysica Acta (BBA)-Biomembranes, 1995. **1240**(1): p. 34-40.
46. Matsui, H., et al., *Loss of binding and entry of liposome-DNA complexes decreases transfection efficiency in differentiated airway epithelial cells.* Journal of Biological Chemistry, 1997. **272**(2): p. 1117-1126.
47. Malam, Y., M. Loizidou, and A.M. Seifalian, *Liposomes and nanoparticles: nanosized vehicles for drug delivery in cancer.* Trends Pharmacol Sci, 2009. **30**(11): p. 592-9.
48. Moghimi, S.M. and J. Szebeni, *Stealth liposomes and long circulating nanoparticles: critical issues in pharmacokinetics, opsonization and protein-binding properties.* Progress in Lipid Research, 2003. **42**(6): p. 463-478.
49. Bangham, A.D., *Liposomes - the Babraham Connection.* Chemistry and Physics of Lipids, 1993. **64**(1-3): p. 275-285.
50. Campos, S.M., et al., *The clinical utility of liposomal doxorubicin in recurrent ovarian cancer.* Gynecologic Oncology, 2001. **81**(2): p. 206-212.
51. Brannon-Peppas, L., *Recent advances on the use of biodegradable microparticles and nanoparticles in controlled drug delivery.* International Journal of Pharmaceutics, 1995. **116**(1): p. 1-9.
52. Alexis, F., et al., *Factors affecting the clearance and biodistribution of polymeric nanoparticles.* Molecular Pharmaceutics, 2008. **5**(4): p. 505-515.
53. Zhang, L., et al., *Nanoparticles in medicine: Therapeutic applications and developments.* Clinical Pharmacology & Therapeutics, 2008. **83**(5): p. 761-769.
54. Mundargi, R.C., et al., *Nano/micro technologies for delivering macromolecular therapeutics using poly(D,L-lactide-co-glycolide) and its derivatives.* Journal of Controlled Release, 2008. **125**(3): p. 193-209.
55. Farokhzad, O.C., et al., *Nanoparticle-aptamer bioconjugates a new approach for targeting prostate cancer cells.* Cancer research, 2004. **64**(21): p. 7668-7672.
56. Reis, C.P., et al., *Nanoencapsulation I. Methods for preparation of drug-loaded polymeric nanoparticles.* Nanomedicine: Nanotechnology, Biology and Medicine, 2006. **2**(1): p. 8-21.
57. Panyam, J. and V. Labhasetwar, *Biodegradable nanoparticles for drug and gene delivery to cells and tissue.* Advanced Drug Delivery Reviews, 2012. **64**: p. 61-71.
58. Sahana, D., et al., *PLGA nanoparticles for oral delivery of hydrophobic drugs: influence of organic solvent on nanoparticle formation and release behavior in vitro and in vivo using estradiol as a model drug.* Journal of pharmaceutical sciences, 2008. **97**(4): p. 1530-1542.
59. Barichello, J.M., et al., *Encapsulation of hydrophilic and lipophilic drugs in PLGA nanoparticles by the nanoprecipitation method.* Drug Development and Industrial Pharmacy, 1999. **25**(4): p. 471-476.
60. Bittner, B., et al., *Bovine serum albumin loaded poly(lactide-co-glycolide) microspheres: the influence of polymer purity on particle characteristics.* Journal of Microencapsulation, 1998. **15**(4): p. 495-514.

61. Carrasquillo, K.G., et al., *Non-aqueous encapsulation of excipient-stabilized spray-freeze dried BSA into poly(lactide-co-glycolide) microspheres results in release of native protein.* Journal of Controlled Release, 2001. **76**(3): p. 199-208.
62. Kumar, M.N.V.R., et al., *Cationic poly(lactide-co-glycolide) nanoparticles as efficient in vivo gene transfection agents.* Journal of Nanoscience and Nanotechnology, 2004. **4**(8): p. 990-994.
63. Kumari, A., S.K. Yadav, and S.C. Yadav, *Biodegradable polymeric nanoparticles based drug delivery systems.* Colloids and Surfaces B: Biointerfaces, 2010. **75**(1): p. 1-18.
64. Sun, B., B. Ranganathan, and S.S. Feng, *Multifunctional poly(D,L-lactide-co-glycolide)/montmorillonite (PLGA/MMT) nanoparticles decorated by Trastuzumab for targeted chemotherapy of breast cancer.* Biomaterials, 2008. **29**(4): p. 475-486.
65. Crooks, R.M., et al., *Dendrimer-encapsulated metal nanoparticles: Synthesis, characterization, and applications to catalysis.* Accounts of Chemical Research, 2001. **34**(3): p. 181-190.
66. Scott, R.W.J., O.M. Wilson, and R.M. Crooks, *Synthesis, characterization, and applications of dendrimer-encapsulated nanoparticles.* Journal of Physical Chemistry B, 2005. **109**(2): p. 692-704.
67. Kainz, Q.M. and O. Reiser, *Polymer- and Dendrimer-Coated Magnetic Nanoparticles as Versatile Supports for Catalysts, Scavengers, and Reagents.* Accounts of Chemical Research, 2014. **47**(2): p. 667-677.
68. Medley, C.D., et al., *Gold nanoparticle-based colorimetric assay for the direct detection of cancerous cells.* Analytical chemistry, 2008. **80**(4): p. 1067-1072.
69. Corsi, F., et al., *Towards Ideal Magnetofluorescent Nanoparticles for Bimodal Detection of Breast‐Cancer Cells.* Small, 2009. **5**(22): p. 2555-2564.
70. Gupta, A.K. and M. Gupta, *Synthesis and surface engineering of iron oxide nanoparticles for biomedical applications.* Biomaterials, 2005. **26**(18): p. 3995-4021.
71. Gallo, J.M. and U. Hafeli, *Preclinical experiences with magnetic drug targeting: Tolerance and efficacy and clinical experiences with magnetic drug targeting: A phase I study with 4'-epidoxorubicin in 14 patients with advanced solid tumors.* Cancer Research, 1997. **57**(14): p. 3063-3064.
72. Scarberry, K.E., et al., *Selective removal of ovarian cancer cells from human ascites fluid using magnetic nanoparticles.* Nanomedicine-Nanotechnology Biology and Medicine, 2010. **6**(3): p. 399-408.
73. Patolsky, F., et al., *Electrical detection of single viruses.* Proceedings of the National Academy of Sciences of the United States of America, 2004. **101**(39): p. 14017-14022.
74. Bunimovich, Y.L., et al., *Electrochemically programmed, spatially selective biofunctionalization of silicon wires.* Langmuir, 2004. **20**(24): p. 10630-10638.
75. Wang, A.Z., R. Langer, and O.C. Farokhzad, *Nanoparticle Delivery of Cancer Drugs.* Annual Review of Medicine, Vol 63, 2012. **63**: p. 185-198.
76. Baneyx, F., *Recombinant protein expression in Escherichia coli.* Curr Opin Biotechnol, 1999. **10**(5): p. 411-21.
77. Schmidt, F.R., *Recombinant expression systems in the pharmaceutical industry.* Applied Microbiology and Biotechnology, 2004. **65**(4): p. 363-372.
78. Ikonomou, L., Y.-J. Schneider, and S. Agathos, *Insect cell culture for industrial production of recombinant proteins.* Applied microbiology and biotechnology, 2003. **62**(1): p. 1-20.
79. Birch, J.R. and S.J. Froud, *Mammalian-Cell Culture Systems for Recombinant Protein-Production.* Biologicals, 1994. **22**(2): p. 127-133.
80. Scheffel, U., et al., *Albumin microspheres for study of the reticuloendothelial system.* J Nucl Med, 1972. **13**(7): p. 498-503.

81. Lohcharoenkal, W., et al., *Protein Nanoparticles as Drug Delivery Carriers for Cancer Therapy.* Biomed Research International, 2014.
82. Marty, J.J., R.C. Oppenheim, and P. Speiser, *Nanoparticles--a new colloidal drug delivery system.* Pharm Acta Helv, 1978. **53**(1): p. 17-23.
83. Estrada, L.H., S. Chu, and J.A. Champion, *Protein nanoparticles for intracellular delivery of therapeutic enzymes.* J Pharm Sci, 2014. **103**(6): p. 1863-71.
84. Carter, D.C., et al., *Three-dimensional structure of human serum albumin.* Science, 1989. **244**(4909): p. 1195-1198.
85. Carter, D.C. and J.X. Ho, *Structure of serum albumin.* 1994.
86. Carter, D.C. and J.X. Ho, *Structure of serum albumin.* Adv Protein Chem, 1994. **45**: p. 153-203.
87. John, T.A., et al., *Quantitative analysis of albumin uptake and transport in the rat microvessel endothelial monolayer.* American Journal of Physiology-Lung Cellular and Molecular Physiology, 2003. **284**(1): p. L187-L196.
88. Desai, N., V. Trieu, and Z. Yao, *Increased antitumor activity, intratumor paclitaxel concentrations, and endothelial cell transport of cremophor-free, albumin-bound paclitaxel, ABI-007, compared with cremophor-based paclitaxel (vol 12, pg 1317, 2006).* Clinical Cancer Research, 2006. **12**(12): p. 3869-3869.
89. Peters, T., *Serum albumin.* Advances in protein chemistry, 1985. **37**: p. 161-245.
90. Babson, A.L. and T. Winnick, *Protein Transfer in Tumor-Bearing Rats.* Cancer Research, 1954. **14**(8): p. 606-611.
91. Hobbs, S.K., et al., *Regulation of transport pathways in tumor vessels: Role of tumor type and microenvironment.* Proceedings of the National Academy of Sciences of the United States of America, 1998. **95**(8): p. 4607-4612.
92. Maeda, H., et al., *Tumor vascular permeability and the EPR effect in macromolecular therapeutics: a review.* Journal of Controlled Release, 2000. **65**(1-2): p. 271-284.
93. Matsumura, Y. and H. Maeda, *A New Concept for Macromolecular Therapeutics in Cancer-Chemotherapy - Mechanism of Tumoritropic Accumulation of Proteins and the Antitumor Agent Smancs.* Cancer Research, 1986. **46**(12): p. 6387-6392.
94. Yuan, F., et al., *Vascular-Permeability in a Human Tumor Xenograft - Molecular-Size Dependence and Cutoff Size.* Cancer Research, 1995. **55**(17): p. 3752-3756.
95. Noguchi, Y., et al., *Early phase tumor accumulation of macromolecules: a great difference in clearance rate between tumor and normal tissues.* Japanese Journal of Cancer Research, 1998. **89**(3): p. 307-314.
96. Kratz, F. and U. Beyer, *Serum proteins as drug carriers of anticancer agents: A review.* Drug Delivery, 1998. **5**(4): p. 281-299.
97. Stehle, G., et al., *Plasma protein (albumin) catabolism by the tumor itself - implications for tumor metabolism and the genesis of cachexia.* Critical Reviews in Oncology/Hematology, 1997. **26**(2): p. 77-100.
98. Gradishar, W.J., et al., *Phase III trial of nanoparticle albumin-bound paclitaxel compared with polyethylated castor oil-based paclitaxel in women with breast cancer.* Journal of Clinical Oncology, 2005. **23**(31): p. 7794-7803.
99. Stehle, G., et al., *The loading rate determines tumor targeting properties of methotrexate-albumin conjugates in rats.* Anti-Cancer Drugs, 1997. **8**(7): p. 677-685.
100. Di Stefano, G., et al., *Doxorubicin coupled to lactosaminated human albumin remains confined within mouse liver cells after the intracellular release from the carrier.* Digestive and Liver Disease, 2003. **35**(6): p. 428-433.

101. Zeltins, A., *Construction and characterization of virus-like particles: a review.* Mol Biotechnol, 2013. **53**(1): p. 92-107.
102. Kushnir, N., S.J. Streatfield, and V. Yusibov, *Virus-like particles as a highly efficient vaccine platform: diversity of targets and production systems and advances in clinical development.* Vaccine, 2012. **31**(1): p. 58-83.
103. Bachmann, M.F. and R.M. Zinkernagel, *Neutralizing antiviral B cell responses.* Annu Rev Immunol, 1997. **15**: p. 235-70.
104. Brun, A., et al., *Current strategies for subunit and genetic viral veterinary vaccine development.* Virus Res, 2011. **157**(1): p. 1-12.
105. Bachmann, M.F. and M.R. Dyer, *Therapeutic vaccination for chronic diseases: a new class of drugs in sight.* Nat Rev Drug Discov, 2004. **3**(1): p. 81-8.
106. Bachmann, M.F., et al., *The influence of antigen organization on B cell responsiveness.* Science, 1993. **262**(5138): p. 1448-1451.
107. Frazer, I.H., *Prevention of cervical cancer through papillomavirus vaccination.* Nature Reviews Immunology, 2004. **4**(1): p. 46-55.
108. Pumpens, P., et al., *Construction of novel vaccines on the basis of the virus-like particles: Hepatitis B virus proteins as vaccine carriers.* Medicinal Protein Engineering. CRC Press, Boca Raton, Florida, 2008.
109. Lamarre, B. and M.G. Ryadnov, *Self-Assembling Viral Mimetics: One Long Journey with Short Steps.* Macromolecular Bioscience, 2011. **11**(4): p. 503-513.
110. Seow, Y. and M.J. Wood, *Biological Gene Delivery Vehicles: Beyond Viral Vectors.* Molecular Therapy, 2009. **17**(5): p. 767-777.
111. Phelps, D.K., B. Speelman, and C.B. Post, *Theoretical studies of viral capsid proteins.* Current Opinion in Structural Biology, 2000. **10**(2): p. 170-173.
112. Zlotnick, A. and S. Mukhopadhyay, *Virus assembly, allostery and antivirals.* Trends in Microbiology, 2011. **19**(1): p. 14-23.
113. Landry, N., et al., *Influenza virus-like particle vaccines made in Nicotiana benthamiana elicit durable, poly-functional and cross-reactive T cell responses to influenza HA antigens.* Clinical Immunology, 2014. **154**(2): p. 164-177.
114. Li, M., et al., *Mumps virus matrix, fusion, and nucleocapsid proteins cooperate for efficient production of virus-like particles.* Journal of virology, 2009. **83**(14): p. 7261-7272.
115. Lopez-Macias, C., et al., *Safety and immunogenicity of a virus-like particle pandemic influenza A (H1N1) 2009 vaccine in a blinded, randomized, placebo-controlled trial of adults in Mexico.* Vaccine, 2011. **29**(44): p. 7826-7834.
116. Landry, N., et al., *Preclinical and Clinical Development of Plant-Made Virus-Like Particle Vaccine against Avian H5N1 Influenza.* Plos One, 2010. **5**(12).
117. Agnandji, S.T., et al., *First results of phase 3 trial of RTS, S/AS01 malaria vaccine in African children.* The New England journal of medicine, 2011. **365**(20): p. 1863-75.
118. Vazquez, E. and A. Villaverde, *Engineering building blocks for self-assembling protein nanoparticles.* Microbial Cell Factories, 2010. **9**.
119. Glover, D.J., et al., *Multifunctional protein nanocarriers for targeted nuclear gene delivery in nondividing cells.* Faseb Journal, 2009. **23**(9): p. 2996-3006.
120. Domingo-Espin, J., et al., *RGD-based cell ligands for cell-targeted drug delivery act as potent trophic factors.* Nanomedicine-Nanotechnology Biology and Medicine, 2012. **8**(8): p. 1263-1266.
121. Domingo-Espin, J., et al., *Nanoparticulate architecture of protein-based artificial viruses is supported by protein-DNA interactions.* Nanomedicine, 2011. **6**(6): p. 1047-1061.

122. Subramanian, G.M., et al., *Albinterferon alpha-2b: a genetic fusion protein for the treatment of chronic hepatitis C.* Nature Biotechnology, 2007. **25**(12): p. 1411-1419.
123. Melder, R.J., et al., *Pharmacokinetics and in vitro and in vivo anti-tumor response of an interleukin-2-human serum albumin fusion protein in mice.* Cancer Immunology Immunotherapy, 2005. **54**(6): p. 535-547.
124. Chang, K.L., et al., *Efficient Gene Transfection by Histidine-Modified Chitosan through Enhancement of Endosomal Escape.* Bioconjugate Chemistry, 2010. **21**(6): p. 1087-1095.
125. Vazquez, E., et al., *Protein nanodisk assembling and intracellular trafficking powered by an arginine-rich (R9) peptide.* Nanomedicine, 2010. **5**(2): p. 259-268.
126. Vazquez, E., et al., *Internalization and kinetics of nuclear migration of protein-only, arginine-rich nanoparticles.* Biomaterials, 2010. **31**(35): p. 9333-9339.
127. Xu, S., et al., *Targeting receptor-mediated endocytotic pathways with nanoparticles: rationale and advances.* Adv Drug Deliv Rev, 2013. **65**(1): p. 121-38.
128. Zhang, S., et al., *Spontaneous assembly of a self-complementary oligopeptide to form a stable macroscopic membrane.* Proc Natl Acad Sci U S A, 1993. **90**(8): p. 3334-8.
129. Koutsopoulos, S., et al., *Controlled release of functional proteins through designer self-assembling peptide nanofiber hydrogel scaffold.* Proceedings of the National Academy of Sciences, 2009. **106**(12): p. 4623-4628.
130. Unzueta, U., et al., *Non-amyloidogenic peptide tags for the regulatable self-assembling of protein-only nanoparticles.* Biomaterials, 2012. **33**(33): p. 8714-8722.
131. Unzueta, U., et al., *Intracellular CXCR4(+) cell targeting with T22-empowered protein-only nanoparticles.* International Journal of Nanomedicine, 2012. **7**: p. 4533-4544.
132. Cespedes, M.V., et al., *In Vivo Architectonic Stability of Fully de Novo Designed Protein-Only Nanoparticles.* Acs Nano, 2014. **8**(5): p. 4166-4176.
133. Maeda, H., H. Nakamura, and J. Fang, *The EPR effect for macromolecular drug delivery to solid tumors: Improvement of tumor uptake, lowering of systemic toxicity, and distinct tumor imaging in vivo.* Adv Drug Deliv Rev, 2013. **65**(1): p. 71-9.
134. Matsumura, Y. and H. Maeda, *A new concept for macromolecular therapeutics in cancer chemotherapy: mechanism of tumoritropic accumulation of proteins and the antitumor agent smancs.* Cancer Res, 1986. **46**(12 Pt 1): p. 6387-92.
135. Gottesman, M.M., T. Fojo, and S.E. Bates, *Multidrug resistance in cancer: role of ATP-dependent transporters.* Nat Rev Cancer, 2002. **2**(1): p. 48-58.
136. Ferrara, N., *VEGF as a therapeutic target in cancer.* Oncology, 2005. **69**: p. 11-16.
137. Van Cutsem, E., et al., *Cetuximab and Chemotherapy as Initial Treatment for Metastatic Colorectal Cancer.* New England Journal of Medicine, 2009. **360**(14): p. 1408-1417.
138. Albanell, J. and J. Baselga, *Trastuzumab, a humanized anti-HER2 monoclonal antibody, for the treatment of breast cancer.* Drugs of Today, 1999. **35**(12): p. 931-946.
139. Wang, A.Z., et al., *Biofunctionalized targeted nanoparticles for therapeutic applications.* Expert Opinion on Biological Therapy, 2008. **8**(8): p. 1063-1070.
140. McCarthy, J.R., et al., *Targeted nanoagents for the detection of cancers.* Molecular Oncology, 2010. **4**(6): p. 511-528.
141. Zhang, H.L., Y. Ma, and X.L. Sun, *Recent Developments in Carbohydrate-Decorated Targeted Drug/Gene Delivery.* Medicinal Research Reviews, 2010. **30**(2): p. 270-289.
142. Pouton, C.W., et al., *Targeted delivery to the nucleus.* Adv Drug Deliv Rev, 2007. **59**(8): p. 698-717.

143. Shiraishi, T., R. Hamzavi, and P.E. Nielsen, *Targeted delivery of plasmid DNA into the nucleus of cells via nuclear localization signal peptide conjugated to DNA intercalating bis- and trisacridines.* Bioconjug Chem, 2005. **16**(5): p. 1112-6.
144. Yousif, L.F., K.M. Stewart, and S.O. Kelley, *Targeting Mitochondria with Organelle-Specific Compounds: Strategies and Applications.* Chembiochem, 2009. **10**(12): p. 1939-1950.
145. Yoshikawa, T., et al., *Organelle-targeted delivery of biological macromolecules using the protein transduction domain: potential applications for Peptide aptamer delivery into the nucleus.* J Mol Biol, 2008. **380**(5): p. 777-82.
146. Hoshino, A., et al., *Quantum dots targeted to the assigned organelle in living cells.* Microbiology and Immunology, 2004. **48**(12): p. 985-994.
147. Terlecky, S.R. and J.I. Koepke, *Drug delivery to peroxisomes: Employing unique trafficking mechanisms to target protein therapeutics.* Advanced Drug Delivery Reviews, 2007. **59**(8): p. 739-747.
148. Kirpotin, D.B., et al., *Antibody targeting of long-circulating lipidic nanoparticles does not increase tumor localization but does increase internalization in animal models.* Cancer research, 2006. **66**(13): p. 6732-6740.
149. Choi, C.H.J., et al., *Mechanism of active targeting in solid tumors with transferrin-containing gold nanoparticles.* Proceedings of the National Academy of Sciences, 2010. **107**(3): p. 1235-1240.
150. Davis, M.E., *The first targeted delivery of siRNA in humans via a self-assembling, cyclodextrin polymer-based nanoparticle: from concept to clinic.* Molecular pharmaceutics, 2009. **6**(3): p. 659-668.
151. Talelli, M., et al., *Intrinsically active nanobody-modified polymeric micelles for tumor-targeted combination therapy.* Biomaterials, 2013. **34**(4): p. 1255-1260.
152. Ogris, M., et al., *Tumor-targeted gene therapy: strategies for the preparation of ligand-polyethylene glycol-polyethylenimine/DNA complexes.* Journal of Controlled Release, 2003. **91**(1-2): p. 173-181.
153. Albanese, A., P.S. Tang, and W.C.W. Chan, *The Effect of Nanoparticle Size, Shape, and Surface Chemistry on Biological Systems.* Annual Review of Biomedical Engineering, Vol 14, 2012. **14**: p. 1-16.
154. Choi, H.S., et al., *Renal clearance of quantum dots.* Nat Biotechnol, 2007. **25**(10): p. 1165-70.
155. Petros, R.A. and J.M. DeSimone, *Strategies in the design of nanoparticles for therapeutic applications.* Nat Rev Drug Discov, 2010. **9**(8): p. 615-27.
156. Enochs, W.S., et al., *Improved delineation of human brain tumors on MR images using a long-circulating, superparamagnetic iron oxide agent.* Jmri-Journal of Magnetic Resonance Imaging, 1999. **9**(2): p. 228-232.
157. Veiseh, O., et al., *Specific Targeting of Brain Tumors with an Optical/Magnetic Resonance Imaging Nanoprobe across the Blood-Brain Barrier.* Cancer Research, 2009. **69**(15): p. 6200-6207.
158. Reddy, S.T., et al., *Exploiting lymphatic transport and complement activation in nanoparticle vaccines.* Tissue Engineering Part A, 2008. **14**(5): p. 734-735.
159. Sadauskas, E., et al., *Kupffer cells are central in the removal of nanoparticles from the organism.* Part Fibre Toxicol, 2007. **4**: p. 10.
160. Choi, H.S., et al., *Rapid translocation of nanoparticles from the lung airspaces to the body.* Nature Biotechnology, 2010. **28**(12): p. 1300-U113.
161. Sarfati, G., et al., *Targeting of polymeric nanoparticles to lung metastases by surface-attachment of YIGSR peptide from laminin.* Biomaterials, 2011. **32**(1): p. 152-161.
162. Maeda, H. and Y. Matsumura, *EPR effect based drug design and clinical outlook for enhanced cancer chemotherapy Preface.* Advanced Drug Delivery Reviews, 2011. **63**(3): p. 129-130.

163. Schroeder, A., et al., *Treating metastatic cancer with nanotechnology.* Nat Rev Cancer, 2012. **12**(1): p. 39-50.
164. Gao, H., W. Shi, and L.B. Freund, *Mechanics of receptor-mediated endocytosis.* Proc Natl Acad Sci U S A, 2005. **102**(27): p. 9469-74.
165. Yuan, H., et al., *Variable nanoparticle-cell adhesion strength regulates cellular uptake.* Phys Rev Lett, 2010. **105**(13): p. 138101.
166. Jiang, W., et al., *Nanoparticle-mediated cellular response is size-dependent.* Nature Nanotechnology, 2008. **3**(3): p. 145-150.
167. Carrillo, L., G. Thiel, and A. Bertl, *Molecular Mechanisms of Endocytosis and Exocytosis in Yeast Studied by High-Resolution Membrane Capacitance Measurements.* Biophysical Journal, 2014. **106**(2): p. 310a-310a.
168. Miaczynska, M. and H. Stenmark, *Mechanisms and functions of endocytosis.* Journal of Cell Biology, 2008. **180**(1): p. 7-11.
169. Bareford, L.M. and P.W. Swaan, *Endocytic mechanisms for targeted drug delivery.* Adv Drug Deliv Rev, 2007. **59**(8): p. 748-58.
170. Torchilin, V.P., *Cell penetrating peptide-modified pharmaceutical nanocarriers for intracellular drug and gene delivery.* Biopolymers, 2008. **90**(5): p. 604-10.
171. See, V., et al., *Cathepsin L Digestion of Nanobioconjugates upon Endocytosis.* Acs Nano, 2009. **3**(9): p. 2461-2468.
172. Fischer, H.C., et al., *Exploring Primary Liver Macrophages for Studying Quantum Dot Interactions with Biological Systems.* Advanced Materials, 2010. **22**(23): p. 2520-2524.
173. Gratton, S.E.A., et al., *The effect of particle design on cellular internalization pathways.* Proceedings of the National Academy of Sciences of the United States of America, 2008. **105**(33): p. 11613-11618.
174. Toy, R., et al., *Shaping cancer nanomedicine: the effect of particle shape on the in vivo journey of nanoparticles.* Nanomedicine (Lond), 2014. **9**(1): p. 121-34.
175. Wang, J., et al., *The Complex Role of Multivalency in Nanoparticles Targeting the Transferrin Receptor for Cancer Therapies.* Journal of the American Chemical Society, 2010. **132**(32): p. 11306-11313.
176. Jin, H., et al., *Size-Dependent Cellular Uptake and Expulsion of Single-Walled Carbon Nanotubes: Single Particle Tracking and a Generic Uptake Model for Nanoparticles.* Acs Nano, 2009. **3**(1): p. 149-158.
177. Rastogi, L., A.J. Kora, and A. J, *Highly stable, protein capped gold nanoparticles as effective drug delivery vehicles for amino-glycosidic antibiotics.* Mater Sci Eng C Mater Biol Appl, 2012. **32**(6): p. 1571-7.
178. Yan, J.M., et al., *One-step seeding growth of magnetically recyclable Au@Co core-shell nanoparticles: highly efficient catalyst for hydrolytic dehydrogenation of ammonia borane.* J Am Chem Soc, 2010. **132**(15): p. 5326-7.
179. Skrastina, D., et al., *Silica Nanoparticles as the Adjuvant for the Immunisation of Mice Using Hepatitis B Core Virus-Like Particles.* Plos One, 2014. **9**(12).
180. Rao, J.P. and K.E. Geckeler, *Polymer nanoparticles: Preparation techniques and size-control parameters.* Progress in Polymer Science, 2011. **36**(7): p. 887-913.
181. Zambaux, M.F., et al., *Influence of experimental parameters on the characteristics of poly(lactic acid) nanoparticles prepared by a double emulsion method.* Journal of Controlled Release, 1998. **50**(1-3): p. 31-40.
182. Song, C.X., et al., *Formulation and characterization of biodegradable nanoparticles for intravascular local drug delivery.* Journal of Controlled Release, 1997. **43**(2-3): p. 197-212.

183. Mainardes, R.M. and R.C. Evangelista, *Praziquantel-loaded PLGA nanoparticles: preparation and characterization.* Journal of Microencapsulation, 2005. **22**(1): p. 13-24.
184. Braasch, D.A., et al., *Biodistribution of phosphodiester and phosphorothioate siRNA.* Bioorg Med Chem Lett, 2004. **14**(5): p. 1139-43.
185. Souhami, R.L., H.M. Patel, and B.E. Ryman, *The effect of reticuloendothelial blockade on the blood clearance and tissue distribution of liposomes.* Biochim Biophys Acta, 1981. **674**(3): p. 354-71.
186. Simberg, D., et al., *Biomimetic amplification of nanoparticle homing to tumors.* Proc Natl Acad Sci U S A, 2007. **104**(3): p. 932-6.
187. Dobrovolskaia, M.A. and S.E. McNeil, *Immunological properties of engineered nanomaterials.* Nat Nanotechnol, 2007. **2**(8): p. 469-78.
188. Simpson, C.A., et al., *In vivo toxicity, biodistribution, and clearance of glutathione-coated gold nanoparticles.* Nanomedicine-Nanotechnology Biology and Medicine, 2013. **9**(2): p. 257-263.
189. Yang, L., et al., *Biodistribution and clearance of aminoclay nanoparticles: implication for in vivo applicability as a tailor-made drug delivery carrier.* Journal of Materials Chemistry B, 2014. **2**(43): p. 7567-7574.
190. Alric, C., et al., *The biodistribution of gold nanoparticles designed for renal clearance.* Nanoscale, 2013. **5**(13): p. 5930-5939.
191. Kaiser, C.R., et al., *Biodistribution studies of protein cage nanoparticles demonstrate broad tissue distribution and rapid clearance in vivo.* International Journal of Nanomedicine, 2007. **2**(4): p. 715-733.
192. Mullin, J.M., et al., *Keynote review: epithelial and endothelial barriers in human disease.* Drug Discov Today, 2005. **10**(6): p. 395-408.
193. Groothuis, D.R., *The blood-brain and blood-tumor barriers: a review of strategies for increasing drug delivery.* Neuro Oncol, 2000. **2**(1): p. 45-59.
194. Braet, F. and E. Wisse, *Structural and functional aspects of liver sinusoidal endothelial cell fenestrae: a review.* Comp Hepatol, 2002. **1**(1): p. 1.
195. Zamecnik, J., et al., *Extracellular matrix glycoproteins and diffusion barriers in human astrocytic tumours.* Neuropathol Appl Neurobiol, 2004. **30**(4): p. 338-50.
196. Oliveira, S., et al., *Fusogenic peptides enhance endosomal escape improving siRNA-induced silencing of oncogenes.* Int J Pharm, 2007. **331**(2): p. 211-4.
197. Song, Q., et al., *Cellular internalization pathway and transcellular transport of pegylated polyester nanoparticles in Caco-2 cells.* Int J Pharm, 2013. **445**(1-2): p. 58-68.
198. Li, Y., X. Zhang, and D. Cao, *Nanoparticle hardness controls the internalization pathway for drug delivery.* Nanoscale, 2015. **7**(6): p. 2758-69.
199. Hawkins, B.T. and T.P. Davis, *The blood-brain barrier/neurovascular unit in health and disease.* Pharmacological reviews, 2005. **57**(2): p. 173-185.
200. Davson, H., *The blood-brain barrier.* The structure and function of nervous tissue, 2012. **4**: p. 321-445.
201. Barrier, B.B., *Blood–brain barrier.* Cancer Symptom Science: Measurement, Mechanisms, and Management, 2010: p. 9.
202. Ballabh, P., A. Braun, and M. Nedergaard, *The blood-brain barrier: an overview: structure, regulation, and clinical implications.* Neurobiol Dis, 2004. **16**(1): p. 1-13.
203. Abbott, N.J., *Astrocyte-endothelial interactions and blood-brain barrier permeability.* J Anat, 2002. **200**(6): p. 629-38.
204. Chun, H.B., et al., *The proteome of mouse brain microvessel membranes and basal lamina.* J Cereb Blood Flow Metab, 2011. **31**(12): p. 2267-81.

205. Davis, W., et al., *Exercise pre-conditioning ameliorates blood-brain barrier dysfunction in stroke by enhancing basal lamina.* Neurol Res, 2007. **29**(4): p. 382-7.
206. Abbott, N.J., et al., *Structure and function of the blood-brain barrier.* Neurobiol Dis, 2010. **37**(1): p. 13-25.
207. de Lange, E. and M. Hammarlund-Udenaes, *Translational aspects of blood-brain barrier transport and central nervous system effects of drugs: From discovery to patients.* Clin Pharmacol Ther, 2015. **97**(4): p. 380-94.
208. Pardridge, W.M., *Blood-brain barrier carrier-mediated transport and brain metabolism of amino acids.* Neurochem Res, 1998. **23**(5): p. 635-44.
209. Cisternino, S., et al., *Coexistence of passive and proton antiporter-mediated processes in nicotine transport at the mouse blood-brain barrier.* AAPS J, 2013. **15**(2): p. 299-307.
210. Ohtsuki, S. and T. Terasaki, *Contribution of carrier-mediated transport systems to the blood-brain barrier as a supporting and protecting interface for the brain; importance for CNS drug discovery and development.* Pharm Res, 2007. **24**(9): p. 1745-58.
211. Wang, Y.Y., P.C. Lui, and J.Y. Li, *Receptor-mediated therapeutic transport across the blood-brain barrier.* Immunotherapy, 2009. **1**(6): p. 983-93.
212. Lajoie, J.M. and E.V. Shusta, *Targeting receptor-mediated transport for delivery of biologics across the blood-brain barrier.* Annu Rev Pharmacol Toxicol, 2015. **55**: p. 613-31.
213. Friden, P.M., *Receptor-mediated transport of therapeutics across the blood-brain barrier.* Neurosurgery, 1994. **35**(2): p. 294-8; discussion 298.
214. Molino, Y., et al., *Setting-up an in vitro model of rat blood-brain barrier (BBB): a focus on BBB impermeability and receptor-mediated transport.* J Vis Exp, 2014(88): p. e51278.
215. Jain, K.K., *Nanobiotechnology-based strategies for crossing the blood-brain barrier.* Nanomedicine (Lond), 2012. **7**(8): p. 1225-33.
216. Broadwell, R.D., et al., *Transcytosis of protein through the mammalian cerebral epithelium and endothelium. III. Receptor-mediated transcytosis through the blood-brain barrier of blood-borne transferrin and antibody against the transferrin receptor.* Exp Neurol, 1996. **142**(1): p. 47-65.
217. Pflanzner, T., C.R. Kuhlmann, and C.U. Pietrzik, *Blood-brain-barrier models for the investigation of transporter- and receptor-mediated amyloid-beta clearance in Alzheimer's disease.* Curr Alzheimer Res, 2010. **7**(7): p. 578-90.
218. Dehouck, B., et al., *A new function for the LDL receptor: transcytosis of LDL across the blood-brain barrier.* J Cell Biol, 1997. **138**(4): p. 877-89.
219. Yepes, M., et al., *Tissue-type plasminogen activator induces opening of the blood-brain barrier via the LDL receptor-related protein.* J Clin Invest, 2003. **112**(10): p. 1533-40.
220. Shibata, M., et al., *Clearance of Alzheimer's amyloid-ss(1-40) peptide from brain by LDL receptor-related protein-1 at the blood-brain barrier.* J Clin Invest, 2000. **106**(12): p. 1489-99.
221. Pinzon-Daza, M., et al., *The association of statins plus LDL receptor-targeted liposome-encapsulated doxorubicin increases in vitro drug delivery across blood-brain barrier cells.* Br J Pharmacol, 2012. **167**(7): p. 1431-47.
222. Chang, J., et al., *Characterization of endocytosis of transferrin-coated PLGA nanoparticles by the blood-brain barrier.* Int J Pharm, 2009. **379**(2): p. 285-92.
223. Gan, C.W. and S.S. Feng, *Transferrin-conjugated nanoparticles of poly(lactide)-D-alpha-tocopheryl polyethylene glycol succinate diblock copolymer for targeted drug delivery across the blood-brain barrier.* Biomaterials, 2010. **31**(30): p. 7748-57.
224. Fishman, J.B., et al., *Receptor-mediated transcytosis of transferrin across the blood-brain barrier.* J Neurosci Res, 1987. **18**(2): p. 299-304.

225. Friden, P.M. and L.R. Walus, *Transport of proteins across the blood-brain barrier via the transferrin receptor.* Adv Exp Med Biol, 1993. **331**: p. 129-36.
226. Fukuta, M., et al., *Insulin fragments as a carrier for peptide delivery across the blood-brain barrier.* Pharm Res, 1994. **11**(12): p. 1681-8.
227. Hawkins, R.A., et al., *Glutamate permeability at the blood-brain barrier in insulinopenic and insulin-resistant rats.* Metabolism, 2010. **59**(2): p. 258-66.
228. Kondo, T., et al., *Mice lacking insulin or insulin-like growth factor 1 receptors in vascular endothelial cells maintain normal blood-brain barrier.* Biochem Biophys Res Commun, 2004. **317**(2): p. 315-20.
229. Castellano, J.M., et al., *Low-density lipoprotein receptor overexpression enhances the rate of brain-to-blood Abeta clearance in a mouse model of beta-amyloidosis.* Proc Natl Acad Sci U S A, 2012. **109**(38): p. 15502-7.
230. Kim, J., et al., *Overexpression of low-density lipoprotein receptor in the brain markedly inhibits amyloid deposition and increases extracellular A beta clearance.* Neuron, 2009. **64**(5): p. 632-44.
231. Johnson, L.A., et al., *Apolipoprotein E-low density lipoprotein receptor interaction affects spatial memory retention and brain ApoE levels in an isoform-dependent manner.* Neurobiol Dis, 2014. **64**: p. 150-62.
232. Zheng, M., et al., *ApoE-deficient promotes blood-brain barrier disruption in experimental autoimmune encephalomyelitis via alteration of MMP-9.* J Mol Neurosci, 2014. **54**(2): p. 282-90.
233. Bjelik, A., et al., *Human apoB overexpression and a high-cholesterol diet differently modify the brain APP metabolism in the transgenic mouse model of atherosclerosis.* Neurochem Int, 2006. **49**(4): p. 393-400.
234. Spencer, B.J. and I.M. Verma, *Targeted delivery of proteins across the blood-brain barrier.* Proc Natl Acad Sci U S A, 2007. **104**(18): p. 7594-9.
235. Wagner, S., et al., *Uptake mechanism of ApoE-modified nanoparticles on brain capillary endothelial cells as a blood-brain barrier model.* PLoS One, 2012. **7**(3): p. e32568.
236. Demeule, M., et al., *Involvement of the low-density lipoprotein receptor-related protein in the transcytosis of the brain delivery vector angiopep-2.* J Neurochem, 2008. **106**(4): p. 1534-44.
237. Ruan, S., et al., *Tumor microenvironment sensitive doxorubicin delivery and release to glioma using angiopep-2 decorated gold nanoparticles.* Biomaterials, 2015. **37**: p. 425-35.
238. Gao, H., et al., *Angiopep-2 and activatable cell-penetrating peptide dual-functionalized nanoparticles for systemic glioma-targeting delivery.* Mol Pharm, 2014. **11**(8): p. 2755-63.
239. Boado, R.J., et al., *Engineering and expression of a chimeric transferrin receptor monoclonal antibody for blood-brain barrier delivery in the mouse.* Biotechnol Bioeng, 2009. **102**(4): p. 1251-8.
240. Bray, N., *Biologics: Transferrin' bispecific antibodies across the blood-brain barrier.* Nat Rev Drug Discov, 2015. **14**(1): p. 14-5.
241. Boado, R.J., et al., *Insulin receptor antibody-sulfamidase fusion protein penetrates the primate blood-brain barrier and reduces glycosoaminoglycans in Sanfilippo type A cells.* Mol Pharm, 2014. **11**(8): p. 2928-34.
242. Boado, R.J., et al., *Humanization of anti-human insulin receptor antibody for drug targeting across the human blood-brain barrier.* Biotechnol Bioeng, 2007. **96**(2): p. 381-91.
243. Zhou, Q.H., et al., *Brain penetrating IgG-erythropoietin fusion protein is neuroprotective following intravenous treatment in Parkinson's disease in the mouse.* Brain Research, 2011. **1382**: p. 315-320.
244. Hedrich, J., et al., *Transport across the blood brain barrier with nanoparticle systems.* Acta Physiologica, 2014. **210**: p. 196-198.

245. Ko, Y.T., *Nanoparticle-mediated delivery of oligonucleotides to the blood-brain barrier: in vitro and in situ brain perfusion studies on the uptake mechanisms.* Journal of Drug Targeting, 2013. **21**(9): p. 866-873.
246. Re, F., et al., *Functionalization of liposomes with ApoE-derived peptides at different density affects cellular uptake and drug transport across a blood-brain barrier model.* Nanomedicine-Nanotechnology Biology and Medicine, 2011. **7**(5): p. 551-559.
247. Patel, T., et al., *Polymeric nanoparticles for drug delivery to the central nervous system.* Advanced Drug Delivery Reviews, 2012. **64**(7): p. 701-705.
248. Tian, X.H., et al., *Enhanced brain targeting of temozolomide in polysorbate-80 coated polybutylcyanoacrylate nanoparticles.* International Journal of Nanomedicine, 2011. **6**: p. 445-452.
249. Somani, S. and C. Dufes, *Applications of dendrimers for brain delivery and cancer therapy.* Nanomedicine, 2014. **9**(15): p. 2403-2414.
250. Ruan, S.B., et al., *Tumor microenvironment sensitive doxorubicin delivery and release to glioma using angiopep-2 decorated gold nanoparticles.* Biomaterials, 2015. **37**: p. 425-435.
251. Prades, R., et al., *Delivery of gold nanoparticles to the brain by conjugation with a peptide that recognizes the transferrin receptor.* Biomaterials, 2012. **33**(29): p. 7194-7205.
252. Qiao, R.R., et al., *Receptor-Mediated Delivery of Magnetic Nanoparticles across the Blood-Brain Barrier.* Acs Nano, 2012. **6**(4): p. 3304-3310.
253. Zensi, A., et al., *Human serum albumin nanoparticles modified with apolipoprotein A-I cross the blood-brain barrier and enter the rodent brain.* J Drug Target, 2010. **18**(10): p. 842-8.
254. Zensi, A., et al., *Albumin nanoparticles targeted with Apo E enter the CNS by transcytosis and are delivered to neurones.* J Control Release, 2009. **137**(1): p. 78-86.
255. Duncan, R. and R. Gaspar, *Nanomedicine(s) under the Microscope.* Molecular Pharmaceutics, 2011. **8**(6): p. 2101-2141.
256. Villar-Pique, A., et al., *Using bacterial inclusion bodies to screen for amyloid aggregation inhibitors.* Febs Journal, 2012. **279**: p. 447-447.
257. Tarasova, N., et al., *Fully synthetic self-assembling tumor-targeted virus-like nanoparticles.* Cancer Research, 2013. **73**(8).
258. Peng, X., et al., *Silicified virus-like nanoparticles in an extreme thermal environment: implications for the preservation of viruses in the geological record.* Geobiology, 2013. **11**(6): p. 511-526.
259. Rhee, J.K., et al., *Glycan-Targeted Virus-like Nanoparticles for Photodynamic Therapy.* Biomacromolecules, 2012. **13**(8): p. 2333-2338.
260. Straub, J.E. and D. Thirumalai, *Principles governing oligomer formation in amyloidogenic peptides.* Curr Opin Struct Biol, 2010. **20**(2): p. 187-95.
261. Reddy, G., J.E. Straub, and D. Thirumalai, *Dynamics of locking of peptides onto growing amyloid fibrils.* Proc Natl Acad Sci U S A, 2009. **106**(29): p. 11948-53.
262. Park, J.S., et al., *A highly sensitive and selective diagnostic assay based on virus nanoparticles.* Nat Nanotechnol, 2009. **4**(4): p. 259-64.
263. Nuzzaci, M., et al., *In vitro stability of Cucumber mosaic virus nanoparticles carrying a Hepatitis C virus-derived epitope under simulated gastrointestinal conditions and in vivo efficacy of an edible vaccine.* J Virol Methods, 2010. **165**(2): p. 211-5.
264. Wu, W., et al., *Active protein aggregates induced by terminally attached self-assembling peptide ELK16 in Escherichia coli.* Microbial Cell Factories, 2011. **10**.
265. Zhou, B.H., et al., *Small surfactant-like peptides can drive soluble proteins into active aggregates.* Microbial Cell Factories, 2012. **11**.

266. Collins, L., et al., *Self-Assembly of Peptides into Spherical Nanoparticles for Delivery of Hydrophilic Moieties to the Cytosol.* Acs Nano, 2010. **4**(5): p. 2856-2864.
267. Ferrer-Miralles, N., et al., *Engineering protein self-assembling in protein-based nanomedicines for drug delivery and gene therapy.* Crit Rev Biotechnol, 2013.
268. Lu, M.J., et al., *Peptide for transmigration across blood brain barrier and delivery systems comprising the same*. 2014, Google Patents.
269. Unzueta, U., et al., *Sheltering DNA in self-organizing, protein-only nano-shells as artificial viruses for gene delivery.* Nanomedicine-Nanotechnology Biology and Medicine, 2014. **10**(3): p. 535-541.
270. Bhowmik, A., R. Khan, and M.K. Ghosh, *Blood Brain Barrier: A Challenge for Effectual Therapy of Brain Tumors.* Biomed Res Int, 2015. **2015**: p. 320941.
271. Friedman, A. and D. Kaufer, *Blood-brain barrier in health and disease.* Semin Cell Dev Biol, 2015. **38**: p. 1.
272. Fu, A., et al., *Intravenous treatment of experimental Parkinson's disease in the mouse with an IgG-GDNF fusion protein that penetrates the blood-brain barrier.* Brain Res, 2010. **1352**: p. 208-13.
273. Fu, A., et al., *Neuroprotection in stroke in the mouse with intravenous erythropoietin-Trojan horse fusion protein.* Brain Res, 2011. **1369**: p. 203-7.
274. Lu, J.Z., et al., *Expression in CHO cells and pharmacokinetics and brain uptake in the Rhesus monkey of an IgG-iduronate-2-sulfatase fusion protein.* Biotechnol Bioeng, 2011. **108**(8): p. 1954-64.
275. Loffler, T., et al., *Impact of ApoB-100 expression on cognition and brain pathology in wild-type and hAPPsl mice.* Neurobiol Aging, 2013. **34**(10): p. 2379-88.
276. Wang, D., et al., *Engineering a lysosomal enzyme with a derivative of receptor-binding domain of apoE enables delivery across the blood-brain barrier.* Proc Natl Acad Sci U S A, 2013. **110**(8): p. 2999-3004.
277. Karch, A., et al., *Investigating the association of ApoE genotypes with blood-brain barrier dysfunction measured by cerebrospinal fluid-serum albumin ratio in a cohort of patients with different types of dementia.* PLoS One, 2013. **8**(12): p. e84405.
278. Yainoy, S., et al., *Engineering of chimeric catalase-Angiopep-2 for intracellular protection of brain endothelial cells against oxidative stress.* International Journal of Biological Macromolecules, 2014. **68**: p. 60-66.
279. Xin, H.L., et al., *The brain targeting mechanism of Angiopep-conjugated poly(ethylene glycol)-co-poly(epsilon-caprolactone) nanoparticles.* Biomaterials, 2012. **33**(5): p. 1673-1681.
280. Wei, X.L., et al., *Retro-Inverso Isomer of Angiopep-2: A Stable D-Peptide Ligand Inspires Brain-Targeted Drug Delivery.* Molecular Pharmaceutics, 2014. **11**(10): p. 3261-3268.
281. Demeule, M., et al., *Identification and design of peptides as a new drug delivery system for the brain.* Journal of Pharmacology and Experimental Therapeutics, 2008. **324**(3): p. 1064-1072.
282. Ying, X.Y., et al., *Angiopep-Conjugated Electro-Responsive Hydrogel Nanoparticles: Therapeutic Potential for Epilepsy.* Angewandte Chemie-International Edition, 2014. **53**(46): p. 12436-12440.
283. Shao, K., et al., *A brain-vectored angiopep-2 based polymeric micelles for the treatment of intracranial fungal infection.* Biomaterials, 2012. **33**(28): p. 6898-6907.
284. Rejman, J., et al., *Size-dependent internalization of particles via the pathways of clathrin- and caveolae-mediated endocytosis.* Biochem J, 2004. **377**(Pt 1): p. 159-69.
285. Champion, J.A., A. Walker, and S. Mitragotri, *Role of particle size in phagocytosis of polymeric microspheres.* Pharm Res, 2008. **25**(8): p. 1815-21.
286. Kreuter, J., et al., *Apolipoprotein-mediated transport of nanoparticle-bound drugs across the blood-brain barrier.* J Drug Target, 2002. **10**(4): p. 317-25.

287. Vazquez, E. and A. Villaverde, *Microbial biofabrication for nanomedicine: biomaterials, nanoparticles and beyond.* Nanomedicine (Lond), 2013. **8**(12): p. 1895-8.
288. Chen, G.Q., *New challenges and opportunities for industrial biotechnology.* Microb Cell Fact, 2012. **11**: p. 111.
289. Chithrani, B.D., A.A. Ghazani, and W.C.W. Chan, *Determining the size and shape dependence of gold nanoparticle uptake into mammalian cells.* Nano Letters, 2006. **6**(4): p. 662-668.
290. Peled, A., O. Wald, and J. Burger, *Development of novel CXCR4-based therapeutics.* Expert Opin Investig Drugs, 2012. **21**(3): p. 341-53.
291. Klonisch, T., et al., *Cancer stem cell markers in common cancers - therapeutic implications.* Trends Mol Med, 2008. **14**(10): p. 450-60.
292. Zhu, B., et al., *Tumor margin detection using quantitative NIRF molecular imaging targeting EpCAM validated by far red gene reporter iRFP.* Mol Imaging Biol, 2013. **15**(5): p. 560-8.

Departament de Genètica i Microbiologia
Facultat de biociències.

Zhikun Xu PhD thesis 2015